Molecular and functional characterization of the signaling pathways that mediate TNF- and TRAIL-induced programmed necrosis

Dissertation submitted in fulfillment of the requirements for the degree of *Doctor rerum naturalium* (Dr. rer. nat.) at the Faculty of Mathematics and Natural Sciences at the Christian Albrechts University Kiel

submitted by Justyna Maria Sosna

born August 23rd, 1983 in Rydułtowy

Kiel, 2013

First reviewer:	**Prof. Dr. Dieter Adam**
Second reviewer:	**Prof. Dr. Dr. h.c. Thomas C. G. Bosch**

Date of submission:	26.06.2013
Date of oral examination:	17.07.2013
Dean:	**Prof. Dr. Wolfgang J. Dusch**

Contents

Abbreviations

°C	degree Celsius
3-OMS	3-*O*-methyl-sphingomyelin
(t)AIF	(truncated) apoptosis-inducing factor
APS	ammonium persulfate
A-SMase	acid sphingomyelinase
Atg	autophagy-related protein
(d)ATP	(deoxy)adenosine-5'-triphosphate
Bak	Bcl-2 antagonist/killer
Bax	Bcl-2–associated X protein
BEACH	Beige and Chediak-Higashi
Bcl-2	B-cell lymphoma 2
Bcl-XL	B-cell lymphoma-extra large
Beclin-1	Atg6, coiled-coil myosin-like Bcl-2-interacting protein
BHA	butylated hydroxyanisole
BHT	butylated hydroxytoluene
(t)Bid	(truncated) BH3 interacting domain death agonist
Bmf	Bcl-2 modifying factor
BSA	bovine serum albumin
Caspase	cysteine-dependent aspartic acid-specific protease
Cer	ceramide
(c)FLIP$_{(L/S)}$	(cellular) FADD-like interleukin-1β converting enzyme inhibitory protein (long/short),
CHS	Chediak-Higashi syndrome, beige in mice
CHX	cycloheximide
cIAP(s)	cellular inhibitor of apoptosis protein(s)
CrmA	cytokine response modifier protein A
CYLD	cylindromatosis (turban tumor syndrome)
CypA/D	cyclophilin A/D, peptidylprolyl isomerase, PPIA/PPID
Cyt *c*	cytochrome *c*
D609	tricyclodecan-9-yl-xanthogenate
DAMP(s)	damage/(danger)-associated molecular pattern(s)

DAPI	4',6-diamidino-2-phenylindole
DD	death domain
DED(s)	death effector domain(s)
DISC	death inducing signaling complex
DMEM	Dulbecco's Modified Eagle Medium
DMSO	dimethyl sulfoxide
DR(s)	death receptor(s)
ECL	enhanced chemiluminescence
EDTA	ethylene diamine tetraacetic acid
EF(s)	embryonic fibroblast(s)
EGTA	ethylene glycol tetraacetic acid
ER	endoplasmic reticulum
ERK	extracellular signal-regulated kinase (MAPK)
FACS	fluorescence-activated cell sorting
FADD	Fas-associated protein with death domain
FAN	factor associated with N-SMase activation
FBS	fetal bovine serum
FSC	forward scatter channel
g	$9{,}81\ {}^{m}/_{s^2}$
h	hour(s)
H^+-V-ATPase	vacuolar-type, proton-translocating ATPase complex
HCl	hydrochloric acid
HEPES	4-(2-hydroxyethyl)-1-piperazineethanesulfonic acid
ID	inter domain
IL-1, (6)	interleukin-1, (6)
JNK(s)	c-jun N-terminal kinase(s)
KD	kinase domain
kDa	kilo Dalton
LMP	lysosomal membrane permeability
LPS	lipopolysaccharide
LYST	lysosomal-trafficking regulator, Beige homolog, CHS
µg	microgram
µm	micrometer

mA	milliampere
mAb	monoclonal antibody
MAPK(s)	mitogen-activated protein kinase(s) (ERK)
MEF(s)	mouse embryonic fibroblast(s)
min	minute(s)
mL	milliliter(s)
MLKL	mixed lineage kinase domain-like
(m/μ/n) M	(milli/micro/nano) molar
MNNG	1-methyl-3-nitro-1-nitrosoguanidine
MMS	methyl methanesulfonate
MOMP	mitochondrial outer membrane permeabilization
NAD^+	nicotinamide adenine dinucleotide
Nec-1 (3, 5, 7)	necrostatin-1 (3, 5, 7)
NEMO	NF-κB essential modulator
NF-κB	nuclear factor kappa-light-chain-enhancer of activated B cells
NP-40	Nonidet 40
N-SMase	neutral sphingomyelinase
pAb	polyclonal antibody
PAR	poly(ADP)-ribose
PARP1/2	poly(ADP-ribose) polymerase 1/2
PBS	phosphate-buffered saline
PBS/T	phosphate-buffered saline with Tween 20
PCD	programmed cell death
PDGF-B	platelet derived growth factor, B polypeptide
PGAM5	phosphoglycerate mutase family member 5
PH	pleckstrin homology
PI	propidium iodide
PKC(δ, ξ)	protein kinase C (delta, zeta)
PKB	protein kinase B**,** AKT1
Ras	rat sarcoma
RelA	v-rel reticuloendotheliosis viral oncogene homolog A
RHIM(s)	RIP homotypic interaction motif(s)
RIP	receptor interacting protein

ROS	reactive oxygen species
RPMI	Roswell Park Memorial Institute
S1P	sphingosine 1-phosphate
SD	standard deviation
SDS-PAGE	sodium dodecyl sulfate polyacrylamide gel electrophoresis
siRNA	small interfering ribonucleic acid
SM	sphingomyelin
Smac	second mitochondria-derived activator of caspases
Sph	sphingosine
SPL(s)	sphingolipid(s)
SSC	side scatter channel
TAB2/3	TAK1-binding protein 2/3
TAK1	transforming growth factor-β-activated kinase 1
TLR(s)	Toll-like receptor(s)
TNF-R(1, 2)	tumor necrosis factor receptor (1, 2)
TNF	tumor necrosis factor
TRADD	TNF receptor-associated protein with death domain
TRAF(2/5)	TNF receptor-associated factor (2/5)
TRAIL	TNF-related apoptosis-inducing ligand
Tris	tris(hydroxymethyl)aminomethane
U	unit(s)
UCH-L1	ubiquitin carboxy-terminal hydrolase L1
UPS	ubiquitin proteasome system
UV	ultra violet
V	Volt
v/v	volume per volume
w/v	weight per volume
WB	Western blot
WD repeats	tryptophan (W) – aspartic acid (D) repeats
XIAP	X-linked inhibitor of apoptosis protein
zVAD-fmk (zVAD)	*N*-benzyloxycarbonyl-Val-Ala-Asp-fluoro methyl ketone

I. Introduction

Preface

Detailed knowledge about the mechanisms controlling cell death and survival in response to death receptors, lipids and proteases may be essential for developing strategies to counteract metabolic disorders, to promote the survival of cells or organs and to enhance tumor destruction. It is increasingly becoming clear that the investigation of alternative cell death pathways, distinct from classical apoptosis or from uncontrolled, accidental necrosis (such as programmed necrosis or autophagy) may offer solutions for challenging problems such as controlling cancer elimination or inflammation-based diseases.

Often, the description of cell death processes is being oversimplified, e.g. "caspase activation is equal to apoptosis" and "autophagic vacuolization is equal to autophagic cell death" (Kepp et al., 2011). Therefore, a detailed investigation of the cellular signaling diversity of these processes is required. In recent years, evidence for an involvement of programmed necrosis in various cellular processes has been found, such as the elimination of chondrocytes, virus infection, bacterial infection (Han et al., 2011) or the homeostasis of T cell populations (Ch'en et al., 2011). Moreover, programmed necrosis has been described to trigger pathophysiological alterations such as neurodegeneration (Chavez-Valdez et al., 2012), β-cell elimination form pancreatic islets/development of diabetes, loss of hypertrophic cardiomyocytes during heart failure (Dorn, 2013), Crohn's disease (Declercq et al., 2011), acute pancreatitis, ischemic injury and inflammation (Han et al., 2011, Kang et al., 2013, Kaczmarek et al., 2013)}. Of note, the ongoing evaluation of mouse disease models and human pathologies will most likely reveal further evidence for the importance of programmed necrosis.

1. Programmed cell death

Living cells are regulated by various mechanisms that govern their development, homeostatic maintenance and remodeling. An imbalance of, mutations in or deregulation of those pathways may lead to transformation from a healthy to a malignant state as well as from survival to death of the affected cell. Historically, two major types of cell death have been distinguished, based on biochemical and morphological features such as cell shrinkage, swelling, and fragmentation of the nucleus and the release of pro-inflammatory

factors: a controlled or programmed form of cell death (PCD) called apoptosis, and an uncontrolled, accidental form of cell death known as necrosis. Although apoptotic PCD is the best characterized route of cell death, many studies have observed that despite application of various anti-apoptotic agents, programmed cell death did still occur (Kroemer and Martin, 2005). As e.g. demonstrated by Cauwels and coworkers in an *in vivo* mouse model, the inhibition of caspases (the main proteases involved in apoptosis) did not alleviate but rather exacerbated tumor necrosis factor (TNF)–induced toxicity (Cauwels et al., 2003). This led to the discovery of alternative forms of programmed cell death that do not depend on the activation of caspases, and – in consequence – to the discrimination between caspase-dependent and caspase-independent PCD. Moreover, it has been recognized that often similar molecular components participate in both pathways, although both pathways operate through distinct mechanisms (Jäättelä and Tschopp, 2003, Vandenabeele et al., 2010). Notably, the term programmed caspase-independent PCD has been used interchangeably with the terms programmed necrosis or necroptosis (discussed later, see chapter 1.2.1). Programmed necrosis (also termed "regulated necrosis" when involved in developmental processes) may be triggered by stimuli such as DNA damage by alkylating agents and the ligation of death receptors (Galluzzi et al., 2012). The diversity of cell death pathways is determined by the existence of numerous signaling complexes that have been termed death-inducing signaling complex (DISC), apoptosome, PIDDosome, Toll-like receptor (TLR) complexes, necrosome or ripoptosome, which were reviewed extensively elsewhere (Sabroe et al., 2003, Bao and Shi, 2007, Yuan and Kroemer, 2010, Dickens et al., 2012, Janssens and Tinel, 2012, Long and Ryan, 2012, Mocarski et al., 2012). However, except for apoptosis, the downstream signaling components of these cell death pathways are poorly understood and need extensive investigation. Importantly, minor differences in cellular function or environmental factors can influence the mode of cell death, directing the whole execution machinery from, e.g. caspase-dependent to caspase-independent PCD. The multiplicity of cell death mechanisms, in particular with regard to necroptosis, is presented in the following chapters.

Importantly, it must be noted here that programmed necrosis is not identical to classical necrosis which describes a passive, accidental, uncontrolled cell death induced solely by harsh physico-chemical factors, e.g. freeze–thawing cycles, high concentrations of pro-oxidants, heat, pressure, that (in contrast to programmed necrosis) cannot be inhibited by pharmacological and/or genetic manipulations (Galluzzi et al., 2012).

1.1 Apoptosis

The most comprehensively investigated form of PCD in living organisms – apoptosis – is executed by cysteine-dependent aspartate-directed proteases called caspases. The morphological aspects of apoptosis are well investigated and are defined by cell shrinkage, blebbing of the plasma membrane, formation of apoptotic bodies, and by condensation and fragmentation of the nucleus. Furthermore, the molecular pathways of apoptosis have been studied in detail (Figure 1). Execution of apoptosis through the extrinsic pathway is triggered by (i) death receptor signaling and subsequent activation of caspase-8 (or -10) and the effector (executioner) caspases-3, -6, and -7, or by (ii) death receptor signaling and activation of the caspase-8-tBID-MOMP (mitochondrial outer membrane permeabilization)-caspase-9-caspase-3 cascade via crosstalk with the intrinsic pathway (Galluzzi et al., 2012). The intrinsic route of apoptosis centrally involves mitochondria as sensors and mediators of PCD. It is activated by events such as irradiation, bioenergetic or metabolic catastrophe, followed by multiple mitochondria-dependent executioner mechanisms such as (i) loss of mitochondrial transmembrane potential, (ii) release of proteins from the mitochondrial intermembrane space into the cytosol and (iii) respiratory chain inhibition (Figure 1). Notably, various degradative processes in apoptosis may rely on caspase-independent mechanisms. For example, translocation of apoptosis-inducing factor (AIF) and endonuclease G (EndoG) to the nucleus in order to mediate large-scale DNA fragmentation or the cleavage of a wide range of cellular substrates by the serine protease HtrA2/Omi contributes to apoptosis, although this occurs independent from caspases (Galluzzi et al., 2012).

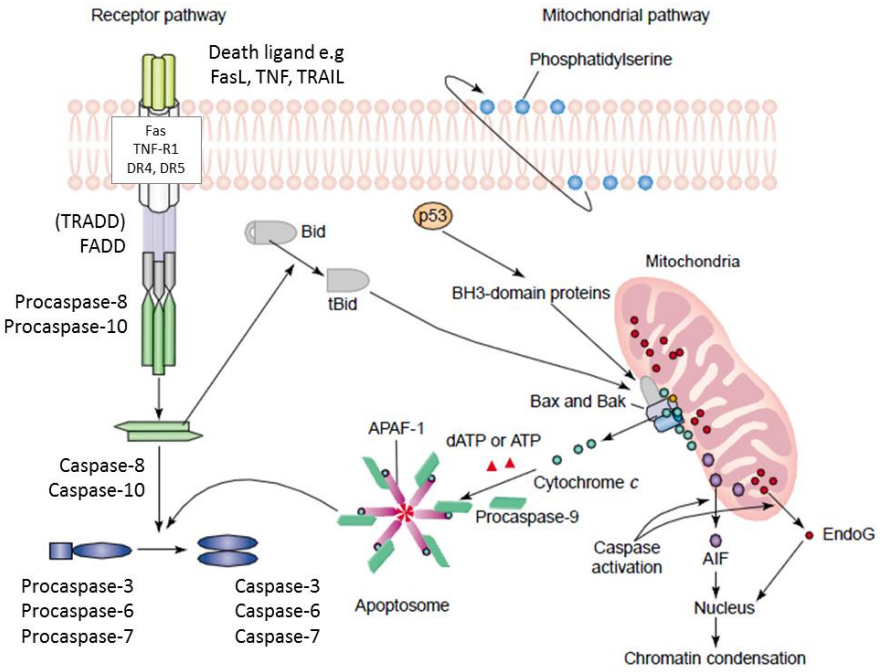

Figure 1. Extrinsic and intrinsic routes of apoptosis/caspase-dependent PCD. In the extrinsic route, after binding of a death ligand, the trimerization of death receptors recruits adapter proteins to their death domains. Death receptors possess C-terminal death domains (DD) and thereby interact directly with the adaptor molecule Fas-associated protein with death domain (FADD, in case of the receptor Fas/CD95/Apo1) or with TNF-R-associated protein with death domain (TRADD, in case of TNF-R1 (tumor necrosis factor receptor 1)) which subsequently binds to FADD. FADD then promotes recruitment of the initiator procaspases-8(/10) through the mutual interaction of death effector domains, resulting in their proteolytic cleavage and activation. Activated caspase-8 cleaves and activates the effector procaspases-3 and/or procaspases-6 and -7. Activated caspases-3 and/or -6 and -7 then execute apoptosis by cleaving various substrate proteins. In the intrinsic route of apoptosis, receptor-independent stimuli, e.g. irradiation causing DNA damage and subsequent activation of p53 lead to Bax- and Bak-mediated MOMP, followed by release of cytochrome *c* and AIF from the mitochondrial intermembrane space into the cytosol. Cytochrome *c*, together with either dATP or ATP binds to apoptotic protease-activating factor 1 (APAF-1) and procaspase-9 to form a complex called apoptosome. Subsequently, the apoptosome containing active caspase-9 induces cleavage and activation of the downstream effector caspases -3, -6 and -7. Additionally, AIF and endonuclease G (EndoG) are released from mitochondria, in either a caspase-dependent or a caspase-independent manner, to translocate to the nucleus, resulting in chromatin condensation. A crosstalk between the extrinsic and intrinsic routes of apoptosis is established by cleavage of Bid to truncated Bid (tBid) by activated caspase-8, followed by the translocation of tBid into mitochondria. There, tBid induces Bax- and Bak-mediated MOMP, followed by release of cytochrome *c* and AIF from the mitochondrial intermembrane space into the cytosol. As one of early markers of apoptosis, phosphatidylserine is translocated in a caspase-dependent or AIF-dependent manner to the outer leaflet of the plasma membrane. Modified after: (Hong et al., 2004, Dickens et al., 2012, Mocarski et al., 2012).

1.2 Programmed necrosis

In addition to the accidental, unregulated necrosis triggered by extreme physical conditions, a programmed type of necrosis has been discovered in an increasing number of studies (Vandenabeele et al., 2010). However, in contrast to apoptosis, programmed necrosis is executed without participation of caspases. Although programmed necrosis resembles accidental necrosis with respect to morphological features such as swelling of mitochondria, irreversible damage of cellular membranes and spilling of the intracellular

content into the surrounding environment, programmed necrosis is executed in a similarly controlled manner as apoptosis. Since programmed necrosis represents a programmed form of cell death, specific signal transduction cascades that eventually lead to cell elimination are executed (Fulda, 2013) (discussed in following chapters). Under conditions of caspase inhibition, programmed necrosis was reported to be induced by different cellular stimuli such as TNF, Fas ligand, TRAIL, double-stranded RNA (dsRNA), interferon-γ (IFN-γ), ATP depletion, ischemia-reperfusion injury and pathogens (Kaczmarek et al., 2013). For example, simultaneous inhibition of caspases and stimulation of TNF-R enhanced cell death in mouse peritoneal RAW246.7 macrophages (Kim and Han, 2001) and mouse fibrosarcoma L929 cells (Thon et al., 2005). In order to inhibit caspases and direct the cell death modus into programmed necrosis, broad spectrum caspase inhibitors, such as zVAD-fmk (z-Val-Ala-Asp**,** zVAD**)**, Q-VD-OPh (Q-Val-Asp**,** quinolyl-valyl-O-methylaspartyl-[-2,6-difluorophenoxy]-methyl ketone), BOC-D-fmk (BOC-Asp**,** *t*-butyloxycarbonyl-Asp(*O*-methyl)-fluoromethylketone) are used. (Chauvier et al., 2007, Wang et al., 2010). In certain cases, inhibition of caspases may lead to programmed necrosis by inducing autocrine TNF production (Wu et al., 2011). Interestingly, inhibition of caspases may influence the formation or stability of various cell death signaling complexes in order to preferably execute programmed necrosis, e.g. through an enhanced binding of the kinases RIP1 and RIP3 (alternatively termed RIPK1 and RIPK3) as the main initiators of programmed necrosis (see chapter 1.2.2) (Cho et al., 2009). Presumably, programmed necrosis can act as an alternative pathway of cell death in cells when the apoptotic machinery is blocked (Christofferson and Yuan, 2010a). For example, naturally occurring viral proteins may efficiently suppress the activity of caspases, and therefore initiate programmed necrosis as an alternative mechanism to limit viral infections (Caspases-8, -1,-4, -5, -6, -10 and granzyme B can be blocked by viral cytokine response modifier A (CrmA) from cowpox virus (Dobo et al., 2006), by SPI-2 from vaccinia virus (Chan et al., 2003), by the cytomegalovirus protein vICA (viral inhibitor of caspase-8 activation (McCormick, 2008), by the murine cytomegalovirus (MCMV)-encoded viral inhibitor of RIP activation (vIRA) (Mocarski et al., 2012) and by the baculovirus anti-apoptotic p53 protein (Fulda et al., 2010)). During programmed necrosis, alternative executive molecules such as calpains, cathepsins, serine proteases and metalloproteases are thought to propagate or support cell death (Schrader et al., 2010) (see chapter 1.2.3).

1.2.1 Necroptosis

Originally, the term “necroptosis” was introduced in order to describe a specific case of programmed necrosis, which is induced by TNF-R1 and mediated by RIP1 kinase (receptor interacting protein kinase 1) (Degterev et al., 2005, Galluzzi et al., 2012). Further analyses identified a specific and potent small-molecule inhibitor of necroptosis, necrostatin-1 (Nec-1), which blocks the kinase function of RIP1 as a critical component of the necroptotic signaling complex. Mechanistically, it was shown that Nec-1 interacts with RIP1 and abrogates the interaction of caspase-8 with FADD (see chapter 1.2.2) (Duprez et al., 2012). Additional studies have identified two other necrostatins: Nec-3 and Nec-5, which target RIP1 and inhibit necroptosis in a mechanism distinct from Nec-1 (Degterev et al., 2008). Although originally defined for TNF-R1, necroptosis can also be triggered by other death receptors such as the receptors for the cytokine TRAIL (Vandenabeele et al., 2010).

TNF- or TRAIL-mediated “classical” necroptosis is dependent mainly on a complex involving the two major Ser/Thr kinases RIP1 and RIP3 which is called the necrosome (Wu et al., 2012). Recent analyses indicate, however, that some exceptions exist and that TNF-mediated necroptosis can be executed in the absence of RIP1, solely through activation of RIP3 (Moujalled et al., 2013). Similarly, in addition to “classical” RIP1-RIP3-dependet necroptosis, distinct forms of caspase-independent cell death such as exclusively RIP3-dependent viral-induced programmed necrosis (Mocarski et al., 2012) or exclusively RIP1-dependent T-cell receptor induced programmed necrosis (Osborn et al., 2010) were identified.

In most cases during TNF- or TRAIL-mediated necroptosis, RIP1 and RIP3 interact through their “RIP homotypic interaction motif” (RHIM) present in both kinases (Duprez et al., 2012). Moreover, it was reported that the phosphorylation of both kinases stabilizes the structure of this pro-necrotic complex (Cho et al., 2009). The most recent analyses identified the cytosolic NAD-dependent deacetylase SIRT2 (sirtuin-2, silent mating type information regulation 2 homolog) as an adaptor molecule which binds constitutively to the carboxy terminus of RIP3 and thereby promotes the formation of the RIP1-RIP3 signaling complex by deacetylating RIP1 in the RHIM domain (Narayan et al., 2012) (see chapter 1.2.2). Recently, a genome wide siRNA screen has identified additional potential regulatory factors in necroptosis. In this study, 32 genes important for TNF-mediated necroptosis in mouse cell lines were identified such as PARP2 (poly(ADP-ribose)

polymerase 2), Bmf (Bcl-2 modifying factor) and CYLD (cylindromatosis) (Hitomi et al., 2008).

1.2.2 Signaling complexes that regulate necroptosis

The balance between pro-survival and pro-cell death properties of cellular receptors depends on the existence of different protein complexes which regulate apoptosis and necroptosis. Binding of TNF to TNF-R1 can either induce the formation of the TNF-R1-associated signaling complex I at the plasma membrane which is responsible for activation of pro-survival pathways or it can trigger assembly of the cytoplasmic signaling complex II which is responsible for apoptosis (Figure 2). The composition of complex I and complex II has been reviewed in detail (Vanlangenakker et al., 2011a, Dickens et al., 2012, Kaczmarek et al., 2013). Complex I recruited to TNF-R1 consists initially of the proteins TRADD, TNF-R-associated factor 2 (TRAF2), TRAF5, cellular inhibitor of apoptosis proteins (cIAPs) and polyubiquitinated RIP1 that engages downstream adaptors such as TAK1-TAB2/3 and NEMO. The formation of complex I promotes NF-κB transcriptional activity, leading in consequence to cell survival, proliferation, or differentiation. By inhibition of cIAPs or deubiquitination of RIP1 by CYLD, complex I may be rearranged into the apoptosis-inducing complex IIa (Figure 2), called death-inducing signaling complex (DISC), which comprises FADD, RIP1, RIP3, procaspase-8 and putatively TRADD (Dickens et al., 2012, Kaczmarek et al., 2013). In comparison, it has been less well explored how the apoptotic complex IIa is transformed into the necroptotic signaling complex IIb under physiologic conditions. However, artificial inhibition of caspase-8 activity by, e.g. zVAD-fmk, CrmA or other factors, deletion of FADD/caspase-8 or induction of RIP3 can lead to formation of the necroptotic complex IIb by preventing RIP1 and RIP3 cleavage (Figure 2). Complex IIb may consist of procaspase-8, FADD, RIP1, RIP3, FLIP and TRADD. However, the involvement of TRADD is controversial. In Jurkat T cells, TRADD is not required and competes with RIP1 for induction of TNF-mediated necroptosis (Zheng et al., 2006), whereas TRADD is necessary for TNF-mediated necroptosis in mouse embryonic fibroblasts (MEFs) (Pobezinskaya et al., 2008). Moreover, deletion or additional association of further components within the signaling complex IIb may lead to formation of alternative complexes that mediate necroptosis. In the cells lacking the capacity to activate caspase-8, the RIP1- and RIP3-containing necroptosis-inducing complexes are termed necrosomes (Declercq et al., 2009, Lu et al., 2011, Wu et

al., 2012). The assembly of the pro-necroptotic RIP1–RIP3 complex is mediated through their RHIM domains. (Moquin and Chan, 2010, Duprez et al., 2012). Both RIP1 and RIP3 possess Ser/Thr kinase domains (KDs) at their N-terminal ends, which are phosphorylated to stabilize the signaling complex for necroptosis (see below). Nec-1 inhibits this stabilization by allosterically binding to the KD of RIP1 (Figure 2).

Recently, independent from the formation of the necrosome complex in death receptor-mediated necroptosis, Feoktistova and coworkers had identified a 2 MDa intracellular complex called "ripoptosome" which depends on TLR signaling. In this complex, similar to the necrosome, the RHIM-dependent interaction of RIP1 and RIP3 is responsible for induction of necroptosis (Feoktistova et al., 2011, Green et al., 2011b). This complex is formed only in the absence of cIAP-1/-2, as described previously by Vanlangenakker and coworkers, and consists of caspase-10 associated with caspase-8, FADD, $cFLIP_{S/L}$ and RIP1. In the absence or after inhibition of cIAPs, inhibition of caspase-8 by $cFLIP_S$ promotes ripoptosome assembly and initiates necroptosis.

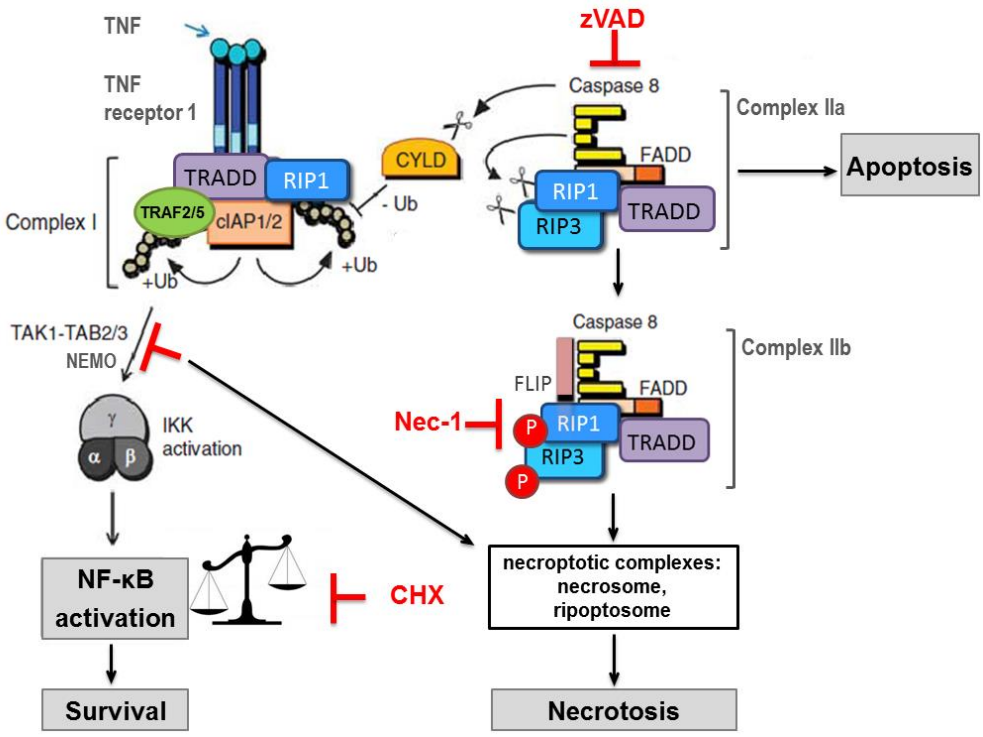

Figure 2. Formation of the signaling complexes after stimulation of TNF receptor 1. TNF induces activation of TNF receptor 1 and promotes formation of complex I (containing the signaling molecules TRADD, TRAF2/5, cIAP1, cIAP2 and RIP1). Polyubiquitination (Ub) of by cIAP1 and cIAP2 enables the interaction of RIP1 with the TAK1 (TGF (transforming growth factor)-β-activated kinase 1)/TAB2 (TAK1 binding protein 2)/3 and NEMO complexes, which in turn activate the survival pathway through the IKK complex and NF-κB pathway. The protein synthesis inhibitor cycloheximide (CHX) (Schneider-Poetsch et al., 2010) blocks the survival pathway and shifts the cellular balance towards cell death. CYLD is a deubiquitinase that removes K63-polyubiquitin chains from RIP1 and regulates its function as a pro-death molecule. Complex IIa can be formed after cIAP inhibition or RIP1 deubiquitination by CYLD, and

subsequent aggregation of RIP3, TRADD (still controversial), FADD and caspase-8. Complex IIa-mediated apoptosis is accompanied by caspase-8-dependent cleavage of RIP1 and RIP3, which prevents formation of the necroptotic complex IIb and contributes to the inhibition of both necroptosis and survival pathways (Lin et al., 1999, Wu et al., 2012). In parallel, caspase-8 cleaves also CYLD, preventing the deubiquitination of RIP1 and thereby, initiation of necroptosis (O'Donnell et al., 2011). An auto-ubiquitination and degradation of cIAP-1 and -2 or its pharmacological inhibition promote apoptosis (Darding et al., 2011). On the other hand, inhibition of caspase-8 activity by, e.g. zVAD-fmk or CrmA, deletion of FADD/caspase-8 prevents RIP1 and RIP3 cleavage and leads to formation of the necroptotic complex IIb. Similarly, formation of heterodimers of procaspase-8 with cellular FADD-like interleukin-1 β-converting enzyme (FLICE)-inhibitory protein long ($cFLIP_L$) in a complex with FADD protects from necroptosis (Feoktistova et al., 2011). RIP1 and RIP3 phosphorylation (P) further stabilizes the signaling complex IIb, allowing further modifications of RIP1-containing necroptotic complexes such as the necrosome or the ripoptosome (discussed in the text). Modified after: (Long and Ryan, 2012).

In addition, numerous regulators of the necroptotic complex IIb have been identified. The kinase TAK1 has been identified as a main negative regulator for the execution of necroptosis. TAK1 inhibits the disassociation of ubiquitinated RIP1 from complex I and prevents formation of complex IIb that results in inhibition of necroptosis. However, in the absence of TAK1, the ligation of TNF leads to execution of necroptosis in which inhibition of caspases (and presence of zVAD-fmk) is dispensable for the formation of the RIP1-mediated necroptotic complex (Figure 2) (Arslan and Scheidereit, 2011). Within the necroptotic complex IIb, a crucial element for the execution of downstream signals is the association of the kinases RIP1 and RIP3, where the phosphorylation of RIP1 by RIP3 at position serine 161 (S161) is one of the earliest events during necroptosis (which is inhibited by Nec-1, thereby abolishing necroptosis). Furthermore, for necroptosis, a phosphorylation loop between RIP1 and RIP3 is crucial (Figure 2 and Figure 3). Especially position serine 199 (S199) within RIP3 is reported to be a necroptotic-specific phosphorylation target site (Cho et al., 2009, Moquin and Chan, 2010, Tsuda et al., 2012). Therefore, analyses of necroptosis have described the kinase RIP3 as the most important "crucial switch" between cell survival and necroptosis. For example, lack of RIP3 in mice failed to induce necroptosis during infection with a virus and resulted in higher mortality of those mice (Cho et al., 2009). Recently, it was found that during necroptosis interactions between RIP1 and RIP3 are followed by formation of a filamentous amyloid-like structure. Those fibrils are generated by regular and strongly associated heterooligomeric 16 RHIM (RIP homotypic interaction motif) residues of RIP1 and 6 RHIM residues of RIP3. Repression in formation of RIP1-RIP3 amyloid-like structures inhibited the signaling complex associations and signal transduction for necroptosis (Li et al., 2012). Moreover, the interactions between RHIM domains of RIP1 and RIP3 are facilitated by the NAD-dependent deacetylase SIRT2 bound to RIP3. Deacetylation of RIP1 at position K530

enables the interaction of RIP1 and RIP3 to trigger necroptosis (Figure 3) (Narayan et al., 2012).

After formation of the necroptotic signaling complex, another autophosphorylation of RIP3 specific for necroptosis at residue serine 227 (S227) enhances the interaction with MLKL (mixed lineage kinase domain-like), a recently discovered downstream signaling molecule. Subsequently, MLKL is phosphorylated at threonine 357 (T357) and serine 358 (S358) (the latter only in mice) in order to activate the necroptotic signaling complex (Figure 3). Formation of the complex can be interrupted necrosulfonamide (NSA), by a novel necroptosis inhibitor (Sun et al., 2012). Downstream the main signaling complex of RIP1-RIP3, other signaling molecules, such as the mitochondrial phosphoglycerate mutase family member 5 (PGAM5), which is anchored with its N-terminus to the outer membrane of mitochondria, ensure a crosstalk between cell death signaling and damage of mitochondria. The splicing variant PGAM5L associates to the death complex of RIP1-RIP3 and MLKL and subsequently with PGAM5S. A putative signaling molecule that relays the signals of PGAM5S is Drp1 (dynamin-related protein 1), which forms a dimer after dephosphorylation at position S637 by PGAM5L/PGAM5S, elevating its GTPase activity and leading to fragmentation of mitochondria (Wang et al., 2012). Moreover, downstream of RIP1-RIP3 a kinase-dead form of MLKL (Figure 3) was identified to interact with yet unknown targets, following generation of ROS and activation of c-Jun N-terminal kinases (JNKs) in the late phase of TNF-mediated necroptosis (Zhao et al., 2012).

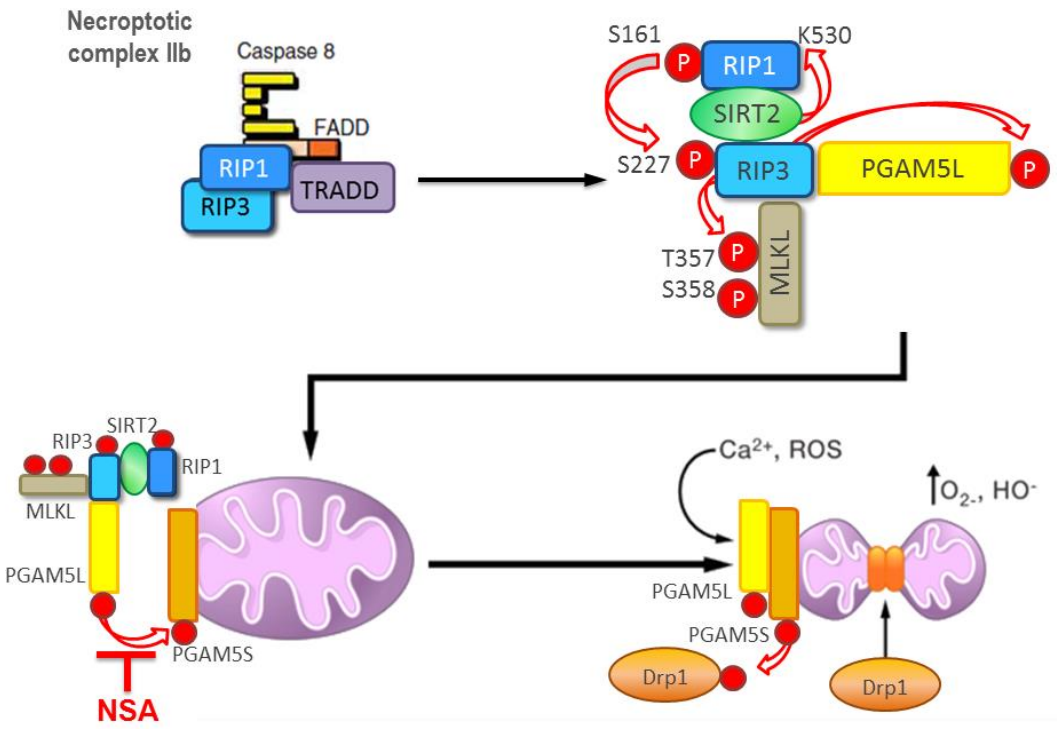

Figure 3. Model for an activation of the necroptotic signaling complex and the execution of necroptosis. At the cytoplasmic necroptotic complex IIb, the deacetylase SIRT2 binds to RIP3 and facilitates interaction of RIP1 and RIP3 by the deacetylation of RIP1. Further, RIP1 is phosphorylated at position S161 (Galluzzi et al., 2012) and it phosphorylates RIP3 at S227. This event leads to recruitment of MLKL and its phosphorylation by RIP3 at positions T357 and S358 (the latter only in mice). These phosphorylation events are important for the signaling complex to recruit the downstream effector molecule PGAM5L. Subsequently, the RIP3 complex phosphorylates PGAM5L, triggering the engagement of the downstream effector PGAM5S bound to mitochondrial membranes. PGAM5S phosphorylation and aggregation of the necroptotic signaling complex with mitochondrial membranes is inhibited by necrosulfonamide (NSA). The phosphorylated complex PGAM5L/PGAM5S dephosphorylates the mitochondrial fission regulator Drp1 at position S637 to induce its dimerization and activation of GTPase activity. Drp1 activity could lead to mitochondrial membrane permeabilization and in consequence reduce energy production, increase ROS generation. The mitochondrial fission may be also activated by calcium flux or a surge of intracellular reactive oxygen species (ROS). Modified after: (Chan and Baehrecke, 2012).

Additional, previously identified regulators of necroptotic as well as apoptotic signaling are the proteins $cFLIP_L$ and $cFLIP_S$ (cFLIP long and cFLIP short) (Green et al., 2011b). The two isoforms are non-catalytic paralogues of caspase-8 (Pop et al., 2011) that can suppress the self-processing of procaspase-8 and thus prevent apoptosis (Figure 4). The $cFLIP_L$ isoform can block necroptosis through remaining caspase-8 proteolytic activity and inactivation of RIP1, RIP3 (Mocarski et al., 2012). Similar to $cFLIP_L$, the anti-apoptotic protein MC159 from the poxvirus *Molluscum contagiosum* that shares sequence homology with the death effector domains of caspase-8 and caspase-10 as well as the E8 protein from equine herpesvirus-2 and K13 from the Kaposi's sarcoma-associated herpesvirus (human herpesvirus-8) (Chan et al., 2003) can inhibit formation of the

necroptotic complex. Thus, the formation of necroptotic RIP1-RIP3 complex is tightly regulated by cFLIP$_L$-caspase-8 interactions (Figure 4) (Oberst et al., 2011). On the other hand, the presence of cFLIP$_S$ can promote RIP1- and RIP3-dependent necroptosis (Figure 4).

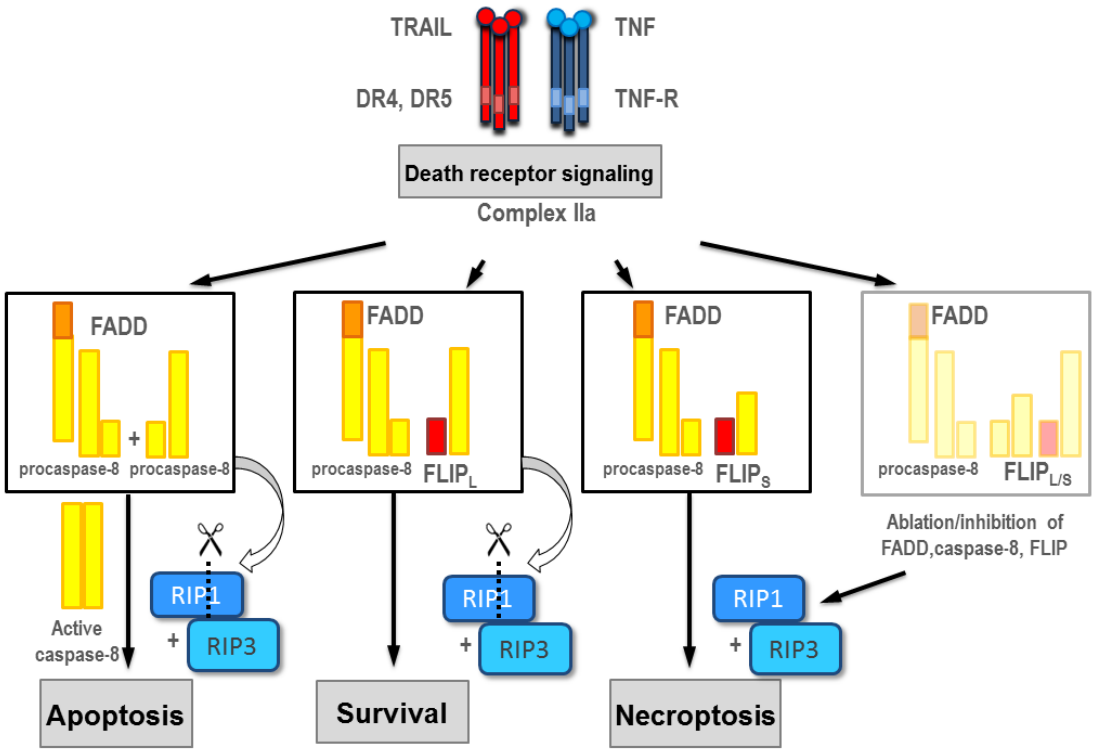

Figure 4. Regulation of the death receptor signaling complexes. Formation of caspase-8 homodimers within the complex results in full catalytic activity and thus apoptosis. Simultaneously, a cleavage of RIP1 occurs within the complex IIa and the necroptosis cannot be executed. The regulatory role of cFLIP is depending on the amount of the particular isoform (L or S). Both forms of cFLIP are recruited to the death inducing signaling complex IIa to prevent procaspase-8 processing and activation followed by abolishment of apoptosis. The formation of caspase-8-cFLIP$_L$ heterodimers results in limited catalytic activity of procaspase-8, which, however, can cleave RIP1 and inactivate necroptosis but is not sufficient to trigger apoptosis. During heterodimerization of procaspase-8 with cFLIP$_S$, both caspase-8 activation and RIP1 cleavage are prevented, thereby necroptosis is executed. Ablation/inhibition of FADD, caspase-8, or FLIP results in RIP1/RIP3-dependent necroptosis (Dickens et al., 2012).

Consequently, under conditions when caspase-8 is not inhibited, the disassociation of the necroptotic complex occurs probably due to a favorable formation of cFLIP$_L$-caspase-8 heterodimers, which suppress RIP1-RIP3-dependent necroptosis (Dillon et al., 2012). However, ablation or inhibition of caspase-8, FADD or FLIP promotes execution of necroptosis. The expression of FLIP protein is regulated by the transcription factor FoxO (forkhead box O), therefore its deletion causes lethality of embryos at day E10.5 as other components of necroptotic pathway do (see chapter 1.2.4) (Park et al., 2009, Green et al.,

2011b). The latest data demonstrate that phosphorylation of FoxO is required for signaling of necroptosis (McNamara et al., 2013).

Another regulatory event for the formation of the necroptotic complex IIb is the association of FADD with RIP1 and RIP3. Deficiency of FADD directs the cells into the necroptotic pathway (Figure 4). However, FADD can differentially regulate Fas-, TRAIL- or TNF-mediated necroptosis. FADD is required for necroptosis triggered by Fas ligand and TRAIL, unlike TNF which, in the absence of FADD, can induce necroptosis when caspases are inhibited (Holler et al., 2000, Vanlangenakker et al., 2012).

The complexity of signaling complexes composed of FADD, caspase-8 and downstream mediators such as RIP1, cFLIP or other factors such as RelA or TRAF2 determines the sensitivity of cells to undergo necroptosis. For example, transformation of PDGF-B or E1A/Ras in MEFs increases susceptibility to TNF-mediated necroptosis (Chau et al., 2011). Moreover, in the absence of caspase-8, TNF-mediated necroptosis can be potentiated by the presence of TNF-R2 (Chan et al., 2003).

1.2.3 Execution of programmed necrosis

In the executive phase of programmed necrosis, multiple effector components have been identified, e. g. cathepsins, μ- and m-calpains, calcium (Ca^{2+}), phospholipases and ceramide, reactive oxygen species (ROS) and cyclophilin D, a component of the mitochondrial permeability transition pore (Festjens et al., 2006, Vandenabeele et al., 2010, Vanlangenakker et al., 2012).

One mechanism that contributes to programmed necrosis is the destabilization of intracellular membranes of the ER and lysosomes. In response to increased levels of cytosolic Ca^{2+}, calpains are activated by autocatalytic hydrolysis, translocate to intracellular membranes and degrade a number of intracellular substrates (Zong and Thompson, 2006). In consequence, lysosomal membrane permeability (LMP) is caused and lysosomal cathepsins are released (Duprez et al., 2009) followed by cytoskeletal protein breakdown and subsequent loss of structural integrity (Yamashima, 2004). As an example, a signaling role of cathepsins D, B, H and L released from lysosomes has been identified during neuronal ischemia (Yamashima, 2004). Although the causative role of cysteine cathepsins was confirmed for staurosporine-mediated programmed necrosis (Dunai et al., 2012), a causative role of cathepsin B was excluded for H_2O_2-mediated

programmed necrosis (Vanlangenakker et al., 2012). Similarly, still it is still controversial whether cathepsins and calpains are crucial for programmed necrosis mediated by death receptors or rather activated as a consequence of cellular degradation. Furthermore, the LMP is regulated by class of lipids called sphingolipids. Inside the lysosomes, acid sphingomyelinase converts sphingolipids into ceramide, which both may serve as signaling molecule or be converted into sphingosine that causes LMP (Zong and Thompson, 2006). Interestingly, ceramide may be a signaling molecule in necroptosis, as inhibition of its production by acid sphingomyelinase increased survival in mouse L929 cells after induction of both TNF- (Strelow et al., 2000, Thon et al., 2005) and TRAIL-mediated necroptosis (Thon et al., 2006).

Mitochondria have been identified as one of the central components that mediate programmed necrosis. For example, it was found that mitochondria are playing an important role in TNF-mediated necroptosis as elimination of the mitochondrial proteins Bax and Bak or overexpression of Bcl-XL protects cells from necroptosis (Irrinki et al., 2011). Independently, analyses have shown an involvement of Drp1 in caspase-independent programmed necrosis. Translocation of Drp1 from the cytosol to mitochondria promotes loss of mitochondrial transmembrane potential, generation of ROS, drop of cellular ATP-levels and facilitates cell death (Bras et al., 2007). Moreover, in some cell systems, ROS represent another component of programmed necrosis that potentially leads to cell death by oxidizing various downstream proteins. Although conflicting reports have been published for necroptosis, it is believed that ROS are oxidizing mitogen-activated protein kinases (MAPKs), which leads to upregulation of the JNK signaling pathway and subsequently, cell death (Christofferson and Yuan, 2010a). Oxidative stress and mitochondrial dysfunction are known to contribute to necroptosis and have been implicated in stroke as well as in Alzheimer’s, Huntington’s and Parkinson’s diseases (Vandenabeele et al., 2010, Yuan and Kroemer, 2010). Therefore, a crosstalk between mitochondria and protein quality control during necroptosis has been implicated (Figure 5).

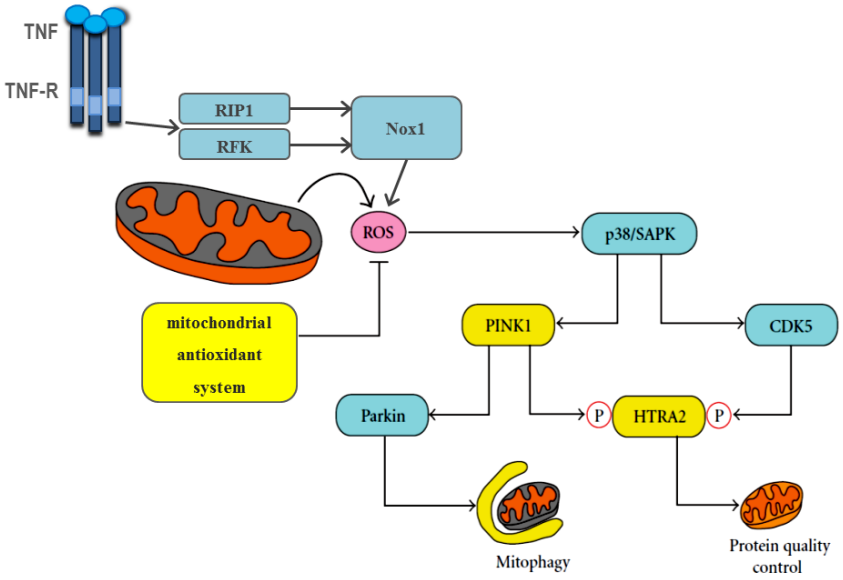

Figure 5. Putative crosstalk between death receptor signaling, integrity of mitochondria and the proteasomal system. The plasma membrane-associated NADPH oxidase 1 (Nox1) forms a complex with RIP1 and is subsequently coupled by riboflavin kinase (RFK) to TNF-R1 to regulate ROS production at the plasma membrane (Moquin and Chan, 2010). Independently, an increased production of ROS by the mitochondria likewise contributes to activation of p38/SAPK (p38/MAPK9) protein kinases. This results in activation of the downstream effectors PINK1 and CDK5 which regulate the proteolytic activity of mitochondrial HtrA2/Omi. The proteolytic activity of this serine protease contributes to the suppression of mitochondrial damage by enhancing protein quality control. Moreover, PINK1 recruits cytosolic Parkin (PARK2, parkinson protein 2, an E3 ubiquitin protein ligase) to damaged mitochondria, in order to remove them by mitophagy. Mitochondrial antioxidant systems such as superoxide dismutase suppress the production of ROS and can therefore negatively regulate necrosis and block signaling from p38 to either PINK1 or CDK5. Yellow: mitochondrial proteins; cyan: cytosolic proteins. Modified after: (Desideri and Martins, 2012).

Additionally, a role of the mitochondrial protein cyclophilin D (CypD) has been proposed for the MOMP event during programmed necrosis, as inhibition of CypD protects mice form ischemic injury (Duprez et al., 2009). Likewise, the mitochondrial serine protease HtrA2/Omi can be released form the intermembrane space of mitochondria which results in cleavage of IAPs or triggers IAP-independent and programmed necrosis (Suzuki et al., 2001). A role of HtrA2/Omi in caspase-independent PCD has been confirmed for virus-infected cells (McCormick et al., 2008). Moreover, the proteolytic activity of HtrA2/Omi has been shown to mediate damage in response to cerebral and cardiac ischemia/reperfusion (Bhuiyan and Fukunaga, 2008, Su et al., 2009), implicating a possible role in programmed necrosis.

Independently, RIP3 was found to accelerate mitochondrial ROS production and mitochondrial metabolism through the activation of glycogen phosphorylase (PYGL), glutamate-ammonia ligase (GLUL), and glutamate dehydrogenase 1 (GLUD1) during necroptosis (Vandenabeele et al., 2010, Wu et al., 2012). The control of protein quality and

protein degradation during cell death is regulated and executed by the ubiquitin proteasome system (UPS). The ubiquitin carboxy-terminal hydrolase L1 (UCH-L1) is one of the most intensively investigated enzymes playing role in cell homeostasis, cell cycle progression and transcriptional regulation. However, it remains unclear if deubiquitinating enzymes such as UCH-L1, A20 (TNFAIP3), cezanne (OTUD7B) or peptidase-21 (USP21) play a role in necroptosis (Vandenabeele et al., 2010). Recently, the RIP1-deubiquitinating enzyme A20 and the linear ubiquitin chain assembly complex (LUBAC) were identified as negative regulators of necroptosis, but in contrast to downregulation of the deubiquitinase CYLD (Figure 3), A20 silencing elevated sensibility of the cells rather than protecting from necroptosis (Vanlangenakker et al., 2011a).

Additionally, a crosstalk between autophagy and programmed necrosis may exist as it was demonstrated that autophagic signaling mediates RIP1-dependent necroptosis in T cells deficient for caspase-8 or FADD (Bell et al., 2008).

1.2.4 (Patho)physiologic role of components of programmed necrosis

The pathophysiologic role of necroptosis has been elucidated in cerebral ischemia, myocardial infarction, pancreatitis, lymphoid homeostasis and the loss of photoreceptor cells as well as intestinal epithelial cells (Vanlangenakker et al., 2012). Infection of cells with viruses and necroptosis promotes the release of intracellular damage/(danger)-associated molecular patterns (DAMPs), which act as endogenous adjuvants to boost the innate immune response (Declercq et al., 2009, Kaczmarek et al., 2013). The chromatin protein high-mobility group B1 (HMGB1) and cytosolic peptidylprolyl cis–trans isomerase cyclophilin A (CypA) are released during necroptotic cell death after early permeabilization of the plasma membrane. Thus, these molecules may be used as biomarkers for early recognition of necroptosis or be recognized by immune system as DAMPs during inflammation processes (Christofferson and Yuan, 2010a).

Detailed analyses of the signaling molecules involved in necroptosis demonstrated that in addition to their role in cell death, they mediate essential functions in embryogenesis, cell cycle, cell migration, cell adhesion, response to pathogens and inflammation (Green et al., 2011b) (Table 1).

Table 1. Pathophysiologic role of various components of necroptosis

Deletion	Phenotype	Implications for PCD	Publication
Caspase-8	defects in yolk sac vascularization and embryonic lethality at day 10.5 past embryogenesis	do not display apoptotic cell death, unregulated necroptosis	(Oberst et al., 2011)
FADD		do not display apoptotic cell death, unregulated necroptosis	(Yeh et al., 1998)
$cFLIP_L$		impaired heart development, highly sensitive to TNF- and Fas-induced apoptosis, rapidly activated caspases	(Yeh et al., 2000)
RIP1	die at day 1-3 after birth	extensive apoptosis in both the lymphoid and adipose tissue; highly sensitive to TNF-induced cell death; do not activate NF-κB	(Kelliher et al., 1998)
RIP3	develop normally	impairment of virus-induced necroptosis	(Newton et al., 2004)
FADD/RIP1	develop normally	defects in B cell activation-induced proliferation	(Zhang et al., 2011)
Caspase-8/RIP3	develop normally	resistant to lethal hepatic injury induced by anti-CD95 antibody, lymphoaccumulative disease – accumulation of $B220^+$, $CD3^+$, $CD4^-$, $CD8^-$T lymphocytes with increasing age	(Kaiser et al., 2011, Oberst et al., 2011, Dillon et al., 2012)
FADD/RIP3	develop normally	resistant to lethal hepatic injury by anti-CD95, lymphoaccumulative disease antibody, defect in activation-induced proliferation of T or B cells	(Dillon et al., 2012)
$cFLIP_L$/RIP3	defects in yolk sac vascularization and embryonic lethality at day 10.5 past embryogenesis	uncontrolled activation of caspase-8, much apoptosis	
FADD/$cFLIP_L$/ RIP3	develop normally	no abnormalities in activation-induced proliferation and activation of NF-κB	

Genetic studies of knockout mice had revealed that during development, FADD, caspase-8, and $cFLIP_L$ counteract RIP1- and RIP3-dependent necroptosis (Vanlangenakker et al., 2012). Moreover, analyses of mice deficient for caspase-8, FADD or RIP3 had shown that many aspects of atopic dermatitis, T cell homeostasis, alteration in response to TLR3 and TLR4 agonists and signaling through TIR domain-containing adaptor protein inducing IFNβ (TRIF) and inflammatory abnormalities are likely to be the consequence of unrestricted necroptosis (Mocarski et al., 2012). For example, analyses of patients with Crohn's disease or ulcerative colitis confirmed that $cFLIP_L$ and $cFLIP_S$ are upregulated in comparison to normal gut, where $cFLIP_S$ is rapidly degraded by the proteasomal pathway. Similarly, ablation of caspase-8 in keratinocytes leads to severe skin inflammation, which is mediated constitutively through the IFN regulatory factor 3 (IFR3) activation pathway

(Kovalenko et al., 2009). Subsequently, epidermis-specific deletion of FADD in mice causes skin inflammation, which was identified as TNF-, CYLD- and RIP1-RIP3-dependent (Bonnet et al., 2011). Importantly, necroptosis may lead to release of necrotic DAMPs which can trigger inflammation by activating pattern recognition receptors (PRRs), including Toll-like receptors (TLRs), NOD-like sensors, and RIG-I-like receptors (Declercq et al., 2011). Thus, many inflammatory diseases may result from activation of necroptosis (Günther et al., 2012) and inhibiting necroptosis may limit extensive tissue damage and inflammatory syndromes (Silke and Strasser, 2013).

Besides a developmental and pro-inflammatory role of necroptosis in mice, an additional role in tumorigenesis has been implicated through an involvement of the tumor suppressors CYLD and EDD1 (embryo-defective-development 1 alias UBR5, ubiquitin protein ligase E3 component n-recognin 5) and several Ras-related proteins, e.g. RAB25 (Ras-related protein Rab-25), RASA4 (RAS p21 protein activator 4) and RASSF7/8 (Ras association (RalGDS/AF-6) domain family (N-terminal) member 7/member 8) in the regulation of necroptosis (Hitomi et al., 2008). Recent studies have shown that inhibition of caspases activates EDD to mediate (independently from the NF-κB pathway) JNK signaling, promote transcription of TNF and thus affecting the execution of TNF-mediated programmed necrosis (Christofferson et al., 2012). Similarly, RIP1 may activate Akt kinases that control autocrine production of TNF, activate JNK kinases and target the mammalian target of rapamycin complex 1 (mTORC1), thereby contributing to the execution of programmed necrosis (McNamara et al., 2013).

1.3 Other types of programmed necrosis

Necrosis has been first associated with accidental cell death in damaged tissue until it was found that programmed necrotic death in specific contexts is orchestrated by many different signaling molecules (Mocarski et al., 2012). Independent from necroptosis induced by death receptors, programmed necrosis is mostly induced by non-specific trauma, injury, calcium overload, oxidative-stress, radiation, UV light or DNA damage factors, e.g. by methylating agents such as MNNG (1-methyl-3-nitro-1-nitrosoguanidine) or MMS (methyl methanesulfonate). Programmed necrosis induced by DNA damage is executed by the hyperactivation of poly(ADP-ribose) polymerase 1 (PARP1) (Figure 6), which depletes the intracellular pool of NAD^+ and ATP and leads to Ca^{2+}-dependent calpain activation. In this type of cell death, the BH3-only protein, Bid is cleaved by

calpains to its truncated form tBid (Cabon et al., 2012). Redistribution of tBid from the cytosol into mitochondria regulates activation of the pro-apoptotic protein Bax, which propagates cleavage and release of AIF from mitochondria (Figure 6). After redistribution of truncated AIF (tAIF) to the nucleus, tAIF forms a complex with histone H2AX (γH2AX) and CypA, resulting in chromatinolysis and finally programmed necrotic death of the cell (Baritaud et al., 2012).

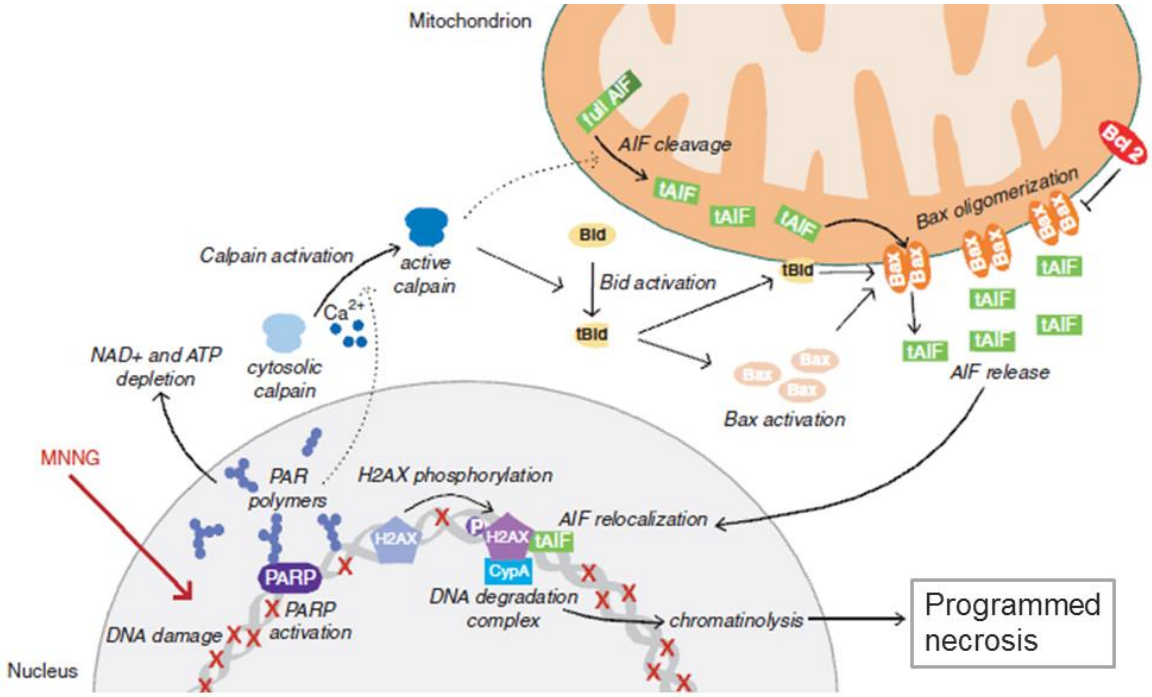

Figure 6. Model of PARP1/AIF-mediated programmed necrosis. MNNG-induced DNA damage activates PARP1, leading to formation of PAR polymers and rapid NAD^+ and ATP depletion. Subsequently, calpains cleave Bid into tBid, which translocates into mitochondria. tBid facilitates Bax oligomerization followed by release of tAIF from mitochondria to the cytosol and nucleus. The anti-apoptotic protein Bcl-2 can prevent this release. Upon transfer to the nucleus, tAIF associates with CypA and γH2AX to generate a complex that promotes chromatinolysis and programmed necrosis (Cabon et al., 2012).

It has been reported that in some cases, programmed necrosis both triggered by the kinases RIP1/RIP3 and by environmental stress factors is dependent on PARP1 activation (Jouan-Lanhouet et al., 2012). Moreover, PARP1 and its activation has been described as the main causative factor during necroptosis mediated by TNF-R1 (Los et al., 2002). Although recent analyses have identified some of the executing factors, e.g. Bcl-2, PARP1, RIP1 and RIP3 as mediators of both necroptosis and programmed necrosis (Vanlangenakker et al., 2012), it is still unknown if death receptor-induced necroptosis and PARP-1-mediated programmed necrosis act through entirely distinct molecular mechanisms or via partially or completely connected signaling cascades. Of note, investigation of programmed necrosis and its further comparison to necroptosis is

especially of interest because many studies have shown a crucial role of programmed necrotic cell death during inflammatory processes, such as ischemia reperfusion damage, hemorrhagic shock, septic shock, lung inflammation, diabetes mellitus and chronic inflammatory disorders such as arthritis and inflammatory bowel diseases (ulcerative colitis and Crohn's disease), allergic encephalomyelitis, multiple sclerosis, uveitis, periodontal inflammation, meningitis, asthma and possibly in various forms of dermal inflammation (Aguilar-Quesada et al., 2007).

In invertebrates, programmed necrosis is involving epithelial sodium channels (ENaCs)/degenerins. Mutations in the degenerins MEC-4, MEC-10, UNC-8, UNC-105 or DEG-1 cause swelling, membrane folding, membrane whorls, and formation of vacuoles that resemble those found in excitotoxic cell death after ischemia, hypoxia, or epilepsy (Kellenberger and Schild, 2002). Degenerins regulate sodium and calcium flux in the cytoplasm. Imbalance in calcium and sodium activates cytoplasmic calpains, which, in concert with the lysosomal compartment, cause the breakdown of the cell and rupturing of the plasma membrane. As an additional mechanism, kinesin-mediated endocytosis facilitates necrotic cell death in concert with autophagy and lysosomal proteolytic mechanisms (Troulinaki and Tavernarakis, 2012).

1.4 Autophagy plays a role in cell death and survival

Autophagy is a self-protective mechanism involved in innate immune responses, cellular homeostasis and protein quality control mechanisms during age-related processes (Walsh and Edinger, 2010, Green et al., 2011a). However, it has also been shown to mediate caspase-independent cell death during the development of *D. melanogaster* or favor cell death in some cancer cells lacking Bax, Bak or caspases (Galluzzi et al., 2012). Autophagy is triggered to sustain the cellular metabolism under conditions of nutrient-deprivation. During autophagy, proteins or whole organelles are sequestrated in autophagosome vesicles and degraded in lysosomes to prevent deprivation of nutrients or accumulation of misfolded proteins. The known molecular mechanisms of autophagy are summarized in Figure 7.

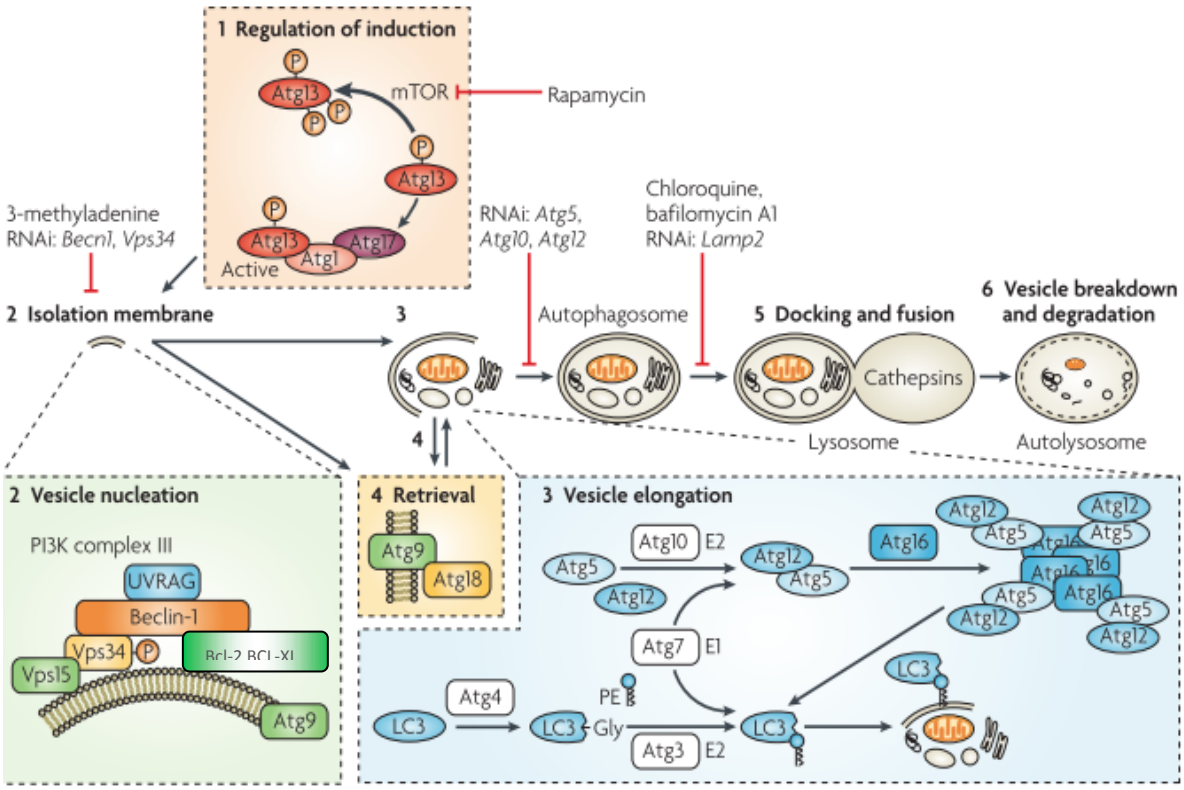

Figure 7. The process of autophagy. Autophagy starts with the sequestration of cytoplasmic material such as cytosol and/or organelles by the phagophore, which is formed by double-membraned vesicles (autophagosomes, also called autophagic vacuoles). The initiation step (1) involves the repression of the mTOR Ser/Thr kinase, which normally inhibits autophagy by phosphorylating autophagy protein-13 (Atg13), preventing the association of Atg13 with the kinases Atg1 and Atg17 in an autophagy-inducing complex. For the next step of vesicle nucleation (2), the activation of mammalian Vps34 (a class III phosphatidylinositol 3-kinase (PI3K), generating phosphatidylinositol-3-phosphate (PtdIns3P)) is required. Vps34 activation depends on the formation of a multiprotein complex with Beclin-1, UVRAG (UV irradiation resistance-associated tumour suppressor gene) and the myristylated kinase Vps15. Bcl-2 and Bcl-XL are regulators of Beclin-1. The following vesicle elongation step (3) requires ubiquitin-like conjugation systems, which conjugate Atg12 (activated by Atg7 and then transferred to Atg10) to Atg5, allowing to bind to Atg16. The complex Atg12-Atg5-Atg16 recruits LC3 bound to phosphatidylethanolamine (PE) by the action of Atg4, Atg7 and Atg3. PE-conjugation leads to the conversion of the soluble form of LC3 (LC3-I) to the autophagic-vesicle-associated form (LC3-II). The last step is the retrieval (4) in which the Atg9 and Atg18 complex participates. After their formation, autophagosomes undergo fusion (5) with lysosomes to create autolysosomes (6). In the autolysosomes, the inner membrane as well as the luminal content of the autophagic vacuoles is degraded by lysosomal enzymes. There are many inhibitors or genes whose downregulation by RNA interference (RNAi) is capable of disrupting distinct steps of autophagy (red indicators). Lamp2: lysosome-associated membrane glycoprotein-2 (Maiuri et al., 2007).

Some indications exist for a crosstalk between autophagy and necroptosis, e.g. a role of ceramide was described for both necroptosis and autophagy after upregulation of Beclin-1 and PKB (Codogno and Meijer, 2005), implicating autophagy as a potential regulator of programmed necrosis.

2. Death receptors and their ligands - functions and mechanisms of action

2.1 TNF and its two receptors TNF-R1 and TNF-R2

Tumor necrosis factor (TNF), also known as cachectin, DIF (differentiation inducing factor), TNFA or TNFSF2 is a type II transmembrane protein of 26 kDa molecular mass, which is processed into the 17-kDa soluble, biologically active form of TNF by the converting enzyme TACE (also called ADAM17). Both the membrane-bound and the soluble form of TNF interact as trimeric proteins with their receptors TNF-R1 (CD120a, TNFRβ, TNF-R55 or p60, TNFRSFR1) or TNF-R2 (CD120b, TNFRα, p75TNFR, p80 or TNFRSF1B) (Cabal-Hierro and Lazo, 2012). The soluble form of TNF selectively activates TNF-R1, however the membrane bound TNF is able to activate both TNF-R1 and TNF-R2. The expression profile of both receptors is distinct. Whereas TNF-R1 is present on the surface of all cell types except for red blood cells, TNF-R2 is found only on oligodendrocytes, astrocytes, T cells, cardiomyocytes, thymocytes, endothelial cells and in human mesenchymal stem cells (Faustman and Davis, 2010). Both TNF-R1 and TNF-R2 contain an extracellular pre-ligand-binding assembly domain (PLAD) which assures trimerization of the receptors after TNF binding (MacEwan, 2002). TNF-R1 contains a cytoplasmic DD motif which is critical for further signaling and association with the adaptor protein TRADD. This facilitates the binding of further adaptor proteins such as TRAF2, cIAP-1, cIAP-2 and RIP1 which together form complex I responsible for triggering survival pathways (Figure 1). Alternatively, activation of TNF-R1 may be followed by deubiquitination of RIP1 by CYLD, recruitment of RIP3, TRADD, FADD and procaspase-8 into the cytosolic complex II, also known as DISC. When caspase-8 is deleted or inhibited, the complex may be rearranged and activate necroptosis (Figure 1). The DD of TNF-R 1 and the adapter proteins TRADD and FADD are responsible for activation of A-SMase (Adam-Klages et al., 1998) through its caspase-dependent cleavage during apoptosis (Edelmann et al., 2011).

TNF-R1 also contains an intracellular sequence called N-SMase activation domain (NSD) (Adam et al., 1996), which binds the adapter molecule FAN (factor associated with N-SMase activation) (Adam-Klages et al., 1996). Together with the molecules RACK1 (receptor of activated protein kinase C 1) and EED (embryonic ectoderm development), FAN is responsible for the activation of neutral sphingomyelinase (N-SMase) (Philipp et

al., 2010). This is followed by production of ceramide, a crucial mediator in the signaling pathways of TNF (Adam-Klages et al., 1996, Adam-Klages et al., 1998) (Figure 8).

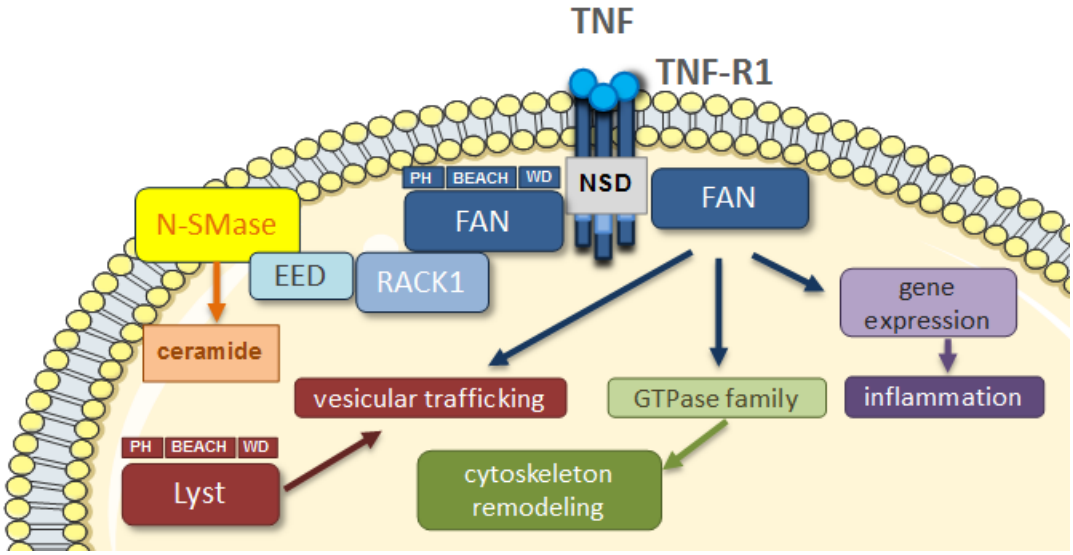

Figure 8. Role of FAN in TNF-R1 signaling pathways. The FAN carboxy-terminal portion possesses WD repeats, which constitutively interact with the N-SMase activation domain (NSD) of TNF-R1 and with the adaptor protein RACK1. By binding to EED, RACK1 recruit N-SMase into the vicinity of TNF-R1, leading to activation of neutral sphingomyelinase (N-SMase). Independently, FAN is required for activation of members of the GTPase family, including cdc42 (cell division control protein 42), Rac and Rho proteins and, in consequence, for cytoskeleton remodeling, e.g. reorganization of filamentous actin. In addition, FAN modulates proinflammatory gene expression, e.g. expression of IL-6. Furthermore, FAN-deficient fibroblasts displayed bigger lysosomes (Möhlig et al., 2007), therefore a role of FAN in vesicular trafficking to and/or from the endolysosomal compartment has been suggested. Lyst (lysosomal trafficking regulator) is a protein homologous to FAN that also possess PH, BEACH and WD repeat domains. Lyst modulates vesicular transport and its deficiency likewise leads to accumulation of giant intracellular vesicles. Modified after: (Montfort et al., 2010).

FAN belongs to the WD repeat protein family, which is involved in signal transduction for motility and migration of cells, e.g. during the process of inflammation (Figure 8). Moreover, FAN possess BEACH and PH domains and therefore belongs to the family of proteins that acts as scaffolding proteins and facilitate membrane events, including both fission and fusion, determined by their binding partners (Cullinane et al., 2013). Similar to FAN, the cytosolic protein Lyst possess a homologous BEACH domain and PH and WD repeat domains. Moreover, Lyst is involved in vesicular trafficking (Figure 8) (Burgess et al., 2009). The Lyst protein is inactivated in patients affected by Chediak-Higashi syndrome. These patients display hypopigmentation and immunological and neurological disorders caused by accumulation of giant intracellular vesicles as a consequence of vesicular transport alterations between the endolysosomal compartments (Montfort et al.,

2010). However, the exact function of proteins that possess PH, BEACH and WD repeat domains in the above processes remains to be elucidated.

TNF-R2 does not possess a DD, but interacts via its cytoplasmic domain with the main adaptor molecule TRAF2, which in turn recruits TRAF1, TRAF3, cIAP-1 and cIAP-2. This complex induces the activation of the transcription factors AP-1 (activator protein 1) and NF-κB (Cabal-Hierro and Lazo, 2012). TNF-R2 is believed to possess a greater affinity to TNF and acts in "ligand-passing" mechanisms, by which TNF-R2 can transmit the ligand to the TNF-R1 complex (MacEwan, 2002). Although normally, TNF-R2 activation triggers pro-survival pathways such as proliferation of cytotoxic T cells, thymocytes, dendrocyte progenitors, or neuron survival, TNF-R2 is able to induce differentiation, cytokine production and even apoptosis. Importantly, signaling through TNF-R2 may be protective in several disorders, including autoimmune diseases, heart disease, demyelinating and neurodegenerative disorders and infectious diseases (Faustman and Davis, 2010).

2.2 TRAIL receptors and their ligands

Tumor necrosis factor (TNF)-related apoptosis-inducing ligand (TRAIL), known alternatively as APO2-L, TL2 or TNFSR10 is a type II transmembrane protein of the tumor necrosis factor family. Similar to TNF, the C-terminal conserved extracellular domain can be proteolytically cleaved from the cell surface (Shirley et al., 2011). In humans, the homotrimeric form of TRAIL binds to the death receptors TRAIL-R1 (DR4) and TRAIL-R2 (DR5) which are able to transduce cell death signals. TRAIL-R1 is expressed in very low levels in most human tissues but TRAIL-R2 is overall equally distributed (Abdulghani and El-Deiry, 2010). TRAIL also binds to the decoy receptors TRAIL-R3 (DcR1) and TRAIL-R4 (DcR2), which lack the functional DD and to osteoprotegerin, which binds TRAIL at low affinity (Hall and Cleveland, 2007). TRAIL-R3 lacks an intracellular domain, but harbors a glycosylphosphatidylinositol (GPI) anchor which drives its location to lipid rafts and competes for TRAIL binding in order to prevent DISC formation. TRAIL-R4 contains an intracellular domain with a truncated DD and inhibits formation of the DISC through interference with the recruitment of FADD and activation of caspase-8 within the complex (Shirley et al., 2011).

TRAIL is able to induce apoptosis in variety of tumor cells while leaving untransformed cells mostly unaffected. Therefore, targeting TRAIL receptors, for example with the human agonistic TRAIL antibodies Mapatumumab and Lexatumumab was shown to be a strategy for selective cancer therapy (Belyanskaya et al., 2007).

A crosstalk exists between ceramide and TRAIL-mediated signals in cell death. It has been suggested that the resistance of various cancer cells to TRAIL is a consequence of ceramide depletion. Consequently, an increase of ceramide was shown to downregulate $cFLIP_L$ and to sensitize cancer cells to TRAIL-mediated apoptosis. Importantly, exogenous ceramide was not able to sensitize cells for cell death, but rather ceramide generated after stimulation of death receptors served as an enhancer or amplifier of cell death signaling (Voelkel-Johnson et al., 2005). Other mechanisms of TRAIL-resistance are associated with activation of NF-κB by TRAIL, followed by activation of the antiapoptotic regulators Mcl-1 (myeloid cell leukemia sequence 1, Bcl-2 related) and cIAP-2. Moreover, a TRAIL/ NF-κB dependent decline in regulators of the intrinsic cell death pathway such as Bax or the BH3-protein Puma (p53 up-regulated modulator of apoptosis, Bcl-2-binding component 3), directs cells into the prosurvival pathway, accounting for TRAIL resistance (Hall and Cleveland, 2007).

3. Role and function of ceramide

3.1 Metabolism of ceramide and its implications

One of the major components of cellular membranes are sphingolipids (SPLs). One of these SPLs, ceramide (Cer, N-acylsphingosine) serves as a precursor for more complex SPLs such as phosphatidylcholine, sphingomyelin (SM), or glycosphingolipids, e.g. glucosylceramide, cerebrosides or gangliosides (Arana et al., 2010). Ceramide, a polar and hydrophobic membrane lipid, is an N-acylsphingosine usually coupled to monosaturated or saturated fatty acids in a length of 2-28 carbon atoms (Stancevic and Kolesnick, 2010). The fatty acyl chains containing 16-24 carbon atoms are most commonly found in mammalian ceramides. Synthetic, water-soluble, short chain analogs such as N-acetylsphingosine (C2-ceramide), N-hexanoylsphingosine (C6-ceramide) or N-octanoylsphingosine (C8-ceramide) have been used in anti-cancer therapy as they can induce apoptosis (Figure 9) (Arana et al., 2010).

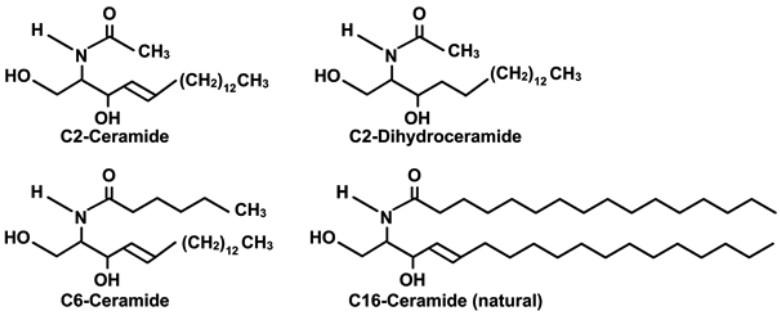

Figure 9. Structures of synthetic and natural ceramide molecules. The synthetic ceramide analogs C2-ceramide, C6-ceramide, and biologically inactive C2-dihydroceramide, as well as the natural C16-ceramide are depicted (Samadi, 2007).

Ceramide, which is required for many different biological processes, is either produced *de novo*, generated from sphingosine by isoenzymes of ceramide synthase (Cer-synthase), or from sphingomyelin by sphingomyelin phosphocholine diesterases (SMPDs, or SMases) (Figure 10). Degradation products of Cer such as sphingosine (Sph) or phosphorylated sphingosine 1-phosphate (S1P) are playing important roles in cell signaling (Figure 10). The balance between ceramide and sphingosine-1-phosphate, referred to as the "ceramide/ sphingosine-1-phosphate rheostat", has been suggested to regulate the balance between cell death and growth and thus to be important for living organisms (Kornhuber et al., 2010). In addition, ceramide-1-phosphate (Cer-1-P), another key regulator of cellular homeostasis which is generated by ceramide kinase (Figure 10) binds directly to targets such as cPLA2 and protein phosphatase 1/2A to regulate inflammatory responses (Chalfant and Spiegel, 2005).

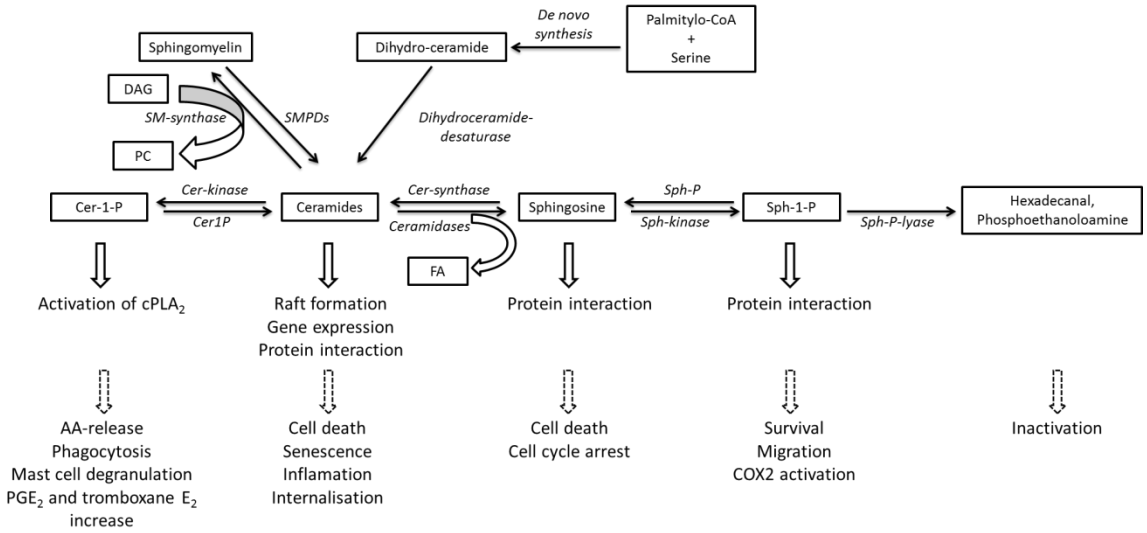

Figure 10. Sphingolipid metabolism and interactions. *De novo* synthesis of ceramide starts with condensation of palmitoyl-CoA with serine yielding a 3-ketosphinganine, which is immediately reduced and acylated by addition of a fatty acid chain by dihydro-ceramide synthase (CerS) to form dihydro-ceramide. Desaturation of the trans-4,5 double bound in dihydro-ceramide yields the final ceramide molecule, which

can be further functionalized by addition of carbohydrates or phosphocholine. Sphingomyelin which is localized in the outer leaflet of the cell membrane can serve as another pool of ceramide through the removal of the polar head group by different classes of sphingomyelin phosphocholine diesterases *alias* sphingomyelinases (SMPDs). Ceramide is degraded by acid ceramidases through hydrolysis of *N*-acyl fatty acids, generating sphingosine which can be further phosphorylated by sphingosine-kinase (Sph-kinase) forming sphingosine-1-phosphate (Sph-1-P). Sph-1-P is known to play an antagonistic role to ceramide and to regulate cell death, cellular differentiation, proliferation and inflammatory responses through activation of cyclooxygenase-2. Sph-1-P is degraded irreversibly by sphingosine-1-phosphate-lyase (Sph-P-lyase). The pool of sphingosine and ceramide can be restored by the activities of sphingosine-1-phosphatase (Sph-P) and ceramide synthase (Cer-synthase), respectively. The main metabolite of ceramide – ceramide-1-phosphate (Cer-1-P) is generated by ceramide-kinase (Cer-kinase). Cer1P: ceramide-1-phosphatase; DAG: diacylglycerol; FA: fatty acid; PC: phosphocholine; PGE_2: prostaglandin E2; SM: sphingomyelin, AA: amino acid; COX2: cyt *c* oxidase subunit II; PGE_2: prostaglandin E2; (Chalfant and Spiegel, 2005, Deigner et al., 2007).

Besides ceramide synthase, one of the major sources of ceramide is the catabolic pathway of sphingomyelin degradation by SMPDs to form phosphocholine and ceramide. While the SMDPs A-SMase and N-SMase are involved in signal transduction processes (Chapter 3.2 and 3.3), alkaline SMase (also named NPP7, nucleotidepyro-phosphatase/phosphodiesterase) is mainly required for digestion processes of the dietary SM in the intestine (Arana et al., 2010). Importantly, the generation of ceramide is conducted mainly through the activity of A-SMase and in cells lacking this enzyme, this deficiency cannot be compensated by N-SMase (Qin and Dawson, 2012). Concerning the cellular localization, compartmentalization and topology of ceramide production or degradation, these determine ceramide function and bioavailability. Of note, synthesis of ceramide in the ER and transport through lipid membranes to the Golgi apparatus, where glycosphingolipids and sphingomyelin are synthesized, is conducted in a non-vesicular manner by ceramide transfer protein (CERT). Similarly, generation of ceramide by SMases in the plasma membrane or in lysosomes exerts its different functions such as clustering of receptors on the cell surface or signaling for necroptosis in lysosomes (Strelow et al., 2000, Thon et al., 2005, Thon et al., 2006, Arana et al., 2010).

Ceramide has been shown to play important roles in signaling of cell death or survival by promoting cell differentiation, growth, migration, angiogenesis and by regulating autophagy (Arana et al., 2010, Jenkins et al., 2011a). Ceramide acts as a potent secondary messenger that can mediate apoptosis through modulation of the plasma membrane exoplasmic leaflet and by forming signaling domains called ceramide-rich platforms or raft structures (Stancevic and Kolesnick, 2010). Such domains are involved in the clustering of receptor molecules and thereby amplify signals for apoptosis (Schenck et al., 2007). This has been described for activation and execution of apoptosis by CD95 (Wagenknecht et al., 2001) or for TNF-R1 in dopaminergic neurons (Martinez et al., 2012). In addition,

ceramide represents a key mediator of necroptosis induced by TNF and TRAIL (Thon et al., 2005, Thon et al., 2006). Moreover, many chemotherapeutic agents activate A-SMase and mediate cell death via ceramide formation (Henry et al., 2011). Mechanistically, ceramide may contribute to apoptosis or programmed necrosis by forming channels in mitochondria, leading to increased permeability of mitochondrial outer membranes, followed by release of cytochrome *c* and other mitochondrial proteins such as AIF, HtrA2/Omi that promote PCD (Stancevic and Kolesnick, 2010). Ceramide was found to function in intracellular signaling processes through segregation of intraluminal vesicles from multivesicular endosomes. Therefore, ceramide is required for direction of cellular components, degradation or extracellular release (Trajkovic et al., 2008). Moreover, ceramide can undergo ‘‘flip-flop” diffusion leading to changes in membrane permeability (Stancevic and Kolesnick, 2010). Independent from its effects on membrane permeability, ceramide interacts with specific proteins which colocalize with ceramide and which mediate ceramide dependent signals such as cathepsin D (Heinrich et al., 1999), JNKs (Reyes et al., 1996), kinase suppressor of Ras (KSR), ceramide-activated protein serine–threonine phosphatases (CAPP) and protein kinase C (PKC) isoforms (Henry et al., 2011). Furthermore, ceramide targets phospholipase D (PLD), which is a key regulatory enzyme responsible for generation of the potent mitogenic agent phosphatidic acid (PA) (Arana et al., 2010). PA in turn is critical for cytoskeletal reorganization, stability and activity of mTOR complexes. Ceramide production has been described in response to signals generated by CD95, TNF, interleukin-1 (IL-1), interferon-γ (INF-γ), oxidative stress, ionizing and ultraviolet radiation as well as heat shock. In general, ceramide appears to regulate inflammatory and stress responses. Therefore, changes in intracellular ceramide levels influence the production of cytokines such as IL-1β or IL-6 (Laulederkind et al., 1995). In agreement, higher levels of TNF, defective production of INF-γ and a lack of IL-1β were reported in A-SMase deficient mice. Independently, ceramide was associated with inflammation linked to increased insulin resistance, possibly as a result of its inhibition of the PI3K/Akt signaling pathway (Horres and Hannun, 2012). The inhibition of Akt kinases by ceramide lead to inactivation of anabolic pathways, e.g. glycogen and protein synthesis, prosurvival enzymes and activation of autophagic enzymes (Bikman and Summers, 2011). Ceramide inhibits Akt through direct targeting of protein phosphatase A2 (PPA2) (Dobrowsky et al., 1993), an enzyme that promotes dephosphorylation of Akt or through prevention of Akt translocation via PKCξ (Bikman and Summers, 2011). Regulation of cell membrane structure by ceramide and its participation in the inflammatory response may

affect various diseases followed by chronic bacterial infections, e.g. cystic fibrosis (Wojewodka et al., 2011). Studies in rodent models revealed that ceramide is involved in the pathogenesis of diabetes, cardiomyopathy, insulin resistance, atherosclerosis, and hepatic steatosis. A disturbed turnover of the ceramide metabolite glucosylceramide lead to Gaucher disease, a disorder characterized by a proinflammatory and insulin-resistant phenotype (Bikman and Summers, 2011). Recent studies have demonstrated that high levels of ceramide in serum are associated with memory impairment and hippocampal volume loss and increased risk of Alzheimer disease (Mielke et al., 2012).

3.2 Biological functions of A-SMases

Acid sphingomyelinase (A-SMase, *Smpd1*, sphingomyelin phosphodiesterase 1) is a soluble hydrolase that generates ceramide and phosphocholine by cleavage of a phosphodiester bond of sphingomyelin at an acidic pH optimum. A-SMase has been observed in caveolae, i.e. SM-enriched microdomains of the plasma membrane (Reynolds et al., 2004). Recently, it was reported that for many signaling processes, e.g. clustering of membrane receptors, A-SMase is translocated to the plasma membrane (Perrotta et al., 2010). A-SMase is activated through various stimuli such as LPS, UV-light, heat, oxidative stress, chemotherapeutic agents, ionizing radiation, accumulation of Cu^{2+} and infection with pathogens such as *Neisseria gonorrhoeae*, *Pseudomonas aeruginosa*, *Staphylococcus aureus*, rhinovirus, Sindbis virus, disruption of integrin signaling, and also by signals of the TNF-receptor superfamily members Fas, CD40, TRAIL-R2, and TNF-R1 (Stancevic and Kolesnick, 2010). Mechanistically, it has been shown that TNF-R1 can activate A-SMase through proteolytic cleavage by caspase-7 (Edelmann et al., 2011). Alternatively, phosphorylation at position Ser 508 (S508) has been reported to cause activation of A-SMase (Zeidan and Hannun, 2007). Third, it has been described that TRAIL can activate A-SMase via a redox mechanism (Dumitru and Gulbins, 2006). Activation of A-SMase has been suggested to play an important role in several pathophysiologic conditions such as atherosclerosis, cancer, diabetes, Alzheimers's disease and cystic fibrosis (Canals et al., 2011). A-SMase deficient mice show a progressive neurodegenerative course; cerebella atrophy, loss of Purkinje cells; foam cells in reticuloendothelial organs and death at the age of 8 months (Horinouchi et al., 1995).

The mechanism of A-SMase activation was described to be dependent on the t-SNARE (target membrane N-ethylmaleimide-sensitive factor attachment protein receptor)

protein syntaxin 4 that mediates translocation of A-SMase from intracellular; cathepsin D-containing compartments to the plasma membrane in an exocytic pathway. After cathepsin D is released into the extracellular milieu, A-SMase is exposed at the cell surface, where it hydrolyzes sphingomyelin to ceramide, inducing death receptor clustering and leading to caspase activation, Akt pathway inhibition, and cell death (Perrotta et al., 2010). Moreover, upregulation of A-SMase expression (e.g. in response to cigarette smoke) following formation of lipid rafts accelerated the production of the TNF-induced pro-inflammatory cytokine IL-6 (Kumagai et al., 2012). Furthermore, A-SMase has been implicated in several diseases such as allograft transplant rejection, asthma, rheumatoid arthritis, atherosclerosis and endometriosis (Jenkins et al., 2011a).

A single A-SMase mRNA gives rise to at least three different splice variants, although only one transcript encodes a functional enzyme. Transcriptional upregulation of A-SMase has been reported in the differentiation of monocytes to macrophages, in senescent fibroblasts from patients with the premature aging disorder Werner syndrome, and in genetic and diet-induced mouse models of obesity (Jenkins et al., 2009). A-SMase is present as an initial 75-kDa prepro form, which is processed to the 72-kDa proform. The 72-kDa proform is cleaved within the lysosomes into the 70-kDa enzyme (Jenkins et al., 2009) and finally processed to a 52-kDa polypeptide (Jenkins et al., 2011b). After proteolytic processing, the endo-lysosomal enzyme A-SMase undergoes posttranslational modifications such as formation of disulfide bonds or glycosylation to ensure proper trafficking, protection from destruction in lysosomes and maintenance of an active conformation. Depending on differences in the oligosaccharide processing of N-glycans of a single protein precursor two, alternative, distinct trafficking forms of A-SMase are present: lysosomal acid sphingomyelinase (L-A-SMase) and secretory acid sphingomyelinase (S-A-SMase). Both forms of A-SMase are metalloenzymes containing several highly conserved Zn^{2+} binding motifs (Stancevic and Kolesnick, 2010). However, whereas the L-A-SMase is Zn^{2+}-independent, the S-A-SMase requires addition of Zn^{2+} for activity (Jenkins et al., 2011b). The L-A-SMase possesses high level of mannose-6-phosphate residues and is targeted to lysosomes mainly through the mannose-6-phosphate receptor system (Schuchman, 2010). S-SMase is trafficked through the distal Golgi pathway (Jenkins et al., 2011b) and the regulated secretion of the S-A-SMase and the generation of ceramide occur in response to inflammatory cytokines. Moreover, enhanced S-A-SMase secretion occurs with concomitant diminution of L-A-SMase activity (Jenkins et al., 2011a).

L-A-SMase mediates ceramide production in lysosomes which is associated with apoptotic signaling, such as Bax activation, mitochondrial injury and cathepsin D release into the cytosol. Various mutations in the *Smpd1* gene lead to loss or reduction of the enzymatic activity of L-A-SMase, which manifests itself in the lysosomal storage disease Niemann-Pick disease type A/B (Simonaro et al., 2006). Epigenetic methylation of *Smpd1* leads to Beckwith–Wiedemann syndrome that possesses the same symptoms as Niemann-Pick disease (Jenkins et al., 2009). While the absence of L-A-SMase activity leads to Niemann-Pick disease, in the pathophysiology of Wilson's disease, overactivation of L-A-SMase by accumulated Cu^{2+} leads to enhanced generation of ceramide and apoptosis (Schenck et al., 2007). The L-A-SMase that residues in lysosomes can be translocated to the cell surface after phosphorylation of a specific serine residue on A-SMase (S508) by PKCδ (Schuchman, 2010).

Accumulation of S-A-SMase in the acidic tumor microenvironment sensitized cells to cell death, e.g. induced by radiation. Moreover, S-A-SMase is elevated in sepsis and secreted after LPS stimulation in mice. S-A-Mase regulates retention of atherogenic lipoproteins and interact with components of extracellular matrix. Furthermore, elevated activity of S-A-SMase in serum has been reported in patients with inflammatory conditions, type II diabetes and chronic heart failure. Similarly, ceramide produced by S-A-SMase in leucocytes influences erythrocytes, leading to their destruction and to subsequent anemia (Jenkins et al., 2009).

There are several pharmacological inhibitors of A-SMase that have been used in functional studies. The most commonly used inhibitor of A-SMase is the xanthate derivative tricyclodecan-9-yl xanthate (D609) that inhibits CERT-dependent ceramide transport and was reported to inhibit A-SMase activity *in vitro* and reduce sphingomyelin synthesis *in vivo* (Perry and Ridgway, 2005). Moreover D609 was described to inhibit phospholipase C, an enzyme upstream of A-SMase, thus indirectly the TNF-dependent activation of A-SMase (Festjens et al., 2006). Furthermore, antidepressants such as desipramine or imipramine are known as inhibitors of A-SMase and were described to attenuate apoptosis, promote cell proliferation (Kornhuber et al., 2008). Recently, Roth and coworkers. demonstrated that several bisphosphonate compounds potently inhibited A-SMase (Roth et al., 2009a, Roth et al., 2009b, Roth et al., 2010). Furthermore, bisphosphonates used for osteoporosis treatment such as zoledronic acid are potent functional inhibitors of A-SMase (Canals et al., 2011).

3.3 Biological functions of N-SMase

The mammalian neutral sphingomyelinase (N-SMase, sphingomyelin phosphodiesterase, neutral membrane) hydrolyses sphingomyelin, producing phosphocholine and the bioactive lipid ceramide. N-SMase exists in three distinct forms: N-SMase1 (*Smpd2*) N-SMase2 (*Smpd3*) and N-SMase3 (*Smpd4*), all of which require Mg^{2+}/Mn^{2+} with a pH optimum in the neutral range. At the cellular level, N-SMase1 localizes to the ER and N-SMase3 to the ER and the Golgi apparatus, whereas N-SMase2 is found in the Golgi apparatus and associated with the inner leaflet of the plasma membrane (Horres and Hannun, 2012). N-SMase1 is enriched in kidneys, N-SMase2 in brain and N-SMase3 ubiquitously present in cells of all organs (Mencarelli and Martinez-Martinez, 2013). Deletion of the *Smpd3* gene encoding N-SMase2 causes profound skeletal dysplasia, suggesting that N-SMase2 plays a direct role in osteoblast development and bone formation (Stoffel et al., 2007). The sequence similarity of N-SMase3 to the other N-SMases is low, suggesting a function different from those of N-SMase1 and N-SMase2. Although all three forms of N-SMase possess *in vivo* sphingomyelin-cleaving activity, only N-SMmase1 and 2 are involved in TNF signaling pathways (Montfort et al., 2010), e.g. apoptosis, and can be inhibited by the inhibitor GW4869 (Luberto et al., 2002). Generation of ceramide by N-SMase is involved in inflammation-associated processes (Horres and Hannun, 2012). Two further inhibitors of N-SMase, 3-*O*-methyl-sphingomyeline (3-OMS) and spiroepoxide, inhibit activation of cyclooxygenase-2 (COX-2) expression (Chen et al., 2009) or abolish IL-1β induced fever, respectively (Chen et al., 2009). Moreover, N-SMase2 is plays a role in several pathophysiological disorders such as chondrodysplasia, dwarfism, Alzheimer's disease, neurodegenerative conditions and aging. Interestingly, N-SMase2 can be activated through a protease cascade involving matrix metalloproteinase-2 (MMP-2) and MMP-14 (matrix metalloproteinase-14 (membrane-inserted), MT1MMP) (Devillard et al., 2010) or through interactions with the EED-Rack-FAN-TNF-R1 complex (Philipp et al., 2010), see chapter 2.1. Since FAN has been implicated in inflammatory responses (e.g. neutrophil and macrophage migration towards wounds or bacterial infections (Boecke et al., 2012) or IL-6 production (Montfort et al., 2009)), a role of N-SMase2 in these processes appears also feasible. N-SMase2 generates ceramide which is involved in cellular responses to p53, DNA-damage, TNF (Adam et al., 1996), ischemia/reperfusion-mediated cell death in cardiomyocytes, cell death associated with JNK activation in hippocampal neurons, and cytokine-induced proliferation (Reynolds et

al., 2004). In contrast to N-SMase2, the roles of N-SMase1 and 3 have been poorly elucidated so far.

Of note, a novel mitochondrial N-SMase which shares sequence similarity with N-SMase2 was identified in zebrafish (*Danio rerio*) (Yabu et al., 2009) and murine cells (*Smdp5*) (Wu et al., 2010a). This mitochondrial N-SMase may generate ceramide in accompanying mitochondria-associated membranes, leading to formation of channels for MOMP and release of mitochondrial proteins. In addition to mitochondria, this isoform of N-SMase has also been identified in the ER, and similarly to other family members also requires Mg^{2+} and Mn^{2+} for its enzymatic activity.

II. Aims of the thesis

In this thesis, the primary goal was the molecular and functional characterization of the signaling pathways that mediate TNF- and TRAIL-induced programmed necrosis.

Within the scope of this goal, the thesis has been divided into two major parts. In the first part, the foremost aim was to understand whether TNF- and TRAIL-induced programmed necrosis (i.e. necroptosis) is mediated by the same pathway that also mediates DNA damage (e.g. MNNG)-induced programmed necrosis (via PARP1) or whether necroptosis and programmed necrosis are two separate and independent pathways. In the latter case, it should be investigated if a possible crosstalk exists.
For this purpose, principal components and events that regulate DNA damage-induced programmed necrosis should be investigated for their involvement in TNF- and TRAIL-induced necroptosis, e.g. activation and general role of PARP1, depletion of intracellular NAD^+ and ATP as well as nuclear translocation of mitochondrial AIF. With regard to a possible crosstalk between necroptosis and programmed necrosis, it should be clarified whether the kinases RIP1 and RIP3 (which are crucial for necroptosis) are similarly essential for programmed necrosis.

The second part of this dissertation should put its focus on the further analysis of the components that mediate the molecular signaling pathways of TNF- and TRAIL-mediated necroptosis to gain insight into the similarities and the differences of the associated signaling pathways.
In particular, an involvement of the necroptotic kinase RIP1 in TRAIL-mediated necroptosis as well as the importance of the sphingolipid ceramide (including the ceramide-generating enzymes A-SMase and N-SMase, and the proteins FADD, TNF-R2, FAN and Lyst) for TNF- and TRAIL-mediated necroptosis should be investigated. An additional aim of this part was to evaluate and validate the role of various classes of proteases in necroptosis, i.e. calpains, cathepsins, metalloproteases and chymotrypsin-like serine proteases. With regard to the latter, a special focus should be put on the role of the serine protease HtrA2/Omi and its putative proteolytic substrates (DBC1, RIP1 and UCH-L1) in necroptosis. As further goals, the importance of ROS in necroptosis and a possible crosstalk between the necroptotic and the autophagic machinery should be investigated.

III. Materials and methods

1. Laboratory equipment

Agfa, Mortsel, Belgium	table top film processor CP1000, developer and rapid fixer for medical x-ray processing
Amaxa, Cologne, Germany	Nucleofector™ II Device
BD Biosciences, Erembodegen, Belgium	Falcon™ tissue culture dish 100 mm, Falcon™ 5 mL polystyrene round-bottom tube 12 x 75 mm
BD Biosciences, Heidelberg, Germany	FACSCalibur Analyser, FACS Flow™ sheath fluid
Bibby Dunn Labortechnik, Asbach, Germany	multi-channel pipette 25-200 µL
Bibby Sterlin, Staffordshire, United Kingdom	Stuart™ horizontal roller mixer SRT6
Biometra, Göttingen, Germany	Power Pack P25T
Brand, Wertheim, Germany	Transferpette® 8 20-100 µL
Eppendorf, Hamburg, Germany	centrifuge 5415D, rotor F45-24-11, centrifuge 5415C, rotor F45-18-11, centrifuge 5417R, rotor F45-30-11, pipettes 10, 20, 100, 200, 1000 µL, thermomixer 5436
Forma Scientific, Marietta, USA	cell culture incubator 3336
Fujifilm, Bedford, U.K.	luminescent image analyzer Las-3000
GE Healthcare, Munich, Germany	Hypercassette™ 18 x 24 cm
Gilson, Limburg-Offheim, Germany	pipettes 10, 20, 100, 200, 1000 µL
Greiner Bio-One, Frickenhausen, Germany	CellStar® filter cap cell culture flask, 25 cm^2, 75 cm^2, 175 cm^2 CellStar® conical tubes 15 mL, 50 mL, CellStar® 6-, 12-, 24-, 48-well cell culture multiwell plates, Cryo.s™ cryogenic vials 1 mL, serological pipettes 1, 5, 10, 25, 50 mL

Hecht-Assistent, Sondheim/Rhön, Germany	horizontal rotating mixer RM5, Neubauer counting chamber, microscope round coverslips 12 mm, microscope slides 76 x 26 mm
Heraeus, Langenselbold, Germany	drying oven T6760
Heraeus, Osterode, Germany	laminAir HB 2472K, Megafuge 1.0R, rotor BS4402/A, Megafuge 16R, rotor TX-400
Hirschmann Laborgeräte, Eberstadt, Germany	pipetus-Accu pipet controller 9907200
IKA, Staufen, Germany	MS 2 minishaker, MS 3 vortex, HS 260 basic shaker, RCT basic hot plate
Julabo, Seelbach, Germany	waterbath U3/8
Kern, Balingen, Germany	precision balance 440-47 N
Kisker Biotech, Steinfurt, Germany	Gel Saver II tips 1-200 µL
Milian, Ghanna, USA	water bath GFL-1003
Millipore, Billerica, MA, USA	Milli-Q water purification system
Molecular Dynamics, Sunnyvale, CA	Personal Densitometer SI model 375
National Labnet, Woodbridge, NS, USA	mini centrifuge C-1200
Nikon, Düsseldorf, Germany	DS-5M-L1 Digital Sight Camera System
Ritter, Schwabmünchen, Germany	ritips 1.25, 12.5 mL
Sartorius, Göttingen, Germany	analytical balance A2005
Scotsman Ice Systems, Vernon Hills, USA	Scotsman ice maker AF-10
Sigma-Aldrich, Munich, Germany	Techne® Dri-Block® heater DB-3
Tecan Group, Männedorf, Germany	Infinite M 200 *microplate* reader, software i-Control 1.3

Thermo Scientific, Roskilde, Denmark	Nunclon Delta Surface 96 microwell plate, flat bottom, clear and white
WTW, Weilheim, Germany	pH-meter pH325, inoLab pH Level1
Zeiss, Göttingen, Germany	microscope Axiovert 10, microscope Axiovert 100, microscope Axiovert 200M

2. Cell culture

2.1 Cell lines

Murine fibrosarcoma L929 cells were purchased from the American Type Culture Collection (ATCC, Manassas, VA, USA) and are subsequently termed L929ATCC throughout this thesis. L929Ts is a TRAIL-sensitive subline of L929, originally derived by prolonged passaging in the laboratory of Dieter Adam (Christian-Albrechts University, Institute for Immunology, Kiel, Germany) (Thon et al., 2006). L929sA is a highly TNF-sensitive subline of L929 that was kindly provided by Peter Vandenabeele (Gent University, Laboratory of Molecular Biology, Belgium). Jurkat human acute leukemia T cells (clone E6-1) were purchased from ATCC and are subsequently termed Jurkat ATCC throughout this thesis. RIP1-deficient Jurkat cells were a gift from Brian Seed (Massachusetts General Hospital, Department of Molecular Biology, Boston, Massachusetts, USA). Jurkat cells deficient for FADD were a kind gift of Harald Wajant (University Hospital Würzburg, Department of Internal Medicine II). Jurkat cells deficient for FADD but additionally stably transfected with TNF-R2 and referred to as Jurkat I.42 were already described (Chan et al., 2003) and a kind gift from Francis Ka-Ming Chan (University of Massachusetts Medical School, Worcester, Massachusetts, USA). The above cell lines were cultivated in Click's RPMI 1640 (A2044,9010, AppliChem, Darmstadt, Germany) (50 %/50 % v/v), supplemented with 10 % (v/v) FBS (S0115, Biochrom, Berlin, Germany), 2 mM L-glutamine (K0282, Biochrom, Berlin, Germany), 100 µg/mL penicillin and streptomycin (A2212, Biochrom, Berlin, Germany) and 50 µM β-mercaptoethanol in 0.9% (w/v) NaCl in a humidified incubator containing 5% (v/v) CO_2 at 37 °C.

NIH3T3 cells naturally expressing or deficient for RIP3 and transfectants stably expressing murine green-fluorescent-protein (GFP) fusions to wildtype or kinase-defective

murine RIP3 in the vector pEGFP-N1 (Takara, Mountain View, CA, USA) were generated and provided by Francis Ka-Ming Chan (University of Massachusetts Medical School, Worcester, Massachusetts, USA). Wildtype and RIP1-deficient MEFs have been previously described (Kelliher et al., 1998).

Primary lung fibroblasts from RIP3- deficient mice and their wildtype littermate controls (that were obtained from Andreas Linkermann (University Medical Center Schleswig-Holstein, Department for Nephrology and Hypertension, Kiel, Germany)) were prepared and cultured as described before (Thon et al., 2005).

Immortalized mouse embryonic fibroblasts deficient for HtrA2/Omi and their wildtype counterparts were originally generated by Julian Downward (Cancer Research UK, Signal Transduction Laboratory, London, U. K. (Martins et al., 2004) and provided by Thomas Langer (University of Cologne, Institute for Genetics).

Embryonic fibroblasts (EF) from wildtype or FAN-deficient mice have been previously described (Kreder et al., 1999). Immortalized Lyst-deficient MCHSF2 fibroblasts and their C572CF wildtype controls were obtained from Diane Ward (University of Utah, Department of Pathology, Salt Lake City, Utah, USA) and have been described previously (Möhlig et al., 2007).

Immortalized MEFs deficient for Atg16L1 and their wild-type controls (Cadwell et al., 2008) were obtained from Paul Saftig (Christian-Albrechts University, Institute of Biochemistry, Unit of Molecular Cell Biology and Transgenic Research, Kiel, Germany). Immortalized MEFs deficient for Atg5 and their wildtype counterparts were obtained from Ingo Schmitz (Helmholtz Centre for Infection Research, Braunschweig, Germany) and generated and described by Noboru Mizushima (Mizushima et al., 2001, Kuma et al., 2004).

Immortalized MEFs, derived from both wild-type and PARP1 KO mice (Munoz-Gamez et al., 2009) were donated by Françoise Dantzer (École Supérieure de Biotechnologie de Strasbourg, Illkirch-Graffenstaden, France).

Wildtype ($CTSD^{+/+}$), cathepsin D-deficient ($CTSD^{-/-}$) and cathepsin D-deficient MEFs stably transfected with the pro-cathepsin D cDNA ($CTSD^{-/-}$reconstituted) were kindly provided by Stefan Schütze (Christian-Albrechts University, Institute for Immunology, Kiel, Germany) and described previously (Heinrich et al., 1999, Heinrich et al., 2004), as have TNF-R1/R2 double-deficient mouse fibroblasts and their transfectants stably re-expressing TNF-R1 (Schneider-Brachert et al., 2004).

The above cell lines were cultivated in DMEM (42430-025, Gibco, Paisley, U.K.),

supplemented with 10 % (v/v) FBS, 100 µg/mL penicillin and streptomycin and 50 µM β-mercaptoethanol in 0.9 % (w/v) NaCl in a humidified incubator containing 5 % (v/v) CO_2 at 37 °C.

Human colon carcinoma HT-29 and A818-6 human pancreatic adenocarcinoma cells were a kind gift of Holger Kalthoff (University Medical Center Schleswig-Holstein, Institute for Experimental Cancer Research, Kiel, Germany) and were kept in McCoy's 5A medium without L-glutamine (F1015, Biochrom, Berlin, Germany) supplemented with 0.5 mM sodium pyruvate (S11.003, PAA, Cölbe, Germany) and 50 µM β-mercaptoethanol in 0.9 % (w/v) NaCl or RPMI 1640 medium (S2400-025, Gibco, Paisley, U.K.) supplemented with sodium pyruvate, respectively, in a humidified incubator containing 5 % (w/v) CO_2 at 37 °C. Cells were routinely passaged every 2-3 days by a wash step with Dulbecco's PBS without Mg^{2+}/Ca^{2+} (L-182-10, Biochrom, Berlin, Germany), short detachment with accutase (L11-007, PAA, Cölbe, Germany), and centrifugation at 100 x g for 6 min at room temperature. Subsequently, cells were stained with 0.4 % (w/v) trypan blue stain (15250, Gibco, Auckland, New Zealand) and counted in a Neubauer counting chamber to determine the quantity of viable cells.

2.2 Reagents used for the treatment of cells

Reagents and chemicals that were used for cell treatment as well as for toxicity assays are listed in Table 2 and Table 3.

Table 2. List of stimuli for induction of apoptosis, necroptosis and necrosis

Name	Product number	Company	Dilution of stock in
cycloheximide (CHX)	C1988	Sigma, Steinheim, Germany	H_2O
hrTNF (TNF), human recombinant		BASF Bioresearch, Ludwigshafen, Germany	
*killer*TRAIL™ (TR, TRAIL), human, recombinant	ALX-201-123	Alexis Biochemicals, Lörrach, Germany	Ready-to-use, pre-dilution in medium
MMS, methyl methanesulfonate	64294	Sigma, Steinheim, Germany	DMSO
MNNG, 1-methyl-3-nitro-1-nitrosoguanidine	M0527	TCI, Zwijndrecht, Belgium	
zVAD-fmk (zVAD)	N-1510	Bachem, Bubendorf, Switzerland	Pure ethanol

Table 3. List of inhibitors and stimuli used for identification of components playing a role in cell death

Name	Product Number	Company	Dilution of stock in
3-AB, 3-aminobenzamide	A0630	TCI Europe, Zwijnchecht, Belgium	H_2O
3-MA, 3-methyladenine	189490	Calbiochem, Darmstadt, Germany	H_2O, heated each time to 100°C
3-OMS, 3-*O*-methyl-sphingomyelin	BML-SL225	Enzo Life Science, Lörrach, Germany	Pure ethanol
Alcohol dehydrogenase from *S. cerevisiae*	A3263	Sigma, Steinheim, Germany	H_2O
ARC39	Synthesized and provided by C. Arenz	Humboldt-University Berlin, Organic and Bioorganic Chemistry, Berlin, Germany	
Bafilomycin A_1	B-1080	LC Laboratories, Woburn, MA, USA	DMSO
BHA, butylated hydroxyanisole	B1253	Sigma, Steinheim, Germany	H_2O
BHT, butylated hydroxytoluene	B1378	Sigma, Steinheim, Germany	
BuOOH, tert-butylhydrogenperoxide, T-HYDRO®	458139	Sigma, Steinheim, Germany	Ready-to-use 70 % in H_2O
Ca-074 Me	4323-v	Peptide Institute, Osaka, Japan	H_2O
CQ, chloroquine diphosphate salt	C6628	Sigma, Steinheim, Germany	
D609	T-6615	Molecular Probes, Leiden, The Netherlands	
Desipramine hydrochloride	D-3900	Sigma, Steinheim, Germany	
DTT, dithiothreitol	D-9779	Sigma, Steinheim, Germany	
E-64,trans-epoxysuccinyl-L-leucylamido-(4-guanidino)butane	E3132	Sigma, Steinheim, Germany	
Fumonisin B_1 from *Fusarium moniliforme*	344850	Calbiochem, Darmstadt, Germany	
GA, geldanamycin	G-4500	LC Laboratories, Woburn, MA, USA	DMSO
GM 6001	364205	Calbiochem, Darmstadt, Germany	
GW4869, N,N′-bis[4-(4,5-dihydro-1H-imidazol-2-yl)phenyl]-3,3′-*p*-phenylene-bis-acrylamide dihydrochloride hydrate	D1692	Sigma, Steinheim, Germany	

Imipramine hydrochloride	I-7379	Sigma, Steinheim, Germany	H_2O
LDN57444	662086	Calbiochem, Darmstadt, Germany	DMSO
LDN91946	662088	Calbiochem, Darmstadt, Germany	
Marimastat	M2699	Sigma, Steinheim, Germany	
Necrostatin-1	480065	Calbiochem, Darmstadt, Germany	
Olaparib, AZD2281	1464	Axon Medchem, Groningen, The Netherlands	
PARG, poly(ADP-ribose) glycohydrolase	ALX-202-045	Enzo Life Science, Lörrach, Germany	Ready-to-use, 0.1 U
PJ34 hydrochloride, *N*-(5,6-Dihydro-6-oxo-2-phenanthridi-nyl)-2-acetamide hydrochloride	3255	Tocris Bioscience, Westwood Bus Park, Ellisville, MO, USA	H_2O
PMSF, phenylmethylsulfonyl fluoride	P-7626	Sigma, Steinheim, Germany	Pure ethanol
Radicicol (RC)	BIA-R1148	Tebu-Bio, Offenbach, Germany	DMSO
Spiroepoxide	270-340-M001	Alexis, Lausen, Switzerland	
TAPI-I	579051	Calbiochem, Darmstadt, Germany	
TPCK, tosyl phenylalanyl chloromethyl ketone	T4376	Sigma, Steinheim, Germany	
Ucf-101 5-[5-(2-nitrophenyl)furfurylidine]-1,3-diphenyl-2-thiobarbituric acid	496150	Calbiochem, Darmstadt, Germany	
zFA-fmk, benzyloxycarbonyl-Phe-Ala-fluoromethylketone	C1480	Sigma, Steinheim, Germany	
zFF-fmk, benzyloxycarbonyl-Phe-Phe-fluoromethylketone	219421	Calbiochem, Darmstadt, Germany	H_2O
Zoledronic acid	Zometa®	Novartis International AG, Basel, Switzerland	

Chemical compounds not listed here were obtained from Sigma (Steinheim, Germany) or Merck (Darmstadt, Germany) in molecular grade purity.

2.3 Flow cytometry analysis

For FACS analyses, cells were seeded in twelve-well plates at a density of 5 x 10^4 cells pro well. Suspension cells were stimulated immediately whereas adherent cells were first cultivated overnight and then treated with the inducers of cell death listed in Table 2 in combination with or without inhibitors and other stimuli listed in Table 3. Subsequently, cells were detached with accutase, centrifuged at 390 x g for 5 min at 4 °C, washed twice with PBS w/o Mg^{2+}/Ca^{2+} supplemented with 5 mM EDTA and stained with 2 µg/ml propidium iodide (PI, Immunochemistry Laboratories, Bloomington, MN, USA). Red fluorescence was measured on a FACSCalibur flow cytometer and analyzed by the BD CellQuest™ Pro software V.4.0.2 (Becton Dickinson, Heidelberg, Germany).

3. Immunoblot analyses

3.1 Preparation of whole cell lysates

For protein-based analyses, 1x10^6 cells were seeded in 10 cm cell culture dishes. Following stimulation, cells were detached with accutase, washed twice with PBS supplemented with 5 mM EDTA, centrifuged at 390 x g for 5 min and lysed at 4 °C in TNE buffer (50 mM Tris pH 8.0, 1 % (v/v) NP-40, 150 mM NaCl, 3 mM EDTA, 1 mM sodium orthovanadate (Na_3VO_4), 5 mM sodium fluoride (NaF), and *complete protease inhibitor* cocktail (Roche, Mannheim, Germany)). After 10 min lysis on ice, samples were centrifuged at 20,800 x g for 10 min at 4 °C and supernatants were used for further analyses.

3.2 Preparation of enriched nuclear and cytosolic fractions

Enriched nuclear fractions and cytosolic fractions were obtained through the procedure of nuclear protein isolation that is common for electrophoretic mobility shift assays (EMSA). 1 x 10^6 cells were washed twice with chilled PBS and centrifuged for 5 min at 390 x g at 4 °C. The cell pellet was lysed with buffer A (10 mM HEPES pH 7.9, 10 mM KCl, 0.1 mM EDTA, 0.1 mM EGTA, freshly supplemented with 1 mM DTT and 1 mM PMSF) for 15 min at 4 °C. Afterwards, 0.6 % NP-40 was added and the lysis solution was shaken for 2 min at 4 °C. Following centrifugation for 2 min at 20,800 x g and 4 °C, the supernatant was kept as the cytosolic fraction and the nuclear pellet was lysed with buffer C (20 mM HEPES pH 7.9, 0.4 M NaCl, 1 mM EDTA, 1 mM EGTA and freshly added 1

mM DTT) by shaking for 30 min at 4 °C. The lysate was centrifuged for 5 min at 20,800 x g at 4 C and the supernatant containing nuclear proteins was gathered and used for further analyses.

Alternatively, purified cytosolic and nuclear fractions were generated with the ProteoJET™ nuclear and cytoplasmic extraction kit (#K0311, Fermentas, St. Leon-Rot, Germany) according to the instructions of the manufacturer.

3.3 SDS-PAGE

The total protein concentration in each sample was measured with the bicinchoninic acid determination method (Pierce® Protein Assay Reagent, Thermo Scientific, Ulm, Germany) or the Bradford assay which uses Coomassie Brilliant Blue R-250 (Thermo Scientific, Ulm, Germany). Identical amounts of protein per lane were resolved by electrophoresis on SDS polyacrylamide gels. Discontinuous SDS-PAGE was performed using the mini Bio-Rad vertical gel apparatus. Different linear non-gradient resolution polyacrylamide gels (7.5 % (w/v), 10 % (w/v) and 12 % (w/v)) were prepared from an acrylamide stock (40 % (w/v), 37.5:1 acrylamide:bis, Serva, Heidelberg, Germany) and 0.375 mM Tris/HCl pH 8.8, 0.1 % SDS (w/v) in glycerin. Those gels were overlaid with stacking gels, which contained 5 % (w/v) total acrylamide, 0.3 mM Tris/HCl pH 6.8 and 0.1 % (w/v) SDS in water. After addition of 1 % (w/v) APS and 1 % (v/v) TEMED, gels were allowed to polymerize overnight at 4 °C. Commercially available gradient gels, precast mini-Protean® TGX 4-20 % (10 well comb, 20 µL, 456-1093, BioRad, Munich, Germany) or AnykD™ (10 well comb, 30 µL, 456-9033, BioRad, Munich, Germany) were used alternatively. Samples were dissolved (1:1) in sample buffer (10 mM Tris/HCl pH 6.8, 1 % SDS (w/v), 2,5 % (v/v) glycerol, 0.05 % (w/v) bromophenol blue and 1 % (v/v) β-mercaptoethanol) and heated in a boiling water bath for 4 min. The electrode buffer contained 25 mM Tris/HCl pH 8.2, 200 mM glycine and 0.1 % SDS (w/v). Electrophoresis was conducted at room temperature at 25 mA per mini gel until the bromophenol blue front reached the end of the gel. The high molecular weight standard PageRuler™ Prestained Protein Ladder (10-170 kDa, Thermo Scientific, Ulm, Germany), was used as a standard for estimation of the protein molecular weights.

3.4 Western blot

Polyacrylamide gels were electrophoretically transferred to 0.2 µm Protran® nitrocellulose transfer membrane (BA83, 10401396, GE Whatman®, Dassel, Germany) in running buffer (25 mM Tris/HCl pH 8.2, 200 mM glycine and 20 % (v/v) methanol) with 100 V for 1 h at 4 °C. Blotted membranes were blocked and incubated at 4 °C overnight with the primary antibodies and the specific conditions listed below (Table 4). Excess of antibodies was removed by washing with PBS supplemented with 0.1 % (v/v) Tween 20 (PBS/T). Afterwards, incubation with the respective secondary antibodies conjugated to horseradish peroxidase (anti-(mouse IgG) or anti-(rabbit IgG), anti-(goat IgG) (Jackson ImmunoResearch, West Grove, Pennsylvania, USA)) diluted 1:10,000 in the corresponding blocking solution was performed for 1 h at room temperature. After three washes with PBS/T, reactive proteins were detected by the addition of luminol chemiluminescent substrate LumiGLO® (Cell Signaling, Danvers, MA; USA). The emitted light was captured on Amersham Hyperfilm™ ECL (GE Healthcare, Munich, Germany).

Table 4. List of all used a2ntibodies, its dilutions and method of incubation

Antibody name	Company	Dilution in PBS/T	Blocking solution
AIF (E-1)	Santa Cruz, sc-13116	1:1,000	5 % non-fat dry milk
α-actin	Santa Cruz, C-11, sc-1615	1:10,000	
ß-actin	Sigma, clone AC-15, A1978	1:10,000	
Cathepsin D	Santa Cruz, sc-6486 (C-20)	1:1,000	
DBC1	Cell Signaling, #5693	1:1,000	5 % BSA
GFP	Clontech, 8369-1	1:1,000	5 % non-fat dry milk
HA, hemagglutinin	Roche, clone 3F10, 11 867 423	1:1,000	
HtrA2/Omi	Abcam, clone E55, ab32092	1:1,000	
LC3	nanoTools, 0231-100/LC3-5F10		
PAR	Enzo, ALX-804-220	1:1,000	
PAR	DB Pharmingen, 551813, component 51-8114KC	1:1,000	
PARP1	Cell Signaling, #9542	1:1,000	
RIP1	BD Bioscience, 610459	1:1,000	
RIP3, murine	Enzo, ADI-905-242-100	1:500	
RIP3, human	Abnova, PAB0287	1:500	5 % BSA
TNF-R1	Santa Cruz, sc-8436 (H-5)	1:1,000	
UCH-L1	monoclonal, kind gift of C. Meyer-Schwesinger (University Medical Center Hamburg-Eppendorf, Department of Internal Medicine, Nephrology Hamburg, Germany)	1:500	5 % non-fat dry milk
UCH-L1	Cedarlane, CL95101	1:3,000	

4. Transfection with siRNA - downregulation of proteins

4.1 List of siRNA used for the experiments

All Silencer®Select siRNA used in this thesis (Table 5) were designed for the coding regions of the selected genes and purchased from Ambion (Life Technologies, Applied Biosystems, Carlsbad, CA, USA).

Table 5. List of siRNAs used for RNA interference assays

siRNA name	Company Number	Specificity	NCBI UniGene ID:
HtrA2/Omi	s654	Human, validated	Hs.469045
HtrA2/Omi (1)	s82293	Mouse, pre-designed	Mm.21880
HtrA2/Omi (2)	s82292	Mouse, pre-designed	Mm.21880
Negative control (siCtr), scrambled siRNA	AM4611	Does not target any gene product, has no significant sequence similarity to human, mouse or rat genes	No data
PARP1	s62053	Mouse, pre-designed	Mm.277779
PARP1	s1097	Human, validated	Hs.177766
RIP1	16104	Mouse, custom annealed Sequence: CACTAGTCTGACTGATGA according to (Yu et al., 2004)	Mm.374799
RIPK3	s80755	Mouse, pre-designed	Mm.46612
UCH-L1	s75710	Mouse, pre-designed	Mm.29807

4.2 Nucleofection of siRNA

Nucleofection was performed using the Amaxa® Cell Line Nucleofector™ kit V (VCA-1001, Amaxa, Cologne, Germany) for L929Ts and Jurkat cells or Nucleofector™ kit R (VCA-1003, Amaxa, Cologne, Germany) for NIH3T3 cells. For one transfection, 1 x 10^6 cells were pelleted at 100 x g for 6 min, resuspended in 100 µL solution V or R and left at room temperature up to 15 min. Afterwards, this cell suspension was mixed in electroporation cuvettes with 25 nM siRNA and nucleofection was carried out with program T-20 for L929Ts, X-001 for Jurkat ATCC and A-24 for NIH3T3 cells. Each transfection experiment was validated by a negative control of scrambled siRNA (siCtr). After nucleofection, cells were resuspended in 6 mL of pre-warmed culture medium in 6 well plates for 48 or 72 h. The efficiency of of the siRNA transfection and the downregulation was analyzed by Western blot analysis for the protein of interest.

4.3 Lipofection of siRNA

Lipofection was performed with HiPerFect transfection reagent (301702, Qiagen, Hilden, Germany). Briefly, 2 x 10^5 Jurkat I.42 cells were pre-plated in 100 µL complete medium in a 24 well plate. 100 µL of serum-free medium was mixed with 3 µL of HiPerFect transfection reagent and 150 nM siRNA. After 15 min incubation at room temperature, 100 µL of this mixture was applied dropwise into 100 µL of pre-plated cell suspension. After 6 additional hours, 400 µL of complete medium was added and cells were left for 48 h and 72 h post-transfection. The efficiency of the siRNA transfection and the downregulation of the protein of interest were analyzed by Western blot.

5. Measurement of intracellular ROS

For measurement of ROS cells were seeded in twelve-well plates at a density of 5 x 10^4 cells pro well. Following stimulation of the cells, determination of intracellular ROS was performed by staining with freshly prepared 10 µM CM-H_2DCFDA for 30 min at 37 °C in the dark. After that, cells were centrifuged, washed with ice-cold PBS (pH 7.2) and suspended in equal volumes of chilled PBS with 2 µg/mL PI staining solution. Finally, cells were analyzed by flow cytometry. Green fluorescence was measured on a FACSCalibur flow cytometer and analyzed by the BD CellQuest Pro software.

6. ATP measurement

For measurement of intracellular ATP, cells were seeded in 96 well plates at a density of 1 x 10^4 cells pro well. For measurement of ATP in whole cell lysates, the bioluminescent assay kit FL-AA (Sigma, Saint Louis, MO, USA), was used following the instructions of the manufacturer. Alternatively, the CellTiterGlow® luminescent cell viability assay (G7570, Promega, Mannheim, Germany) was employed. Luminescence intensity was measured on 96 well, flat bottom white plates by an Infinite M200 microplate reader.

7. NAD^+ measurement

The levels of intracellular NAD^+ after cytotoxicity assays was measured in cells lysed with NAD^+/ATP-lysis buffer (0.5 % (v/v) Triton-X, 10 mM Tris pH 7.5, 1 mM EDTA) for 10 min at 4 °C and centrifuged at 20,800 x g for 20 min at 4 °C. An equal volume of the supernatant was mixed with 100 µL NAD^+-assay buffer (8 % (v/v) ethanol, 1 % (v/v)

polyvinylpyrrolidone (PVP), 0.5 mM EGTA, 50 mM Tris/HCl pH 8.8, 1 mM phenazine ethosulfate (PES), 0.44 mM thiazolyl blue tetrazolium bromide (MTT) and 2 U alcohol dehydrogenase from *S. cerevisiae*) and incubated for 30 min at 37 °C. Afterwards. absorption at 570 nm was measured by a an Infinite M200 microplate reader.

8. Statistical analyses

Cell culture experiments were carried out in triplicates and repeated independently a minimum of three times. Data points were expressed as means ± standard deviation (SD) of three or more experiments in triplicates, unless otherwise indicated. To test the significance of the results, the Student's t-test was performed and *p* values less than 0.05 and 0.01 were considered as significant.

9. Microscopic analyses

9.1 Morphological analyses

Briefly, morphological signs and characteristic features of both necroptosis and apoptosis were observed in cells seeded at a density of 5 x 10^4 cells pro well in 12 well plates by microscopy after stimulation. The ratio of viable cells and cells undergoing cell death was visualized with the Axiovert 10 light microscope by Achrostigmat objectives with resolution 32x/0.40 or 20x/0.30 and digitalized with a Nikon DS-5M-L1 Digital Sight Camera System.

IV. Results

A. Necroptosis and programmed necrosis are two separate and independent pathways

In this thesis, components important for programmed necrosis such as PARP1, AIF, and changes in the bioenergetic status of a cell were analyzed to elucidate their involvement in necroptosis. Moreover, genetic ablation models were used to clarify whether the RIP1-RIP3 complex, an initial component of cytokine-mediated necroptosis, is additionally involved in programmed necrosis.

1. Poly(ADP)-ribose polymerase 1 (PARP1) is not involved in necroptosis

Cleavage of PARP1 is not required for necroptosis in murine and human cells

As a main hallmark of apoptosis, the mature 116-kDa PARP1 protein is cleaved by caspases -3 and -7, resulting in the appearance of an 89-kDa band and release of this PARP1 form from the nucleus (Chaitanya et al., 2010). In contrast to most other cells, all sublines of murine L929 cells do not die by apoptosis but rather by necroptosis when treated with TNF (Strelow et al., 2000, Thon et al., 2005, Thon et al., 2006). In agreement, the cleaved apoptotic 89-kDa fragment of PARP1 was not detected in L929 Ts, ATCC and sA cells after induction of necroptosis by TNF, and also not after induction of PARP1-dependent programmed necrosis by MNNG. Rather, PARP1 displayed an atypical shift/disappearance of the uncleaved protein that had been previously been reported for TNF- and TRAIL-induced necroptosis (Thon et al., 2005). Importantly, the potent PARP1 activator MNNG induced the PARP1 shift more rapidly, with changes already detectable within 4-8 h after treatment, whereas for TNF, this occurred at 10 h of treatment or later (Figure 11).

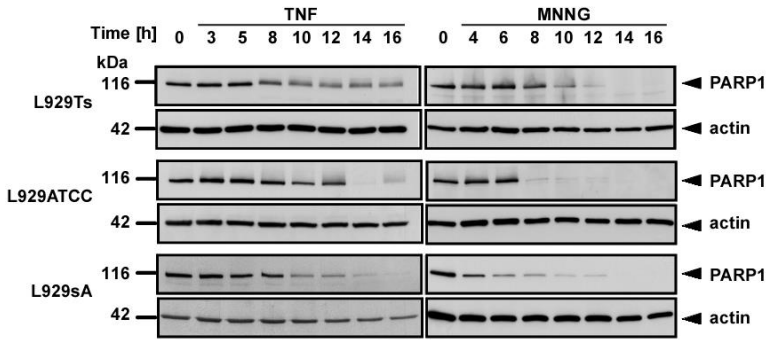

Figure 11. The atypical shift/disappearance of PARP1 occurs with distinct kinetics in response to TNF and MNNG. L929Ts, L929ATCC, and L929sA cells were treated with 0.5 mM MNNG for 15 min (and put into fresh medium without MNNG afterwards) or with 100 ng/mL hrTNF and incubated for indicated times. Afterwards, PARP1 was detected in whole cell lysates. For all Western blots, detection of actin served as a loading control.

This altered timeframe of PARP1 shift/disappearance for TNF-induced necroptosis and MNNG-induced programmed necrosis provided a first indication for a differential importance of PARP1 in both cell death pathways. To clarify the mechanism of the shift/disappearance of PARP1, lysates from L929Ts cells undergoing TNF-induced necroptosis were analyzed for PARP1 in Western blots and reanalyzed for the presence of poly(ADP)-ribose (PAR). As shown in Figure 12 A, the shift/disappearance of PARP1 was accompanied by an increased PARylation of PARP1, indicating that PARP1 is activated during necroptosis, leading to auto-PARylation. This automodification with PAR might cause it to become inaccessible for the detecting antibody. In agreement with this hypothesis, incubation of lysates showing shift/disappearance of PARP1 with PARG, a PAR-removing enzyme, restored the original PARP1 band (Figure 12 B). In summary, these results indicated that induction of necroptosis is accompanied by hyperactivation of PARP1 which causes the atypical shift/disappearance in Western Blots.

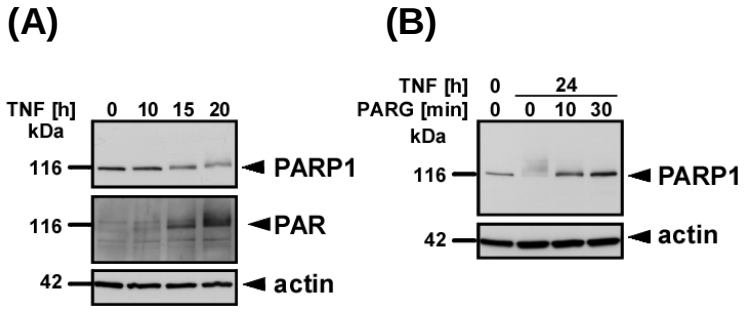

Figure 12. Disappearance PARP1 is due to its hyperactivation. (A) L929Ts were incubated for the indicated periods of time with 100 ng/mL hrTNF and whole cell lysates were prepared. Following detection of PARP1, the membrane was reprobed with an antibody for PAR. **(B)** L929Ts cells were incubated for 24 h with 100 ng/mL hrTNF, followed by whole cell lysis. Afterwards, lysates were incubated for the indicated periods of time at 37 °C with 0.01 U PARG. Antibodies: anti-PARP1 (Cell Signaling), anti-PAR (BD Pharmingen) and anti-actin (Sigma).

Employing additional cell systems, it was next analyzed whether – in addition to its established role in programmed necrosis induced by DNA-damaging agents – PARP1 is also involved in TNF- and TRAIL-mediated necroptosis. Murine L929Ts and NIH3T3 cells and human Jurkat ATCC and HT-29 cells were left untreated (Figure 13, lanes 1, 10) or stimulated with hrTNF or *killer*TRAIL (Figure 13, lanes 2, 11). This treatment induced apoptosis in all cell lines (except for TNF-treated L929Ts cells, in which TNF alone induces caspase-independent necroptosis (Vanlangenakker et al., 2011a, Wu et al., 2011), confirmed by the appearance of the apoptotic 89-kDa cleavage fragment of PARP1 (or a necroptotic shift of the mature 116-kDa PARP1 band in L929Ts cells) (Figure 13, lane 2). When the cells were stimulated with hrTNF or *killer*TRAIL in combination with the broad-spectrum caspase inhibitor zVAD-fmk to induce necroptosis (and the protein biosynthesis inhibitor CHX to sensitize the cells), a necroptotic shift or disappearance of PARP1 but no apoptotic 89-kDa PARP1 fragment was detectable in all cell lines (except for HT-29 cells, where a slight 89-kDa band was visible, possibly due to incomplete inhibition of caspases by zVAD-fmk) (Figure 13, lanes 3, 12). Therefore, the characteristic apoptotic cleavage of PARP1 to an 89-kDa fragment does not occur during necroptosis in multiple murine or human cell lines. Rather, the data presented here indicate an activation of PARP1 (i.e. the shift/disappearance) during necroptosis in murine and human cells.

To determine if the observed disappearance of the full-length PARP1 band is directly linked to PARP1 activation beyond the above experiment with PARG, the PARP1 inhibitors PJ34, 3-AB and olaparib were employed in combination with TNF/zVAD/CHX or TRAIL/zVAD/CHX as inducers of necroptosis. The presence of the inhibitors completely or partially abolished the disappearance of PARP1 in the mouse cell lines L929 and NIH3T3 as well as in human HT-29 cells. This effect was less clearly visible in human Jurkat ATCC cells where induction of necroptosis only modestly induced the disappearance of PARP1 (Figure 13, lanes 4-9 and 13-18).

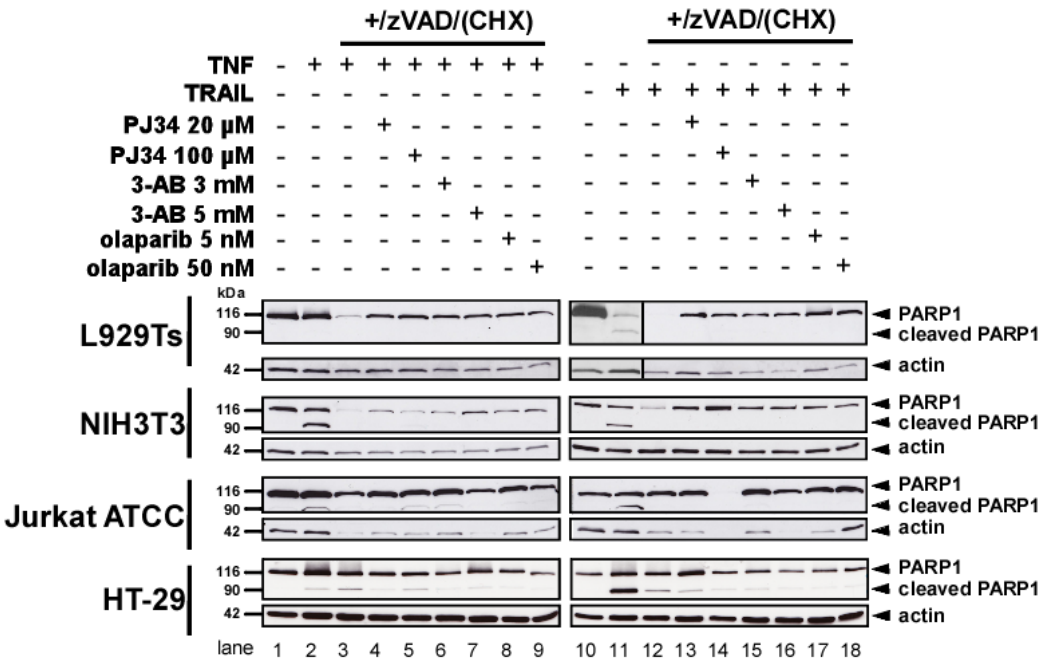

Figure 13. PARP1 cleavage in TNF- and TRAIL-mediated apoptosis and necroptosis. General PARP1 inhibitors (PJ34, 3-AB and olaparib) were used to inhibit PARP1 activation in TNF- and TRAIL-mediated necroptosis. Cells were left untreated or preincubated for 2 h with the indicated concentrations of the PARP1 inhibitors PJ34, 3-AB and olaparib. Afterwards, cells were stimulated in the presence of thePARP1 inhibitors as indicated with 20 µM zVAD-fmk in combination with 100 ng/mL hrTNF or 30 ng/mL *killer*TRAIL for 5 or 14 h respectively for L929Ts cells. NIH3T3 cells were stimulated with 100 ng/mL hrTNF or 50 ng/mL *killer*TRAIL in combination with 20 µM zVAD-fmk for 16 h. HT-29 cell were stimulated with 100 ng/mL hrTNF or 30 ng/mL *killer*TRAIL in combination with 20 µM zVAD-fmk and 5 µg/mL CHX for 16 h. Jurkat ATCC cells were stimulated with 100 ng/mL hrTNF or 50 ng/mL *killer*TRAIL in combination with 50 µM zVAD-fmk and 2 µg/mL CHX for 20 h. PARP1and the loading control actin were detected by Western blot. Antibodies: anti-PARP1 (Cell Signaling) and anti-actin (Santa Cruz).

To clarify whether the PARP1 cleavage to an 89-kDa fragment observed in Figure 13 during necroptosis in human cells was based on residual activity of cysteine proteases (e.g. incomplete inhibition of caspases by zVAD-fmk), TNF- and TRAIL- mediated necroptosis was analyzed in Jurkat ATCC and HT-29 cells in the presence of increasing concentrations of zVAD-fmk. When the lowest concentration of zVAD-fmk (50 µM) was applied, residual cleavage of PARP1 in human cell lines was still observed, especially for TRAIL-mediated necroptosis in Jurkat ATCC cells and both TNF- and TRAIL-mediated necroptosis in HT-29 cells. However, this cleavage was clearly inhibited with increasing concentrations of zVAD-fmk whereas the necroptotic shift/disappearance of PARP1 was not influenced (Figure 14), supporting the assumption that the appearance of the 89-kDa PARP fragment in necroptotic lysates in Figure 13 is due to an insufficient inhibition of caspases in Jurkat ATCC and HT-29 cells.

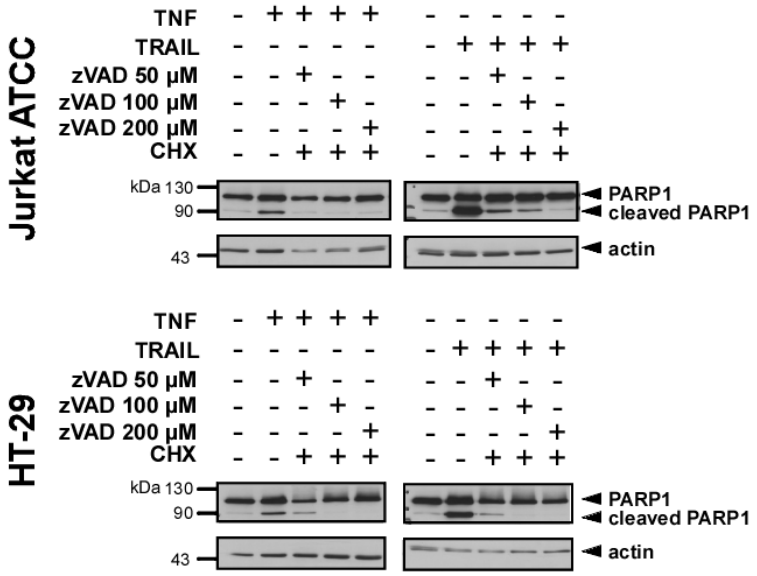

Figure 14. Apoptotic PARP1 cleavage during necroptosis is blocked by zVAD-fmk in a concentration dependent manner in the human cell lines Jurkat ATCC and HT-29. Jurkat ATCC cells were stimulated with 100 ng/mL hrTNF or 50 ng/mL *killer*TRAIL or in combination with increasing concentrations of zVAD-fmk and 2 µg/mL CHX for 20 h. HT-29 cells were stimulated with 100 ng/mL hrTNF or with 30 ng/mL *killer*TRAIL in combination with increasing concentrations of zVAD-fmk and 5 µg/mL CHX for 16 h. PARP1and the loading controls actin were detected by Western blot. Antibodies: anti-PARP1 (Cell Signaling) and anti-actin (Santa Cruz).

Pharmacological inhibition of PARP1 does not consistently protect from necroptosis in murine cells

As an additional experiment to demonstrate that PARP1 undergoes hyperactivation during necroptosis, the formation of PAR was analyzed in presence or absence of the PARP1 inhibitors PJ34, 3-AB and olaparib. As shown in Figure 15 A (lanes 2, 3, 12), an extensive formation of PAR was detected in L929Ts cells after induction of necroptosis by hrTNF or *killer*TRAIL, and also after induction of apoptosis by TRAIL (lane 11), indicating massive PARP1 activation. This formation of PAR chains was efficiently reduced when PARP1 inhibitors were applied (Figure 15 A, lanes 4-9, 13-18), with PJ34 being the most potent inhibitor. To additionally confirm the potency of these inhibitors, L929Ts cells were treated with MNNG as a positive control for induction of PARP1-dependent programmed necrosis. As shown in Figure 15 B, and in agreement with previous reports (De Blasio et al., 2005, Fiorillo et al., 2006), all three inhibitors inhibited MNNG-induced programmed necrosis, validating their efficacy.

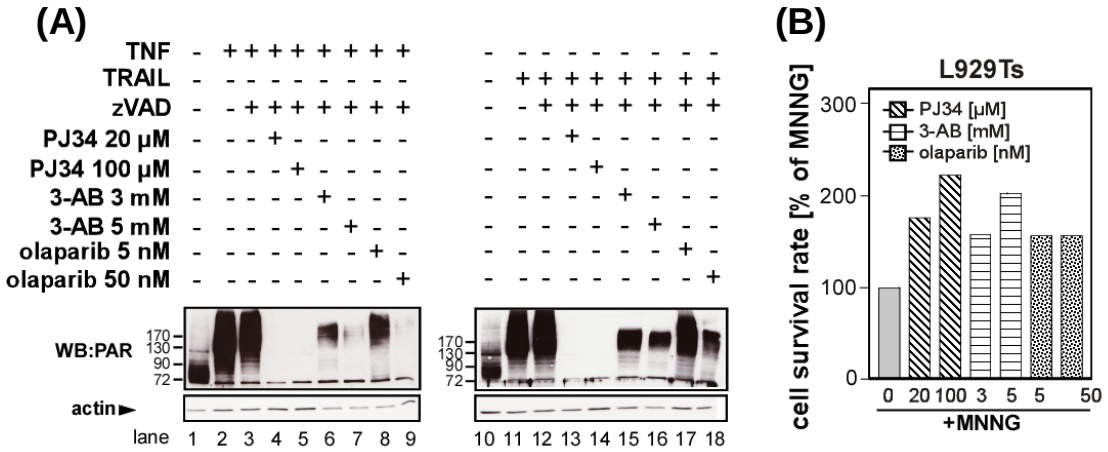

Figure 15. PJ34, 3-AB and olaparib are potent inhibitors of PARP1 activation during TNF- or TRAIL-mediated necroptosis and MNNG-induced programmed necrosis. (A) L929Ts cells were left untreated or preincubated for 2 h with the indicated concentrations of the PARP1 inhibitors PJ34, 3-AB and olaparib. Afterwards, cells were stimulated for 5 h with 100 ng/mL hrTNF or for 14 h with 30 ng/mL *killer*TRAIL in combination with 20 µM zVAD-fmk in the presence of the PARP1 inhibitors as indicated. PAR and the loading control actin were detected by Western blot. Antibodies: anti-PAR (BD Pharmingen), anti-actin (Santa Cruz). **(B)** Cells were preincubated for 2 h with the indicated concentrations of PARP1 inhibitors PJ34, 3-AB and olaparib, followed by stimulation with 0.5 mM MNNG for 15 min and left in fresh medium for 16 h to allow execution of programmed necrosis. Cell survival was determined by flow cytometric measurement of PI-negative cells and is presented relative to cells treated with MNNG only. Values represent the means from one experiment in two repeatitions.

However, and despite their protection from cell death in MNNG-induced programmed necrosis and despite their inhibitory effect on PARP1 activation during TNF- and TRAIL-mediated necroptosis, 3-AB and olaparib failed to protect L929Ts cells from dying after induction of necroptosis by both TNF and TRAIL whereas PJ34 partially inhibited necroptosis in both cases (Figure 16).

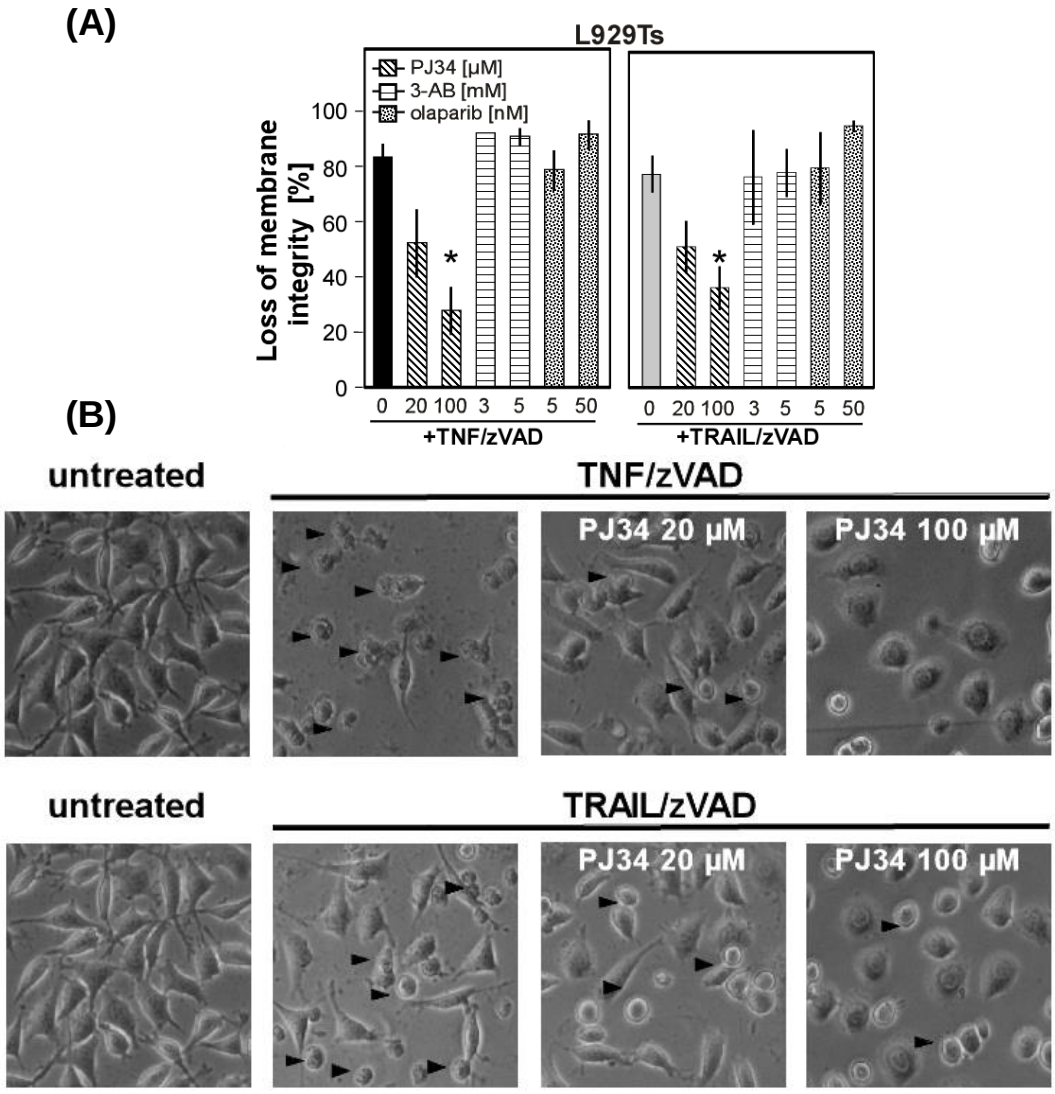

Figure 16. Involvement of PARP1 in TNF- and TRAIL-induced necroptosis in L929Ts cells. (A) Cells were left untreated or preincubated for 2 h with the PARP1 inhibitors PJ34, 3-AB and olaparib in the indicated concentrations. Afterwards, cells were stimulated with 100 ng/mL hrTNF or 30 ng/mL *killer*TRAIL in combination with 20 µM zVAD-fmk for 5 h or 14 h, respectively in the presence of the PARP1 inhibitors. Cell death (i.e. loss of membrane integrity) was measured by flow cytometry counting PI-fluorescence of a sample of 10,000 cells. Values represent the means from at least two independent experiments. Error bars indicate the respective SD. Asterisks indicate statistical significance (t-test $p< 0.01$). **(B)** Morphological analysis of the influence of the PARP1 inhibitor PJ34 on TNF- and TRAIL-mediated necroptosis in murine L929Ts cells. Cells were treated as described in (A). Black arrows indicate typical caspase-independent cell death morphology (i.e. necroptosis). Sample images of untreated cells are shown in comparison to TNF/zVAD and TRAIL/zVAD treated cells with or without the PARP1 inhibitor PJ34. Magnification 320x.

However, when the experiment was repeated in NIH3T3 cells, protection by PJ34 was observed only against TRAIL-mediated necroptosis (Figure 17). Surprisingly, PJ34 did not influence TNF-mediated necroptosis in this cell line. Similarly to the results obtained for L929Ts cells, none of the other PARP1 inhibitors prevented both TNF- and TRAIL-mediated necroptosis.

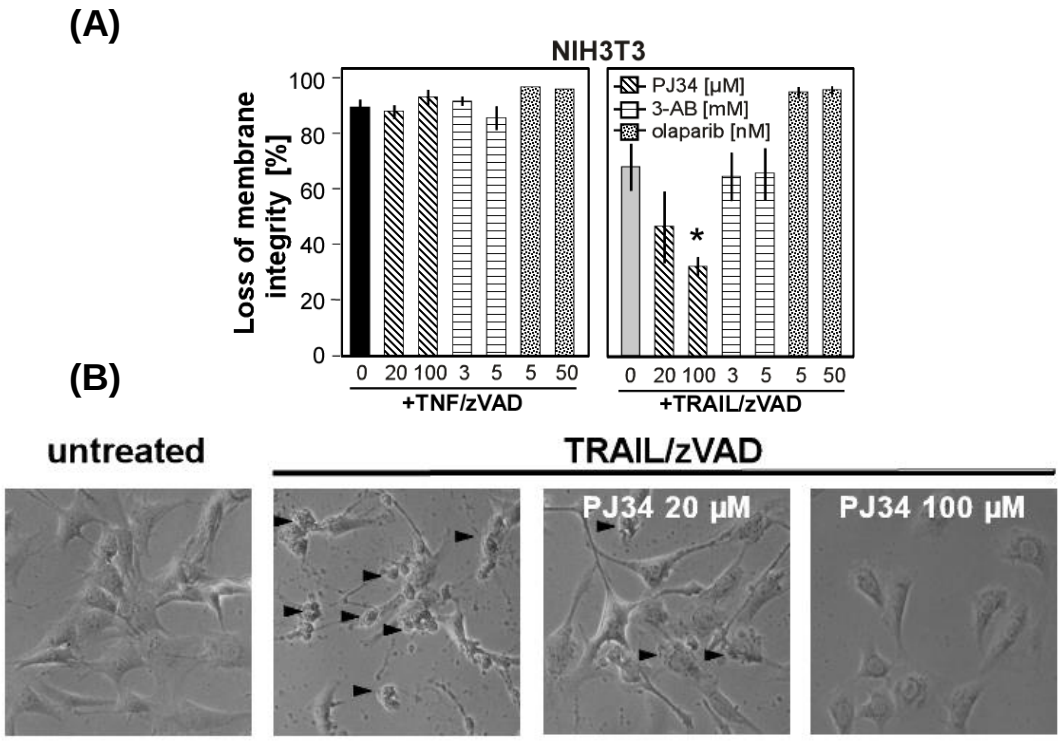

Figure 17. Involvement of PARP1 in TNF- and TRAIL-induced necroptosis in NIH3T3 cells. (A) Cells were left untreated or preincubated for 2 h with the PARP1 inhibitors PJ34, 3-AB and olaparib in the indicated concentrations. Afterwards, cells were stimulated with 100 ng/mL hrTNF or 100 ng/mL *killer*TRAIL in combination with 20 µM zVAD-fmk for 16 h in the presence of the PARP1 inhibitors. Cell death was measured by flow cytometry counting PI-fluorescence of a sample of 10,000 cells. Values represent the means from at least two independent experiments. Error bars indicate the respective SD. Asterisks indicate statistical significance (t-test $p < 0.01$). **(B)** Morphological analysis of the influence of the PARP1 inhibitor PJ34 on TRAIL-mediated necroptosis in murine NIH3T3 cells. Cells were treated as described in (A). Black arrows indicate typical caspase-independent cell death morphology (i.e. necroptosis). Sample images of untreated cells are shown in comparison to TRAIL/zVAD treated cells with or without the PARP1 inhibitor PJ34. Magnification 320x.

For both murine cell lines (L929Ts and NIH3T3), the protective effects of PJ34 were additionally analyzed at the level of cell morphology. The microscopic examination of L929Ts cells treated with necroptotic stimuli in combination with PJ34 demonstrated a slight reduction in cell number, accompanied by morphological changes. Although the cell membrane integrity was apparently preserved, the cells appeared much rounder, resembling cells reattaching after cell division, without long cytoplasmic protrusions, and lacking interconnecting fibers (Figure 16 B). Similarly, in NIH3T3 PJ34 noticeably prevented the cellular disintegration during TRAIL-mediated necroptosis and sustained their plasma membrane integrity, but nevertheless failed to restore the typical healthy appearance of the cells (Figure 17 B). In summary, the morphological analyses suggest that the protective effect of PJ34 is due to a restricted and slowed execution of cell death rather than to a specific blockade of necroptosis. As an additional explanation for the differential effects of PJ34 compared to 3-AB and olaparib, several reports have confirmed that PJ34

unspecifically downregulates ERK1/2 (Ethier et al., 2007) or ROS production (Halmosi et al., 2001, Fiorillo et al., 2006). In summary, the above results indicate that the effects of PJ34 may represent artifacts and that PARP1 is most likely not required for necroptosis in L929Ts and NIH3T3 cells.

Pharmacological inhibition of PARP1 does not protect from necroptosis in human cells

To extend the analyses also to human cells, the effects of PJ34, 3-AB and olaparib on TNF- and TRAIL-induced necroptosis were additionally investigated in Jurkat ATCC and HT-29 cells. Despite their suppressing effects on the shift/disappearance and thus the activation of PARP1 (see Figure 13), none of the inhibitors reproducibly prevented TNF- and TRAIL-induced necroptosis in the two cell lines (Figure 18 and Figure 19). In fact, inhibition of PARP1 by PJ34 in HT-29 cells even led to an increased level of necroptosis (Figure 19).

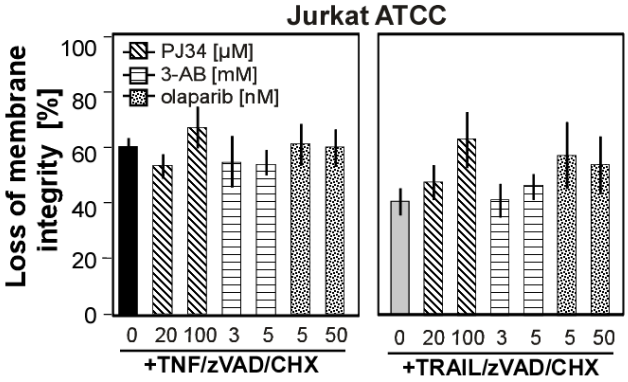

Figure 18. Involvement of PARP1 in TNF- and TRAIL-induced necroptosis in Jurkat cells. Cells were left untreated or preincubated for 2 h with the PARP1 inhibitors PJ34, 3-AB and olaparib in the indicated concentrations. Afterwards, cells were stimulated with 100 ng/mL hrTNF or 50 ng/mL *killer*TRAIL in combination with 50 µM zVAD-fmk and 2 µg/mL CHX for 20 h in the presence of the PARP1 inhibitors. Cell death was measured by flow cytometry counting PI-fluorescence of 10,000 cells for each sample. Values represent the means from at least two independent experiments. Error bars indicate the respective SD.

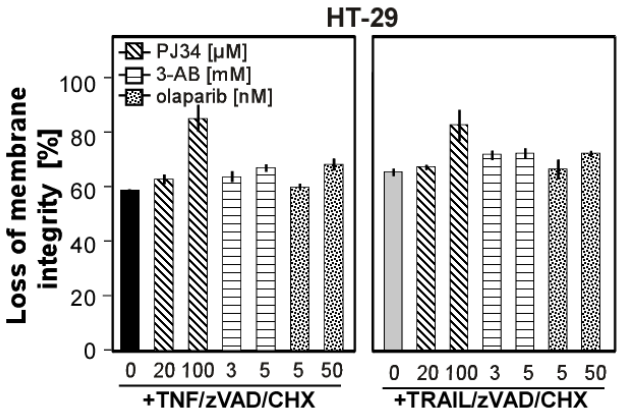

Figure 19. Involvement of PARP1 in TNF- and TRAIL-induced necroptosis in HT-29 cells. Cells were left untreated or preincubated for 2 h with the PARP1 inhibitors PJ34, 3-AB and olaparib in the indicated concentrations. Afterwards, cells were stimulated with 100 ng/mL hrTNF or with 30 ng/mL *killer*TRAIL in combination with 20 µM zVAD-fmk and 5 µg/mL CHX for 16 h in the presence of the PARP1 inhibitors. Cell death was measured by flow cytometry counting PI-fluorescence of 10,000 cells for each sample. Values represent the means from at least two independent experiments. Error bars indicate the respective SD.

In contrast to the results obtained in the mouse cell lines L929Ts and NIH3T3, no protection against necroptosis by any PARP1 inhibitor was observable for human Jurkat and HT-29 cells. These results further support the hypothesis that inhibition of PARP1 activation does not protect from TRAIL- or TNF-induced necroptosis.

PARP1 is not required for necroptosis but indispensable for programmed necrosis

Thompson and coworkers have shown that $PARP^{-/-}$ cells are protected from alkylating agents that induce DNA damage but are still sensitive to apoptosis, implicating a central role of PARP1 in programmed necrosis (Ditsworth et al., 2007). Therefore, it was investigated whether PARP1 was similarly involved in cytokine-mediated necroptosis. Downregulation of PARP1 by RNA interference in mouse L929Ts and human Jurkat ATCC cells clearly protected from MNNG-mediated programmed necrosis, confirming the central role of PARP1 in this signaling pathway, but had no effect on TNF-mediated necroptosis (Figure 20).

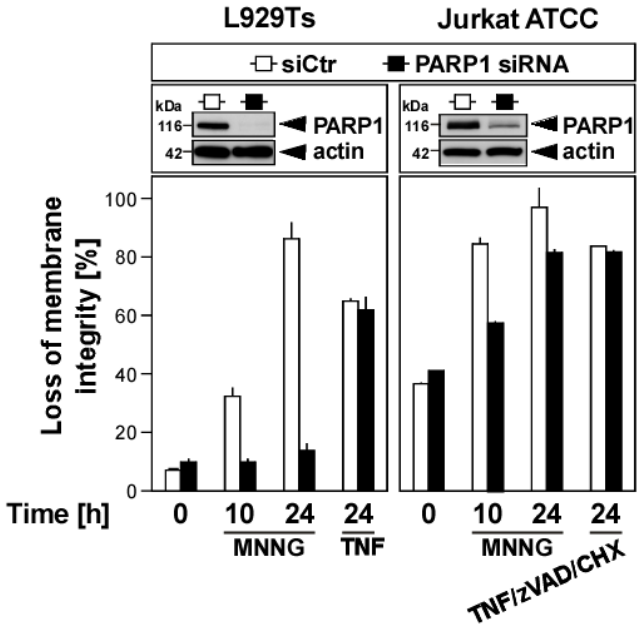

Figure 20. TNF-induced necroptosis is not blocked by downregulation of PARP1. L929Ts or Jurkat ATCC cells were transfected with negative control siRNA (siCtr) or with siRNA specific for murine or human PARP1. Cells were treated for 15 min with 0.5 mM MNNG (and put into fresh medium without MNNG afterwards) or 100 ng/mL hrTNF alone or in combination with 50 µM zVAD-fmk and 2 µg/mL CHX for the indicated periods of time before loss of membrane integrity as a marker for cell death was measured by PI-staining and flow cytometry. Values represent the means form one out of two representative experiments, each in three repetitions. Error bars indicate the respective SD. Insets: control Western blots for endogenous PARP1 (anti-PARP1 form Cell Signaling) and anti-actin (Sigma) for loading control.

Lack of PARP1 does not block, but even enhances TNF- and TRAIL-mediated necroptosis and apoptosis

To validate the hypothesis that TNF- and TRAIL-mediated necroptosis is not PARP1-dependent, cytotoxicity assays were performed in PARP1$^{-/-}$ MEFs or in wildtype MEFs (Figure 21). Moreover, analyses were performed for TNF- and TRAIL-mediated apoptosis (treatment with TNF/CHX or TRAIL/CHX) in order to examine an impact of PARP1-deficieny on caspase-dependent apoptosis. Consistent with an essential role of PARP1 in programmed necrosis induced by DNA-damaging agents, PARP1$^{-/-}$ cells were protected from MNNG-mediated programmed necrosis. Although over time, MNNG treatment killed wildtype cells much more effectively than apoptotic or necroptotic stimuli, necroptosis was not abolished by genetic deletion of PARP1. Likewise, apoptosis was not abolished in PARP1$^{-/-}$ MEFs. Rather, a significant increase in cell death during both apoptosis and necroptosis occurred when PARP1 was absent, possibly because the DNA repair function of PARP1 was also missing.

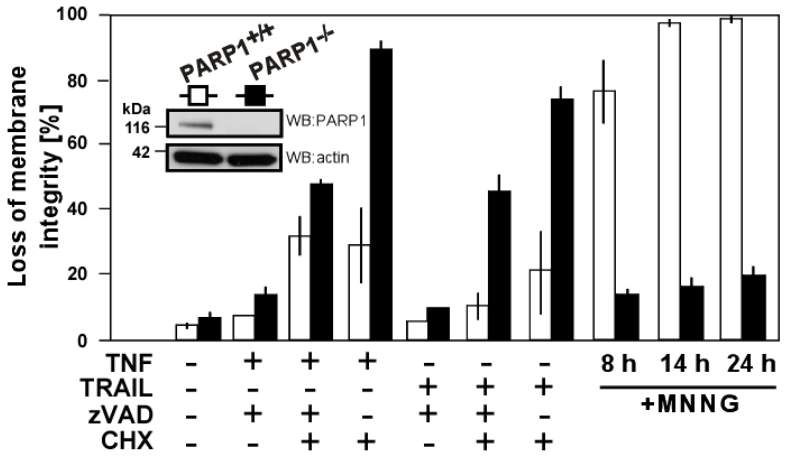

Figure 21. PARP1 is dispensable for TNF- and TRAIL-mediated necroptosis and apoptosis. MEF from PARP1$^{-/-}$ mice and from their wildtype littermates were stimulated with 1µg/ml CHX in combination with 20 µM zVAD-fmk (to induce necroptosis) or without zVAD-fmk (to induce apoptosis) and with 100 ng/mL hrTNF or 50 ng/mL *killer*TRAIL for 24 h. In parallel, cells were stimulated with 0.5 mM MMNG for 15 min and left in fresh medium for 8, 14 or 24 h. Cell death was analyzed after PI-staining by flow cytometric determination of the fraction of PI-positive cells. Values represent the means of three independent experiments, each in three repetitions. Error bars indicate the respective SD. Antibodies: anti-PARP1 (Cell Signaling) and anti-actin (Santa Cruz).

Depletion of intracellular ATP and NAD$^+$ levels does not indicate a role of PARP1 in necroptosis

During programmed necrosis caused by DNA damage, hyperactivation of PARP1 results in a rapid depletion of intracellular NAD$^+$ and ATP (Yu et al., 2002), finally leading to cell lysis. Therefore, it was investigated whether PARP1 had a similar role in TNF- and TRAIL-induced necroptosis.

In the three L929 sublines L929Ts, L929ATCC and L929sA, genotoxic stress induced by MNNG and MMS (a distinct DNA-alkylating agent) caused a rapid depletion of intracellular NAD$^+$ within 30 min post treatment. In contrast, TNF failed to induce changes in NAD$^+$-levels within these early time points, but caused a decrease of NAD$^+$ only after a longer time period (up to 8 h) (Figure 22 A). Similarly, both MNNG and MMS caused the depletion of the intracellular ATP pools promptly within 2 to 4 h, whereas TNF did not induce notable changes in ATP levels within this timeframe (Figure 22 B). Theses clear differences in the changes of the bioenergetic state during TNF- vs. DNA-alkylating agents-induced cell death in the three cell lines provided further evidence for a differential contribution of PARP1 in the corresponding signaling pathways. Whereas the rapid loss of intracellular NAD$^+$ and ATP, induced by MNNG and MMS, clearly prove the rapid activation of PARP1, for TNF-mediated necroptosis, PARP-1 and subsequent individual

components of the associated "PARP-pathway" are apparently activated only late, most likely as an accompanying secondary factor, but rather not as an initial inducer of cellular disintegration.

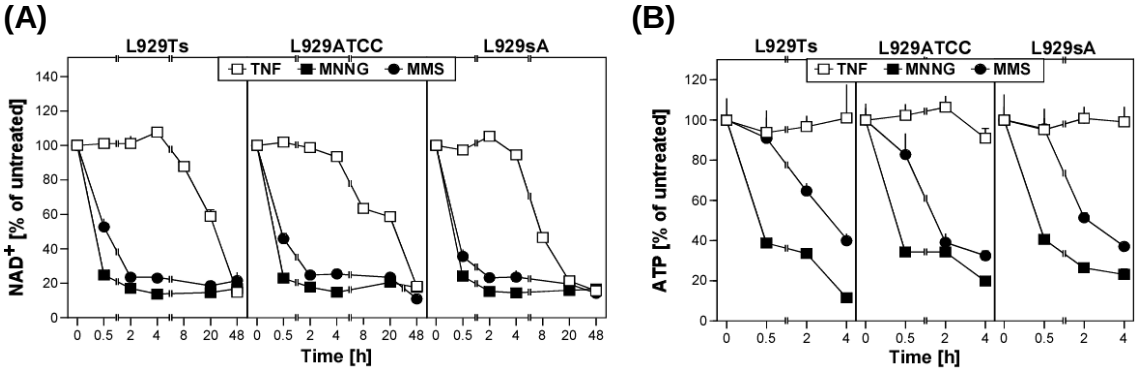

Figure 22. DNA-alkylating agents but not TNF activate the PARP-pathway. L929Ts, L929ATCC and sA cells were stimulated with 0.5 mM MNNG and 25 mM MMS for 15 min and left incubated in fresh medium without MNNG/MMS for the indicated periods of time or were stimulated with 100 ng/mL hrTNF for the indicated time points before their **(A)** intracellular NAD^+ or **(B)** intracellular ATP content was measured. Values represent means of one representative experiment out of three, each in three repetitions. Error bars indicate the respective SD.

The above results were validated and extended by additional experiments, analyzing the depletion of intracellular NAD^+ and ATP pools in combination with the loss of membrane integrity during TNF/zVAD- as well as TRAIL/zVAD-mediated necroptosis in further cell lines. The data presented in (Figure 23) show that in all cases, the NAD^+ and ATP levels did not decrease in the early phase of necroptosis. Rather, the bioenergetic state of the cells stayed stable up to 8 to 10 h after induction of necroptotic cell death. Only in the late phases of necroptosis, dying cells displayed a depletion of intracellular NAD^+ followed by a corresponding decrease in intracellular the ATP pools. However, both events were preceded by a continuous increase in the number of PI-positive cells, reflecting the executive phase of necroptosis. Therefore, in the case of TNF- and TRAIL-mediated necroptosis, the decrease of NAD^+ and ATP levels is rather a result of the loss of cell integrity and disintegration than the activation of PARP1. In summary, these data again confirm that activation of PARP1 is dispensable for TNF- and TRAIL-mediated necroptosis.

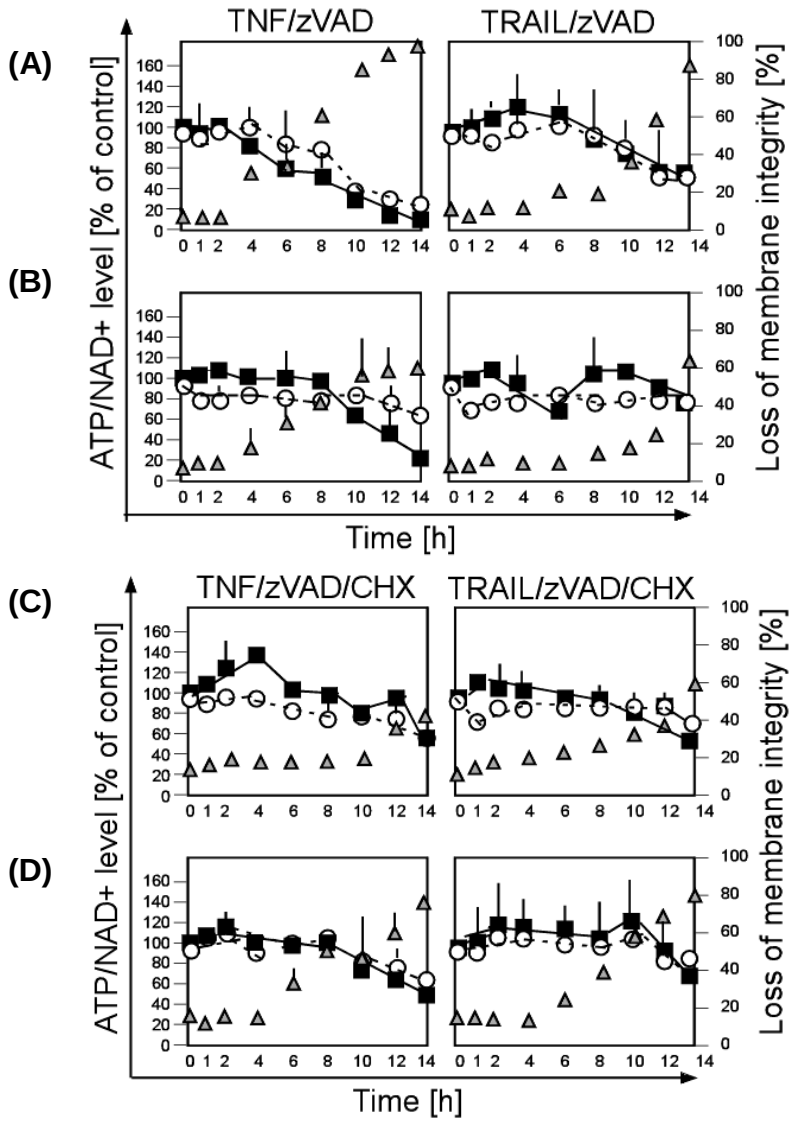

Figure 23. Depletion of intracellular ATP, NAD^+ levels and loss of membrane integrity during TNF- and TRAIL-mediated necroptosis. (A) L929Ts cells were stimulated 20 µM zVAD-fmk in combination with 100 ng/mL hrTNF or 30 ng/mL *killer*TRAIL for the indicated periods of time. **(B)** NIH3T3 cells were incubated with 100 ng/mL hrTNF or 100 ng/mL *killer*TRAIL in combination with 20 µM zVAD-fmk for indicated time points. **(C)** Jurkat cells were stimulated 100 ng/mL hrTNF or 50 ng/mL *killer*TRAIL in combination with 50 µM zVAD-fmk and 2 µg/mL CHX for indicated time. **(D)** HT-29 cells were treated with 100 ng/mL hrTNF or 30 ng/mL *killer*TRAIL in combination with 20 µM zVAD-fmk and 50 µg/mL CHX for the indicated periods of time before their intracellular NAD^+ or intracellular ATP levels were measured. Values are expressed as % of untreated cells. In parallel, cell death was analyzed after PI-staining by flow cytometric determination of the fraction of PI-positive cells. Values represent the means of a minimum of two independent experiments, and are shown (for ATP and NAD^+ levels) relative to untreated cells. Error bars indicate the respective SD.

The enzyme PARP1 is either inactivated or activated depending on whether a cell dies via apoptosis or necrosis. Therefore, estimation of its activity can potentially be used as marker to distinguishing both forms of cell death (Putt et al., 2005). Similarly, the above data show that in the cell lines examined here, PARP1 is highly activated during programmed necrosis induced by DNA damage whereas PARP1 shows only moderate or late activation during necroptosis. Those data demonstrate that during necroptosis, cells do

not die as a consequence of bioenergetic catastrophe, but rather that further execution of necroptosis requires the preservation of the cellular energetic state.

2. Translocation of AIF (apoptosis inducing factor) from mitochondria into the nucleus is not necessary for necroptosis

In response to activation of PARP1 due to DNA damage, the mitochondrial protein AIF translocates into the nucleus, where it essentially mediates programmed necrosis (Figure 6) (Moubarak et al., 2007, Cohausz et al., 2008). In order to augment the above analyses of the signal transduction pathways involved in caspase-independent cell death, the participation of AIF in TNF- and TRAIL-mediated necroptosis was investigated, specifically if translocation of AIF from mitochondria to nucleus occurs during TNF- and TRAIL-mediated necroptosis. Western blots of nuclear and cytoplasmic fractions from murine L929Ts cells demonstrated that the nuclear translocation of AIF is not an early event during necroptosis, but occurs late (Figure 24, lanes 4, 5, 9, 10), most likely as a consequence rather than the cause of the progressing necroptotic cellular disintegration (which is also illustrated by the disappearance of actin at those late time points, Figure 24 and Figure 25, lanes 4, 5, 9, 10). In addition, and consistent with the earlier results shown in Figure 11-Figure 15, PARP1 activation/disappearance, accompanied by the massive generation of PAR chains was again detectable only in the late steps of necroptosis (Figure 24, lanes 3 and 9, 10). Therefore, nuclear translocation of AIF is not an initial, causative process in the signaling pathways by which TNF and TRAIL mediate necroptosis, but rather associated with later stages as a consequence of cellular destruction.

Since the antibody for AIF was directed against its C-terminal end, it also allowed the detection of a shortened form of AIF (AIFsh, AIF short) (Figure 24, lanes 4, 5, 9, 10, asterisks), which has also been described to induce caspase-independent cell death through chromatin condensation and large-scale (50 kb) DNA fragmentation (Delettre et al., 2006). However, similar to full-length AIF, AIFsh was detectable in the nucleus only during the later phases of necroptosis, also as a consequence and not a cause of necroptosis. Interestingly, for TNF-mediated necroptosis in the absence of zVAD-fmk (which occurs in L929Ts cells, but less vigorously than with zVAD-fmk), the AIFsh form was not detected (Figure 23, lane 2 versus lane 5), pointing to differences in the proteolytic processing of AIF in the presence or absence of zVAD-fmk. Moreover, a control for TRAIL-mediated apoptosis (Figure 24, lane 7) did not reveal translocation of AIF or presence of AIFsh in

the nuclear fraction, as these events are not common for apoptosis but abundant for programmed necrosis.

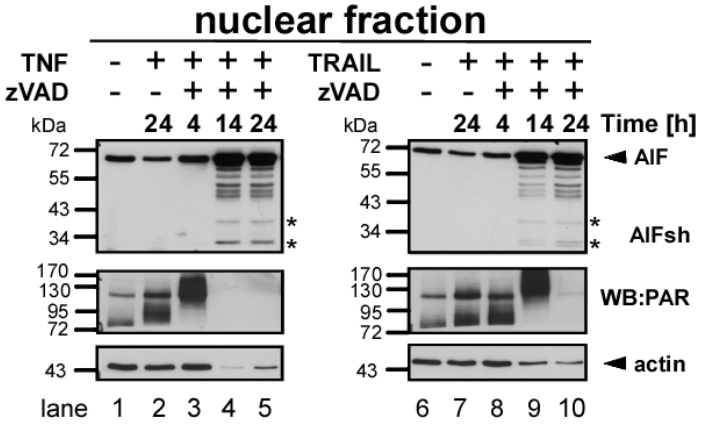

Figure 24. AIF translocation to the nucleus and PARP1 poly(ADP)-ribosylation are late events in TNF- and TRAIL-mediated necroptosis in murine cells. L929Ts cells were left unstimulated or stimulated with 100 ng/mL hrTNF or 30 ng/mL *killer*TRAIL for 24 h. Alternatively, cells were treated with TNF or TRAIL in combination with 20 µM zVAD-fmk for the indicated periods of time. Afterwards, enriched nuclear fractions of the cells were prepared. Antibodies: anti-AIF (D-20, Santa Cruz), anti-PARP1 (Cell Signaling), anti-PAR (BD Pharmingen) anti-actin (Santa Cruz); asterisks indicate the putative presence of AIFsh (AIF short).

In the remaining cytoplasmic/organelle fractions, a decrease of AIF levels was observed only in the late phase of cell death (Figure 25, lanes 4, 5 and 9, 10). Moreover, in the nuclear enzyme PARP1 was not found in the cytoplasmic/organelle fractions. Furthermore, PAR chains that were detected in the nuclear fraction (Figure 24) were not detected in the cytoplasmic/organelle fraction, despite of nonspecific crossreaction with the PAR antibody, creating a smear in the entire lane (Figure 25, lanes 1, 3, 6, 8). A decrease of actin additionally illustrates that both TNF- and TRAIL-mediated necroptosis are extensively executed at timepoints later than 4 h, leading to the degradation of cellular proteins (Figure 24 and Figure 25, lanes 4, 5 and 9, 10).

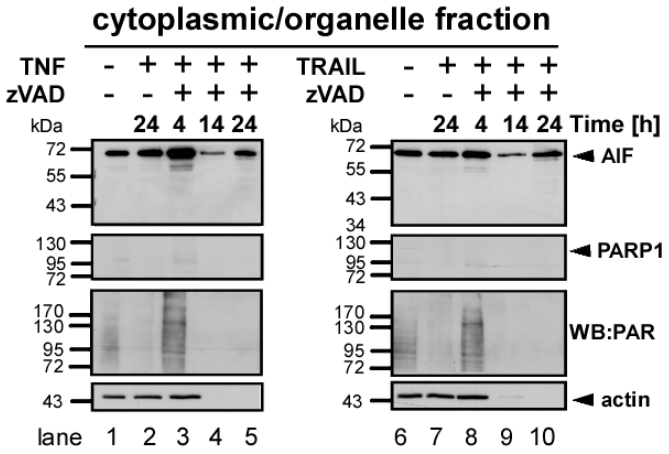

Figure 25. In the late phases of necroptosis, AIF levels decrease in the cytoplasmic/organelle fractions. L929Ts cells were stimulated with 100 ng/mL hrTNF or 30 ng/mL *killer*TRAIL for 24 h alone or in combination with 20 µM zVAD-fmk for the indicated periods of time. Afterwards, cytoplasmic/organelle fractions of the cells were prepared. Antibodies: anti-AIF (D-20, Santa Cruz), anti-PARP1 (Cell Signaling), anti-PAR (BD Pharmingen), anti-actin (Santa Cruz).

3. The RIP1-RIP3 complex is not necessary for MNNG-mediated programmed necrosis but is essential for TNF-mediated necroptosis

Recently, PARP1 was found to regulate the expression of TNF and of adhesion molecules (Jog et al., 2009), thus influencing cell death. Moreover, other members of the TNF receptor family are also influenced by PARP1. For example, an RNA interference study has shown transcriptional regulation of TRAIL-R1 and -R2 (DR4 and DR5) in a PARP1-dependent manner (Cohausz and Althaus, 2009). Independently, it was published that RIP1 controls PARP1-mediated cell death (Xu et al., 2006). Therefore, the next goal of this thesis was to investigate if a crosstalk exists between PARP1 and the RIP1-RIP3-mediated execution of TNF-induced necroptosis.

First, analyses of MEFs deficient for TNF-R1 demonstrated their full resistance to TNF-mediated necroptosis, but the same sensitivity to MNNG-mediated cell death as wildtype MEFs (Figure 26). This indicates that PARP1-mediated cell death does not depend on signals mediated by TNF-R1.

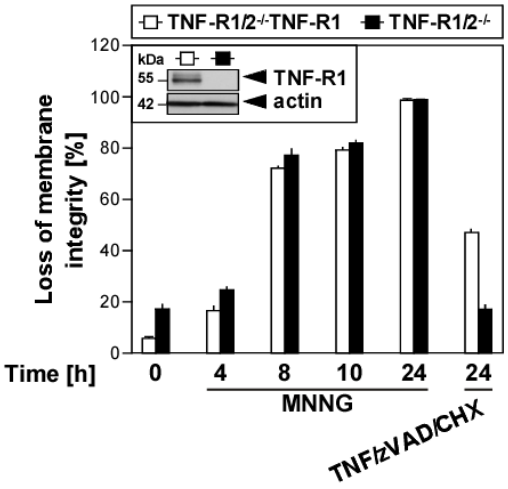

Figure 26. TNF-R1 is not involved in PARP1-dependent programmed necrosis but mediates TNF-induced necroptosis. TNF-R-1/2$^{-/-}$ fibroblasts and TNF-R1/2$^{-/-}$ fibroblasts stably re-expressing TNF-R1 (TNF-R1/2$^{-/-}$TNF-R1) were stimulated for 15 min with 0.5 mM MNNG and subsequently incubated in fresh medium without MNNG for the indicated periods of time. Simultaneously, cells were treated with 100 ng/mL hrTNF in combination with 20 µM zVAD-fmk and 1 µg/mL CHX for 24 h before loss of membrane integrity as a marker for cell death was measured by PI-staining and flow cytometry. Inset: control Western blots for TNF-R1 (Santa Cruz) and actin (Sigma). Error bars indicate the respective SD. One representative experiment out of three independent repetitions performed in triplicates is shown.

In further experiments, it was shown that neither pharmacological inhibition of RIP1 by Nec-1 (Figure 27 A) nor genetic ablation of RIP1 in MEFs (Figure 27 B) nor siRNA-mediated downregulation of RIP1 in murine NIH3T3 cells that naturally express RIP3 (Zhang et al., 2009) (Figure 27 C) protected cells from PARP1-mediated programmed necrosis. Likewise, the rapid loss of intracellular ATP as one of the first steps of MNNG/PARP1-induced programmed necrosis was not affected by presence or absence of RIP1 (Figure 27 B and C). In contrast, pharmacologic or genetic interference with RIP1 consistently abolished TNF-mediated necroptosis (Figure 27). These data suggest that in the cell systems examined here, RIP1 is not necessary for PARP1-mediated programmed necrosis but is indispensable for TNF-mediated necroptosis.

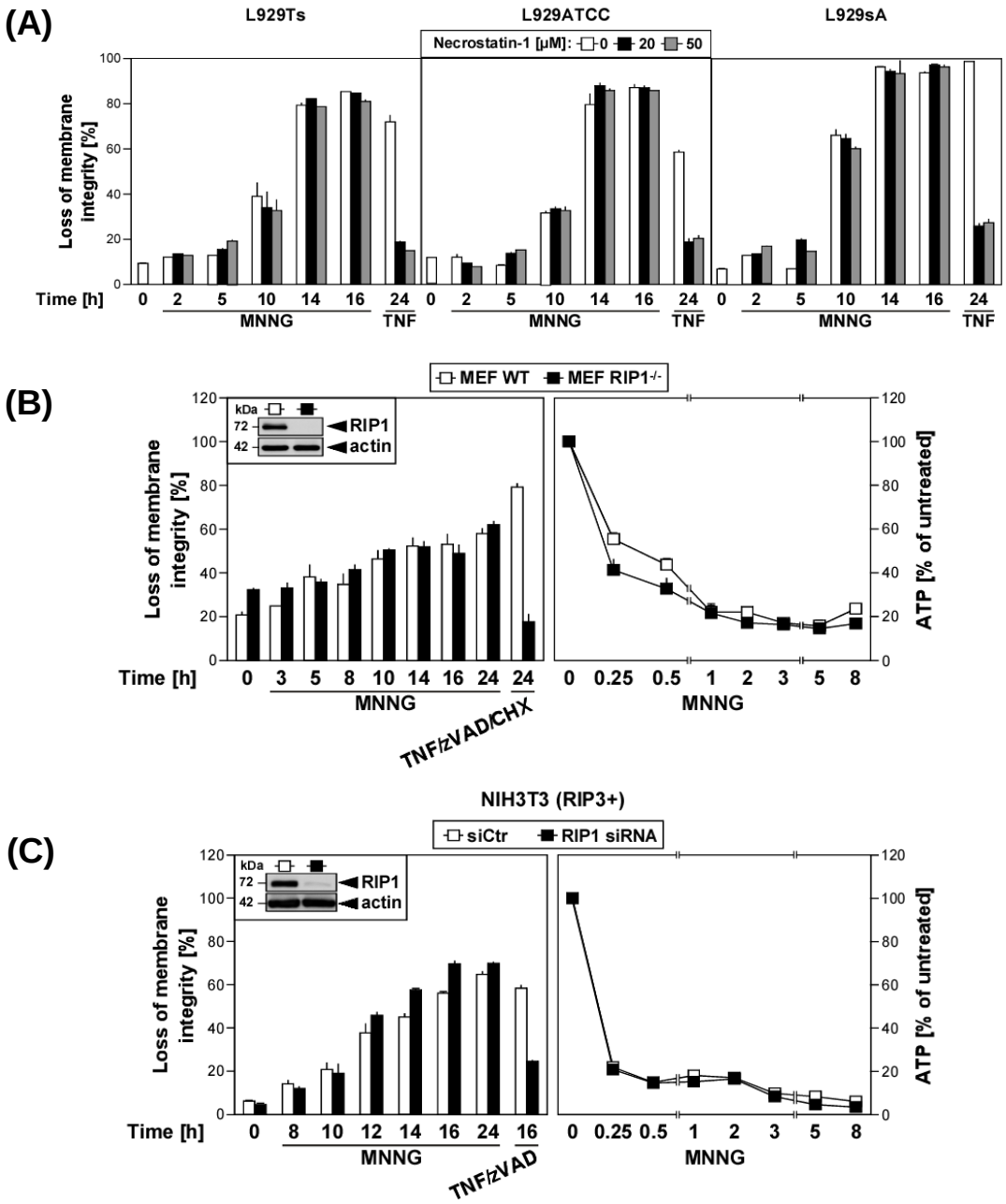

Figure 27. RIP1 is not necessary for PARP1-mediated programmed necrosis but is indispensable for TNF-mediated necroptosis in L929 cells, MEFs and NIH3T3 cells. (A) L929Ts, ATCC and sA cells were pre-stimulated for 2 h with the indicated concentrations of Nec-1 and stimulated afterwards with 0.5 mM MNNG for 15 min and subsequently incubated in fresh medium without MNNG and Nec-1, or with 100 ng/mL hrTNF and Nec-1 for the indicated periods of time. Loss of membrane integrity as a marker for cell death was measured by PI-staining and flow cytometry. **(B)** MEFs deficient for RIP1 and wildtype MEFs were stimulated with MNNG or hrTNF as in (A) in combination with 20 μM zVAD-fmk and 1 μg/mL CHX for the indicated periods of time. Loss of membrane integrity in WT and RIP1$^{-/-}$ MEFs was measured by PI uptake. Concurrently, analyses of intracellular ATP levels from MNNG-stimulated cells were performed. Inset: control Western blots for endogenous RIP1. **(C)** NIH3T3 cells naturally expressing RIP3 were transfected with negative control (siCtr) or mouse siRNA specific for RIP1 and stimulated with MNNG or hrTNF in combination with 20 μM zVAD-fmk as in (A) for the indicated periods of time. Loss of membrane integrity was measured by PI uptake. Parallel analyses of intracellular ATP-levels from MNNG stimulated cells were performed. Inset: control Western blots for endogenous RIP1, downregulation of RIP1 (anti-RIP1 from Cell Signaling) and actin (anti-actin from Sigma). One representative experiment out of three independent repetitions performed in triplicates is shown for each panel. Error bars indicate the respective SD.

Additionally examined RIP1-deficient Jurkat cells likewise proved resistant against TNF-induced necroptosis, but, other than MEFs and NIH3T3 cells, displayed a certain, transient protection from MNNG-mediated cell death in the early phase of the cell death, which however not prevented the final execution of programmed necrosis (Figure 28). Identical to L929 cells, MEFs and NIH3T3 cells, the rapid loss of intracellular ATP during MNNG/PARP1-induced programmed necrosis was not affected by presence or absence of RIP1. This suggests that the transient protection of RIP1-deficient Jurkat cells from MNNG/PARP1-induced programmed necrosis is not due to an action of RIP1 in the early, but rather in later, secondary steps of the PARP-pathway.

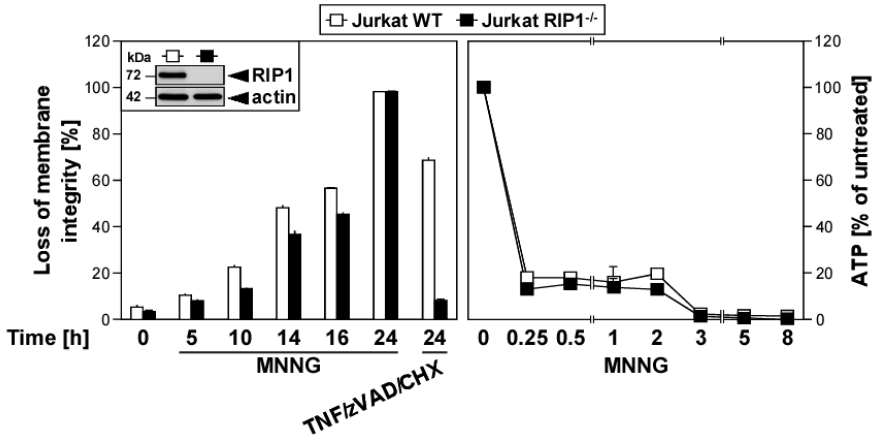

Figure 28. RIP1 provides a transient protection from PARP1-mediated programmed necrosis in human T cells. Wildtype and Jurkat cells lacking RIP1 were treated with 0.5 mM MNNG for 15 min and subsequently incubated in fresh medium without MNNG or with 100 ng/mL hrTNF in combination with 50 µM zVAD-fmk and 2 µg/mL CHX for the indicated periods of time before loss of membrane integrity as a marker for cell death was measured by PI-staining and flow cytometry. Inset: control Western blots for endogenous RIP1 (anti-RIP1 from Cell Signaling) and actin as loading control (Sigma). Simultaneously, analyses of intracellular ATP-levels from MNNG-stimulated cells were performed. Values represent the means of one out of three independent experiments in three replications each. Error bars indicate the respective SD.

Latest analyses have implicated PARP1 as an active effector downstream of the RIP1-RIP3 signaling complex in TRAIL-mediated necroptosis (Jouan-Lanhouet et al., 2012). Therefore, a crosstalk between RIP3 and PARP1 in programmed necrosis was additionally analyzed. For this purpose, naturally RIP3-deficient NIH3T3 cells (Zhang et al., 2009) and stable transfectants overexpressing wildtype RIP3 kinase or a kinase dead form of RIP3 were investigated as above. Similar to RIP1-deficient Jurkat cells, RIP3-deficient NIH3T3 cells displayed a transient attenuation, but not protection from MNNG-mediated cell death, while being fully resistant against TNF/zVAD-induced necroptosis (Figure 29 A). Importantly, the stable re-expression of kinase-defective RIP3 did not confer a transient or permanent protection from PARP1-mediated cell death. This indicates that the kinase activity of RIP3 is not required for a function of RIP3 in the PARP1-pathway. This is

adverse to TNF/zVAD-mediated necroptosis, for which a functional kinase domain and the physical presence of RIP3 is essential.

Subsequently, RIP3 was downregulated in NIH3T3 cells that naturally express RIP3 (Zhang et al., 2009). Similar to previous data, depletion of RIP3 protected naturally RIP3-expressing NIH3T3 cells from TNF-induced necroptosis while only transiently attenuating PARP1-mediated programmed necrosis (Figure 29 B). The rapid loss of ATP during MNNG-induced programmed necrosis occurred identically in RIP3-deficient, -downregulated or -retransfected cells, implicating that like RIP1, the transient protection of RIP3-deficient or -downregulated NIH3T3 cells from PARP1-induced programmed necrosis is due to an action of RIP3 in the later, secondary steps of the PARP-pathway.

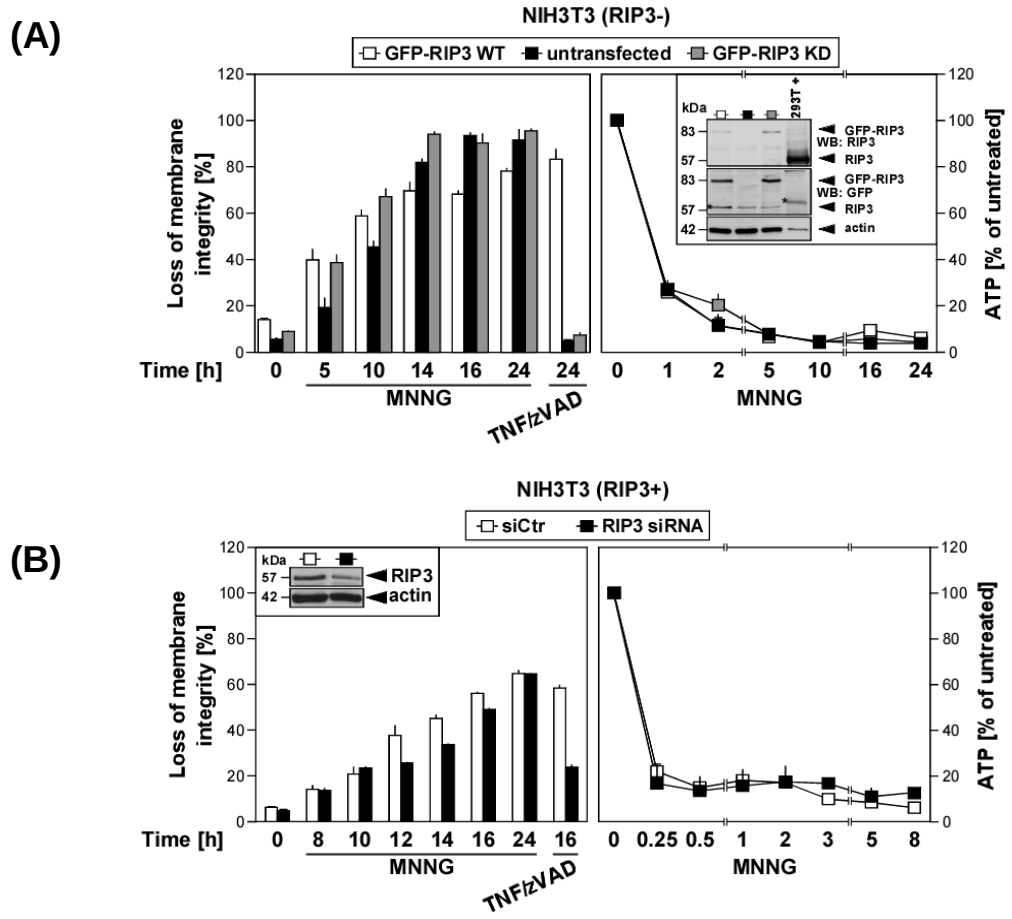

Figure 29. RIP3 provides a transient protection from PARP1-mediated programmed necrosis and is indispensable for necroptosis in mouse 3T3 cells. (A) NIH3T3 cells naturally lacking RIP3 and cells retransfected with wildtype RIP3 (GFP-RIP3 WT) or RIP3 with a non-functional kinase domain (GFP-RIP3 KD) were stimulated with 0.5 mM MNNG for 15 min and subsequently incubated in fresh medium without MNNG or stimulated with 100 ng/mL hrTNF in combination with 20 µM zVAD-fmk for the indicated periods of time. Loss of membrane integrity as a marker for cell death was measured by PI-staining and flow cytometry. Inset: control Western blot for murine RIP3 (anti-RIP3 form Enzo, top), GFP (anti-GFP from Clontech, middle) or actin (anti-actin form Sigma, bottom) to verify expression of the constructs, absence of endogenous murine RIP3, and equal loading. Asterisks indicate unspecific bands. **(B)** NIH3T3 cells naturally possessing RIP3 were transfected with negative control (siCtr) or mouse siRNA specific for RIP3 and stimulated as described in (A). Inset: control Western blot for endogenous and downregulated RIP3 (anti-

RIP3 from Abnova) and anti-actin (Sigma) as loading control. Simultaneously, analyses of intracellular ATP-levels from MNNG-stimulated cells were performed. One representative experiment out of three independent repetitions performed in triplicates is shown. Error bars indicate the respective SD.

Additional analyses were performed in primary mouse embryonic fibroblast deficient for RIP3 (Figure 30 A) and freshly prepared lung fibroblast lacking RIP3 (Figure 30 B). In these cells, TNF/zVAD/CHX-induced necroptosis was completely blocked, whereas the course of MNNG-induced necrosis was not altered. Again, the absence of RIP3 did not prevent the MNNG-induced rapid loss of intracellular ATP as an early step of the PARP-pathway Figure 30 in line with the above results. Therefore, in the examined MEFs and lung fibroblasts, RIP3 has no function in the PARP1-pathway, in contrast to its essential function in TNF-induced necroptosis.

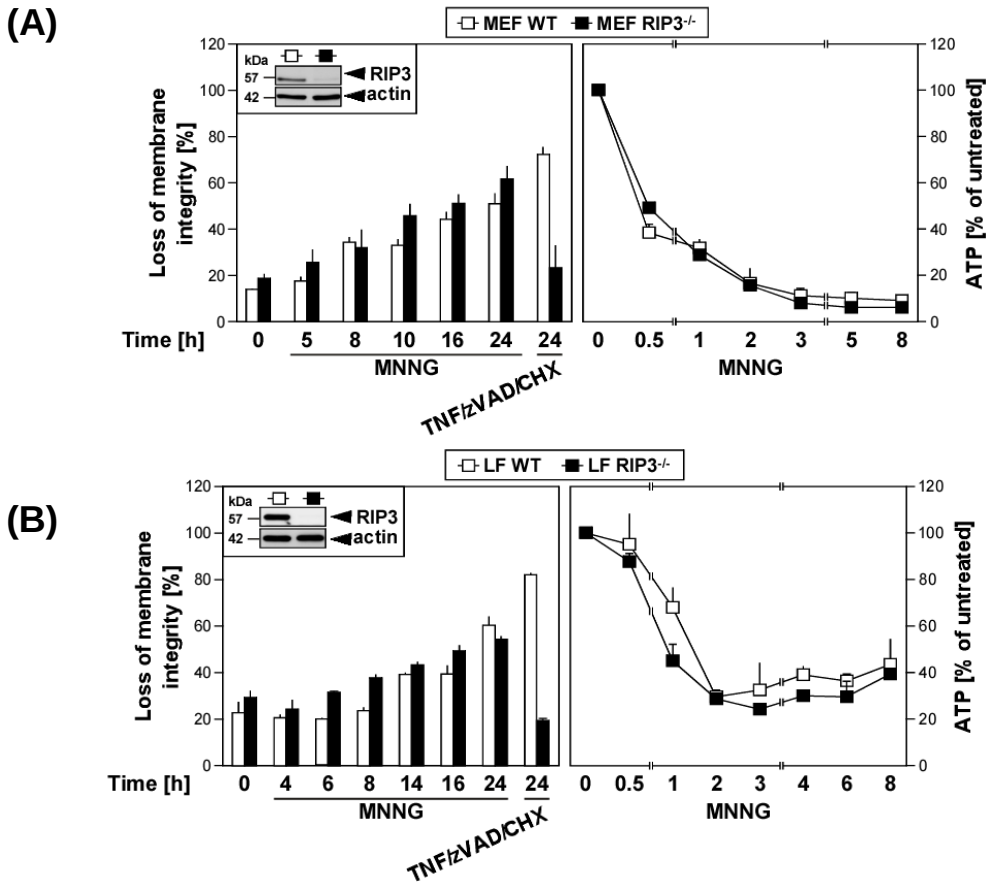

Figure 30. RIP3 is dispensable for PARP1-mediated programmed necrosis but is indispensable for TNF-mediated necroptosis in MEFs and lung fibroblasts. (A) primary MEFs and **(B)** freshly prepared lung fibroblasts (LF) deficient for RIP3 and their wildtype counterparts were stimulated for 15 min with 0.5 mM MNNG and subsequently incubated in fresh medium without MNNG or with 100 ng/mL hrTNF in combination with 20 µM zVAD-fmk and 1 µg/mL CHX for 24 h for the indicated periods of time. Loss of membrane integrity as a marker for cell death was measured by PI-staining and flow cytometry. Insets: control Western blots for endogenous RIP3 (anti-RIP3 form Abnova) and anti-actin (Sigma) as loading control. Simultaneously, analyses of intracellular ATP-levels from MNNG stimulated cells were performed. One representative experiment out of three independent repetitions performed in triplicates is shown. Error bars indicate the respective SD.

In summary, the above data confirm that while RIP1 is clearly crucial for TNF-induced necroptosis in a cell type-independent manner; its contribution to MNNG-induced necrosis appears to be of more limited importance and cell type-specific. Although previously not investigated, the data obtained here indicate that the same is also true for RIP3.

B. Analysis of the molecular signaling pathways of TNF- and TRAIL-mediated necroptosis

Of interest for this part of the thesis were molecular mechanisms which define the necroptotic capabilities of the two cytokines TNF and TRAIL. The comparison of the necroptotic signaling pathways mediated by those two cytokines was expected to provide further insight into the complexity and variability of necroptosis. Furthermore, a better understanding of necroptosis induced by these two members of the TNF superfamily is of potential significance for various therapies, as this type of cell death has been implicated in a broad range of pathophysiological states.

1. RIP1 triggers TRAIL-mediated necroptosis

Previous work had revealed that the protein kinase RIP1 is indispensable for TNF-mediated necroptosis (Thon et al., 2005). By utilizing Jurkat cells deficient for RIP1-expression it was shown that TRAIL-induced necroptotic cell death is abolished in these cells (Figure 31 A). Independently, treatment with radicicol (RC) which acts similarly to geldanamycin (GA), an ATP-competitive inhibitor of Hsp90 and indirectly reduces RIP1 protein levels (Lewis et al., 2000) significantly increased the survival of murine L929Ts and NIH3T3 cells as well as human Jurkat cells after induction of TRAIL-mediated necroptosis (Figure 31 B), in summary confirming the role of RIP1 as a main component also of TRAIL-mediated necroptosis.

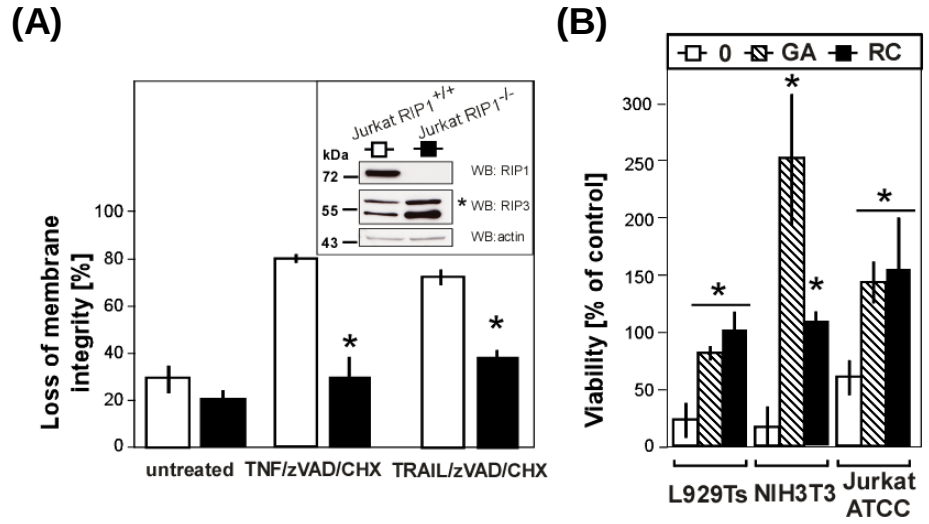

Figure 31. RIP1 transmits the death signal in TNF- and TRAIL- mediated necroptosis. (A) Wildtype and RIP1-deficient (RIP1$^{-/-}$) Jurkat cells were left untreated or stimulated with 50 ng/mL *killer*TRAIL or 100 ng/mL hrTNF in combination with 50 µM zVAD-fmk and 2 µg/mL CHX for 20 h before cell death was examined by flow cytometry, counting PI-fluorescence of a sample of 10,000 cells. Data were obtained from

minimum three independent experiments. Error bars indicate the respective SD. Asterisks indicate statistical significance (t-test) $p<0.01$. Insets: control Western blots for endogenous RIP1 and RIP3. Actin served as a loading control. Asterisk in Western blot: unspecific band. **(B)** L929Ts, NIH3T3 and Jurkat ATCC cells were left untreated or preincubated with 1 µg/mL GA (geldanamycin) or 5 µg/mL RC (radicicol) for 24 h. Afterwards, L929Ts and NIH3T3 cells were left untreated or stimulated with 20 µM zVAD-fmk in combination with 30 ng/mL or 100 ng/mL of *killer*TRAIL, respectively. Jurkat wildtype cells were left untreated or stimulated with 50 µM zVAD-fmk and 2 µg/mL CHX in combination with 50 µg/mL *killer*TRAIL. After 24 h of incubation, cell death was analyzed by flow cytometric counting of PI-positive cells. Data were obtained from three experiments in each a sample of 10,000 cells was analyzed. The fraction of surviving cells is displayed relative to cells that were treated as above, except that no TRAIL/zVAD (TRAIL/zVAD/CHX) was added. Error bars indicate the respective SD. Values represent the means of a minimum of three independent experiments. Asterisks indicate statistical significance (t-test) $p<0.01$.

2. Ceramide generation is important for necroptosis

2.1 A-SMase and N-SMase are involved in TNF-and TRAIL-induced necroptosis in murine cells

Ceramide was described to mediate non-apoptotic caspase independent cell death (Kim et al., 2005), particularly generated by A-SMase after stimulation of TNF-R1 (Thon et al., 2005). Previously, a pharmacological approach using the inhibitors D609, desipramine, imipramine for A-SMase, GW4869 and spiroepoxide for N-SMase as well as fumonisin B_1 for ceramide synthase had been performed to determine the enzyme which generated ceramide during necroptosis (Sosna, 2010). The results from these experiments had confirmed the crucial role of A-SMase and (less pronounced) N-SMase for generation of ceramide involved in TNF-mediated necroptotic signaling. In order to obtain further insight into the role of ceramide generated through A-SMase or N-SMase not only in TNF- but also in TRAIL-induced necroptosis, the three novel A-SMase inhibitors ARC39, TP102, TP064/14e (Appendix, Figure 84) (Roth et al., 2009a, Roth et al., 2009b, Roth et al., 2010) together with zoledronic acid as well as the N-SMase inhibitors 3-OMS (3-*O*-methyl-sphingomyelin) and spiroepoxide were investigated.

In murine L929Ts cells, inhibition of A-SMase by the novel potent inhibitor ARC39 was sufficient to significantly reduce the rate of both TNF- and TRAIL-induced necroptosis (Figure 32 A and B). Similarly, in NIH3T3 cells, inhibition of A-SMase by ARC39 showed a protective effect (Figure 33 A and B). However, another bisphosphonate-based inhibitor (zoledronic acid) inhibited necroptosis with statistical significance only in L929Ts but not in NIH3T3 cells. Subsequently, the inositol-bisphosphate-based inhibitor TP064/14e did not prevent either TNF- or TRAIL-mediated necroptosis in both murine cell lines (Figure 32 A, B and Figure 33 A, B). Similarly, TP102, another inositol-

bisphosphate-based inhibitor failed to protect murine L929Ts cells from TNF- and TRAIL-mediated necroptosis (Appendix, Figure 85). These results suggest that the various inhibitors differ in their effectiveness to suppress A-SMase activity, possibly depending on their chemical composition, composition (bisphosphonate-based vs. inositol-based), and even exerting cell line-specific effects.

Independently, in both murine L929Ts and NIH3T3 cells, TNF- and TRAIL-induced necroptosis was impaired by inhibition of N-SMase with spiroepoxide and 3-OMS (Figure 32 A, B and Figure 33 A, B), pointing to an involvement of ceramide generated not only by A-SMase, but also by N-SMase.

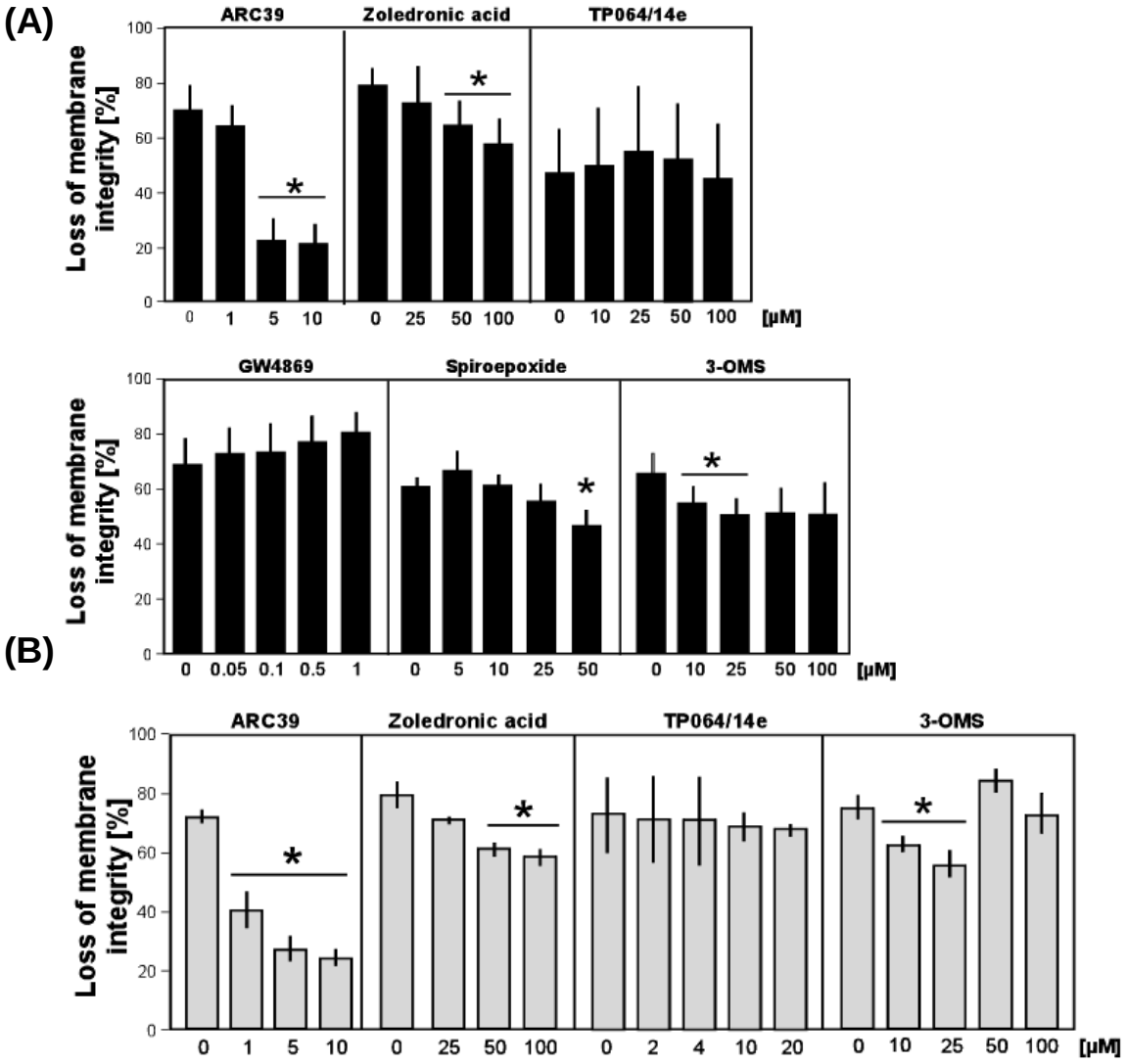

Figure 32. Inhibition of A-SMase or N-SMase protects murine L929Ts cells from TNF and TRAIL-mediated necroptosis. Cells were pre-treated for 2 h with the indicated concentrations of inhibitors and subsequent addition of **(A)** 100 ng/mL hrTNF for 5 h or **(B)** 30 ng/mL *killer*TRAIL for 14 h in combination with 20 µM zVAD-fmk. Cell death was analyzed after PI-staining by flow cytometric determination of the fraction of PI-positive cells. Values represent the means of a minimum of two independent experiments. Error bars indicate the respective SD. Asterisks indicate statistical significance (t-test) $p<0.01$.

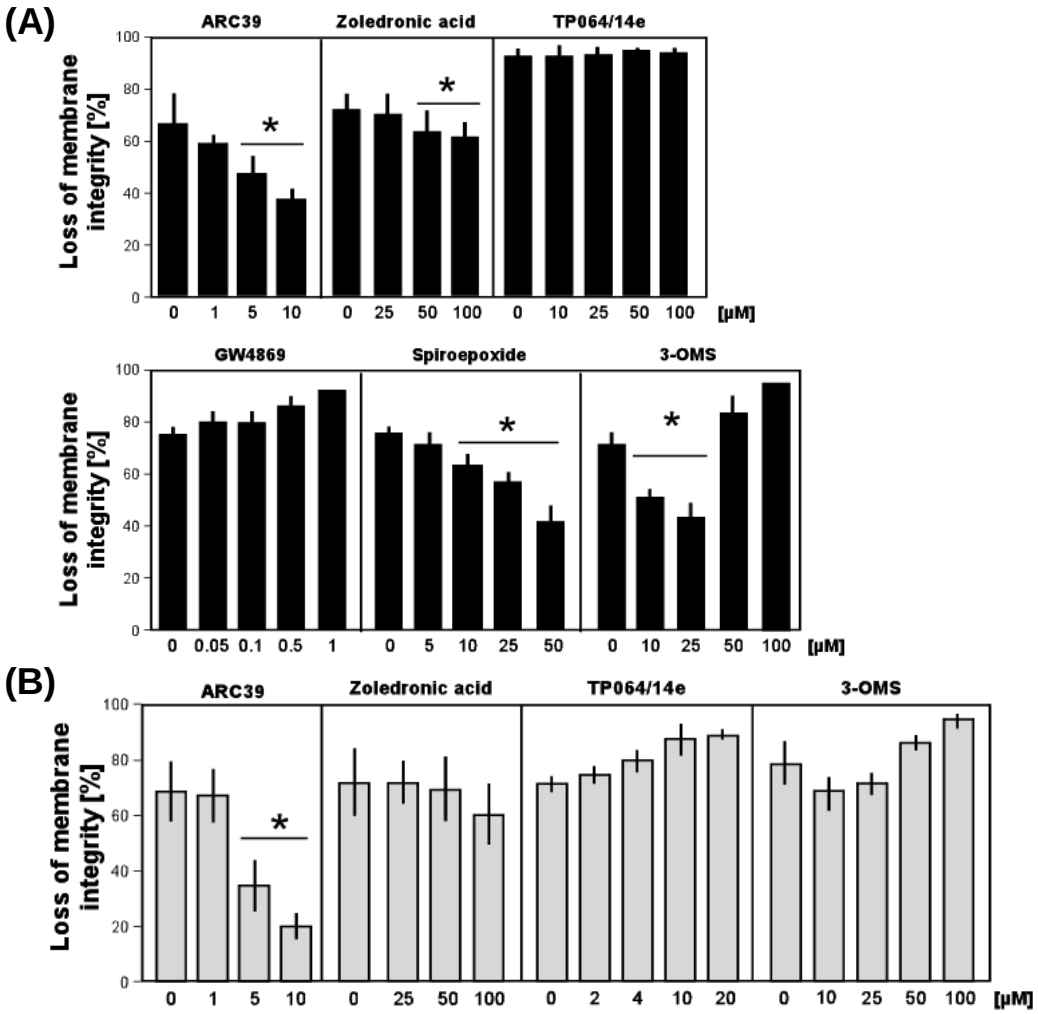

Figure 33. Inhibition of A-SMase or N-SMase protects murine NIH3T3 cells from TNF- and TRAIL-mediated necroptosis. Cells were pre-treated for 2 h with the indicated concentrations of inhibitors and subsequnet addition of **(A)** 100 ng/mL hrTNF or **(B)** 100 ng/mL killerTRAIL in combination with 20 µM zVAD-fmk for 16 h. Cell death was analyzed after PI-staining by flow cytometric determination of the fraction of PI-positive cells. Values represent the means of a minimum of two independent experiments. Error bars indicate the respective SD. Asterisks indicate statistical significance (t-test) $p<0.01$.

2.2 A-SMase is involved in TNF-induced necroptosis in human cells

To obtain a deeper insight into the role of ceramide during TNF- and TRAIL-induced necroptosis in human cells, the cell lines HT-29 and Jurkat ATCC were analyzed. In HT-29 cells, none of the A-SMase inhibitors showed a significant protection against TNF- and TRAIL-mediated necroptosis (Figure 34 A, B). Similarly, in the human cell line Jurkat ATCC, neither TNF- nor TRAIL-induced necroptosis was impaired by inhibition of A-SMase (Figure 35 A, B). Moreover, there was no evidence for a role of N-SMase during necroptosis in human cells. In HT-29 and Jurkat ATCC cells, similarly to mouse cell lines, ceramide synthase was also not involved in necroptosis.

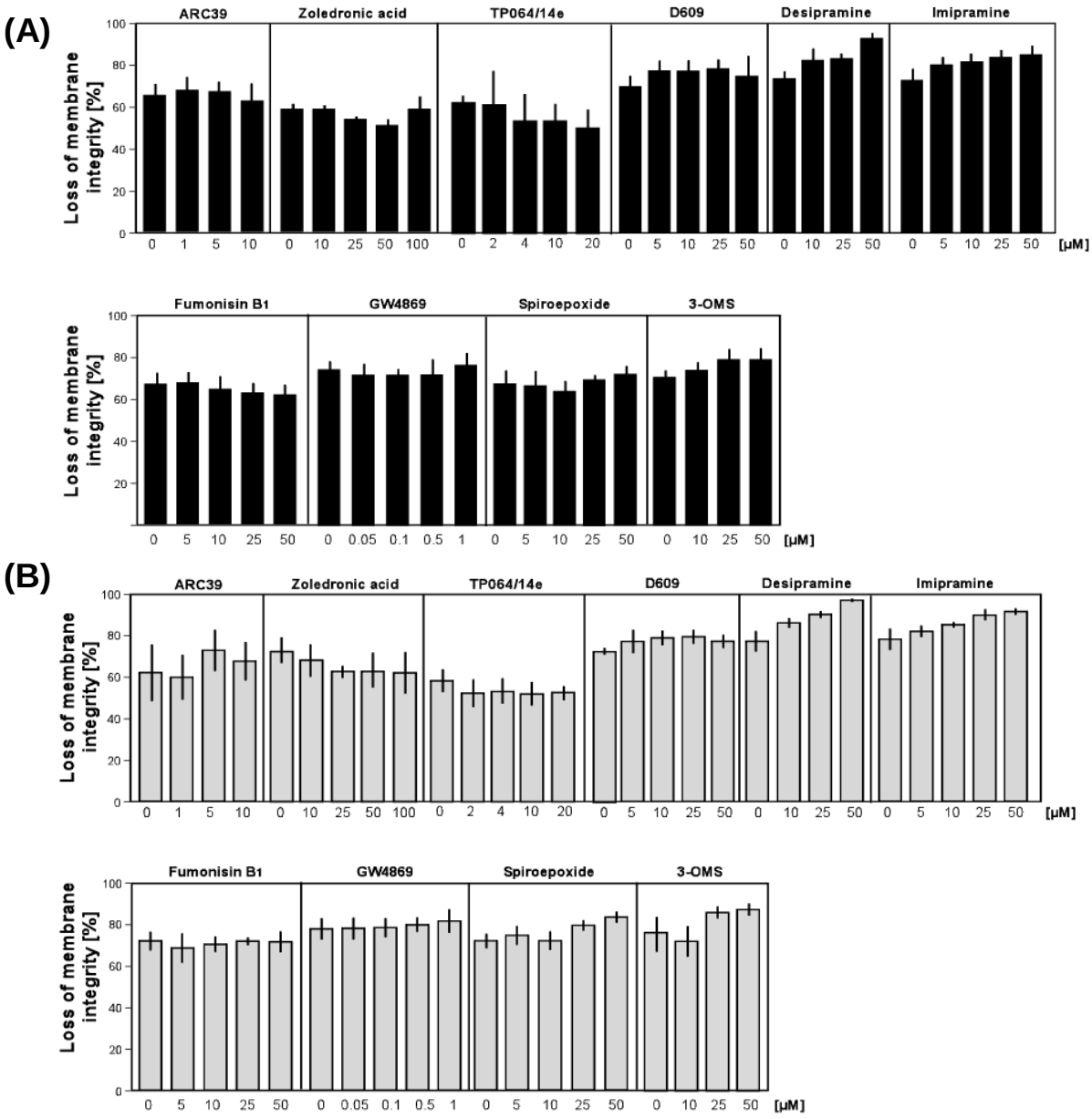

Figure 34. Effects of A-SMase and N-SMase inhibitors on TNF- and TRAIL-mediated necroptosis in human HT-29 cells. Cells were pre-treated for 2 h with the indicated concentrations of inhibitors and subsequent addition of **(A)** 100 ng/mL hrTNF or **(B)** 30 ng/mL *killer*TRAIL in combination with 20 µM zVAD-fmk and 5 µg/mL CHX for 16 h. Cell death was analyzed after PI-staining by flow cytometric determination of the fraction of PI-positive cells. Values represent the means of a minimum of two independent experiments. Error bars indicate the respective SD.

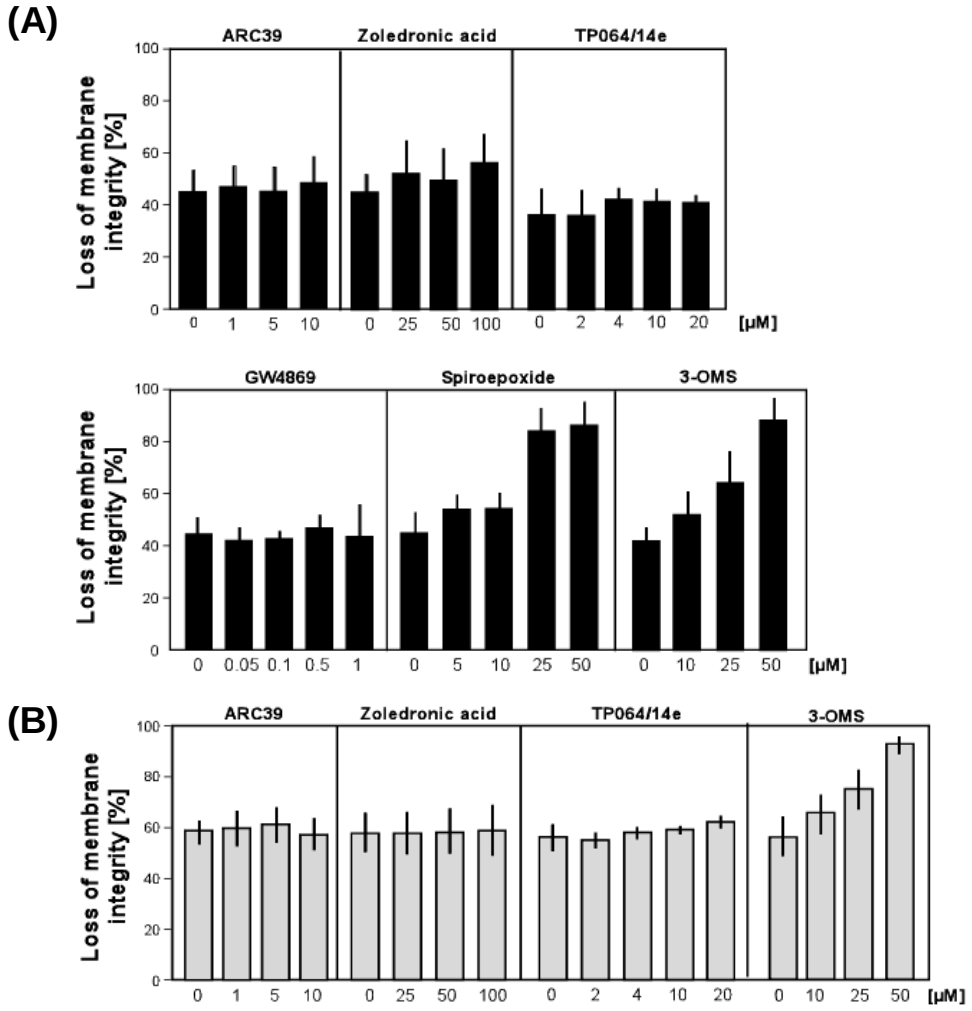

Figure 35. Neither A-SMase nor N-SMase inhibitors protect human Jurkat ATCC cells from TNF- and TRAIL-mediated necroptosis. Cells were pre-treated for 2 h with the indicated concentrations of inhibitors and subsequent addition of **(A)** 100 ng/mL hrTNF or **(B)** 100 ng/mL *killer*TRAIL in combination with 50 µM zVAD-fmk and 2 µg/mL CHX for 20 h. Cell death was analyzed after PI-staining by flow cytometric determination of the fraction of PI-positive cells. Values represent the means of a minimum of two independent experiments. Error bars indicate the respective SD.

However, the results from HT-29 and Jurkat ATCC cells were obtained in the presence of the protein biosynthesis inhibitor CHX, which is not required for effective induction of necroptosis in the murine cell lines L929Ts and NIH3T3. To exclude that the additional sensitization by CHX interfered with protection from necroptosis by the above inhibitors, experiments were performed in additional human cell lines that are sensitive to TNF- and TRAIL-induced necroptosis without the need to add CHX. The Jurkat subline I.42 is deficient for FADD and stably transfected with TNF-R2 (Chan et al., 2003) and susceptible to TNF-mediated cell death in the absence of CHX. To assure that cell death indeed occurred by necroptosis, any action of caspases was blocked by zVAD-fmk and TNF/zVAD-mediated necroptosis was confirmed by using the RIP1 inhibitor Nec-1 in a control experiment (Figure 36). Although not all inhibitors showed a protective effect, the

A-SMase inhibitor ARC39 and the N-SMase inhibitor spiroepoxide inhibited TNF-mediated necroptosis in Jurkat I.42 cells in the absence of CHX (Figure 36) and demonstrated that both enzymes generating ceramide are involved in necroptosis also in human cells. However, similar to results obtained for murine cells, the A-SMase inhibitor TP102 failed to protect human Jurkat I.42 cells from TNF-mediated necroptosis (Appendix, Figure 85).

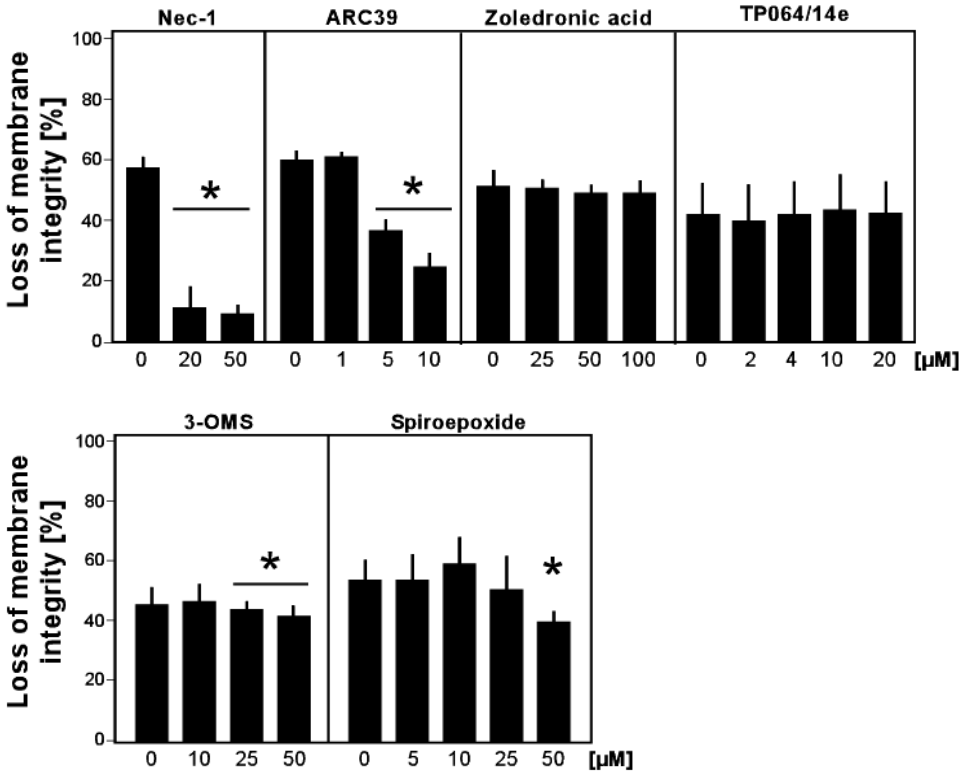

Figure 36. Inhibitors of A-SMase or N-SMase protect human Jurkat I.42 cells from TNF-mediated necroptosis. Cells were pre-treated for 2 h with the indicated concentrations of inhibitors and stimulated afterwards with 100 ng/mL hrTNF in combination with 50 µM zVAD-fmk for 6 h. Cell death was analyzed after PI-staining by flow cytometric determination of the fraction of PI-positive cells. Values represent the means of a minimum of two independent experiments, each in three repetitions. Error bars indicate the respective SD. Asterisks indicate statistical significance (t-test) $p<0.01$.

As another human cell line sensitive to TRAIL-mediated necroptosis in presence of zVAD-fmk, but without requirement for CHX (Appendix, Figure 86), the human pancreatic adenocarcinoma cell line A818-6 was utilized. In line with the results from Jurkat I.42 cells (Figure 36), ARC39 clearly protected A818-6 cells from TRAIL-induced necroptosis (Appendix, Figure 86). Since A818-6 cells were not sensitive to TNF-induced necroptosis in the absence of CHX (Appendix, Figure 88 A), they were additionally tested with regard to TNF- and TRAIL-induced necroptosis after addition of CHX. As shown in Appendix, Figure 88 ARC39 uniformly protected the cells also in the presence of CHX, in summary clearly supporting the role of A-SMase in necroptosis also in human cells. The

protection of A818-6 cells by ARC39 was independently confirmed by microscopic analysis of the cell morphology (Appendix, Figure 87, Appendix, Figure 89).

2.3 Influence of FADD and TNF-R2 on A-SMase-generated ceramide signaling in necroptosis

In the above experiments, sensitization of human HT-29 and Jurkat ATCC cells by CHX interfered with protection from necroptosis by the A-SMase inhibitors. Nevertheless, the importance of A-SMase-generated ceramide for necroptosis could be demonstrated by using Jurkat I.42 cells, which do not require sensitization by CHX to undergo TNF-mediated necroptosis (Figure 37). Notably, Jurkat I.42 cells are deficient for FADD and retransfected with TNF-R2 (Chan et al., 2003) (which is not expressed in regular Jurkat ATCC cells), which may explain their enhanced sensitivity for TNF-induced necroptosis. To further explore the role of FADD and TNF-R2, Jurkat I.42 cells (Figure 37 A) were compared to FADD-deficient Jurkat cells not transfected with TNF-R2 (Figure 37 B, C). Both Jurkat sublines are unable to activate caspases in response to TNF-induced cell death signaling due to their deficiency for FADD (Chan et al., 2003) and thus undergo necroptosis regardless of whether zVAD-fmk is added or not. This was verified through inhibition of TNF-induced cell death by Nec-1 (Figure 37) .

When ceramide generation by A-SMase was inhibited by ARC39 in these cells, a statistically significant protection from necroptosis was observed in Jurkat FADD-deficient cells only when TNF-R2 was stably expressed (Figure 37 A) or when zVAD-fmk was applied in cells that do not express TNF-R2 (Figure 37 C). Blocking the function of A-SMase in the absence of zVAD-fmk and TNF-R2 did not abrogate TNF-induced necroptosis with statistical significance, although a certain inhibition could be detected (Figure 37 B). These data argue that inhibition of apoptotic signaling through caspases by zVAD-fmk or by genetic deletion of FADD enhances ceramide-mediated necroptotic cell death. Moreover, these data suggest that in FADD-deficient cells, where the apoptotic signaling complex is partially disrupted or/and disordered, additional factors such as zVAD-fmk or TNF-R2 can enhance ceramide-mediated necroptosis.

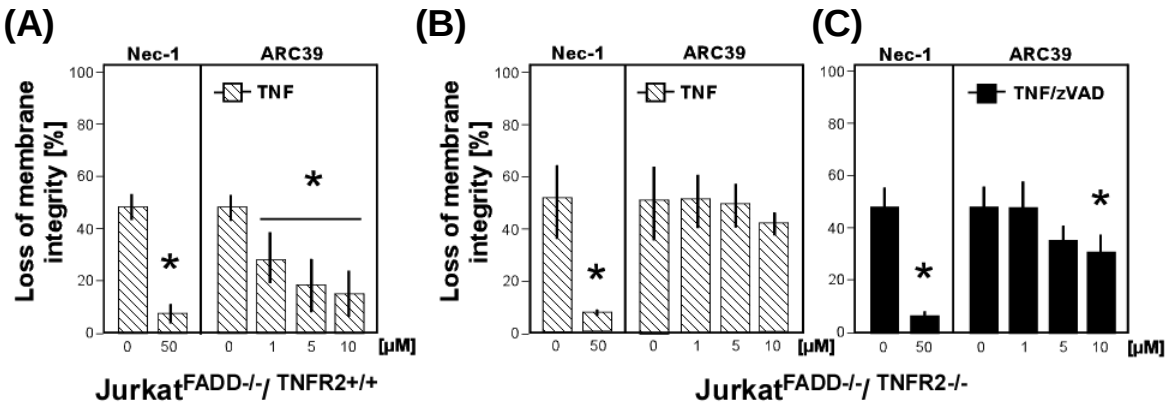

Figure 37. Ceramide-mediated necroptosis in FADD-deficient Jurkat cells is enhanced by TNF-R2 or pharmacological inhibition of caspases. Cells were pre-stimulated for 2 h with 50 µM Nec-1 and subsequent addition of 100 ng/mL hrTNF alone or in combination with 50 µM zVAD-fmk for 6 h **(A)** or for 20 h **(B)** and **(C)**. **(A)** FADD-deficient Jurkat I.42 cells retransfected with TNF-R2 were pre-stimulated for 2 h with increasing concentrations of ARC39 with subsequent addition of 100 ng/mL hrTNF for 6 h. **(B)** and **(C)** FADD-deficient Jurkat cells not transfected TNF-R2 were pre-treated for 2 h with the indicated concentrations of ARC39 and subsequent addition of 100 ng/mL hrTNF alone or in combination with 50 µM zVAD-fmk for 20 h. Cell death was analyzed after PI-staining by flow cytometric determination of the fraction of PI-positive cells out of 10,000 measured events. Values represent the means of a minimum of three independent experiments, each in three repetitions. Error bars indicate the respective SD. Asterisks indicate statistical significance (t-test) $p<0.01$.

Analyses that were carried out had updated the data from previous work and achieved a complete picture of A-SMase, N-SMase and ceramide synthase inhibition in murine L929Ts and NIH3T3 cells, as well as in human Jurkat ATCC and HT-29, Jurkat I.42 and A-818-6 cells during TNF- (Table 6) and TRAIL-induced necroptosis (Table 7). These results support previous findings (Thon et al., 2005) arguing against a function of ceramide synthase in necroptosis. They further confirm that A-SMase is involved in both TNF- and TRAIL-mediated necroptosis. Previously unknown, N-SMase was also implicated in necroptosis in murine and human cells by these data. To verify and confirm this novel finding, murine cells lacking FAN protein, which is a direct binding partner for TNF receptor and essential for N-SMase-activation by TNF, were used for further investigations (see paragraph 2.4.). The summary of all results gathered in a previous study (Thon et al., 2005), as well as own data generated previously (Sosna, Master Thesis, 2010) and in this Ph.D. thesis are presented in Table 6 and Table 7. Altogether, the presented results strongly support the concept that ceramide generated through the activity of A-SMase and N-SMase is necessary for TNF- and TRAIL-mediated necroptosis.

Table 6. Summary of experiments investigating the role of A-SMase, N-SMase and ceramide synthase in TNF-mediated necroptosis in murine L929Ts, NIH3T3 and human Jurkat, HT-29 and A818-6 cells. For the study of A-SMase, the inhibitors ARC39, D609, desipramine, imipramine and zoledronic acid were used. N-SMase was pharmacologically inhibited by GW4869, 3-OSM and spiroepoxide. Fumonisin B_1 is an inhibitor of ceramide synthase. Necroptosis was induced according to previously described settings in Figure 32 to Figure 36. The (+) sign indicates protection against TNF-induced necroptosis. The (-) sign indicates lack of protection by the respective inhibitor against TNF-induced necroptosis in each cell line. Black signs indicate analyses that have been performed in this thesis, and grey signs data obtained by previous researchers (see (Thon et al., 2005)). n.d.: no data

			INHIBITORS									
			A-SMase						**N-SMase**			**Ceramide synthase**
STIMULI	**CELL LINE**		ARC39	D609	Desipramine	Imipramine	Zoledronic acid	TP064/14e	GW4869	3-OMS	Spiroepoxide	Fumonisin B_1
TNF/zVAD	murine	**L929Ts**	+	+	-	-	+	-	-	+	+	-
		NIH3T3	+	+	-	-	+	-	-	+	+	-
TNF/zVAD/CHX	human	**Jurkat ATCC**	-	+	-	-	-	-	-	-	-	-
		HT-29	-	-	-	-	-	-	-	-	-	-
TNF/zVAD		**Jurkat I.42**	+	**n.d.**	**n.d.**	**n.d.**	-	-	**n.d.**	-	+	**n.d.**
TNF/zVAD/CHX		**A818-6**	+	**n.d.**	**n.d.**	**n.d.**	**n.d.**	**n.d.**	**n.d.**	**n.d.**	**n.d.**	**n.d.**

Table 7. Summary of experiments investigating the role of A-SMase, N-SMase and ceramide synthase in TRAIL-mediated necroptosis in murine L929Ts, NIH3T3 and human Jurkat, HT-29 and A818-6 cells. For the study of A-SMase, the inhibitors ARC39, D609, desipramine, imipramine and zoledronic acid were used. N-SMase was pharmacologically inhibited by GW4869, 3-OSM and spiroepoxide. Fumonisin B_1 is an inhibitor of ceramide synthase. Necroptosis was induced according to previously described settings in Figure 32 to Figure 36. The (+) sign indicates protection against TRAIL-induced necroptosis. The (-) sign indicates lack of protection by the respective inhibitor against TRAIL-induced necroptosis in each cell line. Black signs indicate analyses that have been performed in this thesis and grey signs the data summarized in my previous master thesis (Sosna, 2010). n.d.: no data

			INHIBITORS									
			A-SMase						**N-SMase**			**Ceramide synthase**
STIMULI	**CELL LINE**		ARC39	D609	Desipramine	Imipramine	Zoledronic acid	TP064/14e	GW4869	3-OMS	Spiroepoxide	Fumonisin B_1
TRAIL/zVAD	murine	**L929Ts**	+	+	-	-	+	-	-	+	+	-
		NIH3T3	+	+	-	-	-	-	-	-	+	-
TRAIL/zVAD/CHX	human	**Jurkat ATCC**	-	+	-	-	-	-	-	-	-	-
		HT-29	-	-	-	-	-	-	-	-	-	-
TRAIL/zVAD		**A818-6**	+	**n.d.**	**n.d.**	**n.d.**	**n.d.**	**n.d.**	**n.d.**	**n.d.**	**n.d.**	**n.d.**
TRAIL/zVAD/CHX			+	**n.d.**	**n.d.**	**n.d.**	**n.d.**	**n.d.**	**n.d.**	**n.d.**	**n.d.**	**n.d.**

2.4 Impact of N-SMase, FAN and Lyst on necroptosis

Factor associated with N-SMase activation (FAN) contributes to TNF-mediated necroptosis and apoptosis

As shown above (Figure 32 to Figure 37), pharmacological inhibition of N-SMase significantly decreased the levels of TNF- and TRAIL-induced necroptosis. Since the protein FAN has been described as a component of the signaling pathway between TNF-R1 and N-SMase (Adam-Klages et al., 1996), cell death was investigated in FAN-deficient MEFs. As shown in (Figure 38), both TNF-mediated necroptosis and apoptosis were significantly decreased in FAN-deficient cells. Notably, increasing the concentration of CHX boosted the level of TNF-mediated necroptosis and apoptosis but deficiency for FAN still significantly protected from cell death (Figure 38 A, *versus* B). This finding indicates that N-SMase is involved in both TNF-mediated necroptosis and apoptosis and that FAN might serve as an association partner for other proteins associated with necroptotic and apoptotic cell death signaling. Obstructing a more detailed analysis, wildtype MEFs were resistant to necroptosis and apoptosis triggered by TRAIL. Of note, FAN-deficiency moderately enhanced TRAIL-mediated apoptosis but not necroptosis (Figure 38), suggesting a differential role of FAN in TRAIL- *versus* TNF-mediated cell death signaling. The protection of FAN-deficient cells from TNF-mediated necroptosis and apoptosis was independently confirmed at the level of cell morphology (Figure 39).

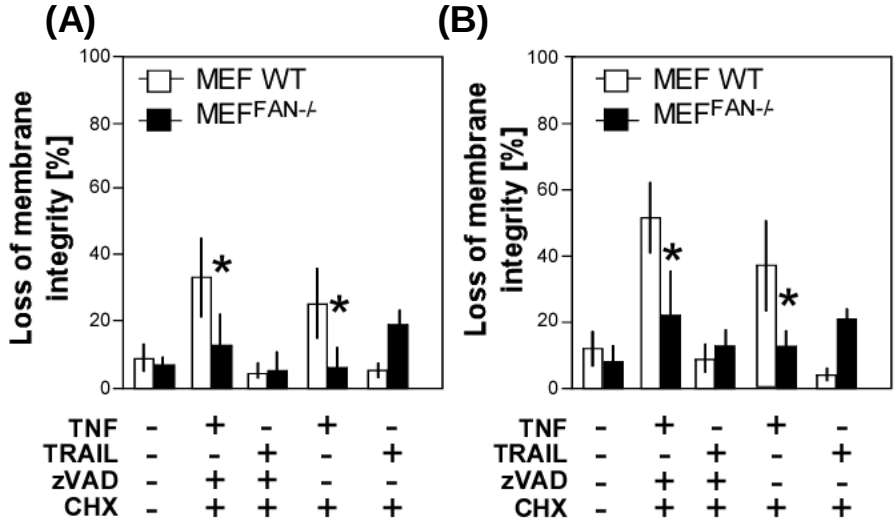

Figure 38. Deficiency for FAN protects from both TNF-mediated necroptosis and apoptosis in murine cells. FAN-deficient ($MEF^{FAN-/-}$) and wildtype (MEF WT) MEFs were prestimulated with **(A)** 1 µg/mL CHX or **(B)** 2 µg/mL CHX in combination with (for necroptosis) or without (for apoptosis) 20 µM zVAD-fmk for 30 min with subsequent addition of 100 ng/mL hrTNF for 12 h or 100 ng/mL *killer*TRAIL for 20 h. Cell death was analyzed after PI-staining by flow cytometric determination of the fraction of PI-positive cells. Values represent the means of a minimum of three independent experiments, each in three repetitions. Error bars indicate the respective SD. Asterisks indicate statistical significance (t-test) $p<0.01$.

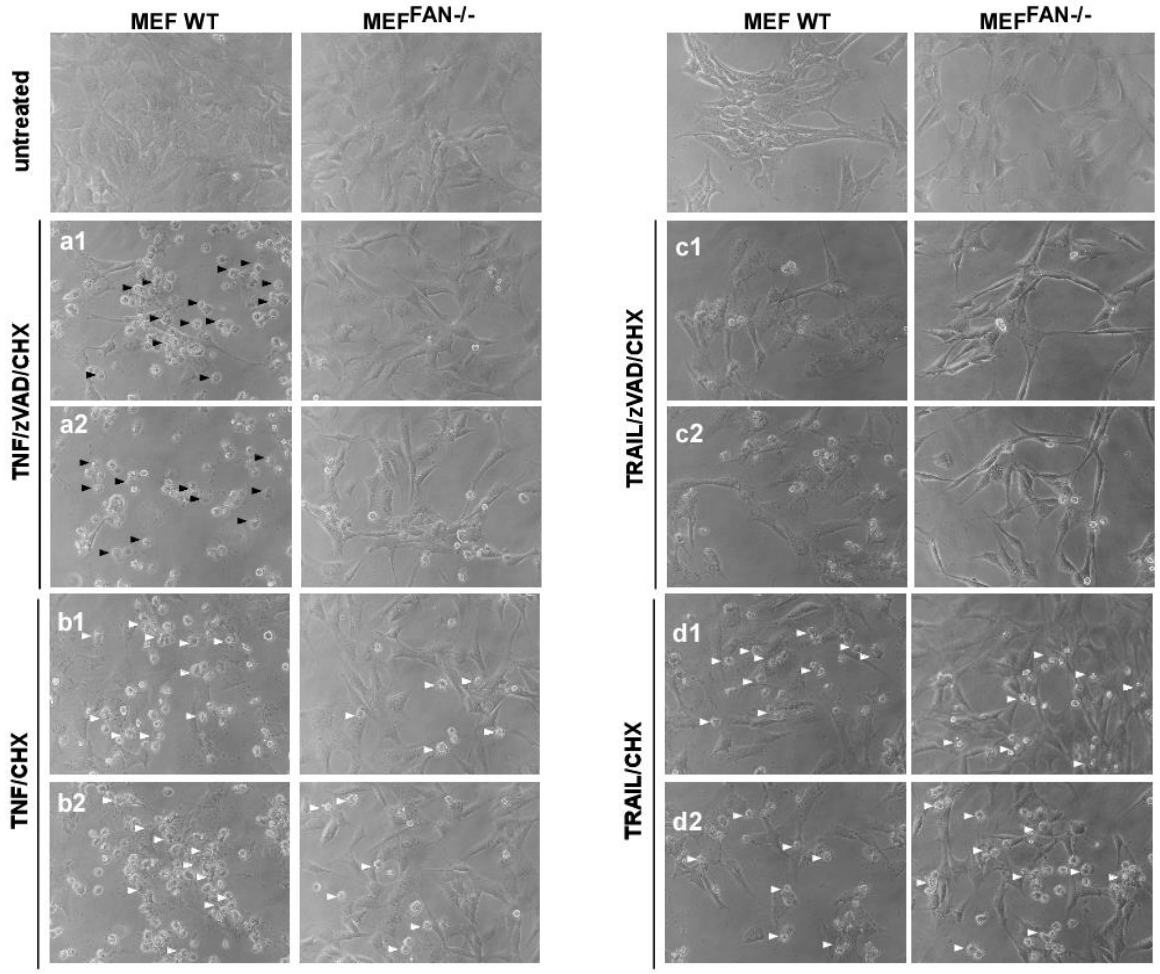

Figure 39. Morphological analyses of the influence of FAN on necroptosis and apoptosis in MEFs. FAN-deficient ($MEF^{FAN-/-}$) and wildtype (MEF WT) MEFs were prestimulated with **(a1), (b1)** 1 µg/mL CHX or **(a2), (b2)** 2 µg/mL CHX in combination with (for necroptosis) or without (for apoptosis) 20 µM zVAD-fmk for 30 min with subsequent addition of 100 ng/mL hrTNF for 12 h. In order to induce TRAIL-mediated cell death, the cells were prestimulated with **(c1), (d1)** 1 µg/mL CHX or **(c2), (d2)** 2 µg/mL CHX in combination with (for necroptosis) or without (for apoptosis) 20 µM zVAD-fmk for 30 min with subsequent addition of 100 ng/mL *killer*TRAIL for 20 h. The images show morphological changes during necroptosis and apoptosis in FAN wildtype and -deficient cells. Black arrows indicate typical necroptotic morphology. White arrows indicate blebbing and apoptotic bodies characteristic for apoptosis. Magnification 320x.

Lyst, a homolog of FAN contributes to TNF-mediated necroptosis and apoptosis

After the requirement for FAN was confirmed for TNF-mediated necroptosis and apoptosis, further experiments were conducted to investigate the FAN-homologous protein Lyst. FAN and Lyst both share a similar overall structure and are both involved in the regulation of vesicle size (Möhlig et al., 2007). Functional inactivation of Lyst leads to the lethal Chediak-Higashi syndrome in humans, manifested by formation of giant, perinuclear vesicles (lysosomes, melanosomes) in many cells (Montfort et al., 2010). A role of Lyst in signaling by N-SMase or in TNF-induced necroptosis had however not been investigated

so far.

To determine the role of Lyst in TNF- and TRAIL-mediated necroptosis and apoptosis, mouse fibroblasts lacking Lyst and their wildtype counterparts were analyzed. Similar to FAN (shown in Figure 38 A), lack of Lyst prevented TNF- and TRAIL-mediated necroptosis, suggesting a possible involvement of the lysosomal compartment in necroptosis (Figure 40 A). Moreover, data obtained in these experiments suggest that synthesis of proteins may be required for resistance against necroptosis in cells lacking Lyst. Inhibition of protein synthesis by CHX resulted in a lack of protection against both TNF- and TRAIL-mediated necroptosis in both Lyst-deficient as in wildtype cells (Figure 40 B). Moreover, Lyst-deficient cells were protected with statistical significance against TNF- but not TRAIL-induced apoptosis (Figure 40 B).

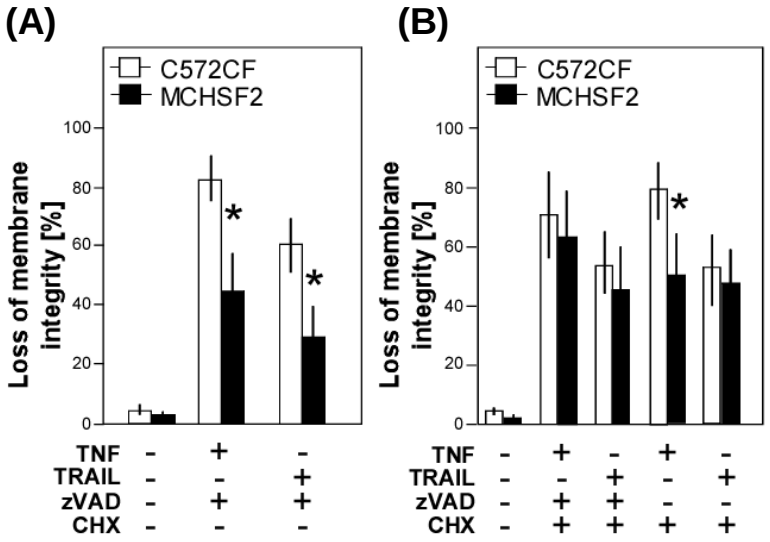

Figure 40. TNF- and TRAIL-mediated necroptosis and apoptosis are mediated through Lyst in murine cells. Lyst-deficient fibroblasts from MCHSF2 mice and their wildtype counterparts from mice were prestimulated with **(A)** 20 µM zVAD-fmk for 30 min with subsequent addition of 100 ng/mL hrTNF or 100 ng/mL *killer*TRAIL for 14 h. **(B)** Cells were pre-stimulated as in (A) with 1 µg/mL CHX in combination with or without 20 µM zVAD-fmk for 30 min and subsequent addition of hrTNF or *killer*TRAIL for 14 h. Cell death was analyzed after PI-staining by flow cytometric determination of the fraction of PI-positive cells. Values represent the means of a minimum of three independent experiments, each in three repetitions. Error bars indicate the respective SD. Asterisks indicate statistical significance (t-test) $p<0.01$.

Additional morphological observations confirmed that Lyst-deficient cells are protected from TNF- and TRAIL-mediated necroptosis and TNF-mediated apoptosis (although less clearly visible for apoptosis) (Figure 41 A and Figure 42) but are uniformly executing necroptosis in the presence of CHX (Figure 41 B).

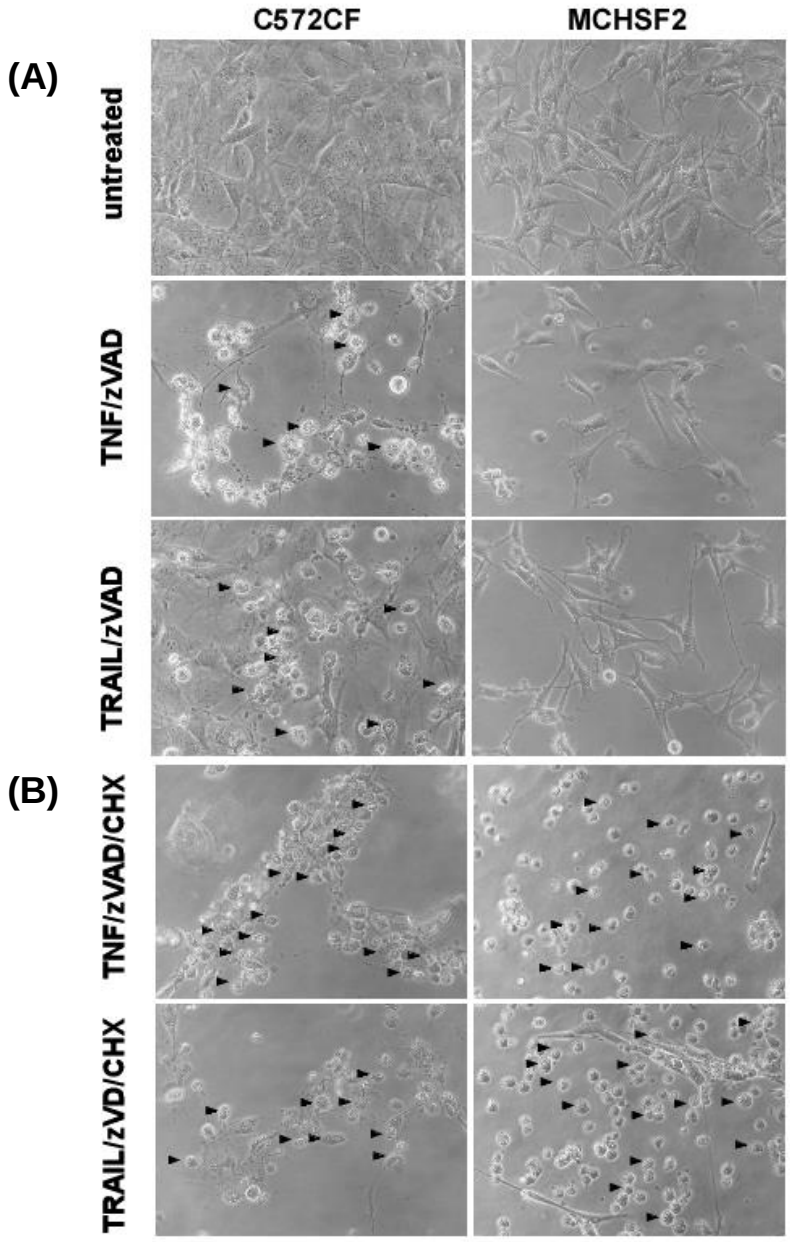

Figure 41. Morphological analyses of necroptosis in the presence or absence of Lyst in mouse fibroblasts. The images show morphological changes during necroptosis in Lyst-deficient (MCHSF2) and wildtype cells (C572CF). All cells were prestimulated with 20 µM zVAD-fmk, additionally **(A)** without or with **(B)** 1 µg/mL CHX for 30 min and subsequent addition of 100 ng/mL hrTNF or 100 ng/mL *killer*TRAIL for 14 h. Black arrows indicate typical necroptotic morphology. Magnification 320x.

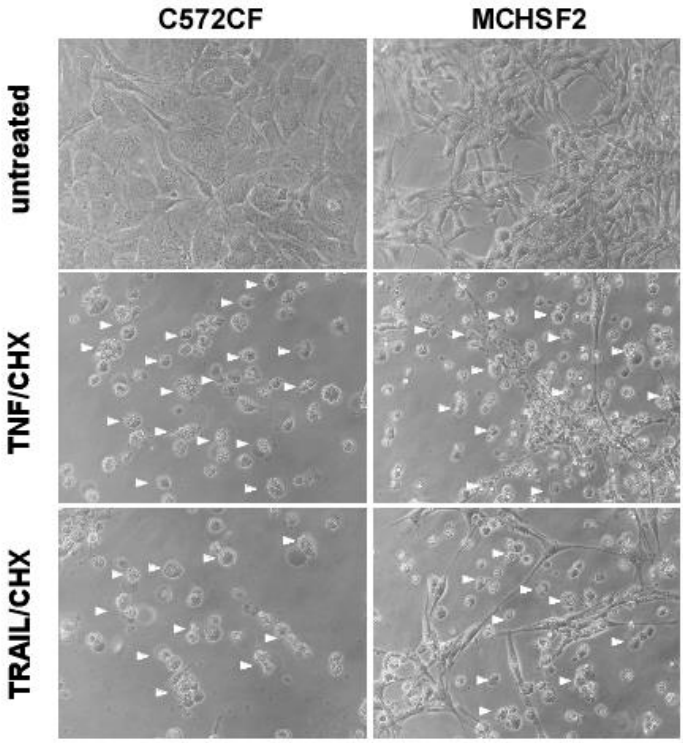

Figure 42. Morphological analyses of apoptosis in the presence or absence of Lyst in mouse fibroblasts. The images show morphological changes during apoptosis in Lyst-deficient (MCHSF2) and wildtype (C572CF) cells. Lyst-deficient mouse fibroblasts and their wildtype counterparts were prestimulated with 1 µg/mL CHX for 30 min with subsequent addition of 100 ng/mL hrTNF or 100 ng/mL *killer*TRAIL for 14 h. White arrows indicate blebbing and apoptotic bodies during apoptosis. Magnification 320x.

3. Which proteases are playing a role in necroptosis?

3.1 Cathepsins and calpains/cysteine proteases are not involved in necroptosis

Cathepsins B and L as well as calpains/cysteine proteases are not required for necroptosis

Data from previous analyses (Appendix, Figure 90) had argued against a role of cathepsins in necroptosis. In extension and further validation of these results, inhibitors of the cysteine proteases cathepsin B and L (zFA-fmk and Ca-074 Me) did not protect L929Ts cells from both TNF- and TRAIL-mediated necroptosis (Figure 43). Likewise, necroptosis was unaffected by the broad spectrum inhibitor E-64 targeting calpains/cysteine proteases, suggesting that cathepsins B and L as well as calpains/cysteine proteases are not essential for neither TRAIL- nor TNF-mediated necroptosis.

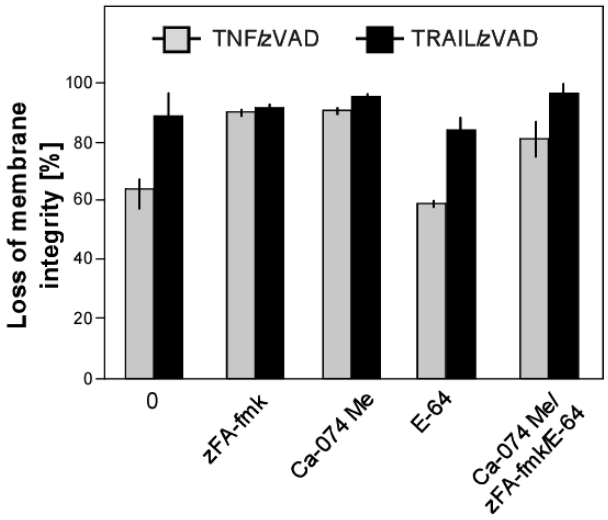

Figure 43. TNF- and TRAIL-mediated necroptosis is not diminished by inhibition of cathepsins B and L or calpains/cysteine proteases. L929Ts cells were preincubated with 20 µM of the listed inhibitors of cathepsins B and L and calpains/cysteine proteases with subsequent addition of either 100 ng/mL hrTNF for 5 h or 30 ng/mL *killer*TRAIL for 14 h or in the presence of 20 µM of zVAD-fmk before cell death was determined. Data were obtained by flow cytometry, counting PI-fluorescence of a sample of 10,000 cells from a minimum of two independent experiments. Error bars indicate the respective SD**.**

To additionally investigate a possible involvement of cathepsin L in necroptosis in more detail, a specific cathepsin L-inhibitor (zFF-fmk, zPhe-Phe-CH_2F) was used alone or

combined with other inhibitors. In line with the previous data, zFF-fmk did not block necroptosis in L929Ts cells (Figure 44).

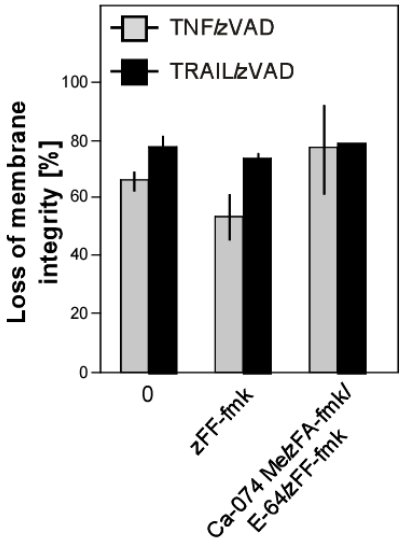

Figure 44. TNF- and TRAIL-mediated necroptosis is not diminished by inhibition of cathepsin L. L929Ts cells were preincubated 20 µM zFF-fmk and other inhibitors of cathepsins with subsequent addition of either 100 ng/mL hrTNF for 5 h or 30 ng/mL *killer*TRAIL for 14 h or in the presence of 20 µM of zVAD-fmk before cell death was determined. Data were obtained by flow cytometry, counting PI-fluorescence of a sample of 10,000 cells from two different experiments in two replications each. Error bars indicate the respective SD.

Overall, the application of the above pharmacological inhibitors demonstrated that neither inhibition of cathepsins B, L nor calpains/cysteine proteases did influence TNF- or TRAIL-mediated necroptosis.

Cathepsin D does not mediate either TNF- or TRAIL-mediated necroptosis

Independently, a genetic approach was used to investigate the role of cathepsin D in necroptosis. To this end, cathepsin D-deficient MEFs ($CTSD^{-/-}$), wildtype cells ($CTSD^{+/+}$) and MEFs in which ectopic expression of CTSD was reconstituted by stable retransfection ($CTSD^{-/-\ reconstituted}$) were compared with regard to their sensitivity to TNF- and TRAIL-mediating necroptosis. The obtained data (Figure 45) indicate that lack of cathepsin D does not protect from TNF- and TRAIL-induced necroptosis (regardless of additional sensitization with CHX or not) and argue against a general role of this protease in necroptosis. Of note, the increased abundance of cathepsin D in $CTSD^{-/-\ reconstituted}$ cells may be responsible for their slightly enhanced sensitivity towards TRAIL/zVAD-mediated necroptosis.

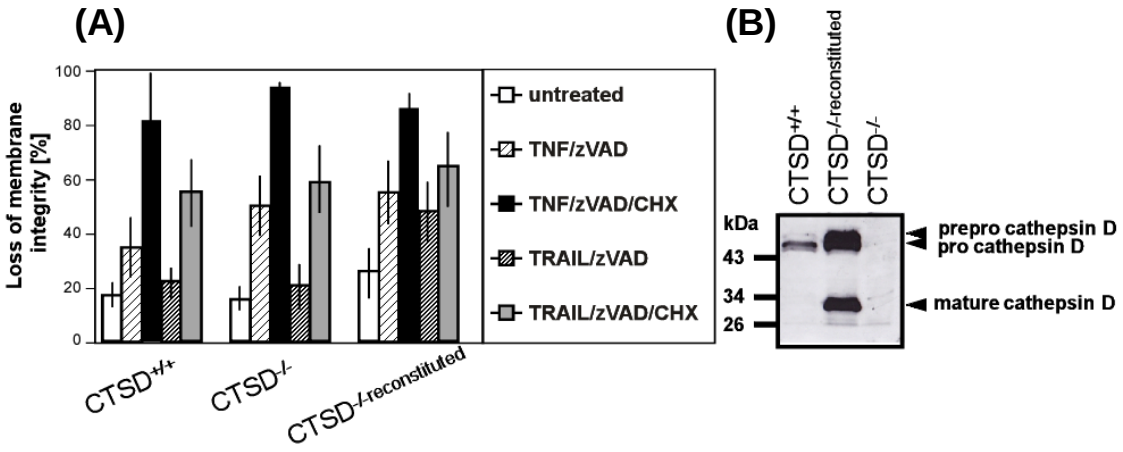

Figure 45. Cathepsin D does not play a role in TNF- and TRAIL-induced necroptosis. **(A)** MEFs derived from wildtype ($CTSD^{+/+}$) or CTSD-deficient mice ($CTSD^{-/-}$) as well as $CTSD^{-/-}$ fibroblasts re-transfected with the CTSD cDNA ($CTSD^{-/-\ reconstituted}$) were incubated for 14 h with 100 ng/mL hrTNF or 30 ng/mL *killer*TRAIL in combination with 20 µM zVAD-fmk in the presence or absence of 5 µg/mL CHX before cell death was measured. Data were obtained by flow cytometry, counting PI-fluorescence of a sample of 10,000 cells from a minimum of three independent experiments. Error bars indicate the respective SD. **(B)** The expression of cathepsin D in each cell line was investigated by Western blot analysis with an anti-cathepsin D antibody (Santa Cruz).

3.2 Inhibition of metalloproteases does not protect murine cells from necroptosis

To explore if metalloproteases propagate necroptosis, a series of pharmacological studies was performed. Inhibitors of metalloproteases (TAPI-1, GM 6001 and marimastat) were used in order to investigate if these proteases are involved in TNF- and TRAIL-mediated necroptosis. Neither TNF- nor TRAIL-mediated necroptosis in murine L929Ts (Figure 46 A) and NIH3T3 (Figure 46 B) cells was diminished after administration of these inhibitors. This suggests that inhibition of metalloproteases is not sufficient to prevent TNF- or TRAIL-mediated necroptosis in murine cells and that these proteases are not critically involved in this form of PCD.

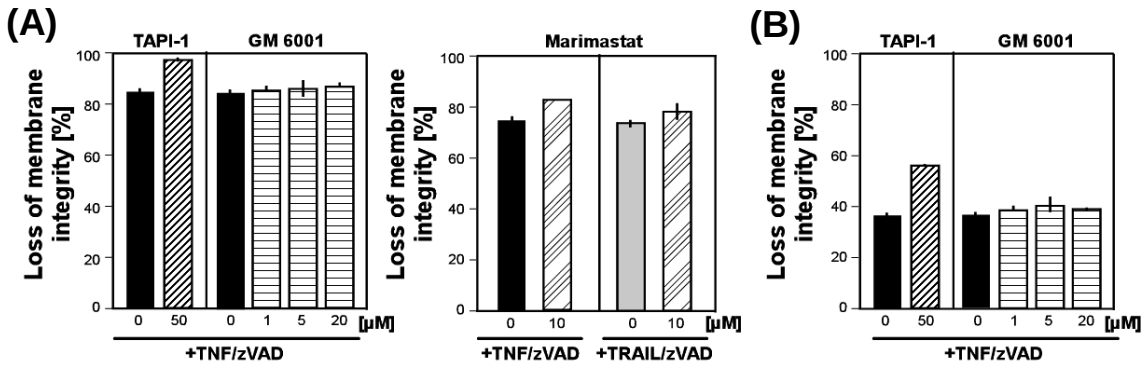

Figure 46. Inhibition of metalloproteases by TAPI-I, GM 6001 and marimastat does not protect from TNF- or TRAIL-mediated necroptosis. Cells were prestimulated for 2 h with the indicated concentrations of inhibitors with subsequent addition of 20 µM zVAD-fmk in combination with either (A) 100 ng/mL hrTNF for 5 h or 30 ng/mL *killer*TRAIL for 14 h for L929Ts or (B) 100 ng/mL hrTNF and 20 µM zVAD-fmk for 16 h for NIH3T3 cells. Cell death was analyzed after PI-staining by flow cytometric determination of the fraction of PI-positive cells from 10,000 measured events. Values represent the means of one independent experiment in three repetitions. Error bars indicate the respective SD.

3.3 Chymotrypsin-like serine proteases participate in TNF- and TRAIL-induced necroptosis

As cathepsins and calpains were shown not to be involved in TNF- and TRAIL-mediated necroptosis, the contribution of cellular serine proteases was evaluated in the next set of experiments. In previous experiments, the broad-spectrum chymotrypsin-like serine protease inhibitor TPCK had increased the survival of L929Ts cells during TNF- and TRAIL-mediated necroptosis (Appendix, Figure 91). These analyses were extended with the additional murine cell line NIH3T3 and the two human cell lines Jurkat ATCC and HT-29, showing that serine proteases participate in TNF- and TRAIL-mediated necroptosis in these cell lines (Figure 47). Moreover, morphological analyses of L929Ts and HT-29 cells revealed that although definitive signs of cell death were present, the integrity of the plasma cell membrane and the complexity of the cells were maintained in the presence of TPCK (Figure 47 B and C). This supports the assumption that cytoplasmic serine proteases contribute to later phases of necroptosis.

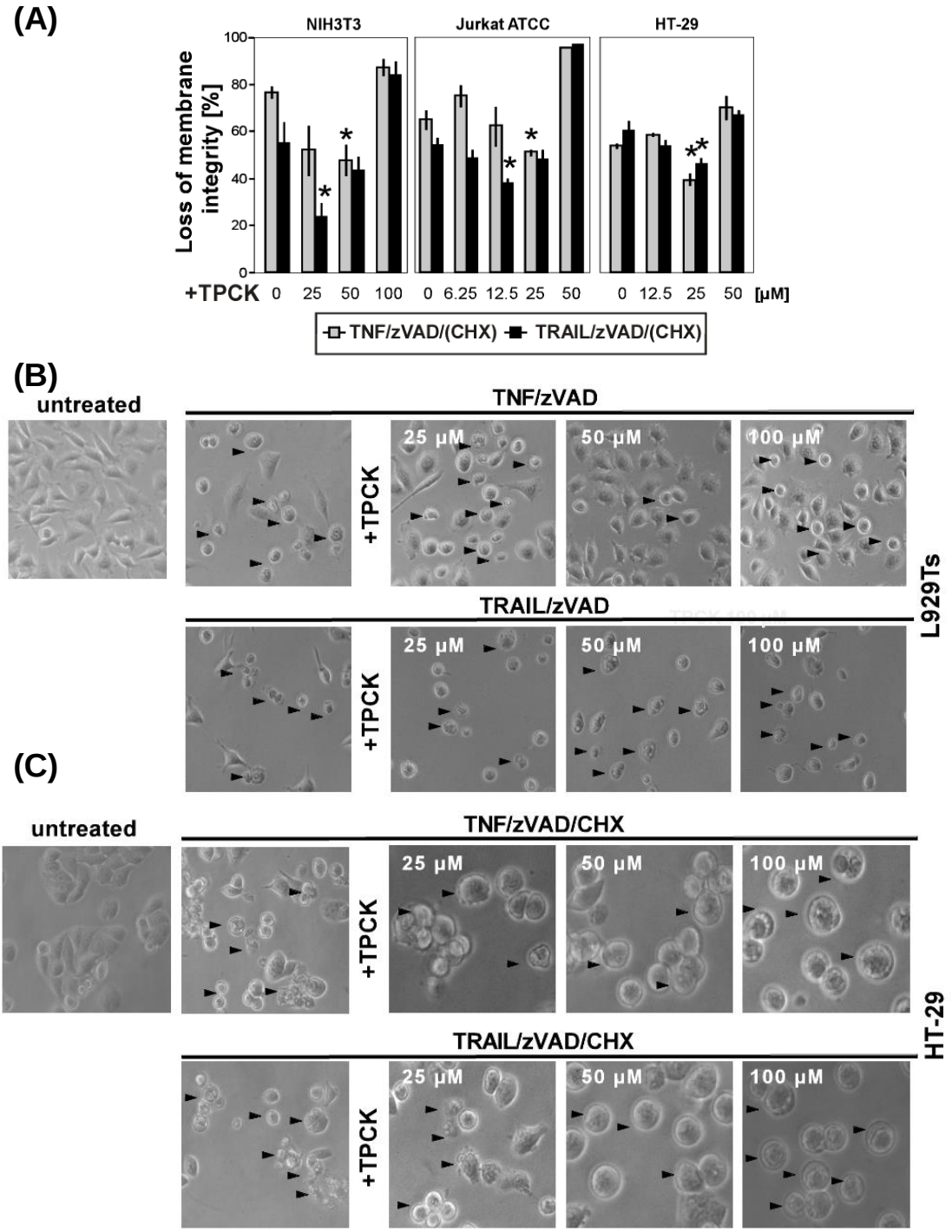

Figure 47. TPCK protects murine and human cells from TNF- and TRAIL-mediated necroptosis. (A) Cells were stimulated with 20 µM zVAD-fmk in combination with 100 ng/mL hrTNF or with *killer*TRAIL 100 ng/mL (NIH3T3 for 16 h), 50 ng/mL (Jurkat ATCC for 20 h) or 30 ng/mL (HT-29 for 16 h) in the presence of the indicated concentrations of TPCK. Additionally for Jurkat ATCC cells 2 µg/mL, and for HT-29 cells 5 µg/mL of CHX were added. TNF- and TRAIL-induced necroptosis was analyzed by flow cytometric determination of the fraction of PI-positive cells out of 10,000 events. Values represent the means of a minimum of three independent experiments. Error bars indicate the respective SD. Asterisks indicate statistical significance (t-test) $p<0.01$ or $p<0.05$. **(B)** L929Ts cells were stimulated with 100 ng/mL hrTNF in combination with 20 µM zVAD-fmk for 5 h or **(C)** HT-29 cells were stimulated as described in (A). Morphological changes were analyzed by microscopy. Magnification 320x. Black arrows indicate cells dying by necroptosis.

3.4 Role of the serine protease HtrA2/Omi and its substrates in necroptosis

As the above experiments had shown that serine-like proteases are playing a role in necroptosis and since accumulating evidence suggested that mitochondria are playing a central role in necroptosis (Deerberg et al., 2009), the possible involvement of the mitochondrial serine protease HtrA2/Omi in necroptosis was further investigated. As an additional indication for a function of this serine protease in caspase-independent PCD, staurosporine-induced cell death in HeLa cells occurring in the presence of caspase inhibitors could be abrogated by siRNA-mediated downregulation of HtrA2/Omi (Kuninaka et al., 2005).

HtrA2/Omi mediates necroptosis and apoptosis in murine cells

Pharmacological inhibition of HtrA2/Omi with Ucf-101, an inhibitor specific for the serine protease activity of HtrA2/Omi (Cilenti et al., 2003), resulted in protection of L929Ts cells from TNF- as well as TRAIL-mediated necroptosis. Moreover, and confirming previous studies (Suzuki et al., 2001, Verhagen et al., 2002), inhibition of HtrA2/Omi protected also from TNF- and TRAIL-mediated apoptosis (Figure 48 A). Additional analyses of cell morphology confirmed that the changes in cellular integrity during TNF-mediated necroptosis as well as apoptosis were dependent on the protease activity of HtrA2/Omi (Figure 48 B). For TRAIL-mediated necroptosis and apoptosis, definite and clear signs of cell death were visible despite HtrA2/Omi inhibition although the integrity of the cell membrane was still preserved. These results point to an involvement of HtrA2/Omi in TNF-mediated necroptosis (and apoptosis) but also indicate that during TRAIL-mediated cell death, serine proteases other than HtrA2/Omi must participate.

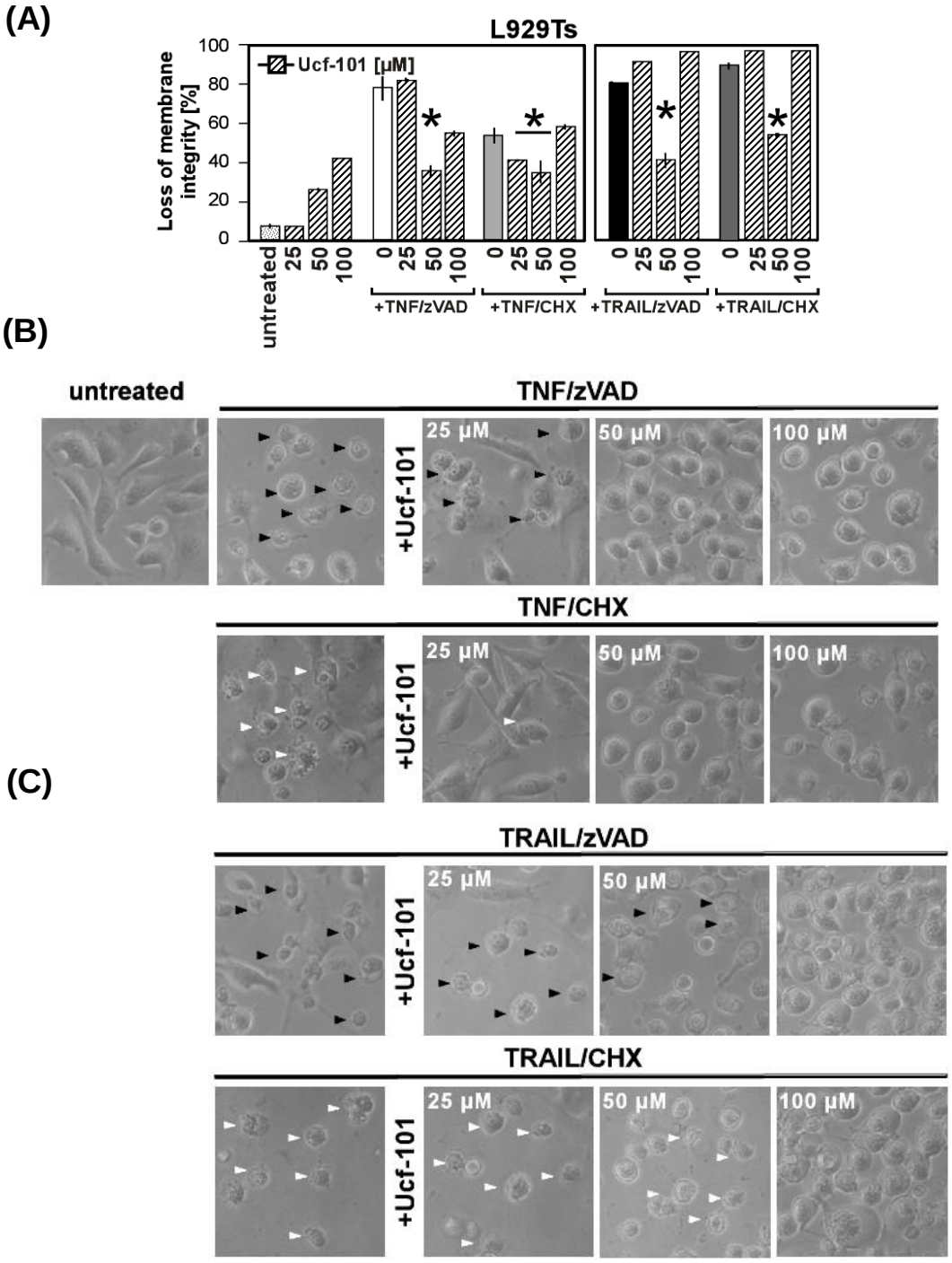

Figure 48. Inhibition of HtrA2/Omi in murine L929Ts cells protects against TNF- and TRAIL-mediated necroptosis and apoptosis. (A) L929Ts cells were pretreated for 2 h with the indicated concentrations of Ucf-101 with subsequent addition of 100 ng/mL hrT NFα for 5 h or with 30 ng/mL *killer*TRAIL for 14 h in combination with 20 µM zVAD-fmk (for necroptosis) or 5 µg/mL CHX (for apoptosis). Cell death was analyzed after PI-staining by flow cytometric determination of the fraction of PI-positive cells. Values represent the means of two independent experiments, each in two repetitions. Error bars indicate the respective SD. Asterisks indicate statistical significance (t-test) $p<0.01$. **(B)** Morphological analyses of the influence of Ucf-101 on TNF- and TRAIL-mediated necroptosis and apoptosis. Cells were stimulated as in (A). Black arrows indicate cell morphology typical for necroptosis. White arrows indicate blebbing of the cells and apoptotic bodies. Magnification 320x.

To exclude that the above results were due to non-specific off-target activities of Ucf-101 or to cell-specific responses of L929Ts cells, necroptosis was investigated in HtrA2/Omi-deficient and wildtype MEF. In addition, the presence of both RIP1 and RIP3 as crucial components of TNF- and TRAIL-mediated necroptosis was verified in these cells. As shown in Figure 49 A, HtrA2/Omi-deficient cells were clearly more resistant to TNF- and TRAIL-mediated necroptosis than their wildtype counterparts. This was additionally verified by morphological analyses (Figure 49 B) and, consistent with the results in L929Ts cells using Ucf-101, altogether demonstrates a predominant role of HtrA2/Omi in TNF- and TRAIL-mediated necroptosis.

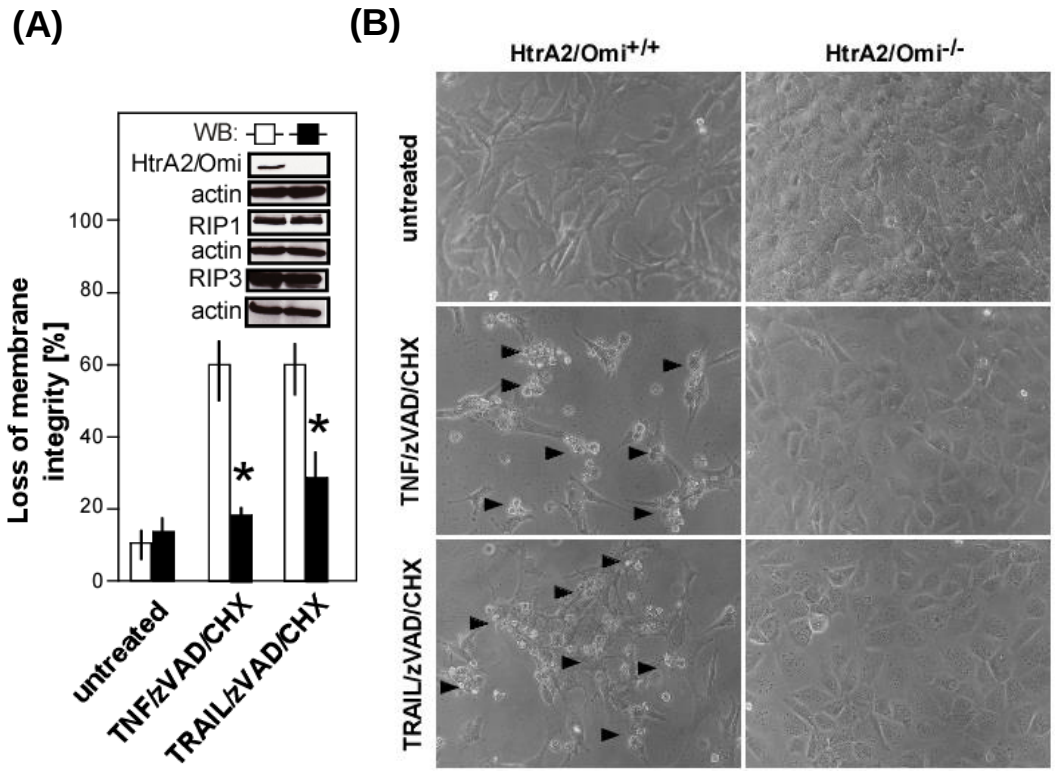

Figure 49. Lack of HtrA2/Omi protects MEFs from TNF- and TRAIL-mediated necroptosis. (A) Wildtype (white bars) or HtrA2/Omi-deficient (black bars) MEFs were incubated with 100 ng/mL hrTNF or 30 ng/mL *killer*TRAIL in combination with 20 µM zVAD-fmk and 1 µg/mL CHX for 16 h. Cell death was analyzed after PI-staining by flow cytometric determination of the fraction of PI-positive cells. Values represent the means of three independent experiments, each in two repetitions. Error bars indicate the respective SD. Asterisks indicate statistical significance (t-test) $p<0.01$. The genotype of wildtype and HtrA2/Omi-deficient cells was verified by Western blot analysis for presence of HtrA2/Omi, and additionally RIP1 and RIP3. **(B)** Impact of HtrA2/Omi-deficiency on the morphology of MEFs undergoing TNF- and TRAIL-mediated necroptosis. Cells were stimulated as in (A). Black arrows indicate cell morphology typical for necroptosis. Antibodies: anti-HtrA2/Omi (Abcam), anti-RIP1 (BD Bioscience), anti-RIP3 (Enzo), anti-actin (Santa Cruz).

HtrA2/Omi is required for necroptosis in human cell lines

The results obtained for HtrA2/Omi as a mediator of necroptosis and apoptosis in murine cells were next validated in human cell lines. Similar to murine cells, TNF- and TRAIL-mediated necroptosis in HT-29 cells was also inhibited by application of Ucf-101 (Figure 50 A). However, TNF- and TRAIL-mediated apoptosis in these cells was not reversed by application of the HtrA2/Omi inhibitor, which is in line with previous studies performed in human cells (Vande Walle et al., 2010). Subsequently analyses of cell morphology confirmed the protection against TNF- and TRAIL-mediated necroptosis while HtrA2/Omi was inhibited, whereas during apoptosis, characteristic apoptotic bodies and cell blebbing were observed regardless of presence or absence of Ucf-101 (Figure 50 B).

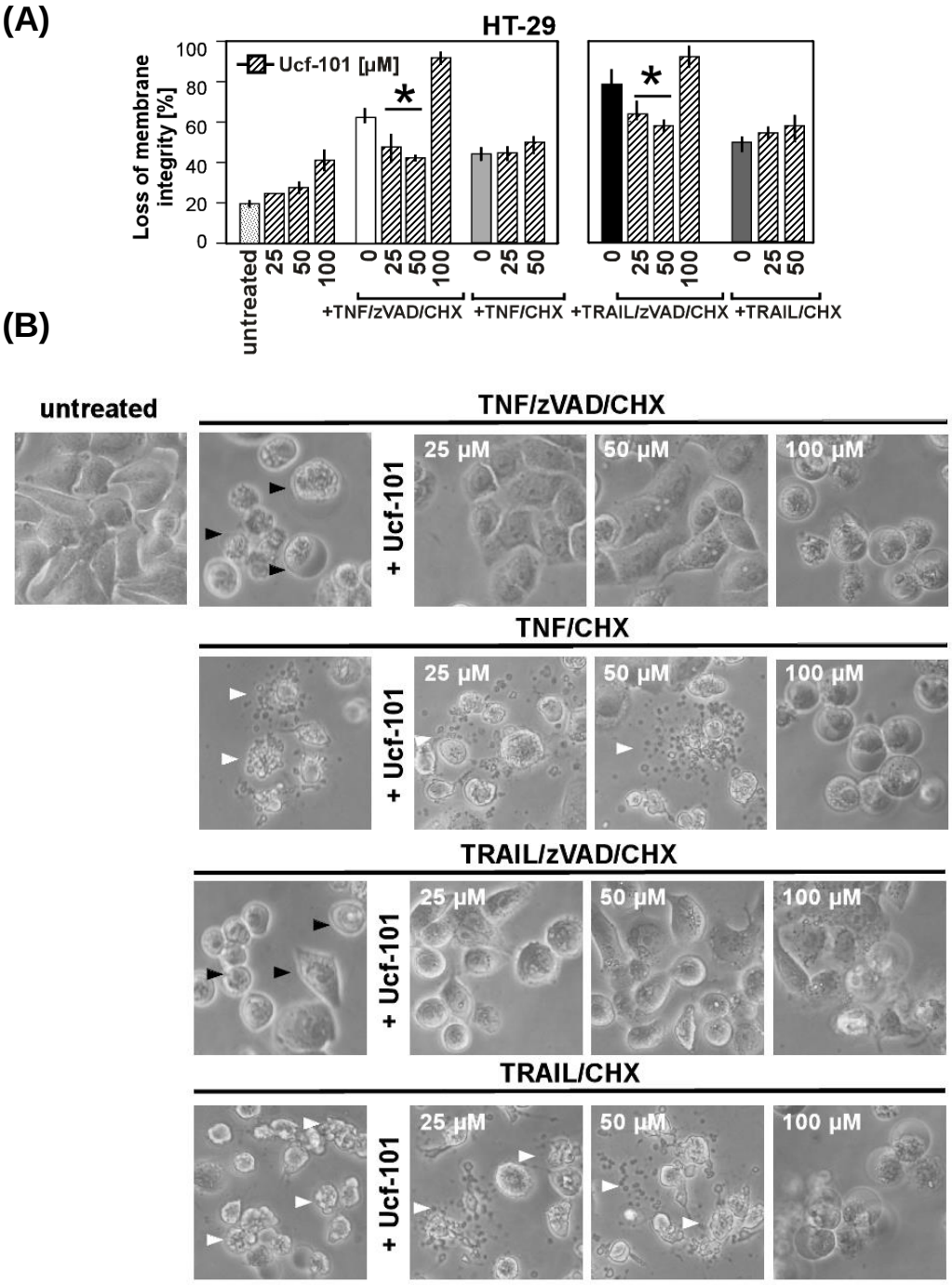

Figure 50. Inhibition of HtrA2/Omi blocks TNF- and TRAIL-mediated necroptosis but not apoptosis in human HT-29 cells. (A) Cells were preincubated for 2 h with the indicated concentrations of Ucf-101 with subsequent addition of 100 ng/mL hrTNF or 30 ng/mL *killer*TRAIL in combination with 20 µM zVAD-fmk and/or 5 µg/mL CHX for 16 h. Cell death was analyzed after PI-staining by flow cytometric determination of the fraction of PI-positive cells. Values represent the means of at least two independent experiments, each in two repetitions. Error bars indicate the respective SD. Asterisks indicate statistical significance (t-test) $p<0.01$. **(B)** Images of cell morphology from HT-29 cells treated as in (A) demonstrating protection against both TNF- and TRAIL-mediated necroptosis but not apoptosis after administration of Ucf-101. Black arrows indicate cell morphology typical for necroptosis. White arrows indicate blebbing of the cells and apoptotic bodies. Magnification 320x.

Notably, human Jurkat cells treated with Ucf-101 were not protected from either TNF- and TRAIL-mediated necroptosis or apoptosis (Figure 51). However, this may be due to

the additional sensitization by CHX required in this cell line which may interfere with protection from necroptosis by Ucf-101, as also seen above for inhibitors for A-SMase and N-SMase (Figure 35).

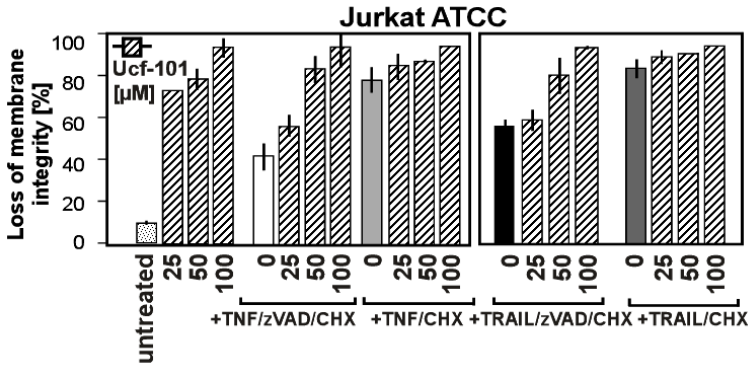

Figure 51. Inhibition of HtrA2/Omi does not protect from TNF- and TRAIL-mediated necroptosis and apoptosis in human Jurkat ATCC cells. Cells were preincubated for 2 h with the indicated concentrations of Ucf-101 with subsequent addition of 100 ng/mL hrTNF or 30 ng/mL *killer*TRAIL in combination with 20 µM zVAD-fmk and 5 µg/mL CHX for 16 h. Cell death was analyzed after PI-staining by flow cytometric determination of the fraction of PI-positive cells. Values represent the means of at least two independent experiments, each in two repetitions. Error bars indicate the respective SD.

To further investigate the function of HtrA2/Omi in TNF- and TRAIL-mediated necroptosis, pharmacological studies with Ucf-101were performed in A818-6 cells, which (at least for TRAIL-induced necroptosis) do not require sensitization by CHX. As shown by measurements of both loss of membrane integrity (Appendix, Figure 86) and cell morphology (Appendix, Figure 87), inhibition of HtrA2/Omi by Ucf-101 prevented TRAIL-induced necroptosis in the absence of CHX. Moreover, Ucf-101 reduced both TNF- and TRAIL-mediated necroptosis in the presence of CHX (Appendix, Figure 88 B and Appendix, Figure 89)

As additional human cell systems in which CHX is not required for sensitization to necroptosis and can therefore not interfere with Ucf-101, human I.42 Jurkat cells deficient for FADD and stably transfected with TNF-R2 as well as "regular" FADD-deficient Jurkat cells that do not express TNF-R2 were analyzed. Necroptosis induced by TNF in combination with or without zVAD-fmk in Jurkat I.42 cells was diminished by Ucf-101 (Figure 52 A), but not in "regular" FADD-deficient Jurkat cells that do not express TNF-R2 (Figure 52 B), confirming a previous study which has shown that the absence or presence of TNF-R2 modulates the strength of the cell death signaling complex (Chan et al., 2003). Accordingly, TNF-R2 (together with additional adaptor molecules) may participate in the assembly of caspase-independent cell death signaling complexes, which need to be clarified. Moreover, the results from this study implicate that the composition

and strength of signaling complexes might influence how and if HtrA2/Omi executes necroptosis.

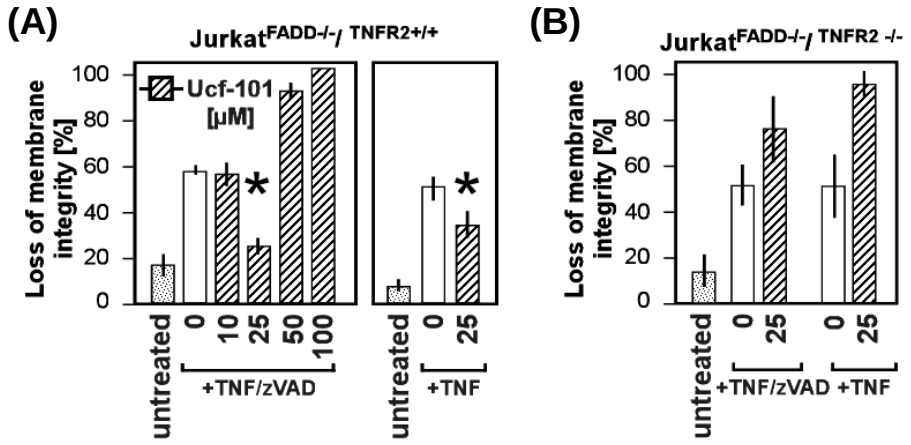

Figure 52. Inhibition of HtrA2/Omi protects from TNF-mediated necroptosis in FADD-deficient human Jurkat I.42 cells transfected with TNF-R2. Jurkat FADD-deficient cells were prestimulated for 2 h with the indicated concentrations of Ucf-101 with subsequent addition of 100 ng/mL hrTNF alone or in combination with 50 µM zVAD-fmk **(A)** for 6 h (TNF-R2$^{+/+}$ cells, I.42) or **(B)** for 20 h (TNF-R2$^{-/-}$ cells). Data were obtained by flow cytometry, counting PI-fluorescence of a sample of 10,000 cells from at least three independent experiments in three replications each. Error bars indicate the respective SD. Asterisks indicate statistical significance (t-test) $p<0.01$.

The above results support the concept that serine proteases in general play an important role in cytokine-mediated necroptosis in murine and human cell lines, with HtrA2/Omi representing the first identified candidate. With regard to a role of HtrA2/Omi in apoptosis, the findings imply a differential role of this protease in murine and human cell lines.

Downregulation of HtrA2/Omi by RNA interference does not protect from necroptosis

The above results showing a protective effect of pharmacological inhibition or genetic deletion of the serine protease HtrA2/Omi on TNF- and TRAIL-mediated necroptosis were complemented by downregulation of HtrA2/Omi in murine L929Ts and human Jurkat I.42 cells. Although the transfected siRNAs effectively downregulated the expression of HtrA2/Omi in murine (Figure 53) and human cells (Figure 54), this did neither protect murine cells from TNF- or TRAIL-mediated necroptosis or apoptosis nor inhibited necroptosis in human Jurkat I.42 cells which are unable to trigger apoptosis due to their FADD-deficiency (Figure 53 and Figure 54). These results are not consistent with the data obtained in HtrA2/Omi-deficient MEFs or by pharmacological inhibition with Ucf-101. As

a likely explanation, the activity of the residual HtrA2/Omi protein that is still present after downregulation may nevertheless be sufficient to support the execution of necroptosis, as similarly observed for downregulation of A-SMase (Thon et al., 2005).

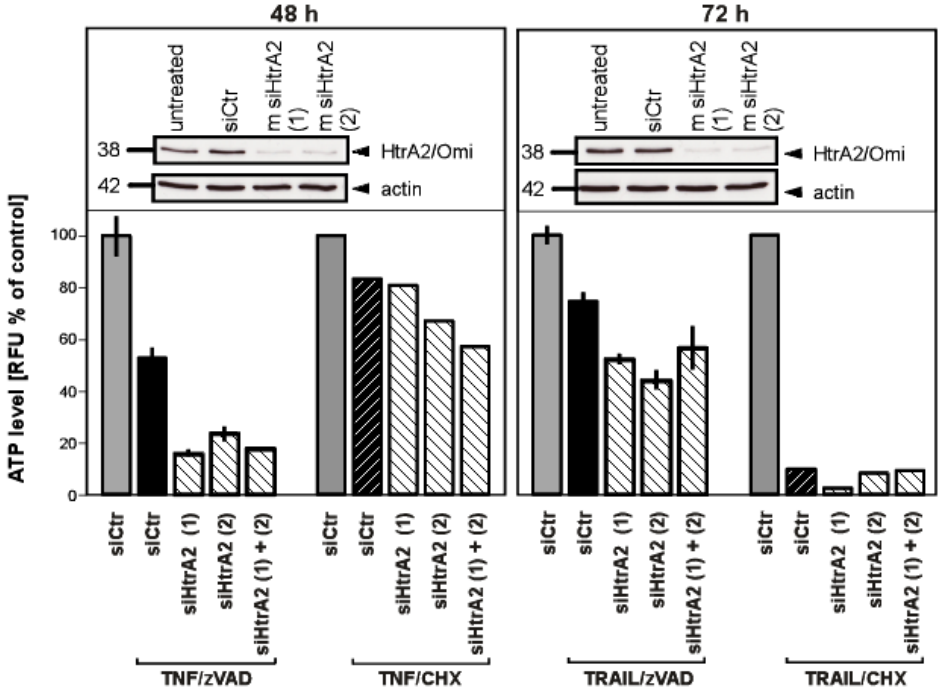

Figure 53. In L929Ts cells, downregulation of HtrA2/Omi does not protect from necroptosis or apoptosis. Cells were nucleofected with control siRNA (siCtr) or siRNA specific for murine HtrA2/Omi (siHtrA2 (1), (2)) and HtrA2/Omi protein levels were analyzed by Western blot. Antibodies: HtrA2/Omi (Abcam), actin (Santa Cruz). Cell death was induced 48 h or 72 h after nucleofection by stimulation with 100 ng/mL hrTNF for 5 h or 30 ng/mL *killer*TRAIL for 14 h in combination with 20 µM zVAD-fmk (for necroptosis) or 5 µg/mL CHX (for apoptosis). The decrease of intracellular ATP levels was determined as a marker for cell death. For necroptosis values represent the means of two independent experiments, each in a minimum of two repetitions and are shown relative to untreated cells. Error bars indicate the respective SD. For apoptosis values represent the means of one experiment in two parallel determinations and are shown relative to untreated cells.

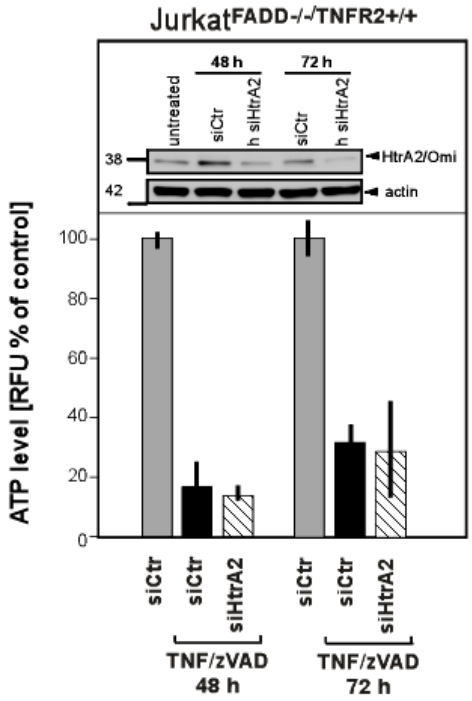

Figure 54. In Jurkat I.42 cells, downregulation of HtrA2/Omi does not protect from necroptosis. Cells were lipofected with control siRNA (siCtr) or siRNA specific for human HtrA2/Omi (h siHtrA2) for 48 and 72 h and HtrA2/Omi protein levels were analyzed by Western blot. Antibodies: anti-HtrA2/Omi (Abcam), anti-actin (Sigma). Subsequently, necroptosis was induced by treatment with 100 ng/mL hrTNF in combination with 50 µM zVAD-fmk for 6 h. The decrease of intracellular ATP levels was determined as a marker for cell death. Values represent the means of one experiment in four parallel determinations and are shown relative to untreated cells. Error bars indicate the respective SD.

RIP1 is cleaved by HtrA2/Omi in necroptosis

A recent study had shown a Bcl-2-dependent cleavage of RIP1 by HtrA2/Omi after growth factor withdrawal. Moreover, it was pointed out that this event is caspase-independent and involved in cell death (Vande Walle et al., 2010). Therefore, a putative cleavage of RIP1 by HtrA2/Omi was investigated for TNF- and TRAIL-mediated necroptosis.

Analyses of the RIP1 cleavage pattern after induction of TNF- and TRAIL-mediated necroptosis in MEFs lacking HtrA2/Omi protein and their wildtype counterparts revealed that cleavage fragments of RIP1 at 25 kDa and at 40 kDa constitutively present in wildtype MEFs were diminished in MEFs lacking HtrA2/Omi (Figure 55 lanes 4, 5, 6), suggesting that RIP1 is a substrate for HtrA2/Omi and that several cleavage sites for HtrA2/Omi exist in RIP. More importantly, necroptosis in wildtype MEFs (as previously shown by uptake of PI and by changes in cell morphology, Figure 49) was accompanied by the decrease of a 30-kDa RIP1 cleavage fragment (Figure 55, lanes 2, 3). In HtrA2/Omi-deficient cells, which do not undergo necroptosis (see Figure 49), the 30 kDa RIP1 band was preserved

(Figure 55, lanes 5, 6). This suggests that processing of the 30-kDa RIP1 fragment is mediated by HtrA2/Omi during necroptosis and therefore indicates that processing of RIP1 by HtrA2/Omi may play a role in necroptosis.

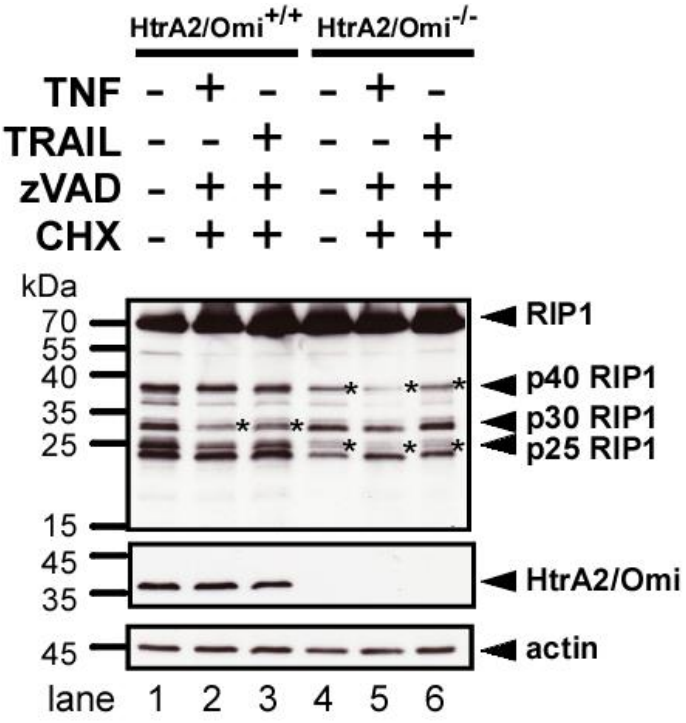

Figure 55. RIP1 is a substrate for proteolytic cleavage by HtrA2/Omi. MEFs deficient for HtrA2/Omi and their wildtype counterparts were stimulated with 100 ng/mL hrTNF or 30 ng/mL *killer*TRAIL in combination with 20 µM zVAD-fmk and 1 µg/mL CHX for 16 h. Cleavage of RIP1was analyzed by Western blot. Full-length RIP1 (72 kDa) and cleavage fragments of 25 kDa, 30 kDa and 40 kDa are marked by arrows. An asterisk indicates reduction of the corresponding cleaved RIP1 fragment. Antibodies: anti-RIP1 (BD Bioscience), anti-actin (Santa Cruz).

To complement the above analyses of RIP1 in MEFs, the cleavage of RIP1 after pharmacological inhibition of HtrA2/Omi was investigated in murine L929Ts cells. In these cells, Ucf-101 inhibited the generation of the 25-kDa, 30-kDa and 40-kDa fragments of RIP1 (Figure 57, lanes 3, 5, 10, 12, 15), similarly as it was observed in HtrA2/Omi-deficient MEFs. This was uniformly detectable in untreated cells and in cells undergoing TNF- or TRAIL-induced necroptosis or apoptosis, indicating that Ucf-101 interferes with a basal cleavage of RIP1 by HtrA2/Omi. Therefore, the relevance of RIP1 as a substrate of HtrA2/Omi for necroptosis will have to be investigated in future experiments.

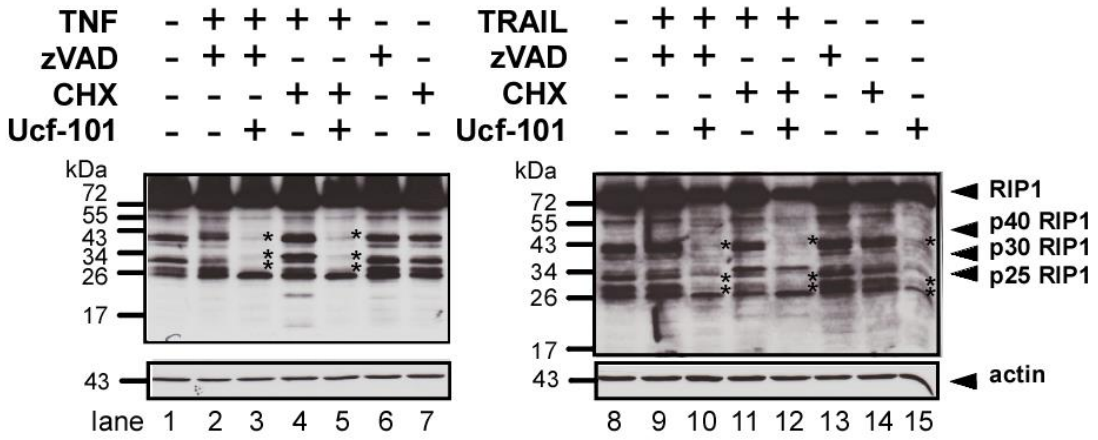

Figure 56. The HtrA2/Omi inhibitor Ucf-101 prevents cleavage of RIP1 in L929Ts cells. L929Ts cells were left untreated or incubated with 100 ng/mL hrTNF or 30 ng/mL *killer*TRAIL in combination with 20 µM zVAD-fmk (for necroptosis) or in combination with 5 µg/mL CHX (for apoptosis), and HtrA2/Omi serine protease activity was inhibited with 50 µM of Ucf-101. Full-length RIP1 (72 kDa) and its cleavage fragments at 25 kDa, 30 kDa and 40 kDa (arrows) were detected by Western blot. The asterisks indicate the predicted positions of the missing cleavage fragments in the Ucf-101-treated samples. Antibodies: anti-RIP1 (BD Bioscience), anti-actin (Santa Cruz).

DBC1 represents a potential substrate for HtrA2/Omi during necroptosis

Recently, the protein DBC1 (deleted in breast cancer-1) had been identified as a substrate of HtrA2/Omi (Vande Walle et al., 2007). Therefore, the cleavage of DBC1 in TNF- and TRAIL-mediated necroptosis in MEFs lacking HtrA2/Omi and their wildtype counterparts was investigated. Induction of necroptosis in wildtype MEFs resulted in the appearance of a cleavage band of DBC1 at 89 kDa (Figure 57, lanes 2 and 3) which was not observed in HtrA2/Omi-deficient MEF (Figure 57, lanes 6, 7). Although these results are still preliminary and require validation in additional experiments, they indicate that DBC1 may indeed represent a substrate for HtrA2/Omi and thus potentially participate in TNF- and TRAIL-mediated necroptosis.

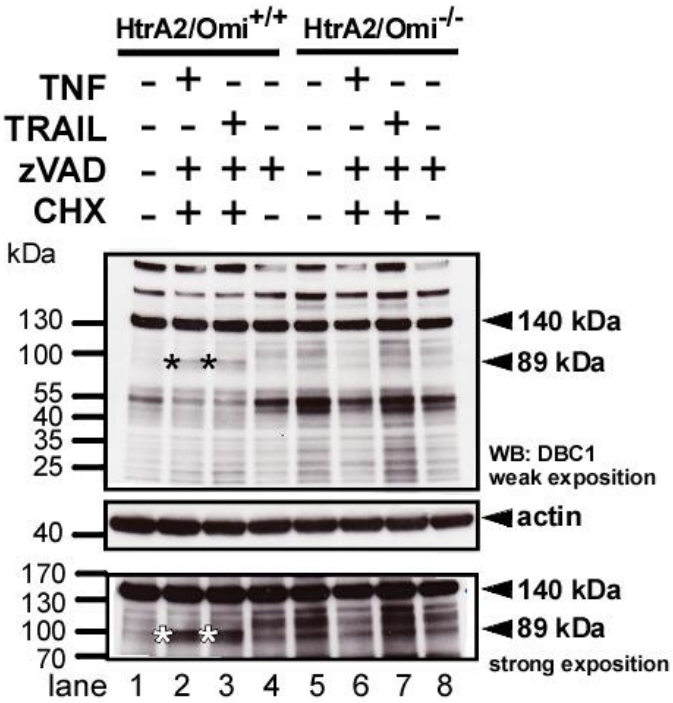

Figure 57. HtrA2/Omi mediates cleavage of DBC1 in TNF- and TRAIL-mediated necroptosis in murine cells. MEFs deficient for HtrA2/Omi and their wildtype counterparts were left untreated or were treated with 100 ng/ml hrTNF or 30 ng/mL *killer*TRAIL in combination with 20 µM zVAD-fmk and 1 µg/mL CHX or with 20 µM zVAD-fmk alone for 16 h. Cleavage of DBC1 was analyzed by Western blot. Full-length DBC1 (140 kDa) and its cleavage fragment of 89 kDa are marked by arrows. The asterisks additionally indicate the DBC1 89-kDa cleaved fragments. Western blot analyses are shown at weak and strong exposure. Antibodies: anti-DBC1 (Cell Signaling), anti-actin (Santa Cruz).

3.5 The protease UCH-L1 regulates TNF-mediated necroptosis

In a previous study, it had been reported that expression level of the ubiquitin carboxyl-terminal esterase L1 (UCH-L1, UCHL-1, PGP9.5, PARK5, gad), an enzyme that recycles free ubiquitin by cleaving ubiquitinated peptides and additionally possess ubiquitin-ubiquitin ligase activity (Liu et al., 2002), correlated with cell proliferation in H1299 lung cancer cells and likewise influenced cell cycle and growth (Liu et al., 2003). However, an impact of UCH-L1 on cell death had not yet been extensively investigated.

TNF- but not TRAIL-mediated necroptosis is regulated by UCH-L1 in murine L929Ts cells

To test whether inhibition of UCH-L1 activity blocks TNF- or TRAIL-mediated necroptosis, LDN57444, a previously described reversible, competitive, active site-directed UCH-L1 inhibitor (Liu et al., 2003) which specifically inhibits UCH-L1 while having no effects on other UCH-L family members, was used. As shown in Figure 58 A, inhibition of

UCH-L1 diminished the level of TNF-mediated necroptosis but did not influence TRAIL-mediated necroptosis. Additionally, analyses of cell morphology (Figure 58 B) confirmed the protective effect of UCH-L1 inhibition during TNF-, but not TRAIL-mediated necroptosis.

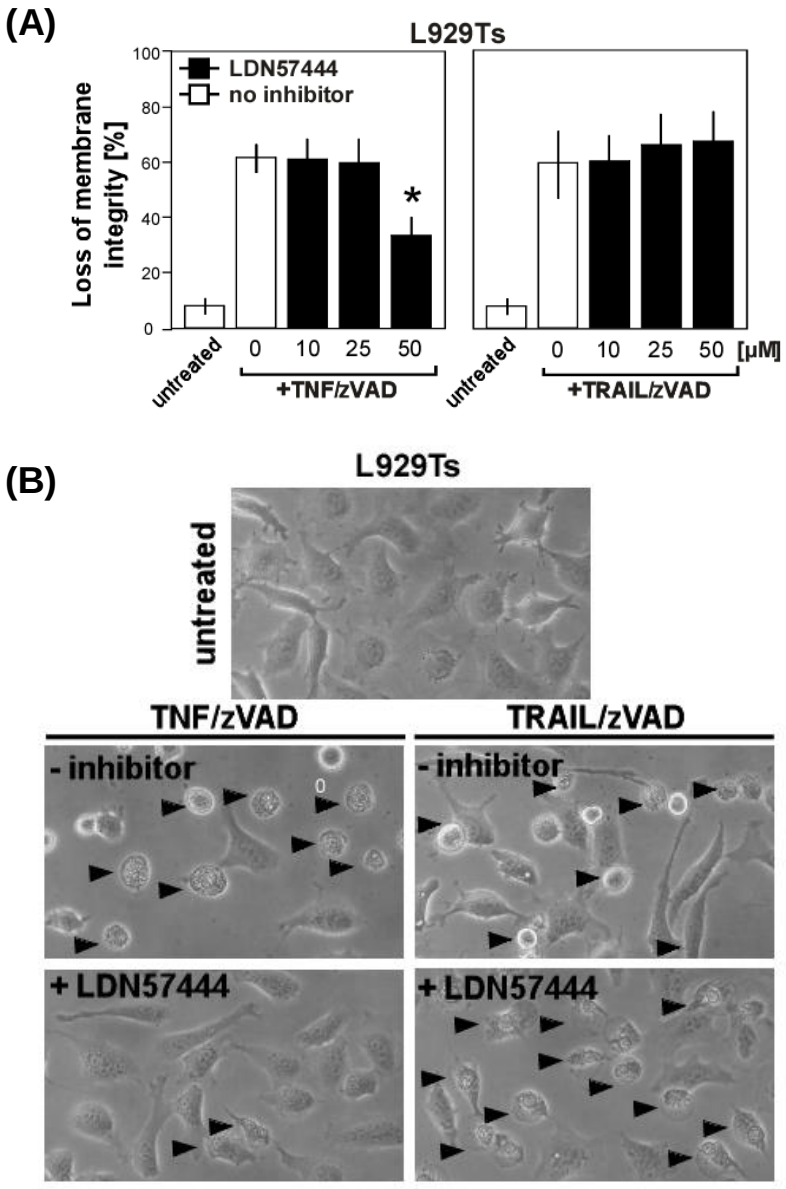

Figure 58. UCH-L1 regulates TNF-mediated necroptosis in murine L929Ts cells. (A) Cells were prestimulated for 3 h with the indicated concentrations of the UCH-L1 inhibitor LDN57444 with subsequent addition of 20 µM zVAD-fmk in combination with either 100 ng/mL hrTNF for 5 h or 30 ng/mL *killer*TRAIL for 14 h. Cell death was analyzed after PI-staining by flow cytometric determination of the fraction of PI-positive cells from 10,000 measured events. Values represent the means of at least three independent experiments, each in three repetitions. Error bars indicate the respective SD. Asterisks indicate statistical significance (t-test) $p<0.01$. **(B)** Morphological changes after inhibition of UCH-L1 during TNF- and TRAIL-mediated necroptosis in murine L929Ts cells treated as in (A). The images demonstrate protection against TNF- but not TRAIL-mediated necroptosis after UCH-L1 inhibition. Black arrows indicate typical necroptotic morphology. Magnification 320x.

The role of UCH-L1 was investigated as well with another UCH-L1 inhibitor, LDN91946, which is a selective and uncompetitive inhibitor that targets the enzyme-substrate complex of UCH-L1, ubiquitin chains and its substrate but not the free UCH-L1 enzyme (Mermerian et al., 2007). Surprisingly, and in contrast to LDN57444, this inhibitor diminished both TNF- and TRAIL-mediated necroptosis (Figure 59), thus suggesting that formation of ubiquitin chains is important for both TNF- and TRAIL-mediated necroptosis, but the UCH-L1 itself is indispensable only for TNF-mediated necroptosis and in TRAIL-mediated necroptosis another ubiquitin ligase, homologous to UCH-L1 may play a role.

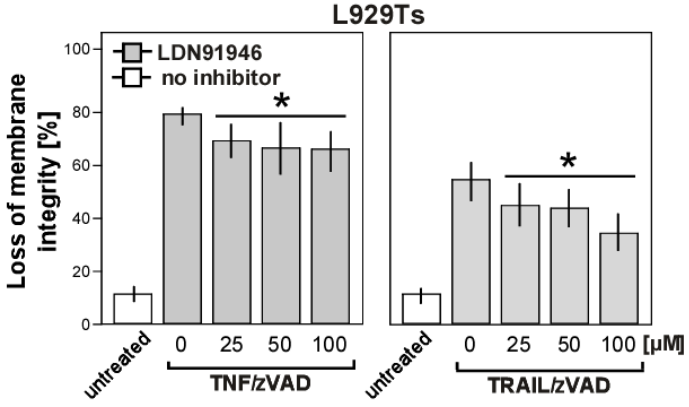

Figure 59. The UCH-L1 inhibitor LDN91946 protects from TNF- and TRAIL-mediated necroptosis in L929Ts cells. Cells were prestimulated for 3 h with the indicated concentrations of the UCH-L1 inhibitor LDN91946 with subsequent addition of 20 µM zVAD-fmk in combination with either 100 ng/mL hrTNF for 5 h or 30 ng/mL *killer*TRAIL for 14 h. Cell death was analyzed after PI-staining by flow cytometric determination of the fraction of PI-positive cells from 10,000 measured events. Values represent the means of three independent experiments, each in three repetitions. Error bars indicate the respective SD. Asterisks indicate statistical significance (t-test) $p<0.01$.

Downregulation of UCH-L1 in murine L929Ts cells protects against TNF- but not TRAIL-mediated necroptosis

To assess the role of UCH-L1 in TNF and TRAIL-induced necroptosis by an independent approach, the expression of endogenous UCH-L1 in murine L929Ts cells was downregulated by transfection with siRNA specific for UCH-L1. Compared to cells transfected with a control siRNA, cells depleted of UCH-L1 exhibited an increased resistance to TNF-induced necroptosis in combination with or without zVAD-fmk. Consistent with the results shown in Figure 58 A, downregulation of UCH-L1 did not influence TRAIL-mediated necroptosis (Figure 60). Simultaneous downregulation of RIP3 as a positive control for protection from necroptosis validated the assay.

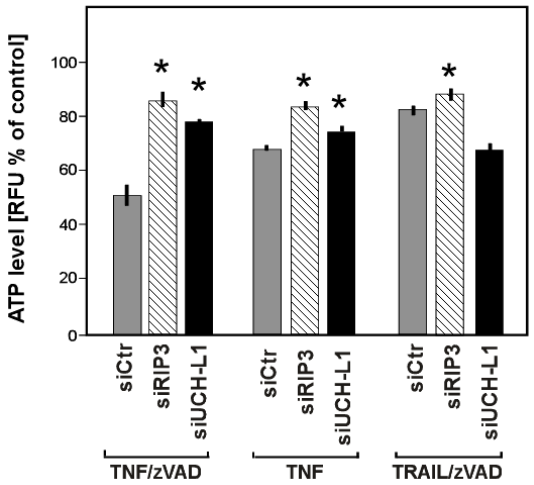

Figure 60. Downregulation of UCH-L1 protects L929Ts cells form TNF- but not TRAIL-mediated necroptosis. Cells were nucleofected with negative control siRNA (siCtr) or with siRNA specific for murine RIP3 or UCH-L1 for 48 h. Afterwards, necroptosis was induced by the stimulation with 100 ng/mL hrTNF in combination with 20 µM zVAD-fmk for 5 h, 100 ng/mL hrTNF alone for 24 h or 30 ng/mL *killer*TRAIL in combination with 20 µM zVAD-fmk for 14 h. Values represent the means of one out of two representative experiments in three parallel determinations. Error bars indicate the respective SD. Asterisks indicate statistical significance (t-test) $p<0.01$.

Inhibition of UCH-L1 does repress TNF-mediated necroptosis in human cells

The role of UCH-L1 in necroptosis was furthermore validated in human cells. Inhibition of UCH-L1 by LDN57444 in Jurkat T cells showed only a partial and moderate protection against TNF-mediated necroptosis (most likely due to the required addition of CHX as a sensitizer, which had also previously impaired protection by inhibition of A-SMase (Figure 35) or by inhibition of HtrA2/Omi (Figure 51)) and in line with previous data did not significantly influence TRAIL-mediated necroptosis (Figure 61).

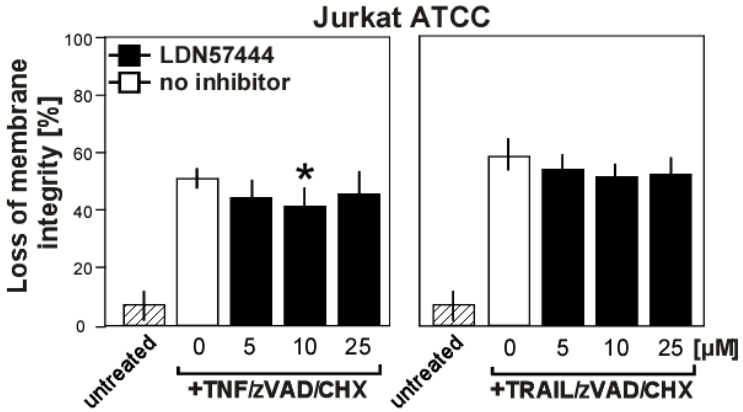

Figure 61. UCH-L1 is involved in TNF-mediated necroptosis in human Jurkat cells. Cells were prestimulated for 3 h with the indicated concentrations of the UCH-L1 inhibitor LDN57444 with subsequent addition of 20 µM *z*VAD-fmk and 2 µg/mL CHX in combination with either 100 ng/mL hrTNF or 50 ng/mL *killer*TRAIL for 20 h. Cell death was analyzed after PI-staining by flow cytometric determination of the fraction of PI-positive cells from 10,000 measured events. Values represent the means of three independent experiments, each in three repetitions. Error bars indicate the respective SD. Asterisks indicate statistical significance (t-test) $p<0.01$.

To test whether the protective effect of UCH-L1 inhibition interfered with formation of the signaling complex for necroptosis, Jurkat I.42 cells deficient for FADD and stably transfected with TNF-R2 were treated with the UCH-L1 inhibitor LDN57444. Unlike downregulation of UCH-L1 in L929Ts cells (Figure 60) or pharmacological inhibition in both L929Ts and Jurkat ATCC cells (Figure 58 and Figure 61), LDN57444 did not protect FADD-deficient T-cells from TNF-induced necroptosis, and this effect was also independent from the caspase inhibitor zVAD-fmk (Figure 62). This suggests that FADD may be necessary for the interaction of UCH-L1 with the necroptotic signaling complex and thus with necroptosis. Probably, the deficiency for FADD may abolishe the regulation of TNF-mediated necroptosis by UCH-L1.

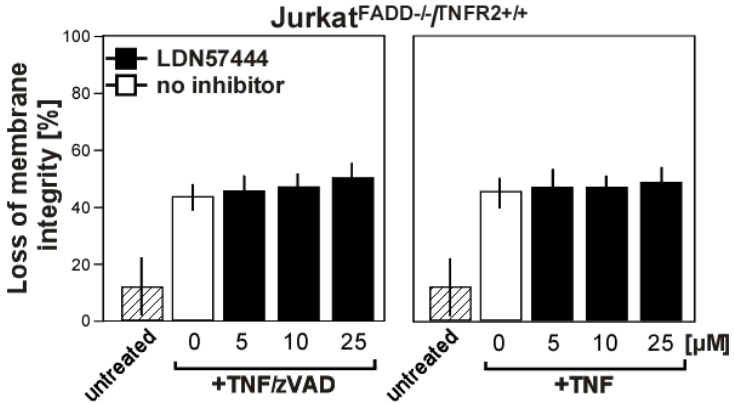

Figure 62. UCH-L1 is dispensable for TNF-mediated necroptosis in FADD-deficient human I.42 Jurkat T cells. Cells were prestimulated for 3 h with the indicated concentrations of the UCH-L1 inhibitor LDN57444 with subsequent addition of 100 ng/mL hrTNF alone or in combination with 50 µM zVAD-fmk for 6 h. Cell death was analyzed after PI-staining by flow cytometric determination of the fraction of PI-positive cells from 10,000 measured events. Values represent the means of at least three experiments in three repetitions each. Error bars indicate the respective SD.

Subsequently, the role of UCH-L1 in necroptosis in human HT-29 cells was investigated. Opposite to results obtained for Jurkat ATCC cells, inhibition of UCH-L1 in human HT-29 cells did not protect from TNF-mediated necroptosis (Figure 63).

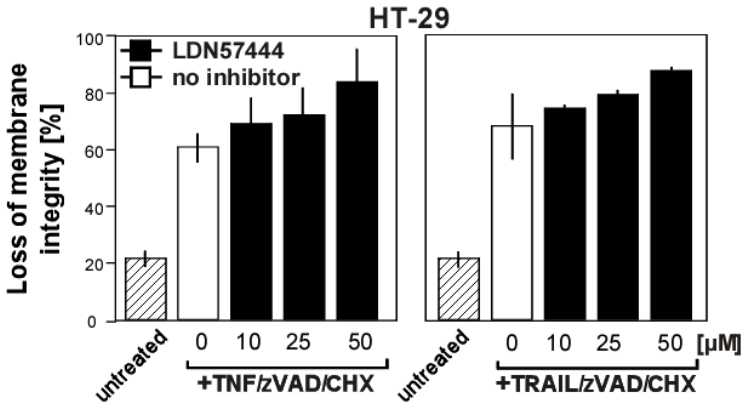

Figure 63. Inhibition of UCH-L1 does not protect from TNF- and TRAIL-mediated necroptosis in human HT-29 cells. Cells were prestimulated for 3 h with the indicated concentrations of the UCH-L1 inhibitor LDN57444 with subsequent addition of 20 µM zVAD-fmk and 5 µg/mL CHX in combination with either 100 ng/mL hrTNF or 30 ng/mL *killer*TRAIL for 16 h. Cell death was analyzed after PI-staining by flow cytometric determination of the fraction of PI-positive cells from 10,000 measured events. Values represent the means of three independent experiments, each in three repetitions. Error bars indicate the respective SD.

Similarly, the investigation of human A818-6 cells confirmed previous results (Figure 58), showing a lack of protection against TRAIL-induced necroptosis (Appendix, Figure 86 and Appendix, Figure 88 B) as well as TNF-mediated necroptosis while CHX was applied in combination with the UCH-L1 inhibitor LDN57444 (Appendix, Figure 88 A).

3.6 UCH-L1 is regulated by HtrA2/Omi during TNF-mediated but not TRAIL-mediated necroptosis

HtrA2/Omi promotes the disappearance of monomeric UCH-L1 during necroptosis in murine cells

Although a previous proteome-wide screen had not identified UCH-L1 as a substrate of the serine protease HtrA2/Omi (Vande Walle et al., 2007), a recent study demonstrated that under apoptotic conditions, UCH-L1 is cleaved by this protease (Park et al., 2011). Notably, the molecular mechanisms that regulate the levels of UCH-L1 protein and a dependence on the serine protease activity of HtrA2/Omi have not been yet elucidated for necroptosis. Therefore, proteolytic degradation of UCH-L1 was investigated in MEFs deficient for HtrA2/Omi and their wildtype counterparts during TNF- and TRAIL-mediated necroptosis. In wildtype cells, the 25-kDa band representing UCH-L1 was clearly diminished after induction of TNF-mediated necroptosis, whereas for TRAIL-mediated necroptosis no changes were observed (Figure 64). This is in line with previous data (Figure 58 and Figure 60), confirming the involvement of UCH-L1 in TNF- but not

TRAIL-mediated necroptosis in murine cells. Moreover, the results shown in Figure 64 demonstrate that the disappearance of UCH-L1 is HtrA2/Omi-dependent, as this was observed for neither TNF- nor TRAIL-mediated necroptosis in HtrA2/Omi-deficient cells. Rather, even the basal levels of UCH-L1 were highly elevated in cells lacking HtrA2/Omi (Figure 64).

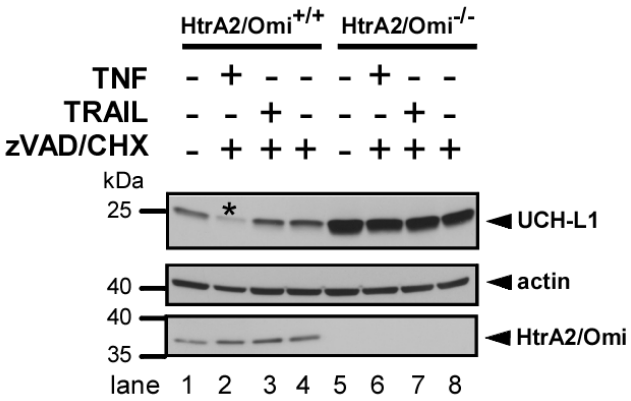

Figure 64. Lack of HtrA2/Omi prevents UCH-L1 degradation during TNF-mediated necroptosis. MEFs deficient for HtrA2/Omi and their wildtype counterparts were left untreated or treated with 100 ng/mL hrTNF or 30 ng/mL *killer*TRAIL in combination with 20 µM zVAD-fmk and 1 µg/mL CHX for 16 h. An asterisk indicates the disappearance of the UCH-L1 band. Antibodies: anti-UCH-L1 (kind gift of C. Meyer-Schwesinger), anti-actin (Sigma), anti-HtrA2/Omi (E55, Abcam).

In the experiment shown in Figure 64, a monoclonal antibody was used which recognizes only the 25-kDa full-length form of UCH-L1. To validate that UCH-L1 is indeed degraded by HtrA2/Omi during TNF-mediated necroptosis, the protein lysates shown in Figure 64 were additionally analyzed with a polyclonal antibody for UCH-L1. As shown in Figure 65, the polyclonal antibody confirmed the reduction of the 25-kDa full-length UCH-L1 band, and also recognized a pattern of multiple additional bands. Unexpectedly, the disappearance of the main band of UCH-L1 in wildtype MEFs undergoing TNF-mediated necroptosis was simultaneously accompanied by the appearance of a band possibly representing an unidentified form of UCH-L1 at 37-kDa (Figure 65, lane 2) rather than by the appearance of smaller cleavage fragments. Interestingly, the 37-kDa fragment of UCH-L1 may be a monoubiquitinated form, in which enzymatic activity is restricted (Cartier et al., 2009, Meray and Lansbury, 2007). In addition, bands at 50-kDa and 75-kDa were recognized by the antibody which may represent previously described dimeric and polymeric forms of UCH-L1 and which possess ubiquitin ligase activity whereas the monomeric form of UCH-L1 possesses only hydrolase activity (Liu et al., 2002). Since the 50-kDa band also slightly increased in wildtype MEFs undergoing TNF-induced necroptosis (Figure 65, lane 2), this may indicate that during TNF-mediated

necroptosis, UCH-L1 loses its hydrolase activity and moderately increases its ligase activity (dimerizing to the 50-kDa form). Notably, the appearance of 37-kDa band of UCH-L1 and the increase of the 50-kDa band is HtrA2/Omi-dependent as it was not observed in HtrA2/Omi-deficient MEFs (Figure 65, lane 6), and also not in cells undergoing TRAIL-mediated necroptosis (Figure 65, lane 3 and lane 7), indicating that these events may be specific for TNF-induced necroptosis.

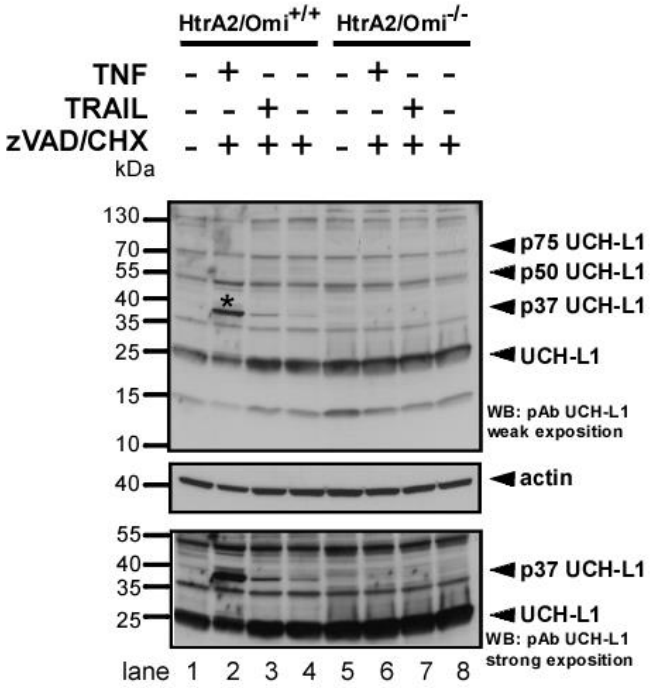

Figure 65. Reactive bands recognized by a polyclonal UCH-L1 antibody in TNF-mediated necroptosis. MEFs deficient for HtrA2/Omi and their wildtype counterparts were left untreated or treated with 100 ng/ml hrTNF or 30 ng/mL *killer*TRAIL in combination with 20 µM zVAD-fmk and 1 µg/mL CHX or with for 16 h. Arrows indicate the expected molecular masses of monomeric and multimeric or modified forms of UCH-L1. The asterisk indicates the appearance of a band potentially corresponding to a modified form of UCH-L1. Antibodies: anti-UCH-L1 (Cedarlane), anti-actin (Sigma).

Despite this assumption, the 37-kDa band recognized by the polyclonal UCH-L1 antibody was also detected (to a much lesser extent) in lysates from wildtype MEFs after induction of necroptosis by TRAIL (Figure 65, lane 3). To clarify this issue, a time kinetic of TNF- and TRAIL-induced necroptosis was performed and lysates of the different time points were analyzed for UCH-L1 modifications. In line with the data shown in Figure 65, early during TNF-mediated necroptosis, a band at 37-kDa was recognized by the polyclonal UCH-L1 antibody in wildtype but not HtrA2/Omi-deficient MEFs (Figure 66 A, lanes 3-6 *versus* lanes 9-12). Simultaneously, a slight disappearance of the main form of UCH-L1 (25-kDa) was observed as the cells gradually underwent TNF-mediated necroptosis. Of note, this was not confirmed for TRAIL-mediated necroptosis, as changes

neither in the main form of UCH-L1 nor (different from Figure 65) an appearance of the 37-kDa band were detected (Figure 66 B). Furthermore, rather tiny changes (moderate upregulation within 2 h after cell death induction) in the dimeric (50-kDa) form of UCH-L1 were detected only for TNF-mediated necroptosis (Figure 66 A, lanes 2-4), in summary indicating that in TNF- but not TRAIL-mediated necroptosis, the protease HtrA2/Omi induces a decrease of the mature, monomeric form of UCH-L1, possibly associated with its modification to forms of higher molecular weight.

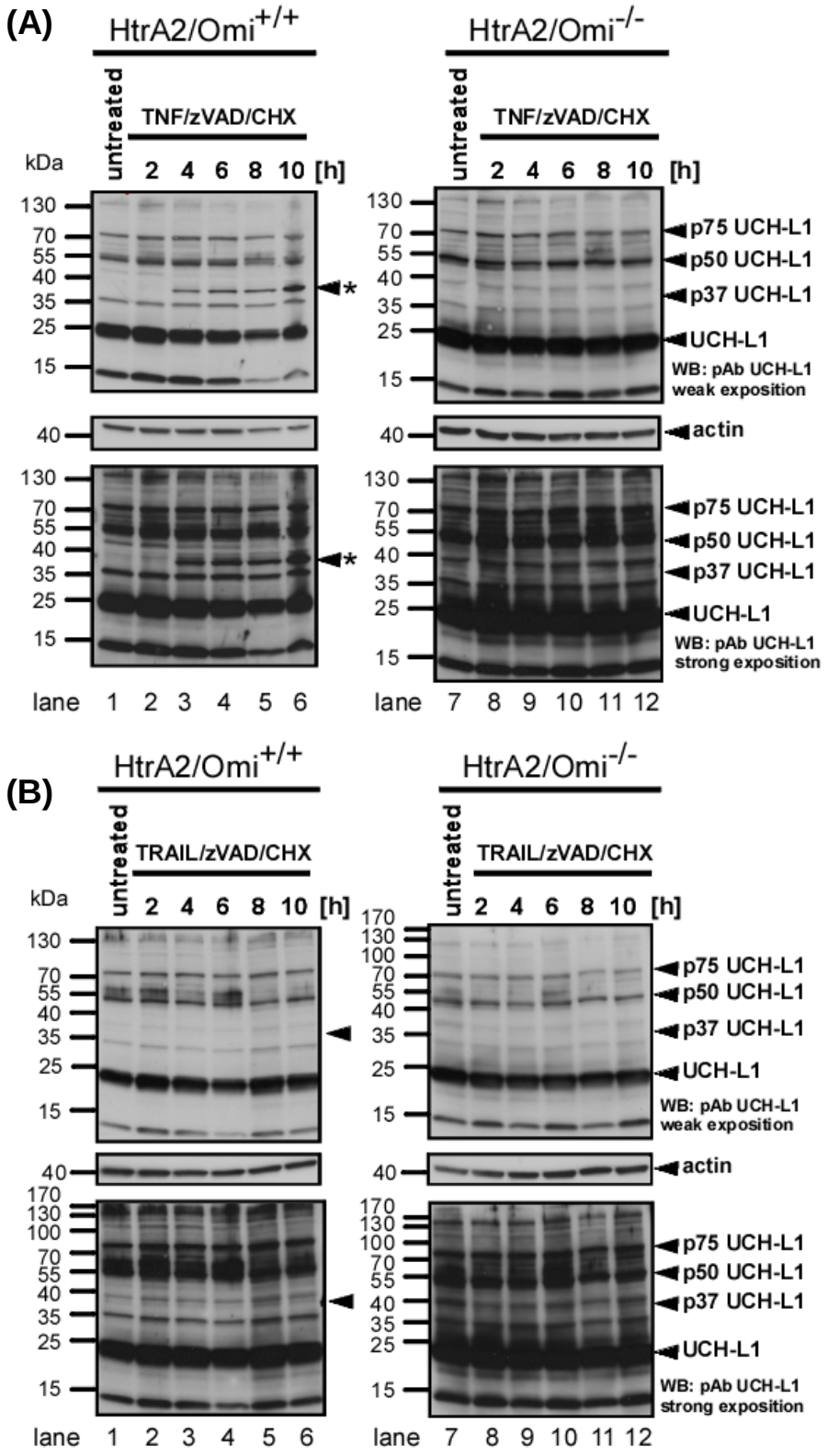

Figure 66. Time course experiment for TNF-mediated necroptosis showing an HtrA2/Omi-dependent increase of the 37-kDa band recognized by the polyclonal UCH-L1 antibody. MEFs deficient for HtrA2/Omi and their wildtype counterparts were left untreated or treated with **(A)** 100 ng/mL hrTNF or **(B)** 30 ng/mL *killer*TRAIL in combination with 20 µM zVAD-fmk and 1 µg/mL CHX for the indicated periods of time. The asterisks indicate an appearance of the modified band of UCH-L1. Antibodies: anti-UCH-L1 (Cedarlane), anti-actin (Sigma).

In order to clarify whether the observed 37-kDa band detected by the polyclonal UCH-L1 antibody was indeed a monoubiquitinated form of UCH-l, an activity-based protein profiling with the use of active-site directed chemical probes was performed. For this purpose, ubiquitin-based electrophilic probes (ubiquitin vinyl methyl ester, Ub-VME) that were epitope-tagged with hemagglutinin (HA) were incubated with cell lysates from untreated or necroptotic wildtype or HtrA2/Omi-deficient MEFs in order to identify and quantify the ability of UCH-L1 to bind ubiquitin (Ub, which leads to a shift of UCH-L1 from 25 kDa to 37 kDa). Notably, a diminished binding of the active-site directed probe (HA-Ub) was detected at 37 kDa in wildtype MEFs undergoing TNF-mediated necroptosis (Figure 67, upper panel, lane 4), indicating that UCH-L1 was already activated in these lysates, and bound to untagged cellular ubiquitin (which is not recognized by the HA-specific antibodies employed in the assay). In contrast, a high amount of the HA-Ub probe was bound in lysates from untreated wildtype MEF (Figure 67, upper panel, lane 2) and from both untreated and necroptotic HtrA2/Omi-deficient cells (Figure 67, upper panel, lanes 6 and 8), most likely because inactive UCH-L1 was not monoubiquitinated by untagged ubiquitin. In reblots with a polyclonal antibody for UCH-L1 (Figure 67, lower panel), a comparison between UCH-L1 modified by the substrate (HA-Ub) (upper band) and the unmodified, main form of UCH-L1 (lower band) demonstrated that indeed binding of Ub to UCH-L1 shifts the 25-kDa band of the enzyme to the 37-kDa form, as observed previously during TNF-mediated necroptosis (Figure 65, lane 2). Furthermore, an increased amount of the dimeric (50-kDa) form of UCH-L1 was detected in lysates from wildtype MEF undergoing TNF-mediated necroptosis (Figure 67, lower panel, lanes 3, 4) but was absent in lysates from HtrA2/Omi-deficient cells resistant to TNF-mediated necroptosis (Figure 67, lower panel, lanes 7, 8).

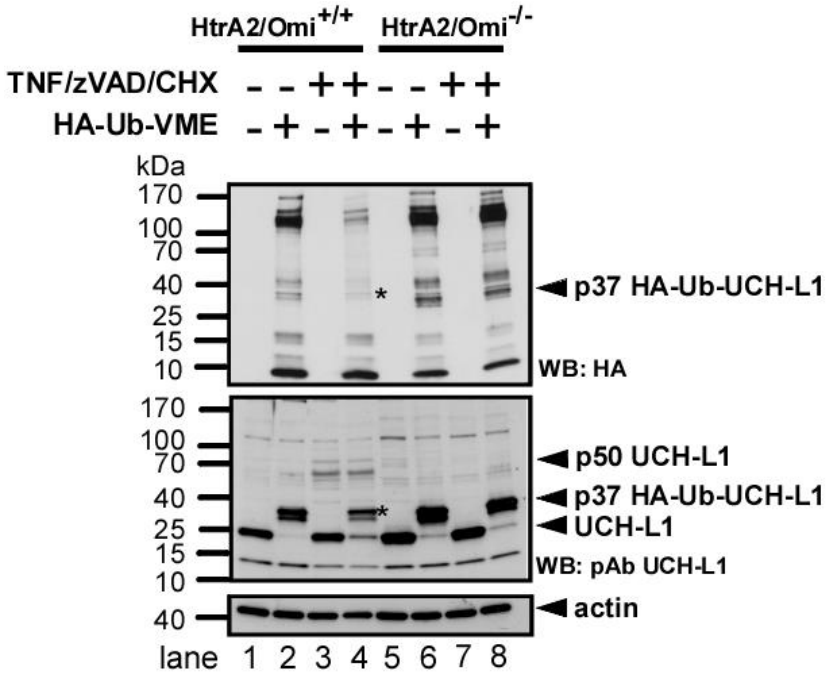

Figure 67. Detection of monoubiquitinated form of UCH-L1 in murine wildtype and HtrA2/Omi-deficient MEFs during TNF-mediated necroptosis. MEFs deficient for HtrA2/Omi and their wildtype counterparts were left untreated or treated with 100 ng/ml hrTNF in combination with 20 µM zVAD-fmk and 1 µg/mL CHX for 16 h. Afterwards, 30 µg of whole cell lysates were incubated with 20 µM of HA-Ub-VME (Enzo Life Science, BML-UW0880) probe in 50 mM Tris, 150 mM NaCl pH 8.0 for 90 min at 37°C. Afterwards, the labeling reactions were quenched by addition of reducing sample buffer, boiled for 10 min and analyzed by SDS-PAGE followed by Western blot. Modified HA-Ub-bound deubiquitinating enzymes were detected by anti-HA antibody (Roche, upper panel). Subsequently, the unmodified (UCH-L1) and monoubiquitinated form (upper band) of UCH-L1 was detected with pAb for UCH-L1 (Cedarlane). The loading control was detected with anti-actin (Sigma). Asterisks indicate the monoubiquitinated form of UCH-L1.

To confirm the data obtained in MEFs, the disappearance of the main band of UCH-L1 and the generation of the 37-kDa putative modified form of UCH-L1 was analyzed in murine L929Ts cells (Figure 68). Surprisingly, in L929Ts cells, the main form of UCH-L1 at 25 kDa was not detected by the monoclonal antibody (Figure 68 A), only by the polyclonal antibody for UCH-L1. Furthermore, the polyclonal antibody did not detect a decrease in the main 25-kDa form of UCH-L1 during TNF-induced necroptosis. Moreover, the increase of the putative 37-kDa form of UCH-L1 was not observed (Figure 68, lanes 2, 4, 6) as in MEFs (Figure 68 B, lane 8). Rather, an increase in the putative 50-kDa form of UCH-L1 was observed early in TNF-mediated necroptosis. UCH-L1 inhibition by LDN57444 slightly inhibited the massive increase of this putative 50-kDa form of UCH-L1. This suggests that in L929Ts cells, the putative dimeric form of UCH-L1 with its ligase activity may participate in TNF-mediated necroptosis whereas in MEFs, UCH-L1 is modified differently after induction of necroptosis by TNF, mainly leading to a

(monoubiquitinated?) form of 37-kDa. In both cases, however, this modification depends on the activity of HtrA2/Omi.

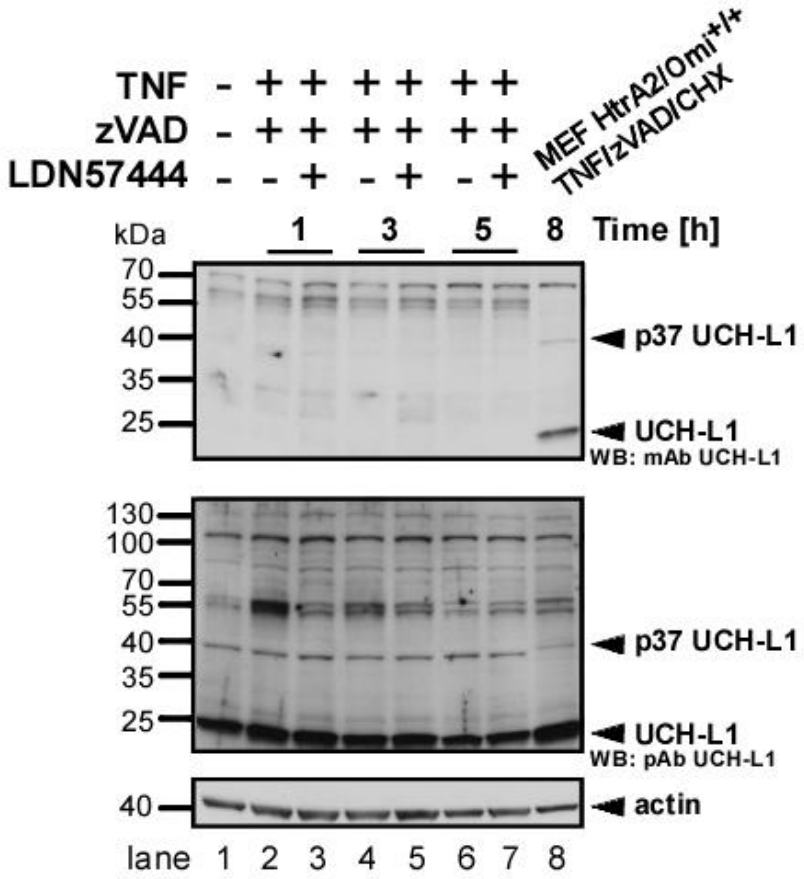

Figure 68. Detection of UCH-L1-reactive bands in murine L929Ts cells in TNF-mediated necroptosis. Cells were pretreated for 3 h with 50 µM LDN57444 or not with subsequent addition of 100 ng/mL hrTNF in combination with 20 µM zVAD-fmk for the indicated times. Lysates of MEFs HtrA2/Omi$^{+/+}$ stimulated for 8 h with 100 ng/mL hrTNF in combination with 50 µM zVAD-fmk and 1 µg/mL CHX were used as a positive control for the appearance of the 25-kDa and putative 37-kDa band of UCH-L1. Antibodies: mAb anti-UCH-L1 (kind gift of C. Meyer-Schwesinger), pAb anti-UCH-L1 (Cedarlane), anti-actin (Sigma).

Taken together, UCH-L1 is regulated by HtrA2/Omi during TNF-mediated necroptosis and may be one of the factors that mediate this form of caspase-independent cell death.

4. Involvement of reactive oxygen species (ROS) in necroptosis

In some cell lines antioxidants reduce production of ROS and abolish TRAIL-mediated necroptosis

Whereas the role of ROS in TNF-induced necroptosis is very well investigated (Thon et al., 2005, Vandenabeele et al., 2010), much less is known about their possible function in necroptosis induced by TRAIL. In order to investigate if ROS are acting downstream of TRAIL signaling in necroptosis, ROS production was analyzed by staining with 2‘-7‘-dichlorodihydrofluorescein diacetate (CM-H_2DCFDA) and compared with the level of cell death. Moreover, it was determined whether application of radical scavengers during TRAIL-induced necroptosis and (as a positive control) BuOOH-induced programmed necrosis may confer protection. As shown in Figure 69, depending on the cell type, TRAIL-induced necroptosis and BuOOH-induced programmed necrosis were accompanied by a strong to modest intracellular ROS production. Interestingly, it was found that in Jurkat ATCC cells, TRAIL-mediated necroptosis induced only a weak production of ROS, which was insensitive for administration of anti-oxidants. For L929Ts and NIH3T3 cells, generation of ROS during both TRAIL-mediated necroptosis and BuOOH-induced programmed necrosis was successfully suppressed by the radical scavenger BHA but not by the related (but obviously less effective) scavenger BHT (Figure 69).

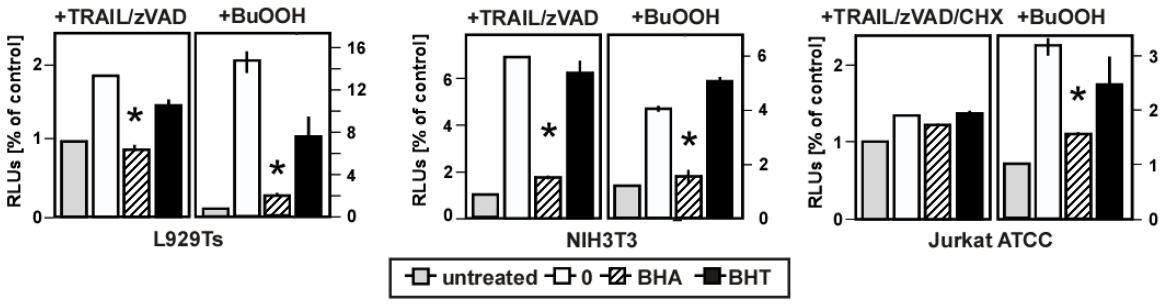

Figure 69. Analysis of ROS in L929Ts, NIH3T3 and Jurkat ATCC cells. All cell lines were pretreated with 150 µM BHA or BHT for 1 h or not with subsequent addition of 30 ng/mL *killer*TRAIL and 20 µM zVAD-fmk for 14 h (L929Ts cells), 100 ng/mL *killer*TRAIL and 20 µM zVAD-fmk for 16 h (NIH3T3 cells) and 50 ng/mL *killer*TRAIL in combination with 50 µM zVAD-fmk and 2 µg/mL CHX for 20 h (Jurkat ATCC cells). Additionally, each cell line was treated with 1 mM BuOOH for 24 h as a positive control for ROS production. The level of ROS was measured by flow cytometry and are shown as relative fluorescence units in comparison to untreated cells. Graphs represent the values of one out of three independent experiments. Error bars indicate the respective SD. Asterisks indicate statistical significance (t-test) $p<0.01$.

Almost identical results were obtained when cell death instead of ROS production was analyzed (Figure 70). In L929Ts and NIH3T3 cells, BHA (but not or only to a much lesser extent, BHT) blocked TRAIL-mediated necroptosis as well as BuOOH-induced programmed necrosis. As expected, scavenging of ROS by BHA in Jurkat cells had no effect on TRAIL-mediated necroptosis but was sufficient to constrain BuOOH-induced programmed necrosis. These findings point to a differential dependence of TRAIL-mediated necroptosis on ROS in different cells. Since an antioxidant such as BHA is sufficient to rescue cells from TRAIL-mediated necroptosis, a therapeutic target was established.

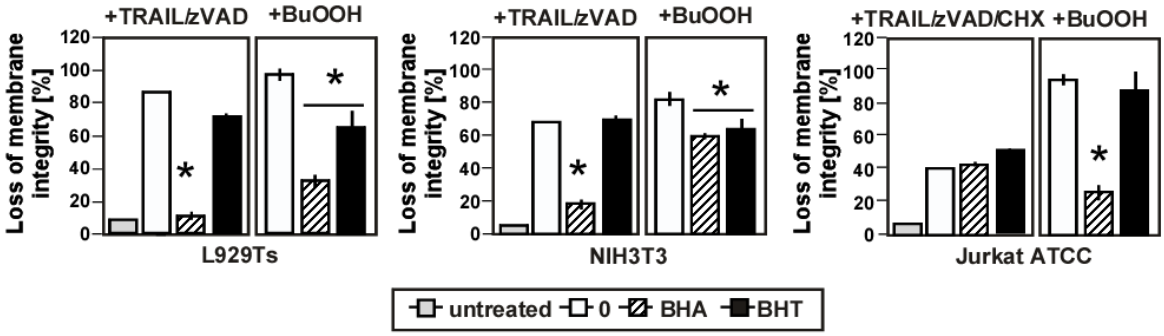

Figure 70. Loss of cell viability in TRAIL-mediated necroptosis after application of radical scavengers. All cell lines were pretreated with 150 µM BHA or BHT for 1 h or not with subsequent addition of 30 ng/mL *killer*TRAIL and 20 µM zVAD-fmk for 14 h (L939Ts cells), 100 ng/mL *killer*TRAIL and 20 µM zVAD-fmk for 16 h (NIH3T3 cells) and 50 ng/mL *killer*TRAIL in combination with 50 µM zVAD-fmk and 2 µg/mL CHX for 20 h (Jurkat ATCC cells). Additionally, each cell line was treated with 1 mM BuOOH for 24 h as a positive control for ROS production. The level of PI-positive cells was measured by flow cytometry measuring 10,000 events. Graphs represent values of one out of three independent experiments. Error bars indicate the respective SD. Asterisks indicate statistical significance (t-test) $p<0.01$.

5. Role of autophagy in TNF and TRAIL-mediated necroptosis

In order to investigate the contribution of "autophagic degradation" to necroptosis, necroptotic cell death was analyzed in different cell lines in the presence or absence of the autophagy inhibitor 3-methyladenine (3-MA). Furthermore, to account for unspecific activities of this inhibitor, other major pharmacological inhibitors were used to block later stages of autophagy, such as chloroquine and bafilomycinA_1 which inhibit autophagic degradation processes inside of the autolysosomes (Figure 7).

Lysosomal acidification and vacuolar-type H^+-V-ATPase but not autophagy regulate necroptosis in murine cells

In murine L929ATCC cells, autophagy is executed independently of caspase inhibition, and even induced by the presence of zVAD-fmk alone (Chen et al., 2011) (Figure 71 A), making this cell line a suitable positive control for autophagy. Correspondingly, zVAD-fmk-induced autophagy was inhibited effectively with 3-MA in L929ATCC cells (Figure 71 A). This inhibitor was unable to rescue the death mediated by both TNF and TRAIL in presence of caspase inhibitor (Figure 71 B and C), thus indicating that autophagy is not involved in necroptosis. In contrast, inhibition of lysosomal function (through disturbance of the acidic environment of endocytic vesicles by chloroquine) or acidification of autophagosomes/lysosomes by the vacuolar-type H^+-V-ATPase (inhibited with bafilomycin A_1) could not rescue from autophagy but had an impact on necroptosis (Figure 71 A). In L929Ts cells, 3-MA did not protect from either TNF- or TRAIL-mediated necroptosis, demonstrating that autophagy is not involved in this type of cell death. For TNF-induced necroptosis, both chloroquine and bafilomycin A_1 protected with statistical significance, indicating that the further execution of necroptosis depends on the formation of lysosomal compartments and the activity of vacuolar-type H^+-V-ATPase (Figure 71 B). In contrast, for TRAIL-induced necroptosis in L929Ts cells, protection was seen only for bafilomycin A_1 (Figure 71 C), indicating that activity of vacuolar-type H^+-V-ATPase was important for this pathway. These results were validated by morphological analyses and confirmed protection against TNF-mediated necroptosis when chloroquine and bafilomycin A_1 were added, whereas for TRAIL-mediated necroptosis only administration of bafilomycin A_1 rescued the cells from necroptosis (Figure 71 D).

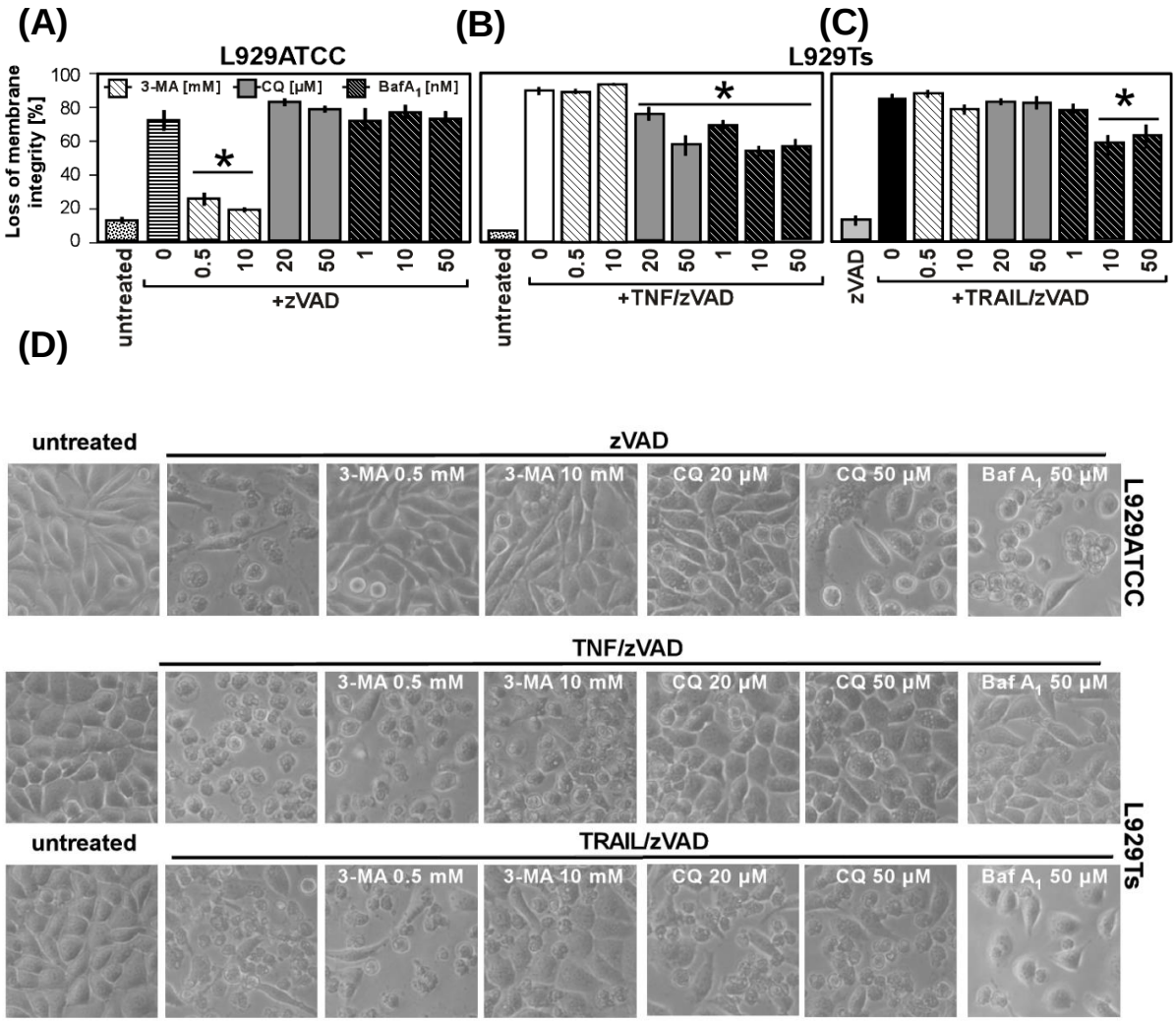

Figure 71. **Autophagy is not playing a crucial role in TNF- or TRAIL- mediated necroptosis in L929Ts cells. (A)** As a positive control for autophagy, L929ATCC cells were stimulated for 24 h with 20 µM zVAD-fmk without or with pretreatment for 2 h with the indicated concentrations of inhibitors of autophagy (3-MA), lysosomal formation (CQ, chloroquine) or vesicle acidification ($BafA_1$, bafilomycin A1). L929Ts cells were pretreated with 3-MA, CQ, or $BafA_1$ as in (A) with subsequent addition of 20 µM zVAD-fmk in combination with **(B)** 100 ng/mL hrTNF for 5 h or **(C)** with 30 ng/mL *killer*TRAIL for 14 h. Data present the rate of cell death, analyzed after PI-staining by flow cytometric determination of the fraction of PI-positive cells. Values represent the means of at least three independent experiments, each in two repetitions. Error bars indicate the respective SD. Asterisks indicate statistical significance (t-test) $p<0.01$. **(D)** Morphological analyses of the influence of 3-MA, CQ, or $BafA_1$ on TNF- and TRAIL-mediated necroptosis and zVAD-fmk-induced autophagy. Cells were stimulated as in (A-C). Magnification 320x.

These data suggest that autophagy is not essential for TNF- or TRAIL-mediated necroptosis, but rather that the components of the lysosomal compartment and the function of vacuolar-type H^+-V-ATPase enhance the necroptotic program in later stages. Furthermore, the obtained results indicate that this contribution of various cellular compartments such as lysosomes or vacuolar-type H^+-V-ATPase is different for TNF- and TRAIL-induced necroptosis.

In human cells, lysosomal acidification and vacuolar-type H^+-V-ATPase, but not autophagy contribute to necroptosis

When the same experiments were performed in human HT-29 and Jurkat cells, the obtained results suggested that none of the autophagic components is playing a role in both TNF- and TRAIL-mediated necroptosis (Figure 72). Neither a role of the lysosomal compartment nor the activity of vacuolar-type H^+-V-ATPase influenced necroptosis in human cells (Figure 72 A and B). However, (as seen above for inhibitors of A-SMase and N-SMase Figure 34 and Figure 35 or for Ucf-101, Figure 51), the required addition of CHX as a sensitizer for necroptosis in these cells might interfere with protection of necroptosis by 3-MA, CQ and $BafA_1$.

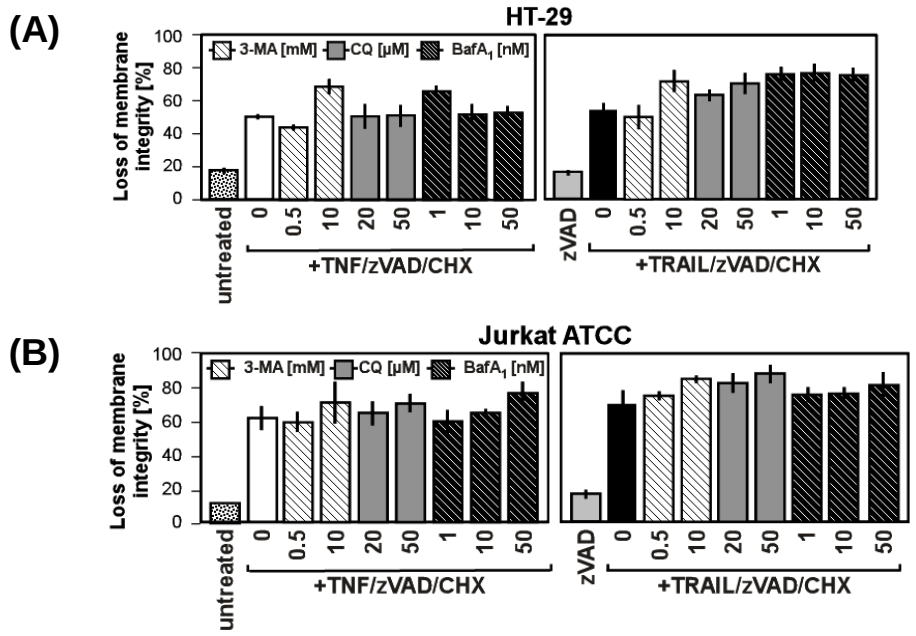

Figure 72. Autophagy is not involved in TNF- or TRAIL-mediated necroptosis in human HT-29 or Jurkat cells. Cells were preincubated for 2 h with the indicated concentrations of inhibitors with subsequent addition of **(A)** 100 ng/mL hrTNF or 30 ng/mL *killer*TRAIL in combination with 20 µM zVAD-fmk and 5 µg/mL CHX for 16 h for HT-29 cells. **(B)** Jurkat cells were stimulated by subsequent addition of 100 ng/mL hrTNF or 50 ng/mL *killer*TRAIL in combination with 50 µM zVAD-fmk and 2 µg/mL CHX for 20 h. Cell death was analyzed after PI-staining by flow cytometric determination of the fraction of PI-positive cells. Values represent the means of at least two independent experiments, each in two repetitions. Error bars indicate the respective SD.

Therefore, and in order to complete the investigation of human cells, Jurkat I.42 cells deficient for FADD and stably transfected with TNF-R2, which do not require sensitization by CHX to undergo TNF-mediated necroptosis were investigated. The obtained results were in line with the previous findings for murine cells (Figure 73), clearly showing that the autophagic sequestration inhibitor 3-MA did not protect the cells from necroptosis. Thus, an impact of autophagy on the executive pathways during necroptosis in human cells

was excluded. Furthermore, the results from Jurkat I.42 cells point to an involvement of lysosomal compartments (inhibited with chloroquine) and the activity of vacuolar-type H^+-V-ATPase (inhibited with bafilomycin A_1) in TNF-mediated necroptosis (Figure 73). However, the impact of inhibition of lysosomal pathway or of the activity of vacuolar-type H^+-V-ATPase on necroptosis was lower in human cells than in murine cells (Figure 71 B and C). Therefore, necroptosis in murine cells may involve elements such as lysosomal compartments and its acidification, but apparently, the role of these compartments in necroptosis in human cell lines is minor.

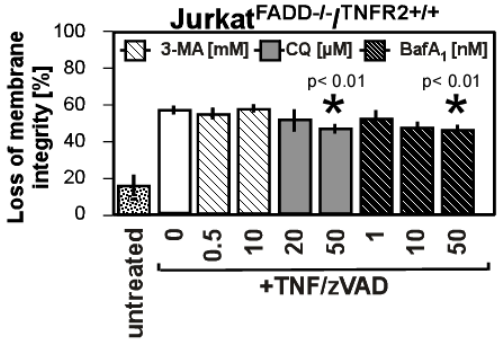

Figure 73. Autophagy is not playing a crucial role in TNF-mediated necroptosis in FADD-deficient human I.42 Jurkat T cells. Jurkat I.42 cells deficient for FADD but stably transfected with TNF-R2 were prestimulated for 2 h with the indicated concentrations of inhibitors of autophagy (3-MA), lysosomal formation (CQ) or vacuolar compartment formation ($BafA_1$). Next, cells were treated for 6 h by addition of 100 ng/mL hrTNF in combination with 50 µM zVAD-fmk. Cell death was analyzed after PI-staining by flow cytometric determination of the fraction of PI-positive cells. Values represent the means of three independent experiments, each in two repetitions. Error bars indicate the respective SD. Asterisks indicate statistical significance (t-test) $p<0.01$.

Subsequently, an involvement of autophagic components in necroptosis was analyzed in the human cell line A818-6. After induction of TRAIL-mediated necroptosis without CHX, the obtained data confirmed previous findings, indicating a minor role of vacuolar-type H^+-V-ATPase but not a role of lysosomes in TRAIL-mediated necroptosis (Appendix, Figure 86 and Appendix, Figure 87) In line with reports for HT-29 and Jurkat cells, the presence of CHX obliterated any CQ- or $BafA_1$-mediated protection from TNF- or TRAIL-mediated necroptosis in this cell line (Appendix, Figure 88 B).

Atg5 is required for both TNF- and TRAIL-mediated necroptosis

A major limitation of inhibitors are non-specific side effects. Therefore, the above pharmacological studies were combined with genetic approaches to more specifically investigate the involvement of autophagy in TNF- and TRAIL-mediated necroptosis.

MEFs deficient for Atg5 were resistant to both TNF- and TRAIL-mediated necroptosis, regardless of the absence or presence of CHX (Figure 74 A). Similarly, morphological observations of the cells confirmed that deficiency of Atg5 is a crucial component in protection against both TNF-and TRAIL-mediated necroptosis (Figure 74 B).

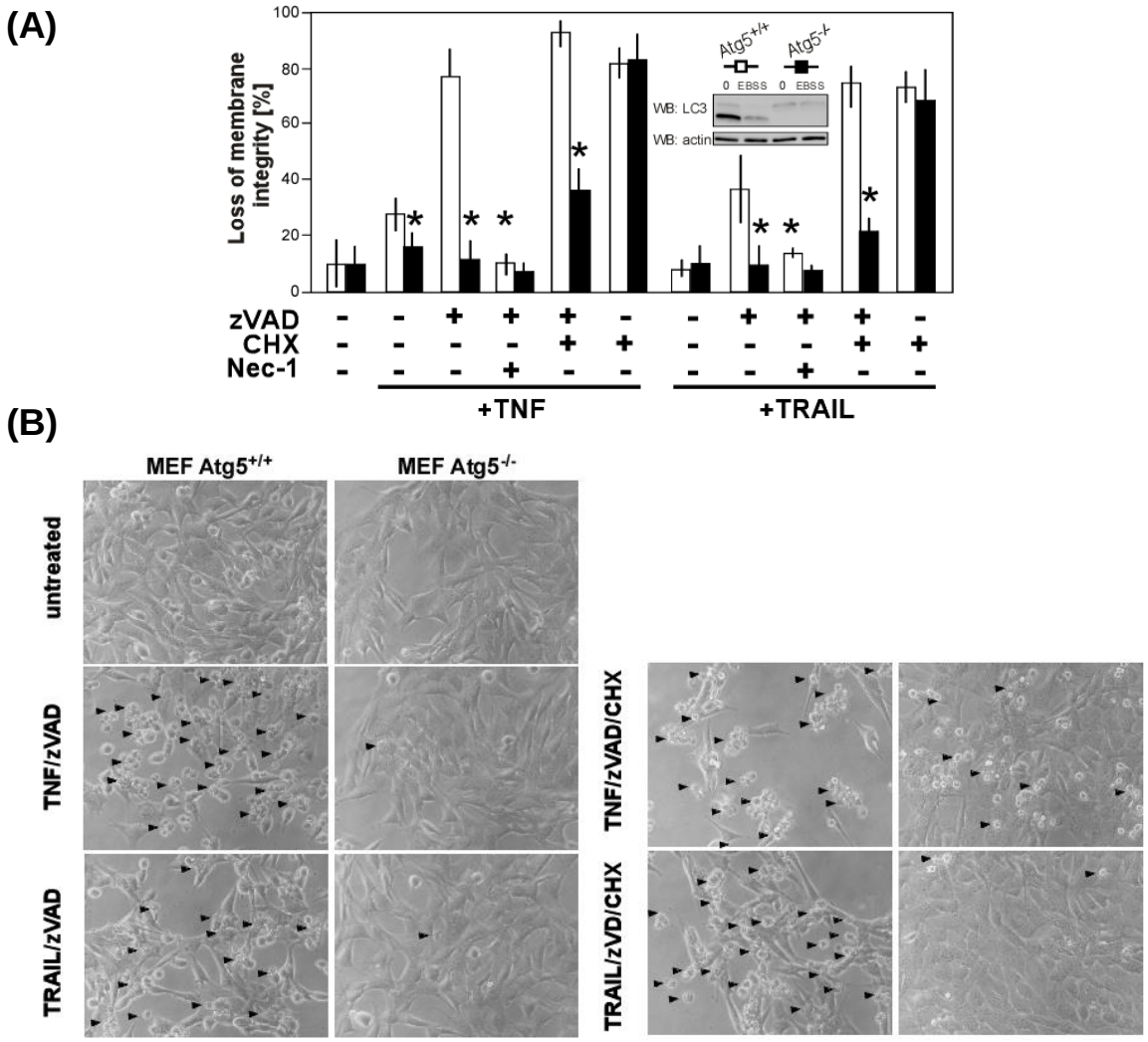

Figure 74. Atg5 is required for both TNF- and TRAIL-mediated RIP1-dependent necroptosis. (A) Atg5-deficient immortalized MEFs and their wildtype counterparts were prestimulated with 50 µM Nec-1 (to verify that cell death occurred by necroptosis) or not for 2 h followed by addition of 100 ng/mL hrTNF or 30 ng/mL *killer*TRAIL together with 20µ M zVAD-fmk and/or 1 µg/mL CHX to induce necroptosis; or 100 ng/mL hrTNF or 30 ng/mL *killer*TRAIL together with 1 µg/mL CHX to induce apoptosis for 18 h. Cell death was analyzed after PI-staining by flow cytometric determination of the fraction of PI-positive cells from 10,000 measured events. Values represent the means of at least three independent experiments, each in two repetitions. Error bars indicate the respective SD. Asterisks indicate statistical significance (t-test) $p<0.01$. In order to verify the authenticity of wildtype and Atg5-deficient MEFs, cells were left untreated in full medium or treated for 2 h with Earle's Balanced Salt Solution (EBSS) to induce autophagy by starvation. Afterwards, whole cell lysates were generated and the appearance of the protein LC3-II as an indicator for autophagy was analyzed. Insets: control Western blot for LC3 under normal and starvation conditions (EBSS). LC3-II is the lowest band. Antibodies: anti-LC3 (nanoTools), anti-actin (Sigma) **(B)** Morphological analyses of necroptosis in Atg5-deficient and wildtype MEFs. Black arrows indicate typical necroptotic morphology. Magnification 320x.

Opposite to the results obtained for necroptosis, deletion of Atg5 did not rescue cells from TNF- or TRAIL-mediated apoptosis (Figure 74 A and Figure 75), in summary suggesting that Atg5 is required for TNF- and TRAIL-mediated necroptosis, but that this protein is dispensable for apoptosis induced by these cytokines.

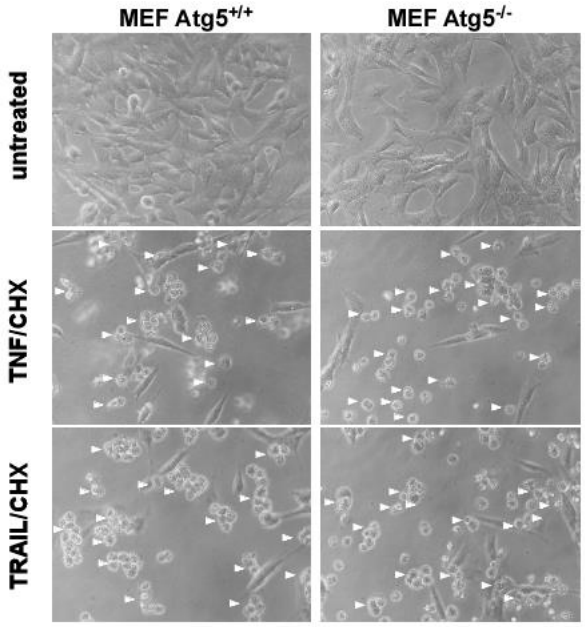

Figure 75. Morphological analyses of TNF- and TRAIL-mediated apoptosis in MEFs lacking Atg5 and their wildtype counterparts. Immortalized MEFs deficient for Atg5 and their wildtype counterparts were stimulated with 100 ng/mL hrTNF or 30 ng/mL *killer*TRAIL together with 1 µg/mL CHX for 18 h. White arrows indicate morphological changes typical for apoptosis. Magnification 320x.

Atg16L1 contributes to TNF-mediated necroptosis

In addition to Atg5-deficient MEFs, MEFs lacking Atg16L1, another factor crucial for autophagy (Figure 7) were investigated. In contrast to the results obtained for Atg5-deficient cells, deletion of Atg16L1 diminished only TNF- but not TRAIL-mediated necroptosis (Figure 76 A). Moreover, the protective effects of Atg16L1 were completely abolished in the presence of CHX, suggesting that Atg16L1 has to be actively translated to be involved in TNF-mediated necroptosis and though differently than Atg5 involved in necroptosis. Furthermore, similarly to the results obtained for Atg5, genetic deficiency for Atg16L1 did not rescue from TNF- and TRAIL-mediated apoptosis (Figure 76 A). The data were confirmed by morphological observations (Figure 76 B), revealing significant protection against TNF- but not TRAIL-mediated necroptosis in Atg16L1 deficient cells.

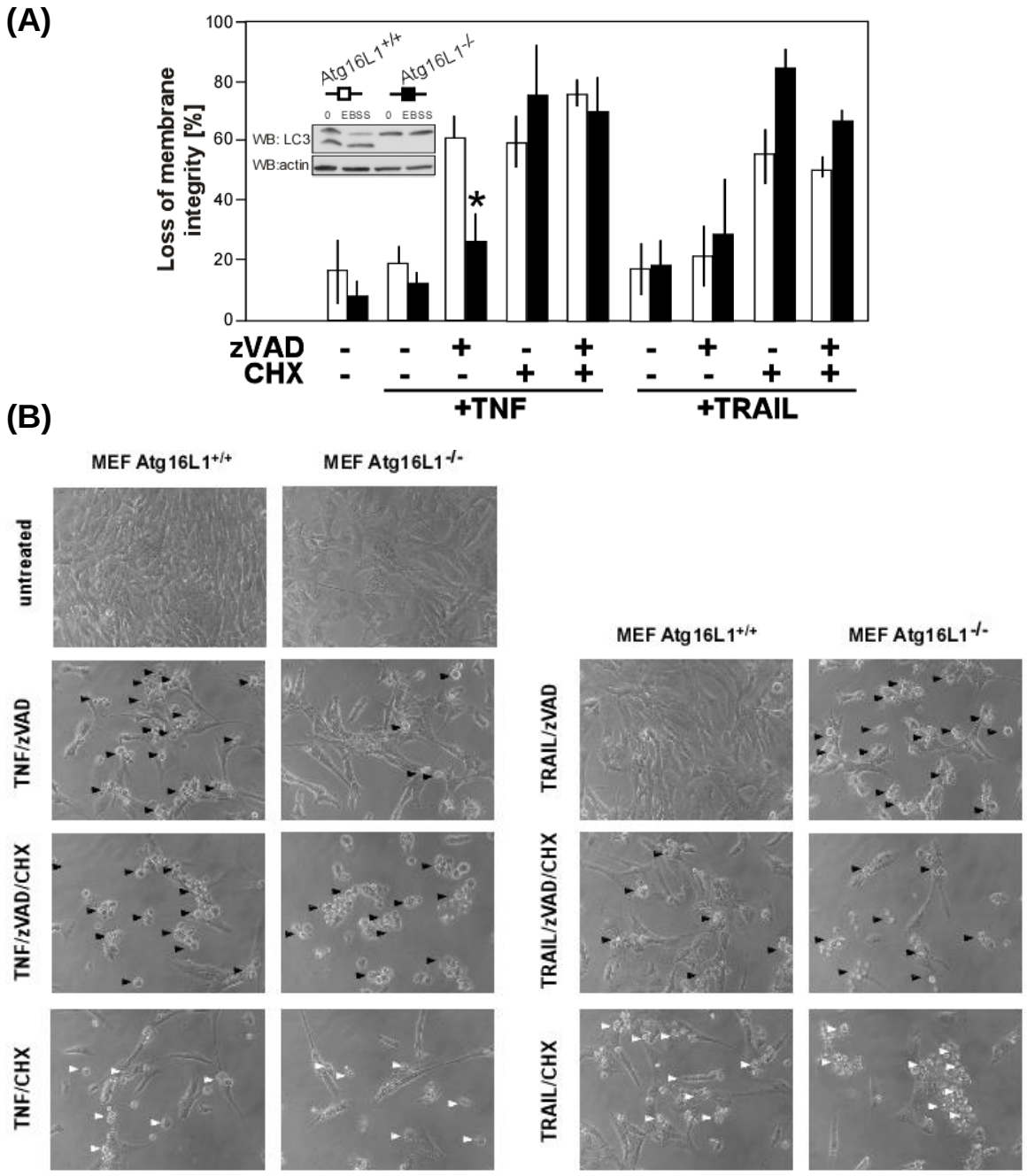

Figure 76. Lack of Atg16L1 protects from TNF-mediated but not TRAIL-mediated necroptosis and does not influence both TNF and TRAIL-mediated apoptosis. (A) Atg16L1-deficient immortalized MEFs and their wildtype counterparts were stimulated with 100 ng/mL hrTNF or 30 ng/mL *killer*TRAIL together with 20 µM zVAD-fmk and/or 1 µg/mL CHX to induce necroptosis; or 100 ng/mL hrTNF or 30 ng/mL *killer*TRAIL together with 1 µg/mL CHX to induce apoptosis for 24 h. Cell death was analyzed after PI-staining by flow cytometric determination of the fraction of PI-positive cells from 10,000 measured events. Values represent the means of at least three independent experiments, each in three repetitions. Error bars indicate the respective SD. Asterisks indicate statistical significance (t-test) $p<0.01$. In order to verify the authenticity of wildtype and Atg16L1-deficient MEFs, cells were left untreated in full medium or treated for 2 h with Earle's Balanced Salt Solution (EBSS) to induce autophagy by starvation. Afterwards, whole cell lysates were generated and the appearance of the protein LC3-II as an indicator for autophagy was analyzed. Insets: control Western blot for LC3 under normal and starvation conditions (EBSS). LC3-II is the lowest band. Antibodies: anti-LC3 (nanoTools), anti-actin (Sigma). **(B)** Morphological analyses of necroptosis and apoptosis in Atg16L1-deficient and wildtype MEFs. Cells were stimulated as in (A) and microscopic observations were conducted. Black arrows indicate typical necroptotic morphology and white arrows indicate blebbing and apoptotic bodies characteristic for apoptosis. Magnification 320x.

In summary, the data obtained above suggest that not autophagy *per se* plays a role in necroptosis, but rather certain elements of the autophagic machinery can also be involved in or interact with components of the necroptotic pathway.

V. Discussion

A. DNA damage/PARP1-induced necrosis and TNF-mediated necroptosis are two separate routes of caspase-independent programmed cell death

Since various previous studies had postulated a crosstalk between components of programmed necrosis and RIP1/RIP3-dependent necroptosis (Galluzzi and Kroemer, 2008, Wu et al., 2012), their involvement in necroptosis was investigated in this thesis. A recent review has suggested a role of various necrotic components such as CypD (*Ppif*), PARP1, JNKs activation, or AIF translocation in necroptosis (Vandenabeele et al., 2010). However, another study had already shown that in activated T cells, necroptosis is executed without CypD (Ch'en et al., 2011), indicating that those components may not necessarily be required for necroptosis. Supporting these initial findings, the data presented here indicate that TNF-induced necroptosis and the PARP-pathway represent two distinct and independent routes to programmed necrosis.

In murine cells, the pan-caspase inhibitor zVAD-fmk effectively blocked PARP1 cleavage typical for apoptosis and even enhanced the TNF-dependent hyperactivation of PARP1. In contrast, in human Jurkat and HT-29 cells, a partial cleavage of PARP1 was detectable, represented by an 89-kDa band during caspase-independent necroptosis. This "background band" may be due to incomplete inhibition by zVAD-fmk, as at concentrations of up to 50 μM it does not block effectively DNA fragmentation (Caserta et al., 2003) and activity of caspase-6 that might cleave PARP1 (Okinaga et al., 2007). On the other hand, the 89-kDa band of PARP1 can appear in human MCF-7 cells independently of inactivation of executioner caspases-7 and -6 and in the absence of caspase-3 (Alam et al., 2011). Alternatively, the cleavage of PARP1 under caspase-independent conditions may be explained by the activity of cathepsins B and D (Chaitanya et al., 2010, Morinaga et al., 2010) or by a cleavage within the PARP1 automodification domain by granzyme B (Zhu et al., 2009) that generates enzymatically inactive product. As it was shown in this thesis that neither calpains nor cathepsins play a role in caspase-independent necroptosis, rather a role of granzyme B in the generation of the 89-kDa band of PARP1 and in the further execution of TNF- and TRAIL-mediated caspase-independent cell death in human cell lines may be possible and thus be of interest for further investigations.

Although many PARP isoenzymes exists, in MNNG-mediated necrosis, only the role of PARP1 has been elucidated and the role of other isoenzymes such as PARP2 was not confirmed (Cohausz and Althaus, 2009). However, for cytokine-mediated necroptosis, Hitomi and coworkers had found that PARP2 may be involved in the execution of this type of cell death. To investigate a possible, redundant function of PARP2 in necroptosis, olaparib, a specific inhibitor of both isoenzymes PARP1 and PARP2 was used in this thesis. Pharmacological inhibition of both PARP1 and PARP2 enzymes by olaparib did not protect cells from TNF- or TRAIL-mediated necroptosis, arguing against a role of both PARP isoforms in necroptosis.

Inhibitors of PARP may exhibit a protective, a neutral, or a sensitizing action during the formation of atherosclerotic plaques (Hans et al., 2008), decrease tissue injury and inflammation after ischemia-reperfusion in cardiovascular disease (Crawford et al., 2010), as well as in neurodegenerative diseases, stroke (Luo and Kraus, 2012), diabetes mellitus (Burkart et al., 1999), hemorrhagic shock, septic shock, and lung inflammation (Aguilar-Quesada et al., 2007). Moreover, inhibitors of PARP1 were shown to be involved in the upregulation of cell death, e.g. in cancer cells expressing a dysfunctional BRCA gene (Underhill et al., 2011). In this thesis, it was shown that although the PARP1/2 inhibitor olaparib decreased the production of PARP-specific poly(ADP)-ribosylated macromolecules, it did not influence TNF- or TRAIL-mediated necroptosis or induce a protective effect. Similarly, the PARP1 inhibitor 3-AB did not rescue cells from TNF- or TRAIL-mediated necroptosis. Surprisingly, the PARP inhibitor PJ34 triggered rather cell-line and cytokine-specific effects on necroptosis. Although some data indicate that PJ34 may effectively block necroptosis, e.g. glutamate-mediated necroptosis in HT-22 cells through reduction of PARP1 activity (Xu et al., 2010), it is still unclear how specific this inhibitor really is. Recent analyses had suggested that PJ34 is also able to target the isoenzymes PARP2 and PARP3, leading to a decrease in the production of pro-inflammatory mediators such as interleukin-1β or TNF (Phulwani and Kielian, 2008). Moreover, PJ34 has been described to exhibit cell-type specific effects on cell survival. In certain cell lines, PJ34 has been found to cause mitotic arrest independently of PARP1 or PARP2 (Madison et al., 2011) or to block glutamate uptake independent from PARP1 inhibition (Nasrabady et al., 2012). Therefore, it is very likely that the protective changes observed after administration of PJ34 during necroptosis in this thesis do not depend completely on PARP1 inhibition, but are caused by non-specific effects of PJ34 in some,

but not other cell lines, e.g. by affecting the expression of genes involved in cell cycle progression, survival or by targeting additional factors such glutamate uptake, e.g. for energy production. The inhibitor 3-AB may as well non-specifically influence cell survival through reduction of NF-κB expression or may influence cell interactions through its influence on matrix metalloprotease-9 (MMP-9) (Koh et al., 2005). In summary, these non-specific side effects of the above PARP inhibitors are most likely responsible for any inconsistencies between cell lines or cytokines that were observed in this thesis, and indicate that a certain caution must be applied when interpreting results obtained by pharmacological inhibitors.

Therefore, genetic cell models and siRNA downregulation studies were utilized in this thesis which independently confirmed that PARP1 is not necessary for neither TNF- nor TRAIL-mediated necroptosis. In PARP1-deficient cells, necroptosis was even enhanced. This may be caused by deregulation of NF-κB signaling cells (Kameoka et al., 2000, Aguilar-Quesada et al., 2007), suggesting that the enhanced sensitivity of PARP1-deficient cells towards necroptosis is a consequence of an inhibition of NF-κB-dependent survival signals. Similarly, an increase of cytokine-mediated apoptosis after deletion of PARP1 was shown to be caused by an impairment of the DNA damage recovery response (Boulares et al., 2001) and by an increased accessibility of chromatin to endonucleases, leading to nuclear disintegration (Oliver et al., 1998). Inhibition or lack of PARP1 may lead to an increase in NAD^+ and in consequence, to activation of SIRT1, which acetylates multiple enzymes, transcription factors and increases the oxidative metabolism of a cell (Bai et al., 2011) and therefore may have an impact on cell viability.

Although a direct role of PARP1 was not found for TNF- and TRAIL-mediated necroptosis, the presence of PAR polymers generated by PARP1 was confirmed in this thesis. It has been described previously that the auto-poly(ADP-ribosyl)ation of PARP1 leads to its auto-inactivation and to the removal of PARP1 from chromatin, thus it reflects PARP1 inactivation, lack of PARP1 protein and the abolishment of PARP1-dependent transcription (Tulin, 2011). Poly(ADP-ribosyl)ated chains attached to various proteins may serve as signaling molecules that could support the execution of necroptosis at later stages, similar to poly(ADP-ribosyl)ated p53 (Komissarova and Rossman, 2010), ribosylated cytochrome *c* reductase and oxidase, the β subunit of F1F0 ATPase, Hsp60, GAPDH (glyceraldehyde 3-phosphate dehydrogenase) and VDAC-1 (voltage-dependent anion-selective channel protein 1) (Lai et al., 2008) which modify the cellular answer.

Accordingly, accumulation of PAR chains was associated with an increase in the vulnerability to (necroptotic?) ischemic brain injury (Cozzi et al., 2006), increased embryonic lethality and enhanced sensitivity to genotoxic stress (Koh et al., 2004). Interestingly, protein ADP-ribosylation may be regulated by SIRT2, an enzyme that is known to be closely regulated by PARG (Tulin et al., 2006) and which also represents one of the regulatory adaptor molecules of RIP3 during necroptosis (Narayan et al., 2012). Therefore, poly(ADP)-ribosylation of proteins may be a consequence of signaling processes in the later stages of necroptosis, and additionally contribute to the necroptotic response. To further investigate a contribution of PAR polymers to necroptosis, analyses of the PAR-degrading enzyme poly(ADP-ribose)glycohydrolase (PARG) should be performed, whose depletion was shown to reduce heat-shock protein (HSP)-70 expression and to worsen ischemic brain injury (Cozzi et al., 2006).

AIF was described to be involved not only in apoptosis but also in caspase-independent cell death (Daugas et al., 2000). For example, Harlequin mice which bear a mutation of *Aifm1* and express reduced amounts of AIF, are protected against necrotic ischemia-reperfusion injury of the brain (Vandenabeele et al., 2010). In this thesis, however, AIF translocation from mitochondria was not found to be required for both TNF and TRAIL-mediated necroptosis but rather occurred late, as a secondary event, identical to AIFsh, a C-terminal amino acid splice variant of AIF. It was already described that AIFsh is involved in caspase-independent programmed cell death, during which it causes large scale DNA fragmentation even in presence of zVAD-fmk, and it induces cell death much more rapidly than AIF (Delettre et al., 2006). Therefore, involvement of the shorten form of AIF (AIFsh) in the late steps of necroptosis and its possible interaction with other executing components of necroptosis, e.g. in order to induce large scale DNA fragmentation could be analyzed in the future.

In this thesis, it was shown that caspase-independent necroptosis is executed in a different manner than DNA damage-mediated necrosis and does not involve PARP1 and AIF. Moreover, previous findings that had described a participation of RIP1 in the PARP-pathway (Xu et al., 2006) were confirmed, nevertheless only in a cell-type specific and limited in its impact, in contrast to the ubiquitous, essential function of RIP1 and RIP3 in TNF-induced necroptosis. Of note, for the first time it was shown that in murine cells, the involvement of RIP3 in DNA damage-induced necrosis is dependent on the presence of the whole protein RIP3 but not on its kinase activity, which in contrast is indispensable for

necroptosis. The results from this thesis strongly support the hypothesis that cytokine-mediated necroptosis and PARP1-mediated necrosis are separate pathways. Although a recent study had reported a RIP1-RIP3-dependent activation of PARP1 in TRAIL-induced necroptosis (Jouan-Lanhouet et al., 2012), here it was shown that PARP1 is not essential for TNF-mediated necroptosis at all. Moreover, the same group had previously reported that in the cell system they studied, caspase activity was required for cell death (Meurette et al., 2007), which is inconsistent with the molecular mechanisms described for necroptosis and thus suggests caution when interpreting the results of this study.

Concluding, it was shown that neither PARP1 nor AIF are involved in the initial phase of TNF- and TRAIL-mediated necroptosis or required for necroptotic PCD, but may be activated as consequence of various cellular programs involved in the late phases of necroptotic cell death. With regard to a future clinical application, the results obtained in this thesis suggest that the simultaneous application of highly specific inhibitors for necroptosis may be a therapeutic approach of choice for an improved treatment for necroptosis/necrosis-based diseases such as colitis, inflammatory lesions in intestinal epithelial cells of the ileum and Crohn's disease (Günther et al., 2011).

B. Analysis of similarities and differences of the molecular signaling pathways of TNF- and TRAIL-mediated necroptosis

Individual members of the TNF-R superfamily show similarities and differences with regard to their intracellular signaling. For each member of the TNF receptor family containing a death domain (i.e. the death receptors), the induction of apoptosis is regulated through common and distinct components. For example, inhibition of the kinases ERK1/2 sensitizes cells to apoptosis elicited by CD95/Fas and TRAIL-R, whereas TNF-R1 signaling is not influenced. As another example, in contrast to CD95/Fas and TRAIL-R, stimulation of TNF-R1 activates mainly the NF-κB pathway, leading to inflammatory and pro-survival signaling (Tran et al., 2001). Differences between the individual death receptors exist also at the level of the signaling molecules that form the DISC, e.g. TRADD is required for TNF-induced apoptosis but not for C95/Fas or TRAIL -induced apoptosis (Jin and El-Deiry, 2006). Also, the death domains of TRAIL receptors have been reported to be weaker inducers of apoptosis than e.g. CD95/Fas (Neumann et al., 2012). In summary, many studies of apoptosis initiated by death receptors for FasL, TNF and TRAIL have revealed similarities, but also differences between the molecular signaling pathways mediated by these receptors. In contrast to death receptor-induced apoptosis, which is very well studied, there is almost no information available with regard to similarities and differences in the necroptotic signaling pathways initiated by death receptors. Therefore, components of the signaling pathways of TNF- and TRAIL-induced necroptosis were analyzed in further detail in this thesis.

RIP1 is responsible for execution of TRAIL-mediated necroptosis

For TRAIL-induced signaling, a role of RIP1 has been controversial. Whereas some studies implicate that mechanisms of TRAIL-induced NF-κB activation and cell survival do not require RIP1 (Grunert et al., 2012), others indicate binding of TRADD and recruitment of RIP1 as responsible for resistance to TRAIL-mediated apoptosis (Cao et al., 2011). On the other hand, RIP1 was found to be required for TRAIL-mediated apoptosis through formation of a complex with caspase-8 and FADD (Abhari et al., 2012), yet downregulation of RIP1 sensitized cancer cells to TRAIL-induced apoptosis (Huang et al., 2013), indicating that RIP1 exerted a protective effect. Although RIP1 and RIP3 are known

as key regulators of TNF-induced necroptosis (Cho et al., 2009), little is known about how they regulate TRAIL-mediated necroptosis, or about their role in MNNG-mediated programmed necrosis.

In this thesis, the combined use of pharmacological and genetic approaches (RIP-1 inhibitors and RIP1-deficient cells) revealed that interference with RIP1 rescues cells from TRAIL-mediated necroptosis. Thus, it was confirmed that RIP1 plays an essential role not only in TNF-, but also in TRAIL-mediated necroptosis. As an additional result, a function of RIP1 (and RIP3) was also found in MNNG-mediated programmed necrosis. However, in the PARP pathway, RIP1 (and RIP3) seem to act only in secondary, later steps, and only with limited impact and in a cell type-specific manner (in contrast to the ubiquitous, essential function of RIP1 (and RIP3) in TNF- and TRAIL-induced necroptosis).

Ceramide generated by A-SMase mediates TNF- and TRAIL-induced necroptosis

For apoptosis, several studies have established a role of ceramide in response to cytokine receptors such as TNF-R1, interleukin-1 receptor (Mizushima et al., 1998) or CD95/Fas (Grassme et al., 2003), as well as environmental factors such as ionizing radiation (Kolesnick and Fuks, 2003) or oxidative stress (Andrieu-Abadie et al., 2001). For necroptosis, the role of ceramide in TNF-mediated signaling had been established in a previous study from our laboratory (Thon et al., 2005). For TRAIL, a second study from our laboratory (Thon et al., 2006) had provided at least some preliminary evidence that ceramide is also involved in necroptosis induced by this cytokine. With regard to the mechanisms of ceramide formation, the activation of SMases, and in particular, A-SMase had been demonstrated as a mode of action.

In this thesis, several pharmacologic inhibitors of ceramide-generating enzymes were employed to demonstrate that ceramide generation is important for necroptosis, revealing that A-SMase is the primary enzyme responsible for ceramide generation in both TNF- and TRAIL-induced necroptosis in murine as well as human cells.
The most potent inhibitor of A-SMase identified is naturally occurring phosphatidylinositol- 3,5-bisphosphate (PtdIns3,5P2) (Roth et al., 2010). ARC39, a novel highly specific and not widely utilized synthetic bisphosphonate-based A-SMase inhibitor

(Roth et al., 2009a) was employed here for the analysis of ceramide-mediated necroptosis. The available data for ARC39 efficacy from previous studies are limited, showing protection against dexamethasone-induced apoptosis in HepG2 cells and a reduction of pulmonary edema in rats (Roth et al., 2009a). Here, the efficacy of this A-SMase inhibitor in necroptosis was investigated for the first time, clearly confirming protection from TNF- and TRAIL-mediated necroptosis in both murine and human cells (despite some interference from the sensitizer CHX in human HT-29 and Jurkat ATCC cells). Interestingly, in A818-6 cells, protection from TRAIL-mediated necroptosis was seen after treatment with ARC39, but this was accompanied by changes in cells morphology. The presence of ARC39 stimulated a foamy-like appearance of the cells (Appendix, Figure 87) similar to the characteristic lipid-laden foam cells observed in bone marrow cells of patients suffering of Niemann-Pick disease (NPD) (Takada et al., 1987). This may be due to the high potency of ARC39 to inhibit A-SMase, as the NPD phenotype was already reported to be associated with decreased A-SMase activity (Kirkegaard et al., 2010) leading to an impairment of the lysosomal compartment (Jenkins et al., 2009). However, a foamy-like morphological appearance of the cells was not observed while necroptosis was executed in combination with the protein synthesis inhibitor CHX. Instead, an impaired appearance of cells was observed (Appendix, Figure 89), although the cells were still protected from both TNF- and TRAIL-mediated necroptosis. As likely explanation, in addition to regulation of cell death, A-SMase may interact with proteins important for survival whose inhibition by CHX is reflected in worsened morphological appearance and condition of cells despite the administration of ARC39 (Figure 77). Recently, the chaperone Hsp70 was identified as such a regulatory protein that influences A-SMase. Hsp70 is associated with activation of A-SMase which in turn regulates sphingomyelin metabolism and thereby increases lysosomal stability (Kirkegaard et al., 2010). Moreover, Hsp70 is assisted by different types of proteins called co-chaperones to function in a myriad of biological processes, modulating polypeptide folding, degradation and translocation across membranes, and protein–protein interactions (Kampinga and Craig, 2010). Therefore the role of Hsp70 in necroptosis will be of interest for future studies.

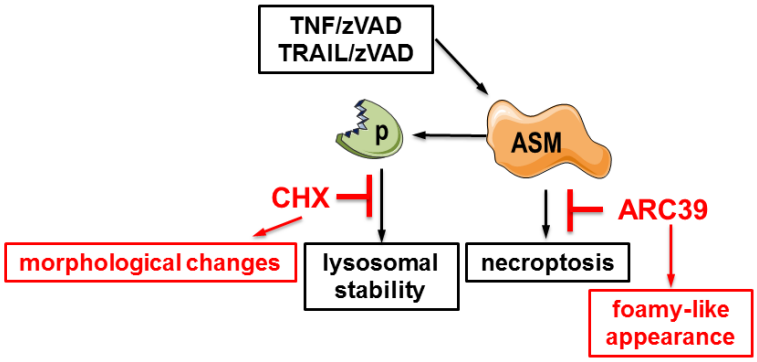

Figure 77. Putative regulation of cell death appearance by A-SMase in A818-6 cells. Administration of ARC39 rescues A818-6 cells from TNF/zVAD- or TRAIL/zVAD-induced necroptosis mediated by A-SMase. Simultaneously, A-SMase may interact with a putative protein (e.g. Hsp70) that mediate pro-survival pathways. Similarly to cells revealing an NPD phenotype, inhibition of A-SMase activity by ARC39 does not decrease cell survival but induces changes in morphology (foamy-like appearance). Inhibition of A-SMase activity during TNF- or TRAIL-mediated necroptosis combined with the application of CHX restricts the execution of TNF- and TRAIL-mediated necroptosis but is coinciding with massive changes in morphological appearance due to putative lysosomal instability and inhibition of survival pathways. ASM – A-SMase, CHX – cycloheximide, p – protein(s)

The results obtained with ARC39 as the most potent and specific A-SMase inhibitor, were confirmed by zoledronic acid, another bisphosphonate-based inhibitor and by the inhibitor D609, a tricyclic xanthate derivative. Although the inhibitor zoledronic acid was described to induce cell death in multidrug-resistant cancer cells (Riganti et al., 2013) by exerting pleiotropic effects such as targeting the mevalonate pathway involved in synthesis of cholesterol, interrupting Ras- and RhoA-dependent downstream signaling pathways and intracellular vesicular transport (Mitrofan et al., 2010), here the inhibitor conferred protection against TNF- and TRAIL-mediated necroptosis. Despite the fact that zoledronic acid is used for anticancer therapy, it may induce protective effects in necroptosis-based pathophysiological events and may be of potential use in anti-necroptotic therapies.

In contrast to PtdIns3,5P2, the inositol ring-based inhibitors TP064/14e and TP102 that are active against A-SMase *in vitro* (Roth et al., 2009b) did not protect against necroptosis *in vivo*. Inositol-based inhibitors may be unsuitable for investigation of necroptosis due to their interaction with Fab1/PIKfyve lipid kinase and antagonistic Fig4/Sac3 lipid phosphatase (Ho et al., 2012) or regulation of endolysosomal trafficking and acidification (Krauss and Haucke, 2007).

Another class of A-SMase inhibitors, the tricyclic antidepressants, desipramine or imipramine failed to protect against TNF- or TRAIL-induced necroptosis, possibly because of inefficient uptake or metabolization within the cells. The potency of desipramine or

imipramine to inhibit A-SMase requires high intra-lysosomal concentrations and translocation of the drug into lysosomal membranes (Kornhuber et al., 2008).

Of note, this thesis has shown for the first time that protective effects of A-SMase inhibition during necroptosis are mediated by bisphosphonate compounds. Since these compounds (like zoledronic acid) are used for treatment of patients with bone metastases (Pouessel and Culine, 2012) or for induction of autophagy in prostate cancer (Lin et al., 2011) and apoptosis in breast cancer (Ma et al., 2012) and since they upregulate TRAIL expression (Rachner et al., 2010), the further study of the role of A-SMase-mediated necroptosis in these processes would be a point of interest for future clinical treatment.

Ceramide generated by N-SMase mediates TNF- and TRAIL-induced necroptosis

A role of N-SMase in the execution of cell death had already been described for apoptosis mediated by stress-inducing factors such as the anti-cancer drug daunorubicin (Ito et al., 2009) or TNF (Luberto et al., 2002). Also, cooperating with the group of Prof. S. Schütze, we had established that a disturbed internalization of TNF-R1 induces N-SMase2-dependent programmed cell death which may represent a protective mechanism to remove deregulated cells (Neumeyer et al., 2006). In this thesis, the use of pharmacological inhibitors had (similar to A-SMase, but to a lesser extent) implicated a contribution of N-SMase to TNF- and TRAIL-mediated necroptosis in murine as well as in TNF-induced necroptosis in human cells. In the performed assays, both spiroepoxide, a selective and irreversible inhibitor of N-SMase, (Arenz and Giannis, 2000) and 3-OMS, a deoxy-sphingomyelin analog reported to efficiently inhibit N-SMase (Lister et al., 1995), moderately diminished TNF- or TRAIL-mediated necroptosis. In contrast, the noncompetitive N-SMase inhibitor GW4869 was ineffective, most likely because the nontoxic concentrations (1 μM and below) that could be employed here did not sufficiently inhibit N-SMase (Canals et al., 2011) (the previously reported dose of 10 μM which inhibits sphingomyelin hydrolysis a cellular system (Luberto et al., 2002), was toxic for the cells analyzed here). Notably, 3-OMS also stabilizes late endosomes/lysosomes, and thus protects against oxidant-induced damage mediated by TNF (Caruso et al., 2005) as well as against TRAIL-mediated apoptosis (Werneburg et al., 2007). This may suggest a role of N-SMase in both TNF- and TRAIL-mediated necroptosis involving an interaction with the

lysosomal compartment.
Interestingly, the TNF-mediated activation of N-SMase has been linked to NADPH oxidase activation followed by ROS accumulation (Barth et al., 2012). Since a role of N-SMase in both TNF- and TRAIL-mediated necroptosis was confirmed in this thesis for the cell lines L929Ts and NIH3T3 which also showed massive ROS production during necroptosis, this ROS production may be dependent on the activity of N-SMase, thereby contributing to necroptosis.

With regard to the molecular mechanism by which ceramide contributes to necroptosis, A-SMase and N-SMase generate this lipid from lysosomal and membrane sphingomyelin, respectively. Therefore ceramide generated during necroptosis may affect vesicular trafficking, may contribute to membrane invagination, budding and reorganization of cell surface receptors (Cremesti et al., 2002) and may thus promote the interactions of proteins gathered in such ceramide-rich microdomains with other cytosolic signaling molecules, finally leading to necroptosis. For future studies, it should also be taken into account that ceramide is converted to subsequent metabolites such as sphingosine-1-phosphate, which has been proposed to be a mediator of TNF-induced N-SMase activation (Hannun and Obeid, 2011). Here, it would be of interest how the converting enzymes, e.g. ceramidases regulate the fate of the cell. In our laboratory, it had been shown that overexpression of acid ceramidase in L929 cells protects against TNF-induced necroptosis (Strelow et al., 2000). Therefore, acid ceramidase may represent a potential target for anti-inflammatory and cancer therapies because it is upregulated in many cancer types (Morad and Cabot, 2013).

Ceramide generated by ceramide synthase does not mediate TNF- and TRAIL-induced necroptosis

As the third enzyme capable of ceramide generation, the role of ceramide synthase in TNF- and TRAIL-mediated necroptosis was likewise investigated in this thesis. Although it was reported that ceramide synthase can mediate apoptosis (Bose et al., 1995), the established ceramide synthase inhibitor fumonisin B_1 consistently failed to protect from TNF- and TRAIL-mediated necroptosis in all experiments. This is not only in line with results from a previous study from our laboratory, but also strongly argues against a function of ceramide synthase in TNF- and TRAIL-mediated necroptosis. In contrast,

ceramide synthase and *de novo* generated C18- and C16-ceramides may even possess pro-survival properties and rescued cells from ER stress-induced apoptosis leading to enhanced growth and development of cancer cells (Senkal et al., 2010).

In these assays (as well as some later experiments using pharmacological inhibitors), it became obvious that inhibition of protein synthesis by CHX can negatively influence the efficacy of some pharmacological inhibitors during necroptosis. This is consistent with previous findings suggesting that factors dependent on protein translation may contribute to necroptosis (Hitomi et al., 2008).

Lack of FADD and presence of TNF-R2 influence signaling of ceramide generated by A-SMase during TNF-mediated necroptosis

Although a role of A-SMase and N-SMase in necroptosis was confirmed for murine cell lines and the human cell lines Jurkat I.42 and A818-6 in this thesis, no evidence for an involvement -of these enzymes in TNF-mediated (Table 6) or TRAIL-mediated (Table 7) necroptosis was found human Jurkat ATCC and HT-29 cell lines. This may be due to the existence of multiple possible execution pathways of necroptosis downstream of the central RIP1-RIP3-SIRT2-MLKL complex, triggered by ceramide, but also by other, components that act independent from ceramide. For example, activation of phospholipase A_2 or lipoxygenases were identified as execution components in addition to ceramide in previous studies (Degterev and Yuan, 2008). Therefore, the differential involvement of A-SMase in the execution of necroptosis seen in this thesis for Jurkat ATCC and HT-29 cells, is possibly dependent on the composition of the necroptotic signaling complex. The use of FADD-deficient Jurkat lymphocytes simplified the analyses of necroptosis, as in those cells apoptosis was blocked, accompanied by an enhanced induction of necroptosis (Degterev et al., 2005). However, during necroptosis induced in the absence of zVAD-fmk, the involvement of A-SMase in the execution of this pathway was minor and not statistically significant (Figure 37 B). This might be due to a decreased stability and formation of the caspase-8-RIP1-RIP3 complex that occurs in the absence of FADD (Wang et al., 2008, Cho et al., 2009, Narayan et al., 2012). This instability may change the preferred signaling of the executing downstream pathways of necroptosis away from the A-SMase/ceramide-dependent module to another, A-SMase/ceramide-independent module, and thereby diminish the protective effects of A-SMase inhibition by ARC39

(Figure 78 A). An additional administration of zVAD-fmk increases the binding of RIP1 and RIP3 to caspase-8 and RIP1 to TNF-R (Cho et al., 2009), and thus may restabilize the necroptotic signaling complex, changing the signaling preference back to the A-SMase/ceramide dependent module (Figure 78 B). In complete agreement with this model, TNF-induced necroptosis in FADD-deficient Jurkat cells was significantly inhibited by ARC39 when zVAD-fmk was present (Figure 37 C). This suggest that presence of zVAD-fmk, according to Cho and coworkers, might increase binding of RIP1 and RIP3 to caspase-8 and RIP1 to TNF-R (Cho et al., 2009) leading to possible stabilization of the necroptotic signaling complex that might assure the involvement of A-SMase to trigger necroptosis. Therefore in FADD-deficient cells lack of zVAD-fmk could lead to activation of RIP1-dependent necroptotic signaling platforms, in which the activity of A-SMase is not essential (Figure 78 A). The modulatory role of zVAD-fmk in the organization of signaling complexes was already reported previously as it prevented the recruitment of TRAF2 into the death-inducing signaling complex (Kataoka and Tschopp, 2004).

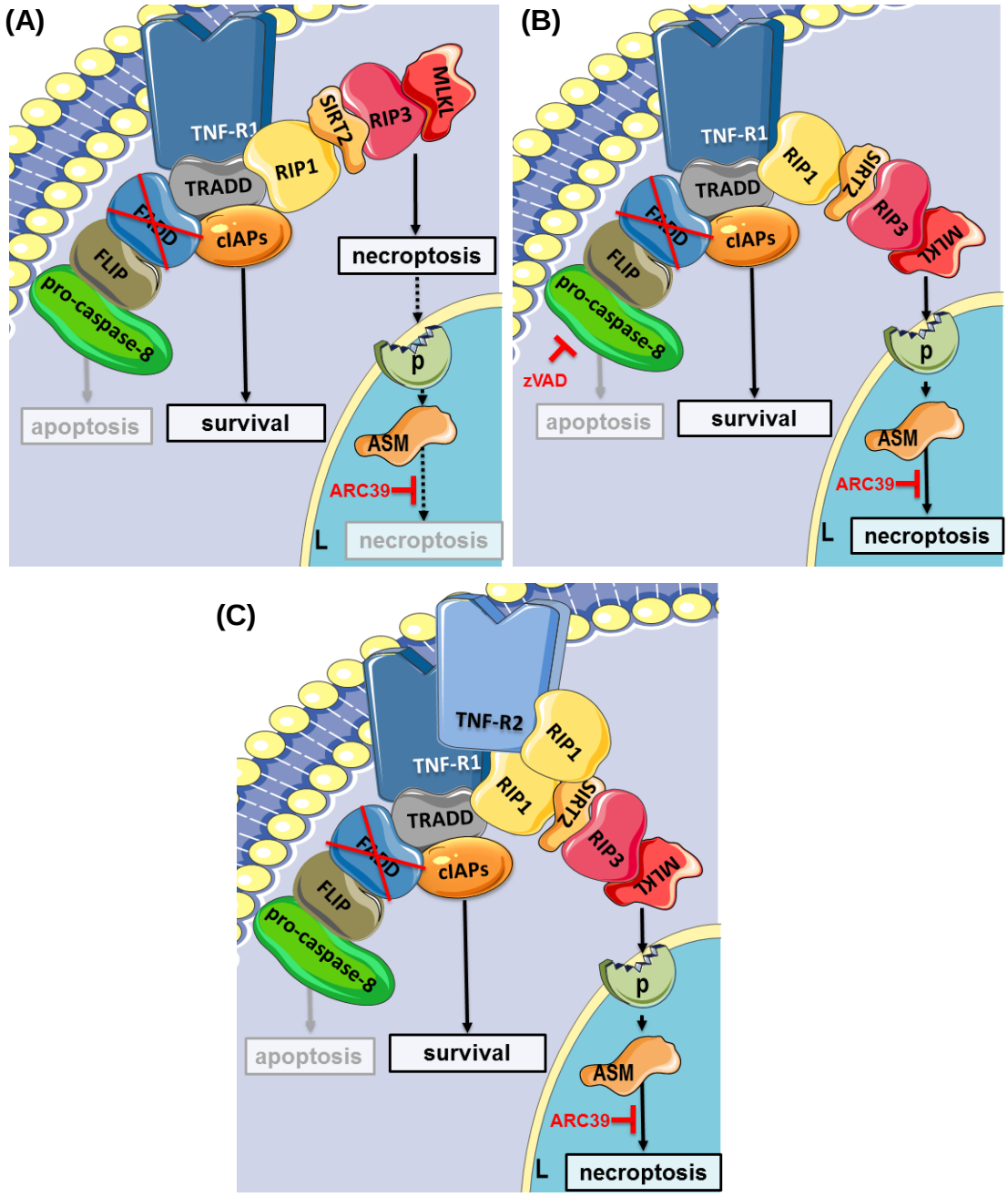

Figure 78. A hypothetical model of the involvement of A-SMase in TNF-mediated necroptosis in human FADD-deficient cells depending on the availability of zVAD-fmk and TNF-R2. (A) In FADD-deficient cells the apoptotic pathway is blocked. Therefore, TNF-mediated necroptosis is executed when TNF is applied alone. Lack of FADD might destabilize the RIP1-RIP3-SIRT2-MLKL complex, leading to execution of necroptosis through downstream pathways which do not involve A-SMase (not shown). In this case, inhibition of A-SMase with ARC39 would not significantly protect form the execution of TNF-mediated necroptosis. **(B)** Additional administration of zVAD-fmk might restabilize the formation of the RIP1-RIP3 signaling complex (Cho et al., 2009) and thereby change the signaling preference back to the A-SMase/ceramide dependent pathway to trigger necroptosis. In consequence, inhibition of A-SMase with ARC39 would again protect from TNF-mediated necroptosis in FADD-deficient human cells. **(C)** As an alternative to zVAD-fmk, the presence of additional (stably expressed) TNF-R2 may likewise restabilize the formation of the RIP1-RIP3 signaling complex and change the signaling preference back to the A-SMase/ceramide dependent pathway. As for zVAD-fmk, inhibition of A-SMase with ARC39 would again protect from TNF-mediated necroptosis. Solid line – significant involvement of components in necroptosis, dotted line –reduced or no involvement, L – lysosomes, p – putative protein(s)

An alternative mechanism of restabilization of the RIP1-RIP3-SIRT2-MLKL complex may involve the presence of TNF-R2. Although TNF-R2 does not contain a cytoplasmic death domain, it is capable of recruiting signaling molecules such as TRAF2, which in turn binds TRAF1, TRAF3, cIAP-1 and cIAP-2 (Cabal-Hierro and Lazo, 2012). It had been already shown that stable re-expression of TNF-R2 in FADD-deficient Jurkat I.42 cells enhanced TNF signaling during apoptosis and necroptosis, caused by TRAF2 degradation followed by recruitment of RIP1 to the TNFR1-signaling complex (Chan et al., 2003). In line with the assumption that, similar to zVAD-fmk, the additional presence of TNF-R2 may restabilize the RIP1-RIP3-SIRT2-MLKL complex, and change the signaling preference back to the A-SMase/ceramide dependent module (Figure 78 C), ARC39 significantly protected Jurkat I.42 cells from TNF-induced necroptosis (Figure 37 A).

In summary, the results obtained in this thesis argue that in FADD-deficient cells, where the caspase-8-RIP1-RIP3 signaling complex is partially destabilized, additional factors such as TNF-R2 or zVAD-fmk can regulate the impact of ceramide generated by A-SMase in the execution phase of necroptosis.

Factor associated with N-SMase (FAN) and its homolog Lyst contribute to the execution of necroptosis and apoptosis

FAN had previously been implicated in filamentous actin polymerization in response to TNF dependent on GTPase proteins (Montfort et al., 2010), migration and chemotaxis of leukocytes, lysosomal permeabilization, IL-6 secretion (Boecke et al., 2012), interaction with N-SMase for mediation of CD40-induced cell death (Segui et al., 1999) and execution of hypoxia/reoxygenation-induced cell death in rat cardiomyocytes (O'Brien et al., 2003). Moreover, it had been shown that FAN is required for TNF-induced generation of ceramide by N-SMase and triggering of apoptosis (Segui et al., 2001). During apoptosis, FAN contributes to increase in lysosomal permeability, release of cathepsin B, cyt *c* and activation of caspase-8 (Werneburg et al., 2004, Montfort et al., 2010). However, an involvement of FAN in caspase-independent cell death had not been investigated until now. In this thesis, it was demonstrated for the first time that FAN is important for TNF-mediated necroptosis. Mechanistically, FAN is required for the recruitment of N-SMase to the TNF signaling complex at the plasma membrane and its subsequent activation (Adam-Klages et al., 1996, Adam et al., 1996, Adam-Klages et al., 1998). In addition, FAN

deficiency impairs the interaction of TNF-R1 with the actin cytoskeleton complex and the reorientation of the Golgi apparatus upon TNF stimulation (Haubert et al., 2007). Thus, FAN might influence vesicular transport or intracellular trafficking, processes which are involved in TNF-mediated necroptosis (as shown in this thesis by a pharmacological approach with chloroquine and bafilomycin A_1). Of note, FAN was described to regulate lysosomal size (Möhlig et al., 2007). Therefore, changes in organization of this compartment might influence ceramide signaling and impair in consequence necroptosis. Similarly, this study confirms previous findings implicating that FAN is responsible for TNF-mediated apoptosis (Segui et al., 2001) and possibly TNF-induced necroptosis may be triggered by vesicular transport of signaling ceramide that is regulated by FAN.

The protein Lyst is known to regulate lysosome size in mammals (Durchfort et al., 2012). The data obtained in this thesis demonstrate for the first time that Lyst-deficient cells were protected from TNF- and TRAIL-mediated necroptosis and TNF-mediated apoptosis. This protection might be due to the Lyst-mediated change of lysosome size that may negatively influence protein signaling, trigger defective vesicular trafficking of Golgi-derived granules (Hammel et al., 2010) necessary for ceramide transport (Mencarelli and Martinez-Martinez, 2013) or cause defects in lysosomal exocytosis (Tchernev et al., 2002). Recently, it was shown that depletion of Lyst affects lysosomal fission via disruption of tubular lysosomes and in consequence leads to an expanded size of lysosomes (Durchfort et al., 2012). It therefore appears likely that a contribution of Lyst in membrane or lysosome tubulation, deformation or/and lysosomal fission may be important for both TNF- and TRAIL-mediated necroptosis.

Lyst possesses evolutionary conserved domains such as the BEACH domain and WD repeats (Montfort et al., 2010). These domains may interact with other proteins that possess a BEACH domain and WD repeats, e.g. neurobeachin (Nbea) (Wang et al., 2000) or LRBA (LPS-responsive vesicle trafficking, beach and anchor containing) which play a role in polarized vesicular trafficking (Jogl et al., 2002). In addition, Lyst may interact with other proteins, e.g. atrophin-1, the importin β-subunit, embryonic-Fyn-substrate (EFS1), a component of SNARE hepatocyte growth factor–regulated tyrosine kinase substrate (HRS) or casein kinase II in order to organize protein complexes important for interaction with (plasma) membrane domains, or to coordinate multi-protein complex assemblies (Tchernev et al., 2002). In line with this assumption, Lyst was found to interact with various proteins that regulate vesicular trafficking and are involved in signal transduction, e.g. 14-3-3-β/τ

(Tchernev et al., 2002). Thus, it may be of interest to investigate the involvement of known Lyst interaction partners in the execution of necroptosis. Moreover, the identification of FAN or Lyst modifiers may uncover further links between organelle biogenesis, turn-over and the execution of cell death.

In order to clarify whether the effects of Lyst on lysosome size and lysosomal trafficking are the major cause for its impact on necroptosis, the effect of vacuolin-1, a drug which rapidly expands late endosomes and lysosomes (Wilson et al., 2008), on necroptosis should be investigated in future experiments. Moreover, the role of Rab proteins should be examined as an interaction of the *Dictyostelium* sp. ortholog of Lyst and Rab14 has been described (Kypri et al., 2013).

In summary, the above experiments demonstrate that both TNF- and TRAIL-mediated necroptosis are impaired in the absence of Lyst and FAN. These results suggest that modification of N-SMase signaling and lysosomal trafficking, regulated by FAN and Lyst, might represent potential therapeutic targets for necroptosis.

Cathepsins and calpains/cysteine proteases and metalloproteases are not required for necroptosis

For the execution of ischemic cell death, a model of ‘‘calpain-cathepsin’’ has been proposed by Yamashima and colleagues. In this model, the μ-calpain-induced cathepsin B release after the disruption of the lysosomal membrane is crucial for this type of cell death (Yamashima et al., 1998). With regard to TNF- and TRAIL-mediated necroptosis however, the results obtained in this thesis demonstrate that inhibitors specific for cathepsins and calpains/cysteine proteases do not inhibit cell death in L929Ts cells. The same was observed in cathepsin D-deficient MEFs, suggesting that these proteases are not crucially involved in necroptosis. They may, however, contribute to cellular events associated with necroptosis, and thereby indirectly support the process of cellular disintegration. As an example, the cathepsin inhibitor Ca-074 Me protected from staurosporine-mediated necroptosis in U937 cells via stabilization of lysosomal compartments (Dunai et al., 2012). Similarly, cathepsin D has been implicated in various lysosomal storage-based diseases (Benes et al., 2008). This is particularly interesting given the role of FAN and Lyst as regulators of both necroptosis and lysosomal size.

In this thesis, inhibition of metalloproteases was likewise found insufficient to prevent TNF- or TRAIL-mediated necroptosis in murine cells. Although GM 6001, an inhibitor of matrix metalloproteinase-9 had been reported to abrogate the seizure-induced brain injury (Hoehna et al., 2012), and although TAPI-I, an inhibitor of ADAM-17 had been described to block the proteolytic shedding of cell surface molecules like amphiregulin, transforming growth factor alpha, syndecan-1 and TNF-R1, and thus to inhibit pro-inflammatory signals (Breshears et al., 2012), these inhibitors were not efficient in the protection from necroptotic cell death. The same results were obtained with marimastat, which is active against all major classes of metalloproteinases. Notably, it has been described that the shedding of TRAIL receptors by ADAM-17 may be a resistance mechanism of cancer cell lines to cell death (Kagawa et al., 2012). In consequence, inhibition of ADAM-17 should even increase the susceptibility of cells to death, and this was in fact observed for both L929Ts and NIH3T3 cells in this thesis. Similarly, the inhibition of metalloproteases by marimastat has been employed as a therapy to decrease the invasiveness and the metastatic potential of various pancreatic carcinomas (Saif, 2006), gastric cancers (Watson et al., 1999), osteosarcoma (Bjornland et al., 2005) and non-small cell lung cancers (Cappuzzo et al., 2003). Therefore, a combination of metalloproteases inhibitors and the induction of TRAIL-mediated necroptosis might be a promising target for a successful and efficient anti-cancer therapy.

Chymotrypsin-like serine proteases participate in TNF- and TRAIL-induced necroptosis

TPCK, an inhibitor of chymotrypsin-like serine proteases, revealed an involvement of serine proteases in TNF- and TRAIL-mediated necroptosis in this thesis. Notably, TPCK itself is highly toxic in concentrations above 50 μM and may cause necrotic cell death (Mlejnek, 2005), which was also seen in this thesis. Independently, TPCK can induce caspase-dependent apoptosis in a variety of cells (Jitkaew et al., 2009), e.g. through inhibition of RNA polymerase and prevention of transcription (Fabian et al., 2009), activation of cell cycle checkpoints and caspase-3, mitochondrial cytochrome *c* release and chromatin condensation (King et al., 2004). However, in the corresponding experiments of this thesis, TPCK-induced apoptosis was prevented by the addition of zVAD-fmk whereas TNF/zVAD- or TRAIL/zVAD-induced necroptosis was in reverse inhibited by TPCK.

Strengthening a function of serine proteases in necroptosis, TPCK was independently used to confirm a role of serine proteases during caspase-independent cell death mediated by the tyrosine-kinase inhibitor imatinib (Gleevec® [USA] or Glivec® [Europe] from Novartis) (Okada et al., 2004).

The serine protease HtrA2/Omi mediates TNF- and TRAIL-induced necroptosis and apoptosis

Previous studies had identified HtrA2/Omi as a factor that ensures mitochondrial homeostasis and controls protein quality and stress responses (Radke et al., 2008, Fulda et al., 2010). A role of HtrA2/Omi had been mainly elucidated for apoptosis and its involvement in caspase-independent cell death had been studied in just a few cases (Bhuiyan and Fukunaga, 2008). With regard to the molecular mechanisms by which HtrA2/Omi contributes to apoptosis, HtrA2/Omi has been reported to interact with XIAP (Suzuki et al., 2001) and cIAPs (Yang et al., 2003). Under apoptotic conditions, e.g. stimulation with UV, staurosporine or TRAIL, HtrA2/Omi is released from mitochondria and interacts with XIAP through its N-terminus, enhancing the activity of caspases (van Loo et al., 2002). Independently, HtrA2/Omi is released into cytosol, and binds and cleaves cIAPs to promote cell death through its serine protease activity (Verhagen et al., 2002). In line, it was found in this thesis that inhibition of HtrA2/Omi rescued murine cells from execution of both TNF- and TRAIL-mediated apoptosis. In contrast to apoptosis, the molecular details of how HtrA2/Omi participates in necroptotic signaling are still unknown. As an obvious possibility, it had been suggested that the role of HtrA2/Omi is dependent on its serine protease activity. This had been reported for necrosis induced by imatinib alone or in combination with the caspase inhibitor zVAD-fmk (Okada et al., 2004) and during ischemia/reperfusion-caused brain injury in rats (Su et al., 2009). Similarly, it had been described for virus-infected cells that HtrA2/Omi can induce cell death after viral inhibition of caspases through its serine protease activity in order to overcome the inhibition of apoptosis and kill the infected cell (McCormick et al., 2008). Likewise, the serine protease activity of HtrA2/Omi had been found to be essential for TNF-induced caspase-independent cell death in human neutrophils (Blink et al., 2004). It had been shown for neutrophils that HtrA2/Omi is not released from mitochondria during TNF-mediated necroptosis, therefore the mechanism how Omi/HtrA2 mediates TNF- and

TRAIL-mediated necroptosis through its serine protease activity from "within" mitochondria requires further investigation. An additional subject of further investigations that remains is whether TNF- and TRAIL-mediated necroptosis are triggered due to cleavage of cIAPs or other substrates by HtrA2/Omi.

Analyses in human cells have reported that the inhibition of the serine protease activity of HtrA2/Omi is not sufficient to inhibit apoptosis (Blink et al., 2004, Vande Walle et al., 2010). In full agreement, in this thesis, a role of HtrA2/Omi in apoptosis of human cells was not confirmed. Rather, in human cells, the serine protease activity of HtrA2/Omi was essential only for necroptosis. However, some human cell lines, e.g. Jurkat ATCC cells, were not protected from necroptosis when HtrA2/Omi was pharmacologically inhibited, which could be due to cell line-specific differences in the involvement of HtrA2/Omi in the execution of PCD. The importance of HtrA2/Omi for necroptosis in human cells was, however, validated by analyses in human A818-6 cells as well as in human FADD-deficient Jurkat I.42 cells that stably express TNF-R2. A comparison with "regular" FADD-deficient Jurkat cells that do not express TNF-R2 additionally indicates that TNF-R2 might modify the involvement of HtrA2/Omi in the execution of necroptosis. However, up to now nothing is known about possible interactions between FADD, HtrA2/Omi and TNF-R2.

Based upon the results obtained in this thesis, a hypothetical model of HtrA2/Omi function in necroptosis in human cell lines is proposed. When FADD and TNF-R2 are absent, a necroptotic complex that does not require the presence of HtrA2/Omi is being formed (Figure 79 A). In the presence of TNF-R2, formation of a modified necroptotic signaling complex is propagated which depends on HtrA2/Omi to trigger necroptosis (Figure 79 B).

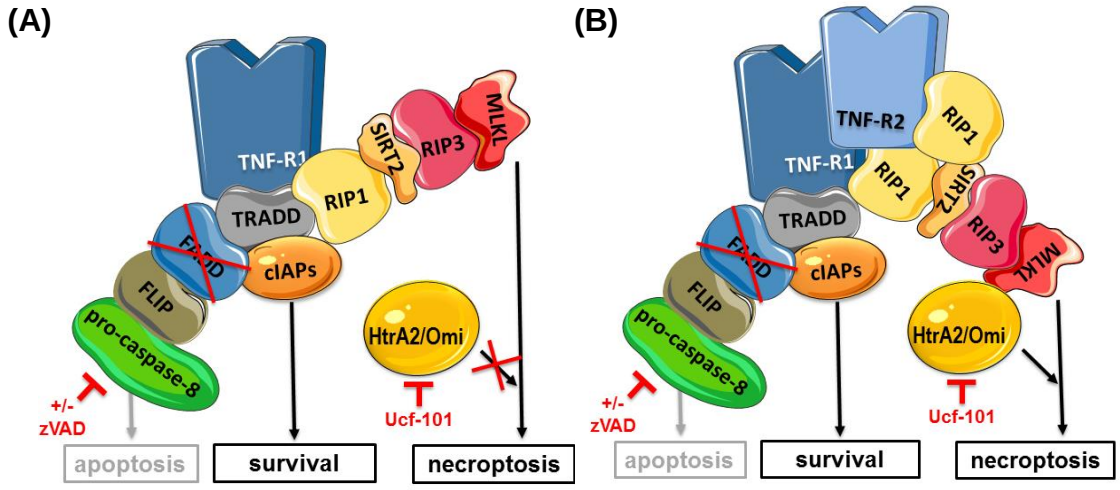

Figure 79. Hypothetical model of HtrA2/Omi function in necroptosis in human cells. (A) In "regular" FADD-deficient cells that do not express TNF-R2, apoptosis is blocked by the absence of FADD. Simultaneously, regardless of presence or absence of the caspase inhibitor zVAD-fmk, a necroptotic signaling complex associates and mediates necroptosis. In the absence of FADD and TNF-R2, the necroptotic signaling complex is too "weak" to recruit HtrA2/Omi for signaling of necroptosis which is switched to an alternative, HtrA2/Omi-independent effector mechanism. In this case, inhibition of HtrA2/Omi by Ucf-101 does not protect from necroptosis. **(B)** In FADD-deficient cells stably expressing TNF-R2, the necroptotic signaling complex is again formed regardless of presence of zVAD-fmk and requires HtrA2/Omi to trigger necroptosis. Probably, additional components which associate with TNF-R2, e.g. RIP1, will allow for the recruitment of HtrA2/Omi to trigger necroptosis.

The ability of TNF-R2 to change the composition of signaling complexes and influence cell death had additionally been previously reported as TNF-R2 is able induce TRAF2 degradation, thereby enhancing TNF-R1-mediated cytotoxicity. Degradation of TRAF2 may inhibit cIAP1/2 and influence the regulation of caspase-8 (Cabal-Hierro and Lazo, 2012). In general, the regulation of necroptotic signaling in FADD-deficient T cells may be influenced differently as in wildtype T cells, as it had been found that in FADD-deficient cells, RIP3 does not appear to associate with RIP1 and necroptosis is dependent upon RIP1 but not RIP3 (Osborn et al., 2010). Certainly, additional studies are needed to investigate which additional components are involved in necroptosis triggered by HtrA2/Omi.

Interestingly, in A818-6 cells, treatment with the HtrA2/Omi inhibitor Ucf-101 nearly completely protected from TRAIL-mediated necroptosis but also caused a foamy-like appearance of the cells, similar to that observed after treatment with the A-SMase inhibitor ARC39 or in bone marrow cells of patients suffering from Niemann-Pick disease (NPD) (Simonaro et al., 2006), suggesting that HtrA2/Omi and A-SMase might be part of the same necroptotic signaling pathway.

In contrast to pharmacological inhibition or genetic deletion of HtrA2/Omi, the downregulation of HtrA2/Omi by RNA interference failed to protect from necroptosis in all tested cell lines, regardless of murine or human. Since a clear downregulation was detected in Western blots, this cannot be a technical issue. However, downregulation also did not protect from TNF- or TRAIL-induced apoptosis, which is in contradiction to previous reports (Martins et al., 2002). As the only explanation currently available, the residual amount of HtrA2/Omi present after downregulation may still suffice to promote necroptosis.

Notably, HtrA2/Omi interacts with the protein kinase WARTS (known as *wts* or *lats* gene, large tumor suppressor), whose downregulation fully protected from UV- or STS-induced caspase-independent cell death (Kuninaka et al., 2005). Since WARTS is downregulated in many aggressive cancers (Takahashi et al., 2005), future analyses of an interplay of WARTS and HtrA2/Omi, in TNF- and TRAIL-mediated necroptosis, may provide novel strategies for optimization of tumor therapy.

Omi/HtrA2 causes cleavage of RIP1 during necroptosis

Cleavage of RIP1 by HtrA2/Omi had already been reported for caspase-independent cell death induced by IL-3 (Vande Walle et al., 2010). In this thesis, it was shown that RIP1 cleavage occurs depending on the serine-protease activity and presence of HtrA2/Omi, which thus might possibly regulate the execution of necroptosis. However, this concept is inconsistent with reports showing that caspase-8-mediated cleavage of RIP1 during TNF-mediated necroptosis in T cells is sufficient to prevent necroptosis (Lu et al., 2011). Moreover, even a partially impaired proteolytic activity of caspase-8 is still sufficient to prevent RIP1-dependent necroptosis (Oberst et al., 2011, Lin et al., 1999). Therefore, further investigations how a cleavage of RIP1 by HtrA/Omi might influence necroptosis are required.

In the literature, several examples exist suggesting how HtrA2/Omi may regulate cell death. It was reported that necroptosis is promoted by the absence of cIAPs and inhibition of caspase activity (Feoktistova et al., 2011), which possibly might be caused by the cleavage of cIAP by HtrA2/Omi (Yang et al., 2003). Furthermore, it was found that cIAP-1 and cIAP-2 limit necroptosis via a post-transcriptional mechanism leading to inhibition of the RIP1-RIP3 necroptosis inducing complex (McComb et al., 2012). Moreover, IAPs

control the formation of a FLIP and caspase-8 complex through ubiquitination of FLIP. In the absence of IAPs, RIP1 can associate with FADD and caspase-8 to form the necroptotic complex (Tenev et al., 2011). Therefore, hypothetically, inhibition of HtrA2/Omi may preserve cIAPs and counteract the formation of the necroptotic signaling complex. Another hypothesis suggest that the serine protease activity of HtrA2/Omi might be involved in downregulation of FLIP and can promote the execution of cell death as it was described during myocardial ischemia (Bhuiyan and Fukunaga, 2007). However, when HtrA2/Omi is blocked by Ucf-101, the complex of FLIP with FADD and caspase-8 may be favored and the execution of necroptosis or apoptosis would be abrogated.

DBC1 is possibly cleaved by HtrA2/Omi in necroptosis

DBC1 is known to be substrate of HtrA2/Omi and is processed to 89- and 14-kDa cleavage fragments (Vande Walle et al., 2007). In TNF-induced apoptosis, an alternative cleavage of DBC1 to 120- and 66-kDa fragments had been described, resulting in relocalization of DBC1 from the nucleus to the cytoplasm (Sundararajan et al., 2005). Similarly, in this thesis, under conditions of caspase inhibition, the 120- and 66-kDa fragments were not identified during necroptosis, but the 89-kDa fragment of DBC1 was shown for the first time to be present during TNF- and TRAIL-mediated necroptosis. Further investigations will have to clarify whether this fragment also relocalizes from the nucleus to the cytoplasm and whether it interacts with cytoplasmic components. It is known that overexpression of this fragment results in mitochondrial clustering and matrix condensation and sensitizes cells to TNF-mediated apoptosis (Sundararajan et al., 2005). Subsequently, DBC1 had been found to colocalize with the NAD^+-dependent deacetylase SIRT1 (Escande et al., 2010), inhibiting its deacetylase activity and is regulated by increasing activity of protein kinase A (PKA) (Nin et al., 2012). Therefore, it will be of interest to investigate if DBC1 regulates metabolic changes during necroptosis via SIRT1 and PKA.

UCH-L1 is involved in TNF-mediated necroptosis

UCH-L1 participates in cell cycle regulation, self-renewal, division and differentiation of cells. (Hurst-Kennedy et al., 2012). Its expression levels had been found to inversely

correlate with the proliferation of cancer cells (Liu et al., 2003), but its importance for cell death had remained unclear.

The results obtained in this thesis suggest that TNF-, but not TRAIL-mediated necroptosis in murine and some human cell lines is regulated by the activity of UCH-L1. Moreover, UCH-L1 was found to be associated with the lysosomal compartment (through interaction with lysosome-associated membrane protein type 2 (LAMP-2) and Hsp-90), (Kabuta et al., 2008), which was shown in this thesis to be involved in TNF- and TRAIL-mediated necroptosis. In line with pharmacological inhibition, downregulation of UCH-L1 in L929Ts cells supported its role in TNF-, but not TRAIL-mediated necroptosis. In future experiments, these results should be complemented by UCH-L1 downregulation in human cells in order to further corroborate the role of UCH-L1 in TNF-mediated necroptosis.

Analyses in mice deficient for UCH-L1 had revealed loss of synaptic vesicles and accumulation of tubule-vesicular structures at the presynaptic nerve terminals (Chen et al., 2010). Thus, UCH-L1 might mediate TNF-induced necroptosis through an involvement in the formation of vesicular and/or tubular structures, and/or early endosomes hypothetically required for the signaling of TNF. Of note, TNF-R1 was described to be internalized through endocytosis (Schneider-Brachert et al., 2004), whereas for TRAIL receptors, conflicting reports claim an involvement of TRAIL receptor internalization for some breast cancers during apoptosis (Zhang and Zhang, 2008) as well as constitutive internalization in hepatic cancer (Akazawa et al., 2009) or describe a lack of clathrin-dependent or -independent endocytotic pathways, e.g. in TRAIL-mediated apoptosis (Kohlhaas et al., 2007).

Of note, UCH-L1 is apparently dispensable for TNF-mediated necroptosis in FADD-deficient human I.42 Jurkat T cells. This suggests that FADD may influence the formation of a necroptotic signaling complex that either depends on the subsequent activity of UCH-L1 for TNF-mediated necroptosis or not (Figure 80).

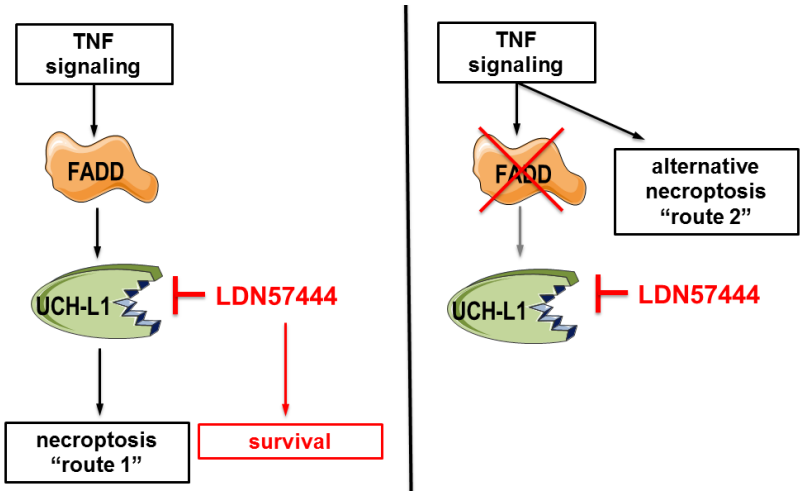

Figure 80. FADD determines the involvement of UCH-L1 in TNF-mediated necroptosis. Left panel: Addition of the UCH-L1 inhibitor LDN57444 abolishes the FADD-dependent necroptotic "route 1" downstream of UCH-L1. Right panel: In the absence of FADD, an alternative route of necroptosis may be triggered that does not depend on UCH-L1 ("route 2").

As described by Park and coworkers UCH-L1 is degraded by HtrA2/Omi under apoptotic conditions (Park et al., 2011). Similarly, in this thesis. the HtrA2/Omi-dependent disappearance of a 25-kDa band representing full-length UCH-L1 was observed during TNF-mediated necroptosis. However, this disappearance was accompanied by an early appearance of a 37-kDa band also recognized by an antibody specific for UCH-L1. Recent reports had identified a similar form of UCH-L1 at around 35 kDa, which is upregulated in NMDA receptor-stimulated neurons and represents a modified monoubiquitinated, active form of UCH-L1 (Cartier et al., 2009). Another study had suggested the existence of a 37-kDa monoubiquitinated form of UCH-L1 that may possess a regulatory role by increasing the availability of free ubiquitin in the cells (Meray and Lansbury, 2007). In summary, monoubiquitination of UCH-L1 could therefore serve as a hypothetical regulatory mechanism for TNF-mediated necroptosis. Monoubiquitinated UCH-L1 might interact with the ubiquitin binding domains of different regulatory proteins or ubiquitin-conjugating enzymes in order to regulate cell death (Meray and Lansbury, 2007). Moreover, the data obtained in this thesis demonstrate that monoubiquitination of UCH-L1 (and thus possible necroptotic downstream effects of UCH-L1) depends on the presence of HtrA2/Omi. However, nothing is known about the mechanism of how HtrA2/Omi might regulate such a monoubiquitination of UCH-L1. Notably, the monoubiquitinated form of UCH-L1 was not found during TNF-mediated necroptosis in L929Ts cells, which rather showed an HtrA2/Omi-dependent increase in the putative dimeric 50-kDa form of UCH-

L1 that exerts ubiquitin ligase activity (Liu et al., 2002). These cell type-specific differences will have to be analyzed in future experiments.

In Parkinson's disease, ROS production results in the activation of p38 MAPK, and activation of the proteolytic activity HtrA2/Omi via PINK1 and CDK5 (Desideri and Martins, 2012). Given the role of UCH-L1 in Parkinson's disease, and the reported impact of caspase-independent necrotic PCD in neuronal tissue (Leist and Jäättelä, 2001), the data obtained in this thesis suggest a possible connection between ROS, activation of the protease activity of HtrA2/Omi and of the ligase activity of UCH-L1 in necroptosis. Therefore, in further work, signaling molecules connecting ROS production and HtrA2/Omi during necroptosis should be investigated.

Role of ROS in TNF- and TRAIL-mediated necroptosis

The results obtained in this thesis show that, for TRAIL-induced necroptosis, ROS production was dramatically increased in L929Ts or NIH3T3 cells, whereas no increase was detected in Jurkat ATCC, suggesting that ROS are required only in a cell type-specific manner during necroptosis. In support of this hypothesis, there are some cell lines which reportedly execute necroptosis through ROS such L929 and MEFs (Christofferson and Yuan, 2010b). However, in some cells of hematopoietic origin (e.g. U937 and Jurkat T cells) and in the colon carcinoma cell line HT-29, ROS are dispensable for execution of necroptosis. For these cell systems, it had been reported that in necroptosis, the interaction between adenine nucleotide translocase (ANT), CypD and the mitochondrial permeability transition pore (mPTP) is disrupted, leading to the loss of ATP followed by cell death without any participation of ROS (Moquin and Chan, 2010). In line, it had been shown that during necroptosis in Jurkat lymphocytes, ROS production was not detected and could not be inhibited by BHA (Degterev et al., 2005), identical to the results obtained in this thesis. For the cell lines in which intracellular ROS play a role in necroptosis, their production can originate from the mitochondria or from the NADPH oxidase complex. Recent studies have shown that ROS involved in TNF-mediated necroptosis in L929 cells were not generated by riboflavin kinase (RFK) and the NADPH oxidases Nox1 or p22phox, but rather other components of the NADPH dehydrogenase (ubiquinone) 1 beta subcomplex 8 (NDUFB8) (subunit of mitochondrial complex I) were described to regulate execution of TNF-mediated necroptosis (Vanlangenakker et al., 2011b).

In summary, the production of ROS does not play an universal role in the execution of necroptosis. Therefore, with regard to future therapies, it has to be kept in mind that scavengers of ROS will exert a protective effect only in the cell lines in which ROS actually contribute to necroptosis.

Although in this thesis, the role of ROS was investigated focusing on TRAIL-induced necroptosis, the wealth of previous data for TNF-mediated necroptosis (Vandenabeele et al., 2010) indicates that there are no major differences between these two pathways with regard to ROS. For both TNF- and TRAIL-induced necroptosis, ROS appear relevant in certain, but not other cell lines. Further investigations are required to precisely clarify an involvement of particular components of the respiratory chain or of oxidases as determinants of necroptotic cell death.

Signaling through the lysosomal compartment, but not autophagy is involved in necroptosis

Autophagy participates in stress-induced cell death, e.g. lung ischemia-reperfusion injury (Zhang et al., 2012). Furthermore, the fact that the necroptotic kinase RIP1 also plays a role in autophagic cell death (Yu et al., 2004), and that caspase-inhibition did not inhibit autophagy (Sirois et al., 2012) could suggest a relationship between necroptosis and autophagy. Although autophagy is required to maintain cell homeostasis and survival, and loss of the essential autophagy-encoding genes leads to metabolic impairment (Rosenfeldt and Ryan, 2011), in some cases deficiency in autophagy does not lead to cell death but to increased survival through upregulation of p62 (sequestosome 1, SQSTM-1, A170) and activation of Nrf2, a critical transcription factor that neutralizes ROS to restore the cellular redox balance (Lau et al., 2010). Interestingly, the zinc finger domain of p62 is able to bind RIP1 and interact with it (Yu et al., 2009). As further discussed below, data presented in this thesis indicate that inhibition of several components of autophagy (Atg16L1, Atg5) leads to increased protection from necroptosis. Therefore, the role of p62, its interaction with RIP1 or activation of Nrf2 during TNF- or TRAIL-induced necroptosis would be or interest for further studies.

It had been reported that in L929 cells, inhibition of caspase-8 by zVAD-fmk induces autophagic cell death (Chen et al., 2011). In full agreement, it was shown in this thesis that in L929ATCC cells (which correspond to the L929 cells used in the study by Chen and

coworkers), 3-MA very efficiently suppressed autophagy induced by zVAD-fmk. However, the same inhibitor was not able to rescue L929 cells or any other analyzed cell line from either TNF- or TRAIL-mediated necroptosis. These results indicate that autophagy is not an integral part of necroptosis, but rather that some components of autophagy may be involved in the executing pathways of necroptosis. In particular, analyses of lysosomal and vacuolar components of the autophagic pathway have revealed a crosstalk between necroptosis and some components of the autophagic machinery. Accordingly, the lysosomotropic agent chloroquine promoted cell death in renal cell carcinoma by preventing autophagy and causing RIP- and ROS-mediated necroptosis (Bray et al., 2012). Importantly, an involvement of ceramide in the induction of autophagy had been reported for MCF-7 cells (Codogno and Meijer, 2005). Therefore, a role of the lysosomal compartment in necroptosis is most likely due to the presence of both sphingomyelin as a substrate for ceramide generation in the lysosomal membranes as well as A-SMase as the ceramide-generating enzyme itself in the lysosome (Jenkins et al., 2011a). In consequence, inhibition of the fusion of autophagic vacuoles with lysosomes by chloroquine (Yoon et al., 2010) may possibly explain the protective effects on TNF-mediated necroptosis. The data presented here suggest that probably by interfering with lysosome function, blockage of vesicle fission is crucial for TNF- but not for TRAL-mediated necroptosis. This indicates very important differences in signaling between TNF- and TRAIL-mediated necroptosis. Obviously, lysosomes are involved as part of a main executioner pathway of TNF-, but not TRAIL-mediated necroptosis.

Of note, the pro-survival role of chloroquine and bafilomycin A_1 during necroptosis probably is not connected to the inhibition of lysosomal proteases as it was reported that chloroquine increased the intralysosomal pH in L929 cells but did not have an influence on the enzymatic activity of cathepsins B and L (Wu et al., 2010b). An additional effect of chloroquine is an inhibition of the proteasome and the accumulation of ubiquitinated proteins (Myeku and Figueiredo-Pereira, 2011), which may potentially contribute to protection. The hypothesis that intralysosomal ubiquitination of proteins may signal TNF- but not TRAIL-mediated necroptosis requires further investigation and would be a point of interest in elucidating the differences in signaling between TNF and TRAIL during necroptosis.

Acidification of lysosomal compartments by H^+-V-ATPase regulates both TNF and TRAIL-induced necroptosis

Recently, Hitomi and coworkers had described a putative role of the vacuolar H^+-ATPase Atp6v1g2 (ATPase, H^+ transporting, lysosomal V1 subunit G2), a multisubunit enzyme that mediates acidification of intracellular compartments, in both TNF-mediated necroptosis and apoptosis in mouse cell lines (Hitomi et al., 2008). In this thesis, it was accordingly shown that bafilomycin A1, a vacuolar type H^+-ATPase inhibitor, protected from both TNF- and TRAIL-mediated necroptosis. H^+-V-ATPase may contribute to necroptosis by maturation or acidification of cargo vesicles, promoting endogenous protein degradation (Yamamoto et al., 1998) or receptor endocytosis (Jefferies et al., 2008). However, since the lysosomal protease inhibitors z-FA-fmk, z-FF-fmk, Ca-074 Me, E-64 did not inhibit necroptosis, inhibition of H^+-V-ATPase by bafilomycin A_1 most likely protects from necroptosis by affecting endosomal trafficking rather than lysosomal calpains and cathepsins. Since H^+-V-ATPase subunits had been associated with detergent-resistant membranes from late endosomes (Lafourcade et al., 2008), a role of H^+-V-ATPase in ceramide-mediated signaling of necroptosis needs further investigation. Interestingly, endosomal trafficking of TNF-R1 regulated by H^+-V-ATPase had been reported to be negatively regulated by β-catenin (Han et al., 2013). Therefore, further investigations should be performed to clarify whether β-catenin-dependent endosomal trafficking regulates necroptosis.

Atg5 and Atg16L1 are necessary for execution of TNF-mediated necroptosis

In this thesis, deletion of Atg5 in MEFs almost completely protected from both TNF- and TRAIL-mediated necroptosis whereas Atg16L1-deficient MEFs were selectively protected from necroptosis induced by TNF. With regard to a potential mechanism how these two proteins could contribute to necroptosis independent from their function in autophagy, work from Lipinski and coworkers has indicated a connection between regulation of autophagy and necroptosis as the main regulatory protein RIP1 was identified to be involved in both pathways (Lipinski et al., 2010).

Components of autophagy might contribute to the execution of necroptosis, as very recent studies have revealed that ceramide-mediated cell death is abolished by

downregulation of Atg3, Atg7, and importantly by genetic deletion of Atg5 (Sentelle et al., 2012). Moreover, a link between ceramide and Atg5 was reported as inhibition of ceramide formation decreased Atg5 cleavage by calpains and suppressed generation of a 24-kDa pro-apoptotic mitochondria-permeabilizing fragment of Atg5 (Lepine et al., 2011) which activates the intrinsic pathway of apoptosis by interaction with Bcl-XL and release of cytochrome *c* (Yousefi et al., 2006, Tran et al., 2001). Unfortunately, little is known how Atg5 contributes to the execution of necroptosis. Therefore, Atg5 cleavage during TNF- and TRAIL-induced ceramide-mediated necroptosis as well as the potential role of the 24-kDa N-terminal fragment of Atg5 in mitochondrial permeabilization should be analyzed in the future. Recent analyses have shown that Atg5 is able to interact with FADD (Pyo et al., 2005), and that the FADD-Atg5-Atg12 complex is recruited to caspase-8 (Bell et al., 2008), indicating that a possible crosstalk might exist between components which mediate autophagy and necroptosis. Another explanation for an involvement of Atg5 in the execution of necroptosis is a possible control of membrane formation by Atg5 during necroptosis, as deletion of Atg5 promoted formation of elongated membranes and abolished further steps of complete membrane closure (Mizushima et al., 2010). Accordingly, results obtained in this thesis with inhibitors of autophagy suggest that formation of specific lysosomal-like or other vesicular structures might be responsible for mediation and execution of both TNF- and TRAIL-mediated necroptosis.

Notably, in this thesis, a role of Atg16L1 was confirmed for TNF-, but not for TRAIL-induced necroptosis. The molecular mechanism how Atg16L1 is involved in the execution of TNF-mediated necroptosis may be explained by the association of Atg16L1 with the plasma membrane, through interaction with the clathrin-heavy chains, in order to form early autophagosome precursors (Ravikumar et al., 2010). This involvement of Atg16L1 in the internalization of portions of the plasma membrane or in the formation of clathrin-bound vesicle structures may also be (independently from autophagy) required for TNF-mediated necroptosis. Atg16L1 is not involved in TRAIL-mediated necroptosis, therefore this type of necroptosis is probably triggered by other mechanisms than Atg16L1-clathrin regulated endocytosis of TRAIL receptors. In addition, Atg16L1 has seven WD repeats at the carboxy terminus (Saitoh et al., 2008), thus it is a potential interaction partner for other adaptor molecules possessing WD repeats such as FAN, RACK1, or EED which form a complex with N-SMase (Philipp et al., 2010). Since SMases can induce the formation of vesicles via local changes in lipid composition and thus the fluidity and curvature of

membranes (Zha et al., 1998), it is conceivable that Atg16L1 may participate in the regulation of this process by N-SMase. However, this hypothesis will have to be validated in future experiments.

Previous reports investigating the role of autophagy in TNF-mediated necroptosis with the use of the autophagy inhibitor 3-MA, Atg5-deficient MEFs and downregulation of Beclin-1 (Atg6), had demonstrated that autophagy is rather a downstream consequence of necroptosis and not a contributive factor (Degterev et al., 2005). Notably, the results obtained in this thesis demonstrate that components that participate in autophagy also are required for TNF- or TRAIL-mediated necroptosis (Figure 81).

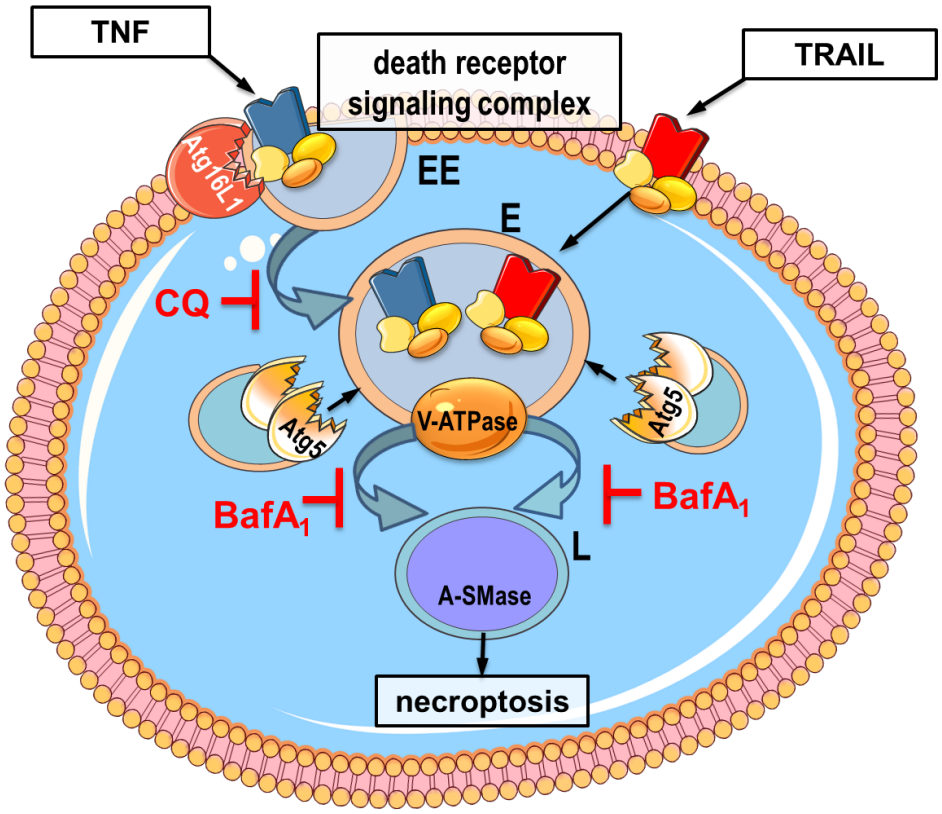

Figure 81. A putative model for the contribution of autophagy-related components to TNF- and TRAIL-mediated necroptosis. Stimulation of TNF-R1 or TRAIL receptors leads to formation of the corresponding death receptor signaling complexes. The TNF-R1-associated complex is internalized with assistance of Atg16L1 that possibly interacts with clathrin chains of the internalization pit. Association of internalized early endosomes (EE) with other membrane structures/vesicles in order to form a late endosome (E) is inhibited by chloroquine (CQ). In TRAIL-mediated necroptosis, the death receptor signaling complex is probably endocytosed by unknown mechanisms that cannot be inhibited by chloroquine and which do not require Atg16L1. The endosomes that contain death receptor signaling complexes are then delivered further to lysosomes (L) by membrane-associated structures with the assistance of Atg5. Endosomes that contain death receptor-associated signaling complex are fused with lysosomes to assure further signaling through, e.g. A-SMase. The fusion step is assured through the activity of H+-V-ATPase, which can be inhibited by bafilomycin A_1 ($BafA_1$).

Importantly, both TNF- and TRAIL-mediated necroptosis were found to be mediated differentially through components of the lysosomal pathway, in which Atg proteins are involved in the formation of various signaling compartments. Of note, the processes and Atg proteins identified here to play a role in necroptosis, are possibly not required to induce canonical autophagy *per se*, but rather could influence the formation of membranous cytoplasmic complexes. Apparently, these complexes might be used during necroptosis for massive membrane rearrangements that could generate compartments either for blocking the procedure of cell death or to separate distorted protein complexes. This is in line with the theory of the origins necroptosis that associates necroptosis with an anti-viral response (He et al., 2011). Such a mechanism of cell compartmentalization could be used by a cell as a mechanism of self-defense to separate viral from cellular components. Similar results were published already for the development of host resistance to infection of human macrophages with murine norovirus (MNV) in response to interferon γ (IFN-γ). The complex of Atg5-Atg12/Atg16L1 proteins was described to play an autophagy-independent role, and that rather, these proteins are used in a "cassette-like" fashion for a pivotal inhibition of viral replication and spreading (Hwang et al., 2012). Finally, several lines of evidence suggest that necroptosis is not a "specialized" type of autophagy as RIP3-dependent necroptosis was not executed through autophagy (i.e. Atg7 was not required for antigen-stimulated caspase-8-deficient cell death in T cells) (Ch'en et al., 2011). However, the precise mechanism by which Atg16L1 and Atg5 are involved in the execution of necroptosis will have to be clarified in future investigations.

C. Hypothetical model of necroptosis triggered by TNF or TRAIL

The data presented in this thesis will hopefully help to better understand the molecular pathways involved in TNF- and TRAIL-mediated necroptosis. Based upon the results obtained in this thesis, the following two models are suggested which provide insight into similarities and differences between TNF- (Figure 82) and TRAIL-mediated necroptosis (Figure 83).

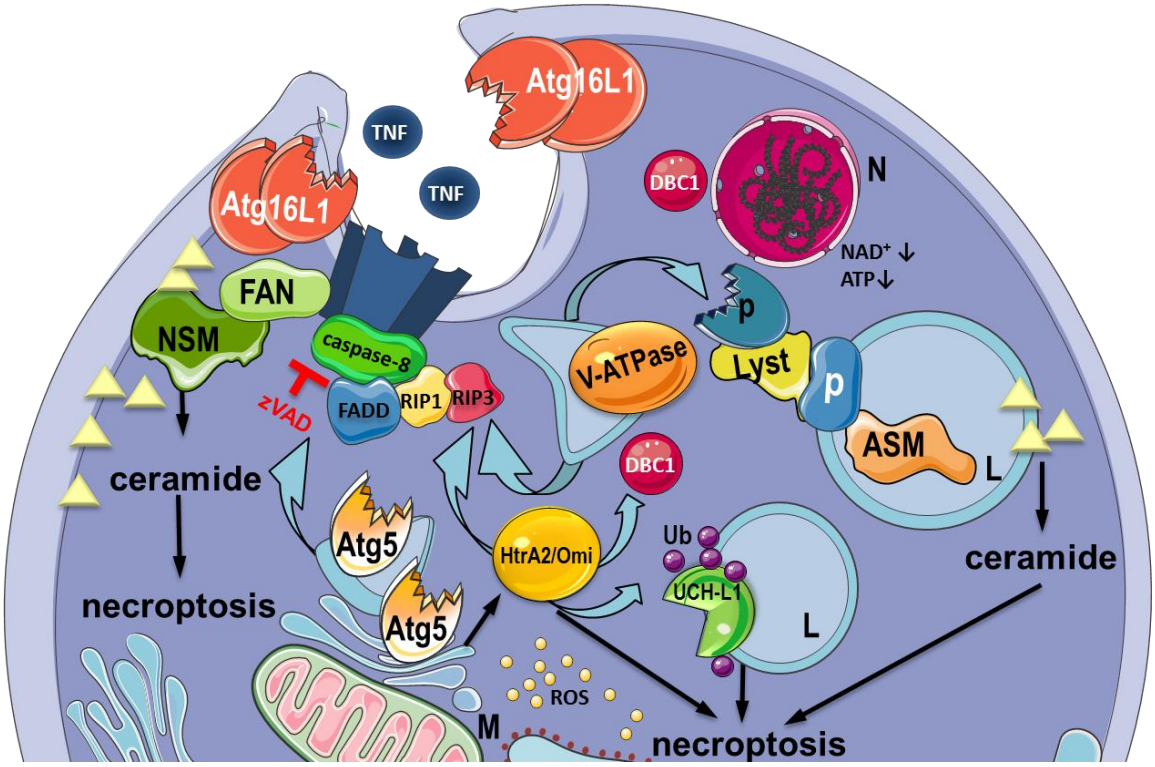

Figure 82. A general model of the signaling pathways in TNF-mediated necroptosis. After activation of TNF-R1 with TNF, the necroptotic signaling complex containing RIP1-RIP3 is formed at the receptor. In addition, TNF-R1 interacts via FAN with the plasma membrane-associated N-SMase (NSM) and generates ceramide (∆) to trigger necroptosis. Atg16L1 might assure the internalization of the necroptotic signaling complex in association with clathrin-coated pits. Clathrin-coated pits are formed and transformed into clathrin-coated vesicles which may fuse with other membranes aggregated with Atg5 or Atg16L1. The TNF-R1/necrosome complex may then fuse with *trans*-Golgi membranes, resulting in the formation of multivesicular endosomes (Schneider-Brachert et al., 2004). Subsequently, the fusion of lysosomes (L) that contain A-SMase (ASM) with these endosomes occurs. This event may be controlled by the activity of H^+-V-ATPase (V-ATPase) and the cytoplasmic protein Lyst or other unknown yet proteins (p). Localized in lysosomes A-SMase is activated, generates ceramide (∆) and further promotes the necroptotic signal. The mitochondria (M) produce necroptosis-promoting ROS and release the serine protease HtrA2/Omi that may possibly proteolytically regulate RIP1. Moreover, execution of necroptosis is influenced by HtrA2/Omi via regulation of UCH-L1 activity, which may be associated with the lysosomal compartment (Kabuta et al., 2008). As a consequence, monoubiquitination (Ub) of UCH-L1 controlled by HtrA2/Omi may serve as a necroptotic signal. The nuclear (N) protein DBC1 is cleaved by HtrA2/Omi and may further contribute to necroptosis, causing a late and secondary PARP1-independent depletion of ATP and NAD^+.

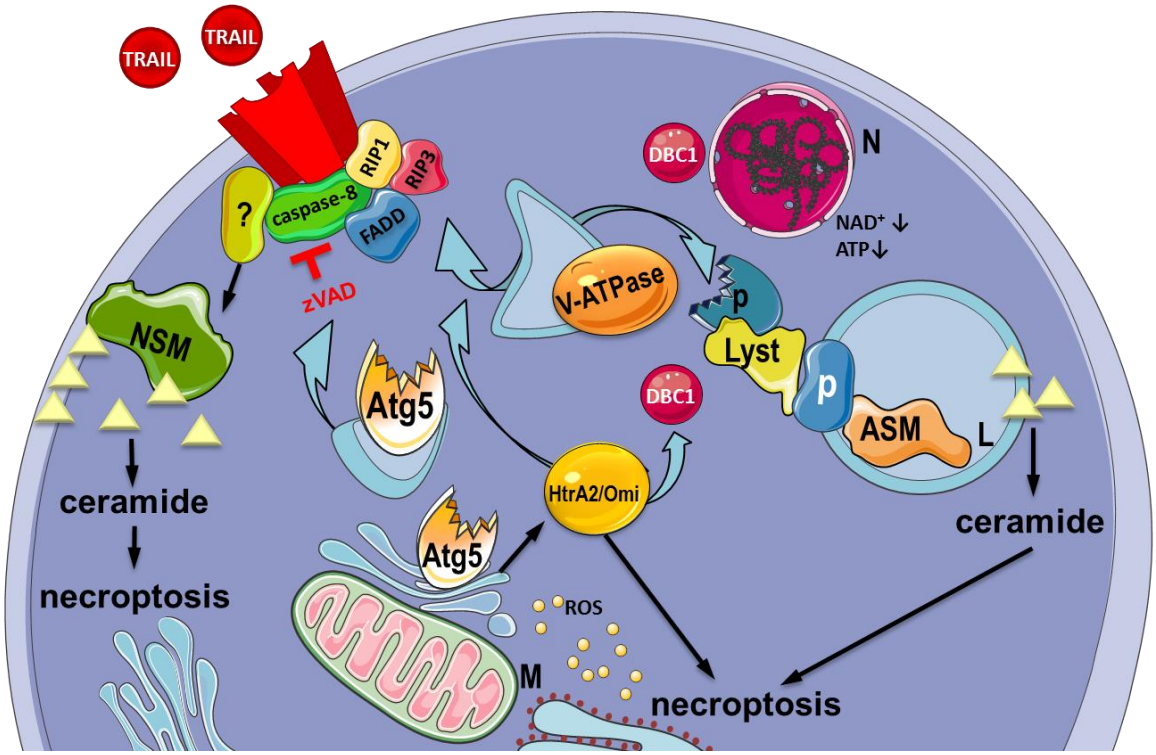

Figure 83. A general model of the signaling pathways in TRAIL-mediated necroptosis. Activation of TRAIL receptors with TRAIL induces formation of the necroptotic signaling complex containing RIP1-RIP3 at the receptor. TRAIL receptors may interact in a similar way as TNF-R1, or through other yet unidentified molecules, with plasma membrane-associated N-SMase (NSM) and generate ceramide (∆) to trigger necroptosis. TRAIL receptors and the necroptotic signaling complex will associate with intracellular membrane structures or vesicles bound to Atg5 and fuse with endosomes that contain H+-V-ATPase (V-ATPase) or lysosomes (L) that contain A-SMase (ASM), regulated by the cytoplasmic protein Lyst, an/or other yet unknown proteins (p). A-SMase is activated and generates ceramide (∆) that mediates progress of the necroptotic pathway. The mitochondria (M) produce necroptosis-promoting ROS and release the serine protease HtrA2/Omi that may possibly proteolytically regulate RIP1. In parallel, the nuclear (N) protein DBC1 is cleaved by HtrA2/Omi and may further contribute to necroptosis, causing a late and secondary PARP1-independent depletion of ATP and NAD^+.

VI. Summary

In this thesis, the signaling pathways that mediate tumor necrosis factor (TNF)- and TNF-related apoptosis-inducing ligand (TRAIL)-induced programmed necrosis (i.e. necroptosis) were characterized at the molecular and functional level.

The results obtained in the first part of this thesis demonstrate that TNF-mediated necroptosis and DNA-damage-induced programmed necrosis represent distinct and independent routes to programmed cell death. It was shown that factors involved in programmed necrosis such as activation of poly(ADP-ribose) polymerase 1 (PARP1), depletion of intracellular NAD^+ and ATP as well as nuclear translocation of mitochondrial AIF are not integral to TNF-induced necroptosis. In reverse, components crucial for the execution of necroptosis e.g. the receptor interacting proteins 1 (RIP1) and 3 (RIP3) were dispensable for the execution of DNA-damage-induced necrosis, also ruling out a crosstalk between both pathways. The results obtained in this part suggest that the currently established model of PARP1-mediated programmed necrosis as being an integral part of TNF-induced necroptosis needs to be revised, with consequences for the development of future therapeutic strategies.

In the second part of this thesis, the components that mediate TNF- and TRAIL-induced necroptosis were analyzed to gain a deeper insight into the similarities and the differences of the associated signaling pathways. It was confirmed that RIP1 is essential not only for TNF- but also for TRAIL-mediated necroptosis. Furthermore, it was demonstrated that both necroptotic pathways are triggered by ceramide generated through both acid sphingomyelinase (A-SMase) and neutral sphingomyelinase (N-SMase), and that Fas-associated protein with death domain (FADD), tumor necrosis factor receptor 2 (TNF-R2) and the caspase inhibitor zVAD-fmk modulate this response. Moreover, functionally associated proteins i.e. factor associated with N-SMase activation (FAN) and lysosomal-trafficking regulator (Lyst) emerged as key regulators of necroptosis. In addition, a role of chymotrypsin-like serine proteases but not of cathepsins, calpain/cysteine proteases, nor metalloproteases in necroptosis was demonstrated. As a particularly interesting protease, the mitochondrial serine protease HtrA2/Omi was identified as an essential regulator of necroptosis, possibly acting by cleavage of RIP1 and the protein deleted in breast cancer-1 (DBC1). Furthermore, an HtrA2/Omi-dependent monoubiquitination of ubiquitin carboxy-terminal hydrolase L1 (UCH-L1) during TNF- but not TRAIL-mediated necroptosis was

discovered in this thesis. Since UCH-L1 was also found to regulate TNF- but not TRAIL-mediated necroptosis, these results provide evidence for differences in the necrotic signaling pathways of TNF and TRAIL. Additional differences between TNF- and TRAIL-mediated necrotic signaling were discovered with respect to several components of the autophagic pathway. For TNF-mediated necroptosis, autophagy-related protein (Atg) Atg5, Atg16L1, lysosomal flux and the activity of vacuolar-type, proton-translocating ATPase (**(**H^+-V-ATPase) were crucial, whereas in necroptosis induced by TRAIL, only Atg5 and H^+-V-ATPase were required. Further analyses indicated a critical, however cell-line specific role of reactive oxygen species (ROS) in the execution of necroptosis. Therefore, the administration of radical scavengers during necroptosis may represent an effective protective strategy in certain cases.

Altogether, the data presented in this thesis demonstrate essential differences between DNA damage-induced programmed necrosis and TNF- and TRAIL-mediated necroptosis, resolving a current misconception in the field of cell death research. More importantly, the results presented here provide a first answer to the recently raised question whether there is one core program or several independent pathways to programmed necrosis, with immediate implications for the future development of necrosis-inhibitory cytoprotective drugs and for the general design of therapeutic strategies. Beyond these results, this thesis also provides deeper insights into the molecular mechanisms of necroptosis/programmed necrosis, highlighting a novel role for several previously unidentified proteins in the execution of TNF- and TRAIL-mediated necroptosis, and thus identifying new potential therapeutic targets.

VII. Zusammenfassung

In der vorliegenden Arbeit wurden die Signalwege der, durch Tumornekrosefaktor (TNF)- oder Tumornekrosefaktor-verwandter Apoptose-induzierender Ligand (TRAIL)-ausgelösten, programmierten Nekrose (d.h., Nekroptose) sowohl auf molekularer als auch auf funktioneller Ebene charakterisiert.

Die Ergebnisse aus dem ersten Teil dieser Arbeit zeigen, dass die durch TNF-ausgelöste Nekroptose und die durch DNA Schäden verursachte programmierte Nekrose zwei klar voneinander getrennte und unabhängige Wege zum programmierten Zelltod darstellen. Spezifisch wurde gezeigt, dass verschiedene Faktoren, die in der programmierten Nekrose eine Rolle spielen, wie die Aktivierung von Poly*(*ADP-ribose*)*-Polymerase 1 (PARP1), die intrazelluläre Abnahme der NAD^+ und ATP Konzentrationen als auch die Translokation von Apoptose induzierender Faktor (AIF) aus den Mitochondrien, keine integralen Bestandteile der TNF-induzierten Nekroptose sind. Im Gegensatz dazu sind Kernkomponenten der Nekroptose wie Rezeptor-interagierende Proteinkinase 1 (RIP1) und 3 (RIP3) nicht essentiell für die programmierte Nekrose. Somit kann, zumindest auf dieser Ebene, eine Überschneidung beider Signalwege ausgeschlossen werden. Diese Ergebnisse deuten darauf hin, dass das bisherige Modell der PARP1-vermittelten programmierten Nekrose als Bestandteil der TNF-induzierten Nekroptose überarbeitet werden muss, mit entsprechenden Konsequenzen für die Entwicklung zukünftiger Strategien in der Therapie.

Im zweiten Teil dieser Arbeit wurden einzelne Komponenten der TNF- bzw. TRAIL-induzierten Nekroptose näher untersucht, um so Gemeinsamkeiten als auch Unterschiede zwischen beiden Signalwegen aufzuklären. Es konnte gezeigt werden, dass RIP1 essentiell für beide Signalwege ist. Des Weiteren zeigen die Ergebnisse, dass sowohl die TNF- als auch die TRAIL-induzierte Nekroptose durch Ceramid, generiert von den sauren und neutralen Sphingomyelinasen, ausgelöst wird. Moduliert wird diese Signalkaskade durch das Fas-assoziierte Protein mit Todesdomäne (FADD), den TNF Rezeptor Typ-2 (TNF-R2) und den Caspaseinhibitor zVAD-fmk. Darüber hinaus wurde deutlich, dass funktionell assoziierte Proteine wie FAN und Lyst Schlüsselfaktoren für die Nekroptose sind. Zusätzlich wurde die Rolle von Chymotrypsin-ähnlichen Serinproteasen, Cathepsinen, Calpain/Cysteinproteasen und Metalloproteasen in der Nekroptose untersucht. Insbesondere die mitochondriale Serinprotease HtrA2/Omi konnte als ein essentieller Regulator der Nekroptose identifiziert werden, möglicherweise durch die Spaltung von RIP1 und der Deacetylase DBC1 (deleted in

breast cancer-1). Weiterhin wurde eine, durch HtrA2/Omi ausgelöste Monoubiquitinierung der Ubiquitin C-terminalen Hydrolase L1 (UCH-L1) während der TNF-induzierten Nekroptose erstmals beschrieben. Dies konnte nicht für die TRAIL-induzierte Nekroptose gezeigt werden und gibt somit Hinweise auf Unterschiede zwischen den beiden nekroptotischen Signalwegen. Zusätzlich wurden weitere Unterschiede zwischen der TNF- und TRAIL-vermittelten Nekroptose in Hinblick auf Komponenten der Autophagie aufgedeckt. Hierbei spielen Autophagie-assozierte Proteine (Atg) Atg5, Atg16L1, lysosomale Kompartimente und die Aktivität der vakuolären Protonen-ATPase (H^+-V-ATPase) eine entscheidende Rolle. Im Gegensatz dazu waren für die TRAIL-induzierte Nekroptose nur Atg5 und H^+-V-ATPase essentiell. Die Ergebnisse von weiteren Analysen deuten auf eine kritische, wenn auch Zelllinien-spezifische Rolle von Reaktiven Sauerstoffspezies (ROS) während der Nekroptose hin. Daher könnte der Einsatz von Radikalfängern eine effektive Behandlung verschiedener Krankheitsbilder ermöglichen.

Zusammengefasst zeigen die Ergebnisse dieser Arbeit essentielle Unterschiede zwischen der, durch DNA Schäden verursachten programmierten Nekrose und der TNF- bzw. TRAIL induzierten Nekroptose und lösen damit ein falsches Modell im Forschungsbereich des Zelltods. Jedoch weitaus interessanter ist, dass die hier vorgestellten Ergebnisse erste Antworten auf die kürzlich aufkommende Frage, ob die programmierte Nekrose durch einen zentralen oder durch mehrere verschiedene Signalwege durchgeführt wird, liefern. Aus der Beantwortung dieser grundlegenden Frage entstehen direkt neue Aspekte und Strategien für die zukünftige Behandlung von Krankheitsbildern, die auf programmierte Nekrose bzw. Nekroptose zurückgeführt werden können. Schließlich geben die Ergebnisse dieser Arbeit weitere Einblicke in die molekularen Mechanismen der programmierten Nekrose bzw. Nekroptose und beschreiben erstmals die Rolle verschiedener, bisher im Zusammenhang mit der TNF- und TRAIL-induzierten Nekroptose unbekannter Proteine. Diese Proteine stellen somit potentiell neue therapeutische Ziele dar.

VIII. References

ABDULGHANI, J. & EL-DEIRY, W. S. 2010. TRAIL receptor signaling and therapeutics. *Expert Opin Ther Targets,* 14, 1091-108.

ABHARI, B. A., CRISTOFANON, S., KAPPLER, R., VON SCHWEINITZ, D., HUMPHREYS, R. & FULDA, S. 2012. RIP1 is required for IAP inhibitor-mediated sensitization for TRAIL-induced apoptosis via a RIP1/FADD/caspase-8 cell death complex. *Oncogene*.

ADAM-KLAGES, S., ADAM, D., WIEGMANN, K., STRUVE, S., KOLANUS, W., SCHNEIDER-MERGENER, J. & KRÖNKE, M. 1996. FAN, a novel WD-repeat protein, couples the p55 TNF-receptor to neutral sphingomyelinase. *Cell,* 86, 937-47.

ADAM-KLAGES, S., SCHWANDNER, R., ADAM, D., KREDER, D., BERNARDO, K. & KRÖNKE, M. 1998. Distinct adapter proteins mediate acid versus neutral sphingomyelinase activation through the p55 receptor for tumor necrosis factor. *J Leukoc Biol,* 63, 678-82.

ADAM, D., WIEGMANN, K., ADAM-KLAGES, S., RUFF, A. & KRÖNKE, M. 1996. A novel cytoplasmic domain of the p55 tumor necrosis factor receptor initiates the neutral sphingomyelinase pathway. *J Biol Chem,* 271, 14617-22.

AGUILAR-QUESADA, R., MUNOZ-GAMEZ, J. A., MARTIN-OLIVA, D., PERALTA-LEAL, A., QUILES-PEREZ, R., RODRIGUEZ-VARGAS, J. M., RUIZ DE ALMODOVAR, M., CONDE, C., RUIZ-EXTREMERA, A. & OLIVER, F. J. 2007. Modulation of transcription by PARP-1: consequences in carcinogenesis and inflammation. *Curr Med Chem,* 14, 1179-87.

AKAZAWA, Y., MOTT, J. L., BRONK, S. F., WERNEBURG, N. W., KAHRAMAN, A., GUICCIARDI, M. E., MENG, X. W., KOHNO, S., SHAH, V. H., KAUFMANN, S. H., MCNIVEN, M. A. & GORES, G. J. 2009. Death receptor 5 internalization is required for lysosomal permeabilization by TRAIL in malignant liver cell lines. *Gastroenterology,* 136, 2365-2376 e1-7.

ALAM, S., BOWSER, B. S., CONWAY, M. J., ISRAR, M., TANDON, A. & MEYERS, C. 2011. Adeno-associated virus type 2 infection activates caspase dependent and independent apoptosis in multiple breast cancer lines but not in normal mammary epithelial cells. *Mol Cancer,* 10, 97.

ANDRIEU-ABADIE, N., GOUAZE, V., SALVAYRE, R. & LEVADE, T. 2001. Ceramide in apoptosis signaling: relationship with oxidative stress. *Free Radic Biol Med,* 31, 717-28.

ARANA, L., GANGOITI, P., OURO, A., TRUEBA, M. & GOMEZ-MUNOZ, A. 2010. Ceramide and ceramide 1-phosphate in health and disease. *Lipids Health Dis,* 9, 15.

ARENZ, C. 2010. Small molecule inhibitors of acid sphingomyelinase. *Cell Physiol Biochem,* 26, 1-8.

ARENZ, C. & GIANNIS, A. 2000. Synthesis of the First Selective Irreversible Inhibitor of Neutral Sphingomyelinase. *Angewandte Chemie International Edition,* 39, 1440-1442.

ARSLAN, S. C. & SCHEIDEREIT, C. 2011. The prevalence of TNFalpha-induced necrosis over apoptosis is determined by TAK1-RIP1 interplay. *PLoS One,* 6, e26069.

BAI, P., CANTO, C., OUDART, H., BRUNYANSZKI, A., CEN, Y., THOMAS, C., YAMAMOTO, H., HUBER, A., KISS, B., HOUTKOOPER, R. H., SCHOONJANS, K., SCHREIBER, V., SAUVE, A. A., MENISSIER-DE MURCIA, J. & AUWERX, J. 2011. PARP-1 inhibition increases mitochondrial metabolism through SIRT1 activation. *Cell Metab,* 13, 461-8.

BAO, Q. & SHI, Y. 2007. Apoptosome: a platform for the activation of initiator caspases. *Cell Death Differ,* 14, 56-65.

BARITAUD, M., CABON, L., DELAVALLEE, L., GALAN-MALO, P., GILLES, M. E., BRUNELLE-NAVAS, M. N. & SUSIN, S. A. 2012. AIF-mediated caspase-independent necroptosis requires ATM and DNA-PK-induced histone H2AX Ser139 phosphorylation. *Cell Death Dis,* 3, e390.

BARTH, B. M., GUSTAFSON, S. J. & KUHN, T. B. 2012. Neutral sphingomyelinase activation precedes NADPH oxidase-dependent damage in neurons exposed to the proinflammatory cytokine tumor necrosis factor-alpha. *J Neurosci Res,* 90, 229-42.

BELL, B. D., LEVERRIER, S., WEIST, B. M., NEWTON, R. H., ARECHIGA, A. F., LUHRS, K. A., MORRISSETTE, N. S. & WALSH, C. M. 2008. FADD and caspase-8 control the outcome of autophagic signaling in proliferating T cells. *Proc Natl Acad Sci U S A,* 105, 16677-82.

BELYANSKAYA, L. L., MARTI, T. M., HOPKINS-DONALDSON, S., KURTZ, S., FELLEY-BOSCO, E. & STAHEL, R. A. 2007. Human agonistic TRAIL receptor antibodies Mapatumumab and Lexatumumab induce apoptosis in malignant mesothelioma and act synergistically with cisplatin. *Mol Cancer,* 6, 66.

BENES, P., VETVICKA, V. & FUSEK, M. 2008. Cathepsin D--many functions of one aspartic protease. *Crit Rev Oncol Hematol,* 68, 12-28.

BHUIYAN, M. S. & FUKUNAGA, K. 2007. Inhibition of HtrA2/Omi ameliorates heart dysfunction following ischemia/reperfusion injury in rat heart in vivo. *Eur J Pharmacol,* 557, 168-77.

BHUIYAN, M. S. & FUKUNAGA, K. 2008. Activation of HtrA2, a mitochondrial serine protease mediates apoptosis: current knowledge on HtrA2 mediated myocardial ischemia/reperfusion injury. *Cardiovasc Ther,* 26, 224-32.

BIKMAN, B. T. & SUMMERS, S. A. 2011. Ceramides as modulators of cellular and whole-body metabolism. *J Clin Invest,* 121, 4222-30.

BJORNLAND, K., FLATMARK, K., PETTERSEN, S., AAASEN, A. O., FODSTAD, O. & MAELANDSMO, G. M. 2005. Matrix metalloproteinases participate in osteosarcoma invasion. *J Surg Res,* 127, 151-6.

BLINK, E., MAIANSKI, N. A., ALNEMRI, E. S., ZERVOS, A. S., ROOS, D. & KUIJPERS, T. W. 2004. Intramitochondrial serine protease activity of Omi/HtrA2 is required for caspase-independent cell death of human neutrophils. *Cell Death Differ,* 11, 937-9.

BOECKE, A., SIEGER, D., NEACSU, C. D., KASHKAR, H. & KRÖNKE, M. 2012. Factor associated with neutral sphingomyelinase activity mediates navigational capacity of leukocytes responding to wounds and infection: live imaging studies in zebrafish larvae. *J Immunol,* 189, 1559-66.

BONNET, M. C., PREUKSCHAT, D., WELZ, P. S., VAN LOO, G., ERMOLAEVA, M. A., BLOCH, W., HAASE, I. & PASPARAKIS, M. 2011. The adaptor protein FADD protects epidermal keratinocytes from necroptosis in vivo and prevents skin inflammation. *Immunity,* 35, 572-82.

BOSE, R., VERHEIJ, M., HAIMOVITZ-FRIEDMAN, A., SCOTTO, K., FUKS, Z. & KOLESNICK, R. 1995. Ceramide synthase mediates daunorubicin-induced apoptosis: an alternative mechanism for generating death signals. *Cell,* 82, 405-14.

BOULARES, A. H., ZOLTOSKI, A. J., YAKOVLEV, A., XU, M. & SMULSON, M. E. 2001. Roles of DNA fragmentation factor and poly(ADP-ribose) polymerase in an amplification phase of tumor necrosis factor-induced apoptosis. *J Biol Chem,* 276, 38185-92.

BRAS, M., YUSTE, V. J., ROUE, G., BARBIER, S., SANCHO, P., VIRELY, C., RUBIO, M., BAUDET, S., ESQUERDA, J. E., MERLE-BERAL, H., SARFATI, M. & SUSIN, S. A. 2007. Drp1 mediates caspase-independent type III cell death in normal and leukemic cells. *Mol Cell Biol,* 27, 7073-88.

BRAY, K., MATHEW, R., LAU, A., KAMPHORST, J. J., FAN, J., CHEN, J., CHEN, H. Y., GHAVAMI, A., STEIN, M., DIPAOLA, R. S., ZHANG, D., RABINOWITZ, J. D. & WHITE, E. 2012. Autophagy suppresses RIP kinase-dependent necrosis enabling survival to mTOR inhibition. *PLoS One,* 7, e41831.

BRESHEARS, L. M., SCHLIEVERT, P. M. & PETERSON, M. L. 2012. A disintegrin and metalloproteinase 17 (ADAM17) and epidermal growth factor receptor (EGFR) signaling drive the epithelial response to Staphylococcus aureus toxic shock syndrome toxin-1 (TSST-1). *J Biol Chem,* 287, 32578-87.

BURGESS, A., MORNON, J. P., DE SAINT-BASILE, G. & CALLEBAUT, I. 2009. A concanavalin A-like lectin domain in the CHS1/LYST protein, shared by members of the BEACH family. *Bioinformatics,* 25, 1219-22.

BURKART, V., WANG, Z. Q., RADONS, J., HELLER, B., HERCEG, Z., STINGL, L., WAGNER, E. F. & KOLB, H. 1999. Mice lacking the poly(ADP-ribose) polymerase gene are resistant to pancreatic beta-cell destruction and diabetes development induced by streptozocin. *Nat Med,* 5, 314-9.

CABAL-HIERRO, L. & LAZO, P. S. 2012. Signal transduction by tumor necrosis factor receptors. *Cell Signal,* 24, 1297-305.

CABON, L., GALAN-MALO, P., BOUHARROUR, A., DELAVALLEE, L., BRUNELLE-NAVAS, M. N., LORENZO, H. K., GROSS, A. & SUSIN, S. A. 2012. BID regulates AIF-mediated caspase-independent necroptosis by promoting BAX activation. *Cell Death Differ,* 19, 245-56.

CADWELL, K., LIU, J. Y., BROWN, S. L., MIYOSHI, H., LOH, J., LENNERZ, J. K., KISHI, C., KC, W., CARRERO, J. A., HUNT, S., STONE, C. D., BRUNT, E. M., XAVIER, R. J., SLECKMAN, B. P., LI, E., MIZUSHIMA, N., STAPPENBECK, T. S. & VIRGIN, H. W. T. 2008. A key role for autophagy and the autophagy gene Atg16l1 in mouse and human intestinal Paneth cells. *Nature,* 456, 259-63.

CANALS, D., PERRY, D. M., JENKINS, R. W. & HANNUN, Y. A. 2011. Drug targeting of sphingolipid metabolism: sphingomyelinases and ceramidases. *Br J Pharmacol,* 163, 694-712.

CAO, X., POBEZINSKAYA, Y. L., MORGAN, M. J. & LIU, Z. G. 2011. The role of TRADD in TRAIL-induced apoptosis and signaling. *FASEB J,* 25, 1353-8.

CAPPUZZO, F., BARTOLINI, S. & CRINO, L. 2003. Emerging drugs for non-small cell lung cancer. *Expert Opin Emerg Drugs,* 8, 179-92.

CARTIER, A. E., DJAKOVIC, S. N., SALEHI, A., WILSON, S. M., MASLIAH, E. & PATRICK, G. N. 2009. Regulation of synaptic structure by ubiquitin C-terminal hydrolase L1. *J Neurosci,* 29, 7857-68.

CARUSO, J. A., MATHIEU, P. A. & REINERS, J. J., JR. 2005. Sphingomyelins suppress the targeted disruption of lysosomes/endosomes by the photosensitizer NPe6 during photodynamic therapy. *Biochem J,* 392, 325-34.

CASERTA, T. M., SMITH, A. N., GULTICE, A. D., REEDY, M. A. & BROWN, T. L. 2003. Q-VD-OPh, a broad spectrum caspase inhibitor with potent antiapoptotic properties. *Apoptosis,* 8, 345-52.

CAUWELS, A., JANSSEN, B., WAEYTENS, A., CUVELIER, C. & BROUCKAERT, P. 2003. Caspase inhibition causes hyperacute tumor necrosis factor-induced shock via oxidative stress and phospholipase A2. *Nat Immunol,* 4, 387-93.

CH'EN, I. L., TSAU, J. S., MOLKENTIN, J. D., KOMATSU, M. & HEDRICK, S. M. 2011. Mechanisms of necroptosis in T cells. *J Exp Med,* 208, 633-41.

CHAITANYA, G. V., STEVEN, A. J. & BABU, P. P. 2010. PARP-1 cleavage fragments: signatures of cell-death proteases in neurodegeneration. *Cell Commun Signal,* 8, 31.

CHALFANT, C. E. & SPIEGEL, S. 2005. Sphingosine 1-phosphate and ceramide 1-phosphate: expanding roles in cell signaling. *J Cell Sci,* 118, 4605-12.

CHAN, F. K. & BAEHRECKE, E. H. 2012. RIP3 finds partners in crime. *Cell,* 148, 17-8.

CHAN, F. K., SHISLER, J., BIXBY, J. G., FELICES, M., ZHENG, L., APPEL, M., ORENSTEIN, J., MOSS, B. & LENARDO, M. J. 2003. A role for tumor necrosis factor receptor-2 and receptor-interacting protein in programmed necrosis and antiviral responses. *J Biol Chem,* 278, 51613-21.

CHAU, H., MIRTSOS, C. & HUANG, H. L. 2011. Regulation of death complexes formation in tumor necrosis factor receptor signaling. *Exp Cell Res,* 317, 1841-50.

CHAUVIER, D., ANKRI, S., CHARRIAUT-MARLANGUE, C., CASIMIR, R. & JACOTOT, E. 2007. Broad-spectrum caspase inhibitors: from myth to reality? *Cell Death Differ,* 14, 387-91.

CHAVEZ-VALDEZ, R., MARTIN, L. J. & NORTHINGTON, F. J. 2012. Programmed Necrosis: A Prominent Mechanism of Cell Death following Neonatal Brain Injury. *Neurol Res Int,* 2012, 257563.

CHEN, B. C., CHANG, H. M., HSU, M. J., SHIH, C. M., CHIU, Y. H., CHIU, W. T. & LIN, C. H. 2009. Peptidoglycan induces cyclooxygenase-2 expression in macrophages by activating the neutral sphingomyelinase-ceramide pathway. *J Biol Chem,* 284, 20562-73.

CHEN, F., SUGIURA, Y., MYERS, K. G., LIU, Y. & LIN, W. 2010. Ubiquitin carboxyl-terminal hydrolase L1 is required for maintaining the structure and function of the neuromuscular junction. *Proc Natl Acad Sci U S A,* 107, 1636-41.

CHEN, S. Y., CHIU, L. Y., MAA, M. C., WANG, J. S., CHIEN, C. L. & LIN, W. W. 2011. zVAD-induced autophagic cell death requires c-Src-dependent ERK and JNK activation and reactive oxygen species generation. *Autophagy,* 7, 217-28.

CHO, Y. S., CHALLA, S., MOQUIN, D., GENGA, R., RAY, T. D., GUILDFORD, M. & CHAN, F. K. 2009. Phosphorylation-driven assembly of the RIP1-RIP3 complex regulates programmed necrosis and virus-induced inflammation. *Cell,* 137, 1112-23.

CHRISTOFFERSON, D. E., LI, Y., HITOMI, J., ZHOU, W., UPPERMAN, C., ZHU, H., GERBER, S. A., GYGI, S. & YUAN, J. 2012. A novel role for RIP1 kinase in mediating TNFalpha production. *Cell Death Dis,* 3, e320.

CHRISTOFFERSON, D. E. & YUAN, J. 2010a. Cyclophilin A release as a biomarker of necrotic cell death. *Cell Death Differ,* 17, 1942-3.

CHRISTOFFERSON, D. E. & YUAN, J. 2010b. Necroptosis as an alternative form of programmed cell death. *Curr Opin Cell Biol,* 22, 263-8.

CILENTI, L., LEE, Y., HESS, S., SRINIVASULA, S., PARK, K. M., JUNQUEIRA, D., DAVIS, H., BONVENTRE, J. V., ALNEMRI, E. S. & ZERVOS, A. S. 2003. Characterization of a novel and specific inhibitor for the pro-apoptotic protease Omi/HtrA2. *J Biol Chem,* 278, 11489-94.

CODOGNO, P. & MEIJER, A. J. 2005. Autophagy and signaling: their role in cell survival and cell death. *Cell Death Differ,* 12 Suppl 2, 1509-18.

COHAUSZ, O. & ALTHAUS, F. R. 2009. Role of PARP-1 and PARP-2 in the expression of apoptosis-regulating genes in HeLa cells. *Cell Biol Toxicol,* 25, 379-91.

COHAUSZ, O., BLENN, C., MALANGA, M. & ALTHAUS, F. R. 2008. The roles of poly(ADP-ribose)-metabolizing enzymes in alkylation-induced cell death. *Cell Mol Life Sci,* 65, 644-55.

COZZI, A., CIPRIANI, G., FOSSATI, S., FARACO, G., FORMENTINI, L., MIN, W., CORTES, U., WANG, Z. Q., MORONI, F. & CHIARUGI, A. 2006. Poly(ADP-ribose) accumulation and enhancement of postischemic brain damage in 110-kDa poly(ADP-ribose) glycohydrolase null mice. *J Cereb Blood Flow Metab,* 26, 684-95.

CRAWFORD, R. S., ALBADAWI, H., ATKINS, M. D., JONES, J. E., YOO, H. J., CONRAD, M. F., AUSTEN, W. G., JR. & WATKINS, M. T. 2010. Postischemic poly

(ADP-ribose) polymerase (PARP) inhibition reduces ischemia reperfusion injury in a hind-limb ischemia model. *Surgery,* 148, 110-8.

CREMESTI, A. E., GONI, F. M. & KOLESNICK, R. 2002. Role of sphingomyelinase and ceramide in modulating rafts: do biophysical properties determine biologic outcome? *FEBS Lett,* 531, 47-53.

CULLINANE, A. R., SCHAFFER, A. A. & HUIZING, M. 2013. The BEACH Is Hot: A LYST of Emerging Roles for BEACH-Domain Containing Proteins in Human Disease. *Traffic*.

DARDING, M., FELTHAM, R., TENEV, T., BIANCHI, K., BENETATOS, C., SILKE, J. & MEIER, P. 2011. Molecular determinants of Smac mimetic induced degradation of cIAP1 and cIAP2. *Cell Death Differ,* 18, 1376-86.

DAUGAS, E., SUSIN, S. A., ZAMZAMI, N., FERRI, K. F., IRINOPOULOU, T., LAROCHETTE, N., PREVOST, M. C., LEBER, B., ANDREWS, D., PENNINGER, J. & KROEMER, G. 2000. Mitochondrio-nuclear translocation of AIF in apoptosis and necrosis. *FASEB J,* 14, 729-39.

DE BLASIO, A., MESSINA, C., SANTULLI, A., MANGANO, V., DI LEONARDO, E., D'ANNEO, A., TESORIERE, G. & VENTO, R. 2005. Differentiative pathway activated by 3-aminobenzamide, an inhibitor of PARP, in human osteosarcoma MG-63 cells. *FEBS Lett,* 579, 615-20.

DECLERCQ, W., TAKAHASHI, N. & VANDENABEELE, P. 2011. Dual face apoptotic machinery: from initiator of apoptosis to guardian of necroptosis. *Immunity,* 35, 493-5.

DECLERCQ, W., VANDEN BERGHE, T. & VANDENABEELE, P. 2009. RIP kinases at the crossroads of cell death and survival. *Cell,* 138, 229-32.

DEERBERG, A., SOSNA, J., THON, L., BELKA, C. & ADAM, D. 2009. Differential protection by wildtype vs. organelle-specific Bcl-2 suggests a combined requirement of both the ER and mitochondria in ceramide-mediated caspase-independent programmed cell death. *Radiat Oncol,* 4, 41.

DEGTEREV, A., HITOMI, J., GERMSCHEID, M., CH'EN, I. L., KORKINA, O., TENG, X., ABBOTT, D., CUNY, G. D., YUAN, C., WAGNER, G., HEDRICK, S. M., GERBER, S. A., LUGOVSKOY, A. & YUAN, J. 2008. Identification of RIP1 kinase as a specific cellular target of necrostatins. *Nat Chem Biol,* 4, 313-21.

DEGTEREV, A., HUANG, Z., BOYCE, M., LI, Y., JAGTAP, P., MIZUSHIMA, N., CUNY, G. D., MITCHISON, T. J., MOSKOWITZ, M. A. & YUAN, J. 2005. Chemical inhibitor of nonapoptotic cell death with therapeutic potential for ischemic brain injury. *Nat Chem Biol,* 1, 112-9.

DEGTEREV, A. & YUAN, J. 2008. Expansion and evolution of cell death programmes. *Nat Rev Mol Cell Biol,* 9, 378-90.

DEIGNER, H. P., GULBINS, E. & CLAUS, R. A. 2007. Sphingolipid Metabolism in Systemic Inflammation. *In:* VINCENT, J.-L. (ed.) *Yearbook of Intensive Care and Emergency Medicine.* Springer Berlin Heidelberg

DELETTRE, C., YUSTE, V. J., MOUBARAK, R. S., BRAS, M., LESBORDES-BRION, J. C., PETRES, S., BELLALOU, J. & SUSIN, S. A. 2006. AIFsh, a novel apoptosis-inducing factor (AIF) pro-apoptotic isoform with potential pathological relevance in human cancer. *J Biol Chem,* 281, 6413-27.

DESIDERI, E. & MARTINS, L. M. 2012. Mitochondrial Stress Signalling: HTRA2 and Parkinson's Disease. *Int J Cell Biol,* 2012, 607929.

DEVILLARD, R., GALVANI, S., THIERS, J. C., GUENET, J. L., HANNUN, Y., BIELAWSKI, J., NEGRE-SALVAYRE, A., SALVAYRE, R. & AUGE, N. 2010. Stress-induced sphingolipid signaling: role of type-2 neutral sphingomyelinase in murine cell apoptosis and proliferation. *PLoS One,* 5, e9826.

DICKENS, L. S., POWLEY, I. R., HUGHES, M. A. & MACFARLANE, M. 2012. The 'complexities' of life and death: death receptor signalling platforms. *Exp Cell Res,* 318, 1269-77.

DILLON, C. P., OBERST, A., WEINLICH, R., JANKE, L. J., KANG, T. B., BEN-MOSHE, T., MAK, T. W., WALLACH, D. & GREEN, D. R. 2012. Survival function of the FADD-CASPASE-8-cFLIP(L) complex. *Cell Rep,* 1, 401-7.

DITSWORTH, D., ZONG, W. X. & THOMPSON, C. B. 2007. Activation of poly(ADP)-ribose polymerase (PARP-1) induces release of the pro-inflammatory mediator HMGB1 from the nucleus. *J Biol Chem,* 282, 17845-54.

DOBO, J., SWANSON, R., SALVESEN, G. S., OLSON, S. T. & GETTINS, P. G. 2006. Cytokine response modifier a inhibition of initiator caspases results in covalent complex formation and dissociation of the caspase tetramer. *J Biol Chem,* 281, 38781-90.

DOBROWSKY, R. T., KAMIBAYASHI, C., MUMBY, M. C. & HANNUN, Y. A. 1993. Ceramide activates heterotrimeric protein phosphatase 2A. *J Biol Chem,* 268, 15523-30.

DORN, G. W., 2ND 2013. Molecular mechanisms that differentiate apoptosis from programmed necrosis. *Toxicol Pathol,* 41, 227-34.

DUMITRU, C. A. & GULBINS, E. 2006. TRAIL activates acid sphingomyelinase via a redox mechanism and releases ceramide to trigger apoptosis. *Oncogene,* 25, 5612-25.

DUNAI, Z. A., IMRE, G., BARNA, G., KORCSMAROS, T., PETAK, I., BAUER, P. I. & MIHALIK, R. 2012. Staurosporine induces necroptotic cell death under caspase-compromised conditions in U937 cells. *PLoS One,* 7, e41945.

DUPREZ, L., BERTRAND, M. J., VANDEN BERGHE, T., DONDELINGER, Y., FESTJENS, N. & VANDENABEELE, P. 2012. Intermediate domain of receptor-interacting protein kinase 1 (RIPK1) determines switch between necroptosis and RIPK1 kinase-dependent apoptosis. *J Biol Chem,* 287, 14863-72.

DUPREZ, L., WIRAWAN, E., VANDEN BERGHE, T. & VANDENABEELE, P. 2009. Major cell death pathways at a glance. *Microbes Infect,* 11, 1050-62.

DURCHFORT, N., VERHOEF, S., VAUGHN, M. B., SHRESTHA, R., ADAM, D., KAPLAN, J. & WARD, D. M. 2012. The enlarged lysosomes in beige j cells result from decreased lysosome fission and not increased lysosome fusion. *Traffic,* 13, 108-19.

EDELMANN, B., BERTSCH, U., TCHIKOV, V., WINOTO-MORBACH, S., PERROTTA, C., JAKOB, M., ADAM-KLAGES, S., KABELITZ, D. & SCHÜTZE, S. 2011. Caspase-8 and caspase-7 sequentially mediate proteolytic activation of acid sphingomyelinase in TNF-R1 receptosomes. *EMBO J,* 30, 379-94.

ESCANDE, C., CHINI, C. C., NIN, V., DYKHOUSE, K. M., NOVAK, C. M., LEVINE, J., VAN DEURSEN, J., GORES, G. J., CHEN, J., LOU, Z. & CHINI, E. N. 2010. Deleted in breast cancer-1 regulates SIRT1 activity and contributes to high-fat diet-induced liver steatosis in mice. *J Clin Invest,* 120, 545-58.

ETHIER, C., LABELLE, Y. & POIRIER, G. G. 2007. PARP-1-induced cell death through inhibition of the MEK/ERK pathway in MNNG-treated HeLa cells. *Apoptosis,* 12, 2037-49.

FABIAN, Z., O'BRIEN, P., PAJECKA, K. & FEARNHEAD, H. O. 2009. TPCK-induced apoptosis and labelling of the largest subunit of RNA polymerase II in Jurkat cells. *Apoptosis,* 14, 1154-64.

FAUSTMAN, D. & DAVIS, M. 2010. TNF receptor 2 pathway: drug target for autoimmune diseases. *Nat Rev Drug Discov,* 9, 482-93.

FEOKTISTOVA, M., GESERICK, P., KELLERT, B., DIMITROVA, D. P., LANGLAIS, C., HUPE, M., CAIN, K., MACFARLANE, M., HACKER, G. & LEVERKUS, M. 2011.

cIAPs block Ripoptosome formation, a RIP1/caspase-8 containing intracellular cell death complex differentially regulated by cFLIP isoforms. *Mol Cell,* 43, 449-63.

FESTJENS, N., VANDEN BERGHE, T. & VANDENABEELE, P. 2006. Necrosis, a well-orchestrated form of cell demise: signalling cascades, important mediators and concomitant immune response. *Biochim Biophys Acta,* 1757, 1371-87.

FIORILLO, C., PONZIANI, V., GIANNINI, L., CECCHI, C., CELLI, A., NASSI, N., LANZILAO, L., CAPORALE, R. & NASSI, P. 2006. Protective effects of the PARP-1 inhibitor PJ34 in hypoxic-reoxygenated cardiomyoblasts. *Cell Mol Life Sci,* 63, 3061-71.

FULDA, S. 2013. Alternative cell death pathways and cell metabolism. *Int J Cell Biol,* 2013, 463637.

FULDA, S., GORMAN, A. M., HORI, O. & SAMALI, A. 2010. Cellular stress responses: cell survival and cell death. *Int J Cell Biol,* 2010, 214074.

GALLUZZI, L. & KROEMER, G. 2008. Necroptosis: a specialized pathway of programmed necrosis. *Cell,* 135, 1161-3.

GALLUZZI, L., VITALE, I., ABRAMS, J. M., ALNEMRI, E. S., BAEHRECKE, E. H., BLAGOSKLONNY, M. V., DAWSON, T. M., DAWSON, V. L., EL-DEIRY, W. S., FULDA, S., GOTTLIEB, E., GREEN, D. R., HENGARTNER, M. O., KEPP, O., KNIGHT, R. A., KUMAR, S., LIPTON, S. A., LU, X., MADEO, F., MALORNI, W., MEHLEN, P., NUNEZ, G., PETER, M. E., PIACENTINI, M., RUBINSZTEIN, D. C., SHI, Y., SIMON, H. U., VANDENABEELE, P., WHITE, E., YUAN, J., ZHIVOTOVSKY, B., MELINO, G. & KROEMER, G. 2012. Molecular definitions of cell death subroutines: recommendations of the Nomenclature Committee on Cell Death 2012. *Cell Death Differ,* 19, 107-20.

GIEFING M., WINOTO-MORBACH S., SOSNA J., DÖRING C., KLAPPER W., KÜPPERS R., BÖTTCHER S., ADAM D., SIEBERT R. & S., S. 2013. Hodgkin-Reed-Sternberg cells in classical Hodgkin lymphoma show alterations of genes encoding the NADPH oxidase complex and impaired reactive oxygen species synthesis capacity. *PLoS One,* submitted for publication.

GRASSME, H., CREMESTI, A., KOLESNICK, R. & GULBINS, E. 2003. Ceramide-mediated clustering is required for CD95-DISC formation. *Oncogene,* 22, 5457-70.

GREEN, D. R., GALLUZZI, L. & KROEMER, G. 2011a. Mitochondria and the autophagy-inflammation-cell death axis in organismal aging. *Science,* 333, 1109-12.

GREEN, D. R., OBERST, A., DILLON, C. P., WEINLICH, R. & SALVESEN, G. S. 2011b. RIPK-dependent necrosis and its regulation by caspases: a mystery in five acts. *Mol Cell,* 44, 9-16.

GRUNERT, M., GOTTSCHALK, K., KAPAHNKE, J., GUNDISCH, S., KIESER, A. & JEREMIAS, I. 2012. The adaptor protein FADD and the initiator caspase-8 mediate activation of NF-kappaB by TRAIL. *Cell Death Dis,* 3, e414.

GÜNTHER, C., MARTINI, E., WITTKOPF, N., AMANN, K., WEIGMANN, B., NEUMANN, H., WALDNER, M. J., HEDRICK, S. M., TENZER, S., NEURATH, M. F. & BECKER, C. 2011. Caspase-8 regulates TNF-alpha-induced epithelial necroptosis and terminal ileitis. *Nature,* 477, 335-9.

GÜNTHER, C., NEUMANN, H., NEURATH, M. F. & BECKER, C. 2012. Apoptosis, necrosis and necroptosis: cell death regulation in the intestinal epithelium. *Gut*.

HALL, M. A. & CLEVELAND, J. L. 2007. Clearing the TRAIL for Cancer Therapy. *Cancer Cell,* 12, 4-6.

HALMOSI, R., BERENTE, Z., OSZ, E., TOTH, K., LITERATI-NAGY, P. & SUMEGI, B. 2001. Effect of poly(ADP-ribose) polymerase inhibitors on the ischemia-reperfusion-induced oxidative cell damage and mitochondrial metabolism in Langendorff heart perfusion system. *Mol Pharmacol,* 59, 1497-505.

HAMMEL, I., LAGUNOFF, D. & GALLI, S. J. 2010. Regulation of secretory granule size by the precise generation and fusion of unit granules. *J Cell Mol Med,* 14, 1904-16.

HAN, J., SRIDEVI, P., RAMIREZ, M., LUDWIG, K. J. & WANG, J. Y. 2013. beta-Catenin-dependent lysosomal targeting of internalized tumor necrosis factor-alpha suppresses caspase-8 activation in apoptosis-resistant colon cancer cells. *Mol Biol Cell,* 24, 465-73.

HAN, J., ZHONG, C. Q. & ZHANG, D. W. 2011. Programmed necrosis: backup to and competitor with apoptosis in the immune system. *Nat Immunol,* 12, 1143-9.

HANNUN, Y. A. & OBEID, L. M. 2011. Many ceramides. *J Biol Chem,* 286, 27855-62.

HANS, C. P., ZERFAOUI, M., NAURA, A. S., CATLING, A. & BOULARES, A. H. 2008. Differential effects of PARP inhibition on vascular cell survival and ACAT-1 expression favouring atherosclerotic plaque stability. *Cardiovasc Res,* 78, 429-39.

HAUBERT, D., GHARIB, N., RIVERO, F., WIEGMANN, K., HOSEL, M., KRONKE, M. & KASHKAR, H. 2007. PtdIns(4,5)P-restricted plasma membrane localization of FAN is involved in TNF-induced actin reorganization. *EMBO J,* 26, 3308-21.

HE, S., LIANG, Y., SHAO, F. & WANG, X. 2011. Toll-like receptors activate programmed necrosis in macrophages through a receptor-interacting kinase-3-mediated pathway. *Proc Natl Acad Sci U S A,* 108, 20054-9.

HEINRICH, M., NEUMEYER, J., JAKOB, M., HALLAS, C., TCHIKOV, V., WINOTO-MORBACH, S., WICKEL, M., SCHNEIDER-BRACHERT, W., TRAUZOLD, A., HETHKE, A. & SCHÜTZE, S. 2004. Cathepsin D links TNF-induced acid sphingomyelinase to Bid-mediated caspase-9 and -3 activation. *Cell Death Differ,* 11, 550-63.

HEINRICH, M., WICKEL, M., SCHNEIDER-BRACHERT, W., SANDBERG, C., GAHR, J., SCHWANDNER, R., WEBER, T., SAFTIG, P., PETERS, C., BRUNNER, J., KRONKE, M. & SCHÜTZE, S. 1999. Cathepsin D targeted by acid sphingomyelinase-derived ceramide. *EMBO J,* 18, 5252-63.

HENRY, B., MÖLLER, C., DIMANCHE-BOITREL, M. T., GULBINS, E. & BECKER, K. A. 2011. Targeting the ceramide system in cancer. *Cancer Lett*.

HITOMI, J., CHRISTOFFERSON, D. E., NG, A., YAO, J., DEGTEREV, A., XAVIER, R. J. & YUAN, J. 2008. Identification of a molecular signaling network that regulates a cellular necrotic cell death pathway. *Cell,* 135, 1311-23.

HO, C. Y., ALGHAMDI, T. A. & BOTELHO, R. J. 2012. Phosphatidylinositol-3,5-bisphosphate: no longer the poor PIP2. *Traffic,* 13, 1-8.

HOEHNA, Y., UCKERMANN, O., LUKSCH, H., STEFOVSKA, V., MARZAHN, J., THEIL, M., GORKIEWICZ, T., GAWLAK, M., WILCZYNSKI, G. M., KACZMAREK, L. & IKONOMIDOU, C. 2012. Matrix metalloproteinase 9 regulates cell death following pilocarpine-induced seizures in the developing brain. *Neurobiol Dis,* 48, 339-47.

HOLLER, N., ZARU, R., MICHEAU, O., THOME, M., ATTINGER, A., VALITUTTI, S., BODMER, J. L., SCHNEIDER, P., SEED, B. & TSCHOPP, J. 2000. Fas triggers an alternative, caspase-8-independent cell death pathway using the kinase RIP as effector molecule. *Nat Immunol,* 1, 489-95.

HONG, S. J., DAWSON, T. M. & DAWSON, V. L. 2004. Nuclear and mitochondrial conversations in cell death: PARP-1 and AIF signaling. *Trends Pharmacol Sci,* 25, 259-64.

HORINOUCHI, K., ERLICH, S., PERL, D. P., FERLINZ, K., BISGAIER, C. L., SANDHOFF, K., DESNICK, R. J., STEWART, C. L. & SCHUCHMAN, E. H. 1995. Acid sphingomyelinase deficient mice: a model of types A and B Niemann-Pick disease. *Nat Genet,* 10, 288-93.

HORRES, C. R. & HANNUN, Y. A. 2012. The roles of neutral sphingomyelinases in neurological pathologies. *Neurochem Res,* 37, 1137-49.

HUANG, Y. Y., LIU, H., LI, Y., PU, L. J., JIANG, C. C., XU, J. C. & JIANG, Z. W. 2013. Down-regulation of RIP1 by 2-Deoxy-D-glucose sensitizes breast cancer cells to TRAIL-induced apoptosis. *Eur J Pharmacol*.

HURST-KENNEDY, J., CHIN, L. S. & LI, L. 2012. Ubiquitin C-terminal hydrolase l1 in tumorigenesis. *Biochem Res Int,* 2012, 123706.

HWANG, S., MALONEY, N. S., BRUINSMA, M. W., GOEL, G., DUAN, E., ZHANG, L., SHRESTHA, B., DIAMOND, M. S., DANI, A., SOSNOVTSEV, S. V., GREEN, K. Y., LOPEZ-OTIN, C., XAVIER, R. J., THACKRAY, L. B. & VIRGIN, H. W. 2012. Nondegradative role of Atg5-Atg12/ Atg16L1 autophagy protein complex in antiviral activity of interferon gamma. *Cell Host Microbe,* 11, 397-409.

IRRINKI, K. M., MALLILANKARAMAN, K., THAPA, R. J., CHANDRAMOORTHY, H. C., SMITH, F. J., JOG, N. R., GANDHIRAJAN, R. K., KELSEN, S. G., HOUSER, S. R., MAY, M. J., BALACHANDRAN, S. & MADESH, M. 2011. Requirement of FADD, NEMO, and BAX/BAK for aberrant mitochondrial function in tumor necrosis factor alpha-induced necrosis. *Mol Cell Biol,* 31, 3745-58.

ITO, H., MURAKAMI, M., FURUHATA, A., GAO, S., YOSHIDA, K., SOBUE, S., HAGIWARA, K., TAKAGI, A., KOJIMA, T., SUZUKI, M., BANNO, Y., TANAKA, K., TAMIYA-KOIZUMI, K., KYOGASHIMA, M., NOZAWA, Y. & MURATE, T. 2009. Transcriptional regulation of neutral sphingomyelinase 2 gene expression of a human breast cancer cell line, MCF-7, induced by the anti-cancer drug, daunorubicin. *Biochim Biophys Acta,* 1789, 681-90.

JÄÄTTELÄ, M. & TSCHOPP, J. 2003. Caspase-independent cell death in T lymphocytes. *Nat Immunol,* 4, 416-23.

JANSSENS, S. & TINEL, A. 2012. The PIDDosome, DNA-damage-induced apoptosis and beyond. *Cell Death Differ,* 19, 13-20.

JEFFERIES, K. C., CIPRIANO, D. J. & FORGAC, M. 2008. Function, structure and regulation of the vacuolar (H+)-ATPases. *Arch Biochem Biophys,* 476, 33-42.

JENKINS, R. W., CANALS, D. & HANNUN, Y. A. 2009. Roles and regulation of secretory and lysosomal acid sphingomyelinase. *Cell Signal,* 21, 836-46.

JENKINS, R. W., CLARKE, C. J., CANALS, D., SNIDER, A. J., GAULT, C. R., HEFFERNAN-STROUD, L., WU, B. X., SIMBARI, F., RODDY, P., KITATANI, K., OBEID, L. M. & HANNUN, Y. A. 2011a. Regulation of CC ligand 5/RANTES by acid sphingomyelinase and acid ceramidase. *J Biol Chem,* 286, 13292-303.

JENKINS, R. W., IDKOWIAK-BALDYS, J., SIMBARI, F., CANALS, D., RODDY, P., RINER, C. D., CLARKE, C. J. & HANNUN, Y. A. 2011b. A novel mechanism of lysosomal acid sphingomyelinase maturation: requirement for carboxyl-terminal proteolytic processing. *J Biol Chem,* 286, 3777-88.

JIN, Z. & EL-DEIRY, W. S. 2006. Distinct signaling pathways in TRAIL- versus tumor necrosis factor-induced apoptosis. *Mol Cell Biol,* 26, 8136-48.

JITKAEW, S., TREBINSKA, A., GRZYBOWSKA, E., CARLSSON, G., NORDSTROM, A., LEHTIO, J., FROJMARK, A. S., DAHL, N. & FADEEL, B. 2009. N(alpha)-tosyl-L-phenylalanine chloromethyl ketone induces caspase-dependent apoptosis in transformed human B cell lines with transcriptional down-regulation of anti-apoptotic HS1-associated protein X-1. *J Biol Chem,* 284, 27827-37.

JOG, N. R., DINNALL, J. A., GALLUCCI, S., MADAIO, M. P. & CARICCHIO, R. 2009. Poly(ADP-ribose) polymerase-1 regulates the progression of autoimmune nephritis in males by inducing necrotic cell death and modulating inflammation. *J Immunol,* 182, 7297-306.

JOGL, G., SHEN, Y., GEBAUER, D., LI, J., WIEGMANN, K., KASHKAR, H., KRÖNKE, M. & TONG, L. 2002. Crystal structure of the BEACH domain reveals an unusual fold and extensive association with a novel PH domain. *EMBO J,* 21, 4785-95.

JOUAN-LANHOUET, S., ARSHAD, M. I., PIQUET-PELLORCE, C., MARTIN-CHOULY, C., LE MOIGNE-MULLER, G., VAN HERREWEGHE, F., TAKAHASHI, N., SERGENT, O., LAGADIC-GOSSMANN, D., VANDENABEELE, P., SAMSON, M. & DIMANCHE-BOITREL, M. T. 2012. TRAIL induces necroptosis involving RIPK1/RIPK3-dependent PARP-1 activation. *Cell Death Differ,* 19, 2003-14.

KABUTA, T., FURUTA, A., AOKI, S., FURUTA, K. & WADA, K. 2008. Aberrant interaction between Parkinson disease-associated mutant UCH-L1 and the lysosomal receptor for chaperone-mediated autophagy. *J Biol Chem,* 283, 23731-8.

KACZMAREK, A., VANDENABEELE, P. & KRYSKO, D. V. 2013. Necroptosis: the release of damage-associated molecular patterns and its physiological relevance. *Immunity,* 38, 209-23.

KAGAWA, K., NAKANO, A., MIKI, H., ODA, A., AMOU, H., TAKEUCHI, K., NAKAMURA, S., HARADA, T., FUJII, S., YATA, K., OZAKI, S., MATSUMOTO, T. & ABE, M. 2012. Inhibition of TACE activity enhances the susceptibility of myeloma cells to TRAIL. *PLoS One,* 7, e31594.

KAISER, W. J., UPTON, J. W., LONG, A. B., LIVINGSTON-ROSANOFF, D., DALEY-BAUER, L. P., HAKEM, R., CASPARY, T. & MOCARSKI, E. S. 2011. RIP3 mediates the embryonic lethality of caspase-8-deficient mice. *Nature,* 471, 368-72.

KAMEOKA, M., OTA, K., TETSUKA, T., TANAKA, Y., ITAYA, A., OKAMOTO, T. & YOSHIHARA, K. 2000. Evidence for regulation of NF-kappaB by poly(ADP-ribose) polymerase. *Biochem J,* 346 Pt 3, 641-9.

KAMPINGA, H. H. & CRAIG, E. A. 2010. The HSP70 chaperone machinery: J proteins as drivers of functional specificity. *Nat Rev Mol Cell Biol,* 11, 579-92.

KANG, T. B., YANG, S. H., TOTH, B., KOVALENKO, A. & WALLACH, D. 2013. Caspase-8 blocks kinase RIPK3-mediated activation of the NLRP3 inflammasome. *Immunity,* 38, 27-40.

KATAOKA, T. & TSCHOPP, J. 2004. N-terminal fragment of c-FLIP(L) processed by caspase 8 specifically interacts with TRAF2 and induces activation of the NF-kappaB signaling pathway. *Mol Cell Biol,* 24, 2627-36.

KELLENBERGER, S. & SCHILD, L. 2002. Epithelial sodium channel/degenerin family of ion channels: a variety of functions for a shared structure. *Physiol Rev,* 82, 735-67.

KELLIHER, M. A., GRIMM, S., ISHIDA, Y., KUO, F., STANGER, B. Z. & LEDER, P. 1998. The death domain kinase RIP mediates the TNF-induced NF-kappaB signal. *Immunity,* 8, 297-303.

KEPP, O., GALLUZZI, L., LIPINSKI, M., YUAN, J. & KROEMER, G. 2011. Cell death assays for drug discovery. *Nat Rev Drug Discov,* 10, 221-37.

KIM, S. O. & HAN, J. 2001. Pan-caspase inhibitor zVAD enhances cell death in RAW246.7 macrophages. *J Endotoxin Res,* 7, 292-6.

KIM, W. H., CHOI, C. H., KANG, S. K., KWON, C. H. & KIM, Y. K. 2005. Ceramide induces non-apoptotic cell death in human glioma cells. *Neurochem Res,* 30, 969-79.

KING, M. A., HALICKA, H. D. & DARZYNKIEWICZ, Z. 2004. Pro- and anti-apoptotic effects of an inhibitor of chymotrypsin-like serine proteases. *Cell Cycle,* 3, 1566-71.

KIRKEGAARD, T., ROTH, A. G., PETERSEN, N. H., MAHALKA, A. K., OLSEN, O. D., MOILANEN, I., ZYLICZ, A., KNUDSEN, J., SANDHOFF, K., ARENZ, C., KINNUNEN, P. K., NYLANDSTED, J. & JÄÄTTELÄ, M. 2010. Hsp70 stabilizes lysosomes and reverts Niemann-Pick disease-associated lysosomal pathology. *Nature,* 463, 549-53.

KOH, D. W., LAWLER, A. M., POITRAS, M. F., SASAKI, M., WATTLER, S., NEHLS, M. C., STOGER, T., POIRIER, G. G., DAWSON, V. L. & DAWSON, T. M. 2004. Failure to degrade poly(ADP-ribose) causes increased sensitivity to cytotoxicity and early embryonic lethality. *Proc Natl Acad Sci U S A,* 101, 17699-704.

KOH, S. H., CHANG, D. I., KIM, H. T., KIM, J., KIM, M. H., KIM, K. S., BAE, I., KIM, H., KIM, D. W. & KIM, S. H. 2005. Effect of 3-aminobenzamide, PARP inhibitor, on matrix metalloproteinase-9 level in plasma and brain of ischemic stroke model. *Toxicology,* 214, 131-9.

KOHLHAAS, S. L., CRAXTON, A., SUN, X. M., PINKOSKI, M. J. & COHEN, G. M. 2007. Receptor-mediated endocytosis is not required for tumor necrosis factor-related apoptosis-inducing ligand (TRAIL)-induced apoptosis. *J Biol Chem,* 282, 12831-41.

KOLESNICK, R. & FUKS, Z. 2003. Radiation and ceramide-induced apoptosis. *Oncogene,* 22, 5897-906.

KOMISSAROVA, E. V. & ROSSMAN, T. G. 2010. Arsenite induced poly(ADP-ribosyl)ation of tumor suppressor P53 in human skin keratinocytes as a possible mechanism for carcinogenesis associated with arsenic exposure. *Toxicol Appl Pharmacol,* 243, 399-404.

KORNHUBER, J., TRIPAL, P., REICHEL, M., MUHLE, C., RHEIN, C., MUEHLBACHER, M., GROEMER, T. W. & GULBINS, E. 2010. Functional Inhibitors of Acid Sphingomyelinase (FIASMAs): a novel pharmacological group of drugs with broad clinical applications. *Cell Physiol Biochem,* 26, 9-20.

KORNHUBER, J., TRIPAL, P., REICHEL, M., TERFLOTH, L., BLEICH, S., WILTFANG, J. & GULBINS, E. 2008. Identification of new functional inhibitors of acid sphingomyelinase using a structure-property-activity relation model. *J Med Chem,* 51, 219-37.

KOVALENKO, A., KIM, J. C., KANG, T. B., RAJPUT, A., BOGDANOV, K., DITTRICH-BREIHOLZ, O., KRACHT, M., BRENNER, O. & WALLACH, D. 2009. Caspase-8 deficiency in epidermal keratinocytes triggers an inflammatory skin disease. *J Exp Med,* 206, 2161-77.

KRAUSS, M. & HAUCKE, V. 2007. Phosphoinositide-metabolizing enzymes at the interface between membrane traffic and cell signalling. *EMBO Rep,* 8, 241-6.

KREDER, D., KRUT, O., ADAM-KLAGES, S., WIEGMANN, K., SCHERER, G., PLITZ, T., JENSEN, J. M., PROKSCH, E., STEINMANN, J., PFEFFER, K. & KRONKE, M. 1999. Impaired neutral sphingomyelinase activation and cutaneous barrier repair in FAN-deficient mice. *EMBO J,* 18, 2472-9.

KROEMER, G. & MARTIN, S. J. 2005. Caspase-independent cell death. *Nat Med,* 11, 725-30.

KUMA, A., HATANO, M., MATSUI, M., YAMAMOTO, A., NAKAYA, H., YOSHIMORI, T., OHSUMI, Y., TOKUHISA, T. & MIZUSHIMA, N. 2004. The role of autophagy during the early neonatal starvation period. *Nature,* 432, 1032-6.

KUMAGAI, T., ISHINO, T. & NAKAGAWA, Y. 2012. Acidic sphingomyelinase induced by electrophiles promotes proinflammatory cytokine production in human bladder carcinoma ECV-304 cells. *Arch Biochem Biophys,* 519, 8-16.

KUNINAKA, S., NOMURA, M., HIROTA, T., IIDA, S., HARA, T., HONDA, S., KUNITOKU, N., SASAYAMA, T., ARIMA, Y., MARUMOTO, T., KOJA, K., YONEHARA, S. & SAYA, H. 2005. The tumor suppressor WARTS activates the Omi / HtrA2-dependent pathway of cell death. *Oncogene,* 24, 5287-98.

KYPRI, E., FALKENSTEIN, K. & DE LOZANNE, A. 2013. Antagonistic Control of Lysosomal Fusion by Rab14 and the Lyst-Related Protein LvsB. *Traffic*.

LAFOURCADE, C., SOBO, K., KIEFFER-JAQUINOD, S., GARIN, J. & VAN DER GOOT, F. G. 2008. Regulation of the V-ATPase along the endocytic pathway occurs

through reversible subunit association and membrane localization. *PLoS One,* 3, e2758.

LAI, Y., CHEN, Y., WATKINS, S. C., NATHANIEL, P. D., GUO, F., KOCHANEK, P. M., JENKINS, L. W., SZABO, C. & CLARK, R. S. 2008. Identification of poly-ADP-ribosylated mitochondrial proteins after traumatic brain injury. *J Neurochem,* 104, 1700-11.

LAU, A., WANG, X. J., ZHAO, F., VILLENEUVE, N. F., WU, T., JIANG, T., SUN, Z., WHITE, E. & ZHANG, D. D. 2010. A noncanonical mechanism of Nrf2 activation by autophagy deficiency: direct interaction between Keap1 and p62. *Mol Cell Biol,* 30, 3275-85.

LAULEDERKIND, S. J., BIELAWSKA, A., RAGHOW, R., HANNUN, Y. A. & BALLOU, L. R. 1995. Ceramide induces interleukin 6 gene expression in human fibroblasts. *J Exp Med,* 182, 599-604.

LEIST, M. & JÄÄTTELÄ, M. 2001. Four deaths and a funeral: from caspases to alternative mechanisms. *Nat Rev Mol Cell Biol,* 2, 589-98.

LEPINE, S., ALLEGOOD, J. C., EDMONDS, Y., MILSTIEN, S. & SPIEGEL, S. 2011. Autophagy induced by deficiency of sphingosine-1-phosphate phosphohydrolase 1 is switched to apoptosis by calpain-mediated autophagy-related gene 5 (Atg5) cleavage. *J Biol Chem,* 286, 44380-90.

LEWIS, J., DEVIN, A., MILLER, A., LIN, Y., RODRIGUEZ, Y., NECKERS, L. & LIU, Z. G. 2000. Disruption of hsp90 function results in degradation of the death domain kinase, receptor-interacting protein (RIP), and blockage of tumor necrosis factor-induced nuclear factor-kappaB activation. *J Biol Chem,* 275, 10519-26.

LI, J., MCQUADE, T., SIEMER, A. B., NAPETSCHNIG, J., MORIWAKI, K., HSIAO, Y. S., DAMKO, E., MOQUIN, D., WALZ, T., MCDERMOTT, A., CHAN, F. K. & WU, H. 2012. The RIP1/RIP3 necrosome forms a functional amyloid signaling complex required for programmed necrosis. *Cell,* 150, 339-50.

LIN, J. F., LIN, Y. C., LIN, Y. H., TSAI, T. F., CHOU, K. Y., CHEN, H. E. & HWANG, T. I. 2011. Zoledronic acid induces autophagic cell death in human prostate cancer cells. *J Urol,* 185, 1490-6.

LIN, Y., DEVIN, A., RODRIGUEZ, Y. & LIU, Z. G. 1999. Cleavage of the death domain kinase RIP by caspase-8 prompts TNF-induced apoptosis. *Genes Dev,* 13, 2514-26.

LIPINSKI, M. M., HOFFMAN, G., NG, A., ZHOU, W., PY, B. F., HSU, E., LIU, X., EISENBERG, J., LIU, J., BLENIS, J., XAVIER, R. J. & YUAN, J. 2010. A genome-wide siRNA screen reveals multiple mTORC1 independent signaling pathways regulating autophagy under normal nutritional conditions. *Dev Cell,* 18, 1041-52.

LISTER, M. D., RUAN, Z. S. & BITTMAN, R. 1995. Interaction of sphingomyelinase with sphingomyelin analogs modified at the C-1 and C-3 positions of the sphingosine backbone. *Biochim Biophys Acta,* 1256, 25-30.

LIU, Y., FALLON, L., LASHUEL, H. A., LIU, Z. & LANSBURY, P. T., JR. 2002. The UCH-L1 gene encodes two opposing enzymatic activities that affect alpha-synuclein degradation and Parkinson's disease susceptibility. *Cell,* 111, 209-18.

LIU, Y., LASHUEL, H. A., CHOI, S., XING, X., CASE, A., NI, J., YEH, L. A., CUNY, G. D., STEIN, R. L. & LANSBURY, P. T., JR. 2003. Discovery of inhibitors that elucidate the role of UCH-L1 activity in the H1299 lung cancer cell line. *Chem Biol,* 10, 837-46.

LONG, J. S. & RYAN, K. M. 2012. New frontiers in promoting tumour cell death: targeting apoptosis, necroptosis and autophagy. *Oncogene,* 31, 5045-60.

LOS, M., MOZOLUK, M., FERRARI, D., STEPCZYNSKA, A., STROH, C., RENZ, A., HERCEG, Z., WANG, Z. Q. & SCHULZE-OSTHOFF, K. 2002. Activation and

caspase-mediated inhibition of PARP: a molecular switch between fibroblast necrosis and apoptosis in death receptor signaling. *Mol Biol Cell,* 13, 978-88.

LU, J. V., WEIST, B. M., VAN RAAM, B. J., MARRO, B. S., NGUYEN, L. V., SRINIVAS, P., BELL, B. D., LUHRS, K. A., LANE, T. E., SALVESEN, G. S. & WALSH, C. M. 2011. Complementary roles of Fas-associated death domain (FADD) and receptor interacting protein kinase-3 (RIPK3) in T-cell homeostasis and antiviral immunity. *Proc Natl Acad Sci U S A,* 108, 15312-7.

LUBERTO, C., HASSLER, D. F., SIGNORELLI, P., OKAMOTO, Y., SAWAI, H., BOROS, E., HAZEN-MARTIN, D. J., OBEID, L. M., HANNUN, Y. A. & SMITH, G. K. 2002. Inhibition of tumor necrosis factor-induced cell death in MCF7 by a novel inhibitor of neutral sphingomyelinase. *J Biol Chem,* 277, 41128-39.

LUEDDE M., LUTZ M., CARTER N., VUCUR M., JACOBY C., FLÖGEL U., KLEIN T., TOLBA R., REISINGER F., SOSNA J., HIPPE H-J., LINKERMANN A., CHALARIS A., ROSE-JOHN S., ADAM D., LUEDDE T., HEIKENWAELDER M. & N., F. 2013. RIP3 mediates inflammation and adverse remodeling after myocardial infarction. *Circulation Research,* submitted for publication.

LUO, X. & KRAUS, W. L. 2012. On PAR with PARP: cellular stress signaling through poly(ADP-ribose) and PARP-1. *Genes Dev,* 26, 417-32.

MA, Y. G., LIU, W. C., DONG, S., DU, C., WANG, X. J., LI, J. S., XIE, X. P., WU, L., MA, D. C., YU, Z. B. & XIE, M. J. 2012. Activation of BK(Ca) channels in zoledronic acid-induced apoptosis of MDA-MB-231 breast cancer cells. *PLoS One,* 7, e37451.

MACEWAN, D. J. 2002. TNF ligands and receptors--a matter of life and death. *Br J Pharmacol,* 135, 855-75.

MADISON, D. L., STAUFFER, D. & LUNDBLAD, J. R. 2011. The PARP inhibitor PJ34 causes a PARP1-independent, p21 dependent mitotic arrest. *DNA Repair (Amst),* 10, 1003-13.

MAIURI, M. C., ZALCKVAR, E., KIMCHI, A. & KROEMER, G. 2007. Self-eating and self-killing: crosstalk between autophagy and apoptosis. *Nat Rev Mol Cell Biol,* 8, 741-52.

MARTINEZ, T. N., CHEN, X., BANDYOPADHYAY, S., MERRILL, A. H. & TANSEY, M. G. 2012. Ceramide sphingolipid signaling mediates Tumor Necrosis Factor (TNF)-dependent toxicity via caspase signaling in dopaminergic neurons. *Mol Neurodegener,* 7, 45.

MARTINS, L. M., IACCARINO, I., TENEV, T., GSCHMEISSNER, S., TOTTY, N. F., LEMOINE, N. R., SAVOPOULOS, J., GRAY, C. W., CREASY, C. L., DINGWALL, C. & DOWNWARD, J. 2002. The serine protease Omi/HtrA2 regulates apoptosis by binding XIAP through a reaper-like motif. *J Biol Chem,* 277, 439-44.

MARTINS, L. M., MORRISON, A., KLUPSCH, K., FEDELE, V., MOISOI, N., TEISMANN, P., ABUIN, A., GRAU, E., GEPPERT, M., LIVI, G. P., CREASY, C. L., MARTIN, A., HARGREAVES, I., HEALES, S. J., OKADA, H., BRANDNER, S., SCHULZ, J. B., MAK, T. & DOWNWARD, J. 2004. Neuroprotective role of the Reaper-related serine protease HtrA2/Omi revealed by targeted deletion in mice. *Mol Cell Biol,* 24, 9848-62.

MCCOMB, S., CHEUNG, H. H., KORNELUK, R. G., WANG, S., KRISHNAN, L. & SAD, S. 2012. cIAP1 and cIAP2 limit macrophage necroptosis by inhibiting Rip1 and Rip3 activation. *Cell Death Differ,* 19, 1791-801.

MCCORMICK, A. L. 2008. Control of apoptosis by human cytomegalovirus. *Curr Top Microbiol Immunol,* 325, 281-95.

MCCORMICK, A. L., ROBACK, L. & MOCARSKI, E. S. 2008. HtrA2/Omi terminates cytomegalovirus infection and is controlled by the viral mitochondrial inhibitor of apoptosis (vMIA). *PLoS Pathog,* 4, e1000063.

MCNAMARA, C. R., AHUJA, R., OSAFO-ADDO, A. D., BARROWS, D., KETTENBACH, A., SKIDAN, I., TENG, X., CUNY, G. D., GERBER, S. & DEGTEREV, A. 2013. Akt Regulates TNFalpha synthesis downstream of RIP1 kinase activation during necroptosis. *PLoS One,* 8, e56576.

MENCARELLI, C. & MARTINEZ-MARTINEZ, P. 2013. Ceramide function in the brain: when a slight tilt is enough. *Cell Mol Life Sci,* 70, 181-203.

MERAY, R. K. & LANSBURY, P. T., JR. 2007. Reversible monoubiquitination regulates the Parkinson disease-associated ubiquitin hydrolase UCH-L1. *J Biol Chem,* 282, 10567-75.

MERMERIAN, A. H., CASE, A., STEIN, R. L. & CUNY, G. D. 2007. Structure-activity relationship, kinetic mechanism, and selectivity for a new class of ubiquitin C-terminal hydrolase-L1 (UCH-L1) inhibitors. *Bioorg Med Chem Lett,* 17, 3729-32.

MEURETTE, O., REBILLARD, A., HUC, L., LE MOIGNE, G., MERINO, D., MICHEAU, O., LAGADIC-GOSSMANN, D. & DIMANCHE-BOITREL, M. T. 2007. TRAIL induces receptor-interacting protein 1-dependent and caspase-dependent necrosis-like cell death under acidic extracellular conditions. *Cancer Res,* 67, 218-26.

MIELKE, M. M., BANDARU, V. V., HAUGHEY, N. J., XIA, J., FRIED, L. P., YASAR, S., ALBERT, M., VARMA, V., HARRIS, G., SCHNEIDER, E. B., RABINS, P. V., BANDEEN-ROCHE, K., LYKETSOS, C. G. & CARLSON, M. C. 2012. Serum ceramides increase the risk of Alzheimer disease: the Women's Health and Aging Study II. *Neurology,* 79, 633-41.

MITROFAN, L. M., CASTELLS, F. B., PELKONEN, J. & MONKKONEN, J. 2010. Lysosomal-mitochondrial axis in zoledronic acid-induced apoptosis in human follicular lymphoma cells. *J Biol Chem,* 285, 1967-79.

MIZUSHIMA, N., KOHSAKA, H. & MIYASAKA, N. 1998. Ceramide, a mediator of interleukin 1, tumour necrosis factor alpha, as well as Fas receptor signalling, induces apoptosis of rheumatoid arthritis synovial cells. *Ann Rheum Dis,* 57, 495-9.

MIZUSHIMA, N., YAMAMOTO, A., HATANO, M., KOBAYASHI, Y., KABEYA, Y., SUZUKI, K., TOKUHISA, T., OHSUMI, Y. & YOSHIMORI, T. 2001. Dissection of autophagosome formation using Apg5-deficient mouse embryonic stem cells. *J Cell Biol,* 152, 657-68.

MIZUSHIMA, N., YOSHIMORI, T. & LEVINE, B. 2010. Methods in mammalian autophagy research. *Cell,* 140, 313-26.

MLEJNEK, P. 2005. Can application of serine protease inhibitors TPCK and TLCK provide evidence for possible involvement of serine protease Omi/HtrA2 in imatinib mesylate-induced cell death of BCR-ABL-positive human leukemia cells? *Leukemia,* 19, 1085-7.

MOCARSKI, E. S., UPTON, J. W. & KAISER, W. J. 2012. Viral infection and the evolution of caspase 8-regulated apoptotic and necrotic death pathways. *Nat Rev Immunol,* 12, 79-88.

MÖHLIG, H., MATHIEU, S., THON, L., FREDERIKSEN, M. C., WARD, D. M., KAPLAN, J., SCHÜTZE, S., KABELITZ, D. & ADAM, D. 2007. The WD repeat protein FAN regulates lysosome size independent from abnormal downregulation/membrane recruitment of protein kinase C. *Exp Cell Res,* 313, 2703-18.

MONTFORT, A., DE BADTS, B., DOUIN-ECHINARD, V., MARTIN, P. G., IACOVONI, J., NEVOIT, C., THERVILLE, N., GARCIA, V., BERTRAND, M. A., BESSIERES, M. H., TROMBE, M. C., LEVADE, T., BENOIST, H. & SEGUI, B. 2009. FAN stimulates TNF(alpha)-induced gene expression, leukocyte recruitment, and humoral response. *J Immunol,* 183, 5369-78.

MONTFORT, A., MARTIN, P. G., LEVADE, T., BENOIST, H. & SEGUI, B. 2010. FAN (factor associated with neutral sphingomyelinase activation), a moonlighting protein in TNF-R1 signaling. *J Leukoc Biol,* 88, 897-903.

MOQUIN, D. & CHAN, F. K. 2010. The molecular regulation of programmed necrotic cell injury. *Trends Biochem Sci,* 35, 434-41.

MORAD, S. A. & CABOT, M. C. 2013. Ceramide-orchestrated signalling in cancer cells. *Nat Rev Cancer,* 13, 51-65.

MORINAGA, Y., YANAGIHARA, K., NAKAMURA, S., HASEGAWA, H., SEKI, M., IZUMIKAWA, K., KAKEYA, H., YAMAMOTO, Y., YAMADA, Y., KOHNO, S. & KAMIHIRA, S. 2010. Legionella pneumophila induces cathepsin B-dependent necrotic cell death with releasing high mobility group box1 in macrophages. *Respir Res,* 11, 158.

MOUBARAK, R. S., YUSTE, V. J., ARTUS, C., BOUHARROUR, A., GREER, P. A., MENISSIER-DE MURCIA, J. & SUSIN, S. A. 2007. Sequential activation of poly(ADP-ribose) polymerase 1, calpains, and Bax is essential in apoptosis-inducing factor-mediated programmed necrosis. *Mol Cell Biol,* 27, 4844-62.

MOUJALLED, D. M., COOK, W. D., OKAMOTO, T., MURPHY, J., LAWLOR, K. E., VINCE, J. E. & VAUX, D. L. 2013. TNF can activate RIPK3 and cause programmed necrosis in the absence of RIPK1. *Cell Death Dis,* 4, e465.

MUNOZ-GAMEZ, J. A., RODRIGUEZ-VARGAS, J. M., QUILES-PEREZ, R., AGUILAR-QUESADA, R., MARTIN-OLIVA, D., DE MURCIA, G., MENISSIER DE MURCIA, J., ALMENDROS, A., RUIZ DE ALMODOVAR, M. & OLIVER, F. J. 2009. PARP-1 is involved in autophagy induced by DNA damage. *Autophagy,* 5, 61-74.

MYEKU, N. & FIGUEIREDO-PEREIRA, M. E. 2011. Dynamics of the degradation of ubiquitinated proteins by proteasomes and autophagy: association with sequestosome 1/p62. *J Biol Chem,* 286, 22426-40.

NARAYAN, N., LEE, I. H., BORENSTEIN, R., SUN, J., WONG, R., TONG, G., FERGUSSON, M. M., LIU, J., ROVIRA, II, CHENG, H. L., WANG, G., GUCEK, M., LOMBARD, D., ALT, F. W., SACK, M. N., MURPHY, E., CAO, L. & FINKEL, T. 2012. The NAD-dependent deacetylase SIRT2 is required for programmed necrosis. *Nature,* 492, 199-204.

NASRABADY, S. E., KUZHANDAIVEL, A., AKRAMI, A., BIANCHETTI, E., MILANESE, M., BONANNO, G. & NISTRI, A. 2012. Unusual increase in lumbar network excitability of the rat spinal cord evoked by the PARP-1 inhibitor PJ-34 through inhibition of glutamate uptake. *Neuropharmacology,* 63, 415-26.

NEUMANN, S., BIDON, T., BRANSCHADEL, M., KRIPPNER-HEIDENREICH, A., SCHEURICH, P. & DOSZCZAK, M. 2012. The transmembrane domains of TNF-related apoptosis-inducing ligand (TRAIL) receptors 1 and 2 co-regulate apoptotic signaling capacity. *PLoS One,* 7, e42526.

NEUMEYER, J., HALLAS, C., MERKEL, O., WINOTO-MORBACH, S., JAKOB, M., THON, L., ADAM, D., SCHNEIDER-BRACHERT, W. & SCHÜTZE, S. 2006. TNF-receptor I defective in internalization allows for cell death through activation of neutral sphingomyelinase. *Exp Cell Res,* 312, 2142-53.

NEWTON, K., SUN, X. & DIXIT, V. M. 2004. Kinase RIP3 is dispensable for normal NF-kappa Bs, signaling by the B-cell and T-cell receptors, tumor necrosis factor receptor 1, and Toll-like receptors 2 and 4. *Mol Cell Biol,* 24, 1464-9.

NIN, V., ESCANDE, C., CHINI, C. C., GIRI, S., CAMACHO-PEREIRA, J., MATALONGA, J., LOU, Z. & CHINI, E. N. 2012. Role of deleted in breast cancer 1 (DBC1) protein in SIRT1 deacetylase activation induced by protein kinase A and AMP-activated protein kinase. *J Biol Chem,* 287, 23489-501.

O'BRIEN, N. W., GELLINGS, N. M., GUO, M., BARLOW, S. B., GLEMBOTSKI, C. C. & SABBADINI, R. A. 2003. Factor associated with neutral sphingomyelinase activation and its role in cardiac cell death. *Circ Res,* 92, 589-91.

O'DONNELL, M. A., PEREZ-JIMENEZ, E., OBERST, A., NG, A., MASSOUMI, R., XAVIER, R., GREEN, D. R. & TING, A. T. 2011. Caspase 8 inhibits programmed necrosis by processing CYLD. *Nat Cell Biol,* 13, 1437-42.

OBERST, A., DILLON, C. P., WEINLICH, R., MCCORMICK, L. L., FITZGERALD, P., POP, C., HAKEM, R., SALVESEN, G. S. & GREEN, D. R. 2011. Catalytic activity of the caspase-8-FLIP(L) complex inhibits RIPK3-dependent necrosis. *Nature,* 471, 363-7.

OKADA, M., ADACHI, S., IMAI, T., WATANABE, K., TOYOKUNI, S. Y., UENO, M., ZERVOS, A. S., KROEMER, G. & NAKAHATA, T. 2004. A novel mechanism for imatinib mesylate-induced cell death of BCR-ABL-positive human leukemic cells: caspase-independent, necrosis-like programmed cell death mediated by serine protease activity. *Blood,* 103, 2299-307.

OKINAGA, T., KASAI, H., TSUJISAWA, T. & NISHIHARA, T. 2007. Role of caspases in cleavage of lamin A/C and PARP during apoptosis in macrophages infected with a periodontopathic bacterium. *J Med Microbiol,* 56, 1399-404.

OLIVER, F. J., DE LA RUBIA, G., ROLLI, V., RUIZ-RUIZ, M. C., DE MURCIA, G. & MURCIA, J. M. 1998. Importance of poly(ADP-ribose) polymerase and its cleavage in apoptosis. Lesson from an uncleavable mutant. *J Biol Chem,* 273, 33533-9.

OSBORN, S. L., DIEHL, G., HAN, S. J., XUE, L., KURD, N., HSIEH, K., CADO, D., ROBEY, E. A. & WINOTO, A. 2010. Fas-associated death domain (FADD) is a negative regulator of T-cell receptor-mediated necroptosis. *Proc Natl Acad Sci U S A,* 107, 13034-9.

PARK, D. W., NAM, M. K. & RHIM, H. 2011. The serine protease HtrA2 cleaves UCH-L1 and inhibits its hydrolase activity: implication in the UCH-L1-mediated cell death. *Biochem Biophys Res Commun,* 415, 24-9.

PARK, S. J., SOHN, H. Y., YOON, J. & PARK, S. I. 2009. Down-regulation of FoxO-dependent c-FLIP expression mediates TRAIL-induced apoptosis in activated hepatic stellate cells. *Cell Signal,* 21, 1495-503.

PERROTTA, C., BIZZOZERO, L., CAZZATO, D., MORLACCHI, S., ASSI, E., SIMBARI, F., ZHANG, Y., GULBINS, E., BASSI, M. T., ROSA, P. & CLEMENTI, E. 2010. Syntaxin 4 is required for acid sphingomyelinase activity and apoptotic function. *J Biol Chem,* 285, 40240-51.

PERRY, R. J. & RIDGWAY, N. D. 2005. Molecular mechanisms and regulation of ceramide transport. *Biochim Biophys Acta,* 1734, 220-34.

PHILIPP, S., PUCHERT, M., ADAM-KLAGES, S., TCHIKOV, V., WINOTO-MORBACH, S., MATHIEU, S., DEERBERG, A., KOLKER, L., MARCHESINI, N., KABELITZ, D., HANNUN, Y. A., SCHÜTZE, S. & ADAM, D. 2010. The Polycomb group protein EED couples TNF receptor 1 to neutral sphingomyelinase. *Proc Natl Acad Sci U S A,* 107, 1112-7.

PHULWANI, N. K. & KIELIAN, T. 2008. Poly (ADP-ribose) polymerases (PARPs) 1-3 regulate astrocyte activation. *J Neurochem,* 106, 578-90.

POBEZINSKAYA, Y. L., KIM, Y. S., CHOKSI, S., MORGAN, M. J., LI, T., LIU, C. & LIU, Z. 2008. The function of TRADD in signaling through tumor necrosis factor receptor 1 and TRIF-dependent Toll-like receptors. *Nat Immunol,* 9, 1047-54.

POP, C., OBERST, A., DRAG, M., VAN RAAM, B. J., RIEDL, S. J., GREEN, D. R. & SALVESEN, G. S. 2011. FLIP(L) induces caspase 8 activity in the absence of interdomain caspase 8 cleavage and alters substrate specificity. *Biochem J,* 433, 447-57.

POUESSEL, D. & CULINE, S. 2012. Complete clinical and biological response to zoledronic acid in castrate-resistant prostate cancer metastatic to bone. *Anticancer Drugs,* 23, 141-2.

PUTT, K. S., BEILMAN, G. J. & HERGENROTHER, P. J. 2005. Direct quantitation of poly(ADP-ribose) polymerase (PARP) activity as a means to distinguish necrotic and apoptotic death in cell and tissue samples. *Chembiochem,* 6, 53-5.

PYO, J. O., JANG, M. H., KWON, Y. K., LEE, H. J., JUN, J. I., WOO, H. N., CHO, D. H., CHOI, B., LEE, H., KIM, J. H., MIZUSHIMA, N., OSHUMI, Y. & JUNG, Y. K. 2005. Essential roles of Atg5 and FADD in autophagic cell death: dissection of autophagic cell death into vacuole formation and cell death. *J Biol Chem,* 280, 20722-9.

QIN, J. & DAWSON, G. 2012. Evidence for coordination of lysosomal (ASMase) and plasma membrane (NSMase2) forms of sphingomyelinase from mutant mice. *FEBS Lett,* 586, 4002-9.

RACHNER, T. D., SINGH, S. K., SCHOPPET, M., BENAD, P., BORNHAUSER, M., ELLENRIEDER, V., EBERT, R., JAKOB, F. & HOFBAUER, L. C. 2010. Zoledronic acid induces apoptosis and changes the TRAIL/OPG ratio in breast cancer cells. *Cancer Lett,* 287, 109-16.

RADKE, S., CHANDER, H., SCHAFER, P., MEISS, G., KRUGER, R., SCHULZ, J. B. & GERMAIN, D. 2008. Mitochondrial protein quality control by the proteasome involves ubiquitination and the protease Omi. *J Biol Chem,* 283, 12681-5.

RAVIKUMAR, B., MOREAU, K., JAHREISS, L., PURI, C. & RUBINSZTEIN, D. C. 2010. Plasma membrane contributes to the formation of pre-autophagosomal structures. *Nat Cell Biol,* 12, 747-57.

REYES, J. G., ROBAYNA, I. G., DELGADO, P. S., GONZALEZ, I. H., AGUIAR, J. Q., ROSAS, F. E., FANJUL, L. F. & GALARRETA, C. M. 1996. c-Jun is a downstream target for ceramide-activated protein phosphatase in A431 cells. *J Biol Chem,* 271, 21375-80.

REYNOLDS, C. P., MAURER, B. J. & KOLESNICK, R. N. 2004. Ceramide synthesis and metabolism as a target for cancer therapy. *Cancer Lett,* 206, 169-80.

RIGANTI, C., CASTELLA, B., KOPECKA, J., CAMPIA, I., COSCIA, M., PESCARMONA, G., BOSIA, A., GHIGO, D. & MASSAIA, M. 2013. Zoledronic acid restores doxorubicin chemosensitivity and immunogenic cell death in multidrug-resistant human cancer cells. *PLoS One,* 8, e60975.

ROSENFELDT, M. T. & RYAN, K. M. 2011. The multiple roles of autophagy in cancer. *Carcinogenesis,* 32, 955-63.

ROTH, A. G., DRESCHER, D., YANG, Y., REDMER, S., UHLIG, S. & ARENZ, C. 2009a. Potent and selective inhibition of acid sphingomyelinase by bisphosphonates. *Angew Chem Int Ed Engl,* 48, 7560-3.

ROTH, A. G., REDMER, S. & ARENZ, C. 2009b. Potent inhibition of acid sphingomyelinase by phosphoinositide analogues. *Chembiochem,* 10, 2367-74.

ROTH, A. G., REDMER, S. & ARENZ, C. 2010. Development of carbohydrate-derived inhibitors of acid sphingomyelinase. *Bioorg Med Chem,* 18, 939-44.

SABROE, I., READ, R. C., WHYTE, M. K., DOCKRELL, D. H., VOGEL, S. N. & DOWER, S. K. 2003. Toll-like receptors in health and disease: complex questions remain. *J Immunol,* 171, 1630-5.

SAIF, M. W. 2006. Anti-angiogenesis therapy in pancreatic carcinoma. *JOP,* 7, 163-73.

SAITOH, T., FUJITA, N., JANG, M. H., UEMATSU, S., YANG, B. G., SATOH, T., OMORI, H., NODA, T., YAMAMOTO, N., KOMATSU, M., TANAKA, K., KAWAI, T., TSUJIMURA, T., TAKEUCHI, O., YOSHIMORI, T. & AKIRA, S.

2008. Loss of the autophagy protein Atg16L1 enhances endotoxin-induced IL-1beta production. *Nature,* 456, 264-8.

SAMADI, A. 2007. Ceramide-induced cell death in lens epithelial cells. *Mol Vis,* 13, 1618-26.

SCHENCK, M., CARPINTEIRO, A., GRASSME, H., LANG, F. & GULBINS, E. 2007. Ceramide: physiological and pathophysiological aspects. *Arch Biochem Biophys,* 462, 171-5.

SCHNEIDER-BRACHERT, W., TCHIKOV, V., NEUMEYER, J., JAKOB, M., WINOTO-MORBACH, S., HELD-FEINDT, J., HEINRICH, M., MERKEL, O., EHRENSCHWENDER, M., ADAM, D., MENTLEIN, R., KABELITZ, D. & SCHUTZE, S. 2004. Compartmentalization of TNF receptor 1 signaling: internalized TNF receptosomes as death signaling vesicles. *Immunity,* 21, 415-28.

SCHNEIDER-POETSCH, T., JU, J., EYLER, D. E., DANG, Y., BHAT, S., MERRICK, W. C., GREEN, R., SHEN, B. & LIU, J. O. 2010. Inhibition of eukaryotic translation elongation by cycloheximide and lactimidomycin. *Nat Chem Biol,* 6, 209-217.

SCHRADER, K., HUAI, J., JOCKEL, L., OBERLE, C. & BORNER, C. 2010. Non-caspase proteases: triggers or amplifiers of apoptosis? *Cell Mol Life Sci,* 67, 1607-18.

SCHUCHMAN, E. H. 2010. Acid sphingomyelinase, cell membranes and human disease: lessons from Niemann-Pick disease. *FEBS Lett,* 584, 1895-900.

SEGUI, B., ANDRIEU-ABADIE, N., ADAM-KLAGES, S., MEILHAC, O., KREDER, D., GARCIA, V., BRUNO, A. P., JAFFREZOU, J. P., SALVAYRE, R., KRONKE, M. & LEVADE, T. 1999. CD40 signals apoptosis through FAN-regulated activation of the sphingomyelin-ceramide pathway. *J Biol Chem,* 274, 37251-8.

SEGUI, B., CUVILLIER, O., ADAM-KLAGES, S., GARCIA, V., MALAGARIE-CAZENAVE, S., LEVEQUE, S., CASPAR-BAUGUIL, S., COUDERT, J., SALVAYRE, R., KRÖNKE, M. & LEVADE, T. 2001. Involvement of FAN in TNF-induced apoptosis. *J Clin Invest,* 108, 143-51.

SENKAL, C. E., PONNUSAMY, S., BIELAWSKI, J., HANNUN, Y. A. & OGRETMEN, B. 2010. Antiapoptotic roles of ceramide-synthase-6-generated C16-ceramide via selective regulation of the ATF6/CHOP arm of ER-stress-response pathways. *FASEB J,* 24, 296-308.

SENTELLE, R. D., SENKAL, C. E., JIANG, W., PONNUSAMY, S., GENCER, S., PANNEER SELVAM, S., RAMSHESH, V. K., PETERSON, Y. K., LEMASTERS, J. J., SZULC, Z. M., BIELAWSKI, J. & OGRETMEN, B. 2012. Ceramide targets autophagosomes to mitochondria and induces lethal mitophagy. *Nat Chem Biol*.

SHIRLEY, S., MORIZOT, A. & MICHEAU, O. 2011. Regulating TRAIL receptor-induced cell death at the membrane : a deadly discussion. *Recent Pat Anticancer Drug Discov,* 6, 311-23.

SILKE, J. & STRASSER, A. 2013. The FLIP Side of Life. *Sci Signal,* 6, pe2.

SIMONARO, C. M., PARK, J. H., ELIYAHU, E., SHTRAIZENT, N., MCGOVERN, M. M. & SCHUCHMAN, E. H. 2006. Imprinting at the SMPD1 locus: implications for acid sphingomyelinase-deficient Niemann-Pick disease. *Am J Hum Genet,* 78, 865-70.

SIROIS, I., GROLEAU, J., PALLET, N., BRASSARD, N., HAMELIN, K., LONDONO, I., PSHEZHETSKY, A. V., BENDAYAN, M. & HEBERT, M. J. 2012. Caspase activation regulates the extracellular export of autophagic vacuoles. *Autophagy,* 8, 927-37.

SOSNA, J. 2010. Characterization of intracellular pathways in caspase-independent programmed cell death. 1-76.

STANCEVIC, B. & KOLESNICK, R. 2010. Ceramide-rich platforms in transmembrane signaling. *FEBS Lett,* 584, 1728-40.

STOFFEL, W., JENKE, B., HOLZ, B., BINCZEK, E., GUNTER, R. H., KNIFKA, J., KOEBKE, J. & NIEHOFF, A. 2007. Neutral sphingomyelinase (SMPD3) deficiency causes a novel form of chondrodysplasia and dwarfism that is rescued by Col2A1-driven smpd3 transgene expression. *Am J Pathol,* 171, 153-61.

STRELOW, A., BERNARDO, K., ADAM-KLAGES, S., LINKE, T., SANDHOFF, K., KRONKE, M. & ADAM, D. 2000. Overexpression of acid ceramidase protects from tumor necrosis factor-induced cell death. *J Exp Med,* 192, 601-12.

SU, D., SU, Z., WANG, J., YANG, S. & MA, J. 2009. UCF-101, a novel Omi/HtrA2 inhibitor, protects against cerebral ischemia/reperfusion injury in rats. *Anat Rec (Hoboken),* 292, 854-61.

SUN, L., WANG, H., WANG, Z., HE, S., CHEN, S., LIAO, D., WANG, L., YAN, J., LIU, W., LEI, X. & WANG, X. 2012. Mixed lineage kinase domain-like protein mediates necrosis signaling downstream of RIP3 kinase. *Cell,* 148, 213-27.

SUNDARARAJAN, R., CHEN, G., MUKHERJEE, C. & WHITE, E. 2005. Caspase-dependent processing activates the proapoptotic activity of deleted in breast cancer-1 during tumor necrosis factor-alpha-mediated death signaling. *Oncogene,* 24, 4908-20.

SUZUKI, Y., IMAI, Y., NAKAYAMA, H., TAKAHASHI, K., TAKIO, K. & TAKAHASHI, R. 2001. A serine protease, HtrA2, is released from the mitochondria and interacts with XIAP, inducing cell death. *Mol Cell,* 8, 613-21.

TAKADA, G., SATOH, W., KOMATSU, K., KONN, Y., MIURA, Y. & UESAKA, Y. 1987. Transitory type of sphingomyelinase deficient Niemann-Pick disease: clinical and morphological studies and follow-up of two sisters. *Tohoku J Exp Med,* 153, 27-36.

TAKAHASHI, Y., MIYOSHI, Y., TAKAHATA, C., IRAHARA, N., TAGUCHI, T., TAMAKI, Y. & NOGUCHI, S. 2005. Down-regulation of LATS1 and LATS2 mRNA expression by promoter hypermethylation and its association with biologically aggressive phenotype in human breast cancers. *Clin Cancer Res,* 11, 1380-5.

TCHERNEV, V. T., MANSFIELD, T. A., GIOT, L., KUMAR, A. M., NANDABALAN, K., LI, Y., MISHRA, V. S., DETTER, J. C., ROTHBERG, J. M., WALLACE, M. R., SOUTHWICK, F. S. & KINGSMORE, S. F. 2002. The Chediak-Higashi protein interacts with SNARE complex and signal transduction proteins. *Mol Med,* 8, 56-64.

TENEV, T., BIANCHI, K., DARDING, M., BROEMER, M., LANGLAIS, C., WALLBERG, F., ZACHARIOU, A., LOPEZ, J., MACFARLANE, M., CAIN, K. & MEIER, P. 2011. The Ripoptosome, a signaling platform that assembles in response to genotoxic stress and loss of IAPs. *Mol Cell,* 43, 432-48.

THON, L., MATHIEU, S., KABELITZ, D. & ADAM, D. 2006. The murine TRAIL receptor signals caspase-independent cell death through ceramide. *Exp Cell Res,* 312, 3808-21.

THON, L., MÖHLIG, H., MATHIEU, S., LANGE, A., BULANOVA, E., WINOTO-MORBACH, S., SCHÜTZE, S., BULFONE-PAUS, S. & ADAM, D. 2005. Ceramide mediates caspase-independent programmed cell death. *FASEB J,* 19, 1945-56.

TRAJKOVIC, K., HSU, C., CHIANTIA, S., RAJENDRAN, L., WENZEL, D., WIELAND, F., SCHWILLE, P., BRUGGER, B. & SIMONS, M. 2008. Ceramide triggers budding of exosome vesicles into multivesicular endosomes. *Science,* 319, 1244-7.

TRAN, S. E., HOLMSTROM, T. H., AHONEN, M., KAHARI, V. M. & ERIKSSON, J. E. 2001. MAPK/ERK overrides the apoptotic signaling from Fas, TNF, and TRAIL receptors. *J Biol Chem,* 276, 16484-90.

TROULINAKI, K. & TAVERNARAKIS, N. 2012. Endocytosis and intracellular trafficking contribute to necrotic neurodegeneration in C. elegans. *EMBO J,* 31, 654-66.

TSUDA, H., NING, Z., YAMAGUCHI, Y. & SUZUKI, N. 2012. Programmed cell death and its possible relationship with periodontal disease. *J Oral Sci,* 54, 137-49.

TULIN, A. 2011. Re-evaluating PARP1 inhibitor in cancer. *Nat Biotechnol,* 29, 1078-9.

TULIN, A., NAUMOVA, N. M., MENON, A. K. & SPRADLING, A. C. 2006. Drosophila poly(ADP-ribose) glycohydrolase mediates chromatin structure and SIR2-dependent silencing. *Genetics,* 172, 363-71.

UNDERHILL, C., TOULMONDE, M. & BONNEFOI, H. 2011. A review of PARP inhibitors: from bench to bedside. *Ann Oncol,* 22, 268-79.

VAN LOO, G., VAN GURP, M., DEPUYDT, B., SRINIVASULA, S. M., RODRIGUEZ, I., ALNEMRI, E. S., GEVAERT, K., VANDEKERCKHOVE, J., DECLERCQ, W. & VANDENABEELE, P. 2002. The serine protease Omi/HtrA2 is released from mitochondria during apoptosis. Omi interacts with caspase-inhibitor XIAP and induces enhanced caspase activity. *Cell Death Differ,* 9, 20-6.

VANDE WALLE, L., VAN DAMME, P., LAMKANFI, M., SAELENS, X., VANDEKERCKHOVE, J., GEVAERT, K. & VANDENABEELE, P. 2007. Proteome-wide Identification of HtrA2/Omi Substrates. *J Proteome Res,* 6, 1006-15.

VANDE WALLE, L., WIRAWAN, E., LAMKANFI, M., FESTJENS, N., VERSPURTEN, J., SAELENS, X., VANDEN BERGHE, T. & VANDENABEELE, P. 2010. The mitochondrial serine protease HtrA2/Omi cleaves RIP1 during apoptosis of Ba/F3 cells induced by growth factor withdrawal. *Cell Res,* 20, 421-33.

VANDENABEELE, P., GALLUZZI, L., VANDEN BERGHE, T. & KROEMER, G. 2010. Molecular mechanisms of necroptosis: an ordered cellular explosion. *Nat Rev Mol Cell Biol,* 11, 700-14.

VANLANGENAKKER, N., BERTRAND, M. J., BOGAERT, P., VANDENABEELE, P. & VANDEN BERGHE, T. 2011a. TNF-induced necroptosis in L929 cells is tightly regulated by multiple TNFR1 complex I and II members. *Cell Death Dis,* 2, e230.

VANLANGENAKKER, N., VANDEN BERGHE, T., BOGAERT, P., LAUKENS, B., ZOBEL, K., DESHAYES, K., VUCIC, D., FULDA, S., VANDENABEELE, P. & BERTRAND, M. J. 2011b. cIAP1 and TAK1 protect cells from TNF-induced necrosis by preventing RIP1/RIP3-dependent reactive oxygen species production. *Cell Death Differ,* 18, 656-65.

VANLANGENAKKER, N., VANDEN BERGHE, T. & VANDENABEELE, P. 2012. Many stimuli pull the necrotic trigger, an overview. *Cell Death Differ,* 19, 75-86.

VERHAGEN, A. M., SILKE, J., EKERT, P. G., PAKUSCH, M., KAUFMANN, H., CONNOLLY, L. M., DAY, C. L., TIKOO, A., BURKE, R., WROBEL, C., MORITZ, R. L., SIMPSON, R. J. & VAUX, D. L. 2002. HtrA2 promotes cell death through its serine protease activity and its ability to antagonize inhibitor of apoptosis proteins. *J Biol Chem,* 277, 445-54.

VOELKEL-JOHNSON, C., HANNUN, Y. A. & EL-ZAWAHRY, A. 2005. Resistance to TRAIL is associated with defects in ceramide signaling that can be overcome by exogenous C6-ceramide without requiring down-regulation of cellular FLICE inhibitory protein. *Mol Cancer Ther,* 4, 1320-7.

WAGENKNECHT, B., ROTH, W., GULBINS, E., WOLBURG, H. & WELLER, M. 2001. C2-ceramide signaling in glioma cells: synergistic enhancement of CD95-mediated, caspase-dependent apoptosis. *Cell Death Differ,* 8, 595-602.

WALSH, C. M. & EDINGER, A. L. 2010. The complex interplay between autophagy, apoptosis, and necrotic signals promotes T-cell homeostasis. *Immunol Rev,* 236, 95-109.

WANG, L., DU, F. & WANG, X. 2008. TNF-alpha induces two distinct caspase-8 activation pathways. *Cell,* 133, 693-703.

WANG, X., HERBERG, F. W., LAUE, M. M., WULLNER, C., HU, B., PETRASCH-PARWEZ, E. & KILIMANN, M. W. 2000. Neurobeachin: A protein kinase A-anchoring, beige/Chediak-higashi protein homolog implicated in neuronal membrane traffic. *J Neurosci,* 20, 8551-65.

WANG, Z., JIANG, H., CHEN, S., DU, F. & WANG, X. 2012. The mitochondrial phosphatase PGAM5 functions at the convergence point of multiple necrotic death pathways. *Cell,* 148, 228-43.

WANG, Z., WATT, W., BROOKS, N. A., HARRIS, M. S., URBAN, J., BOATMAN, D., MCMILLAN, M., KAHN, M., HEINRIKSON, R. L., FINZEL, B. C., WITTWER, A. J., BLINN, J., KAMTEKAR, S. & TOMASSELLI, A. G. 2010. Kinetic and structural characterization of caspase-3 and caspase-8 inhibition by a novel class of irreversible inhibitors. *Biochim Biophys Acta,* 1804, 1817-31.

WATSON, S. A., MORRIS, T. M., COLLINS, H. M., BAWDEN, L. J., HAWKINS, K. & BONE, E. A. 1999. Inhibition of tumour growth by marimastat in a human xenograft model of gastric cancer: relationship with levels of circulating CEA. *Br J Cancer,* 81, 19-23.

WERNEBURG, N., GUICCIARDI, M. E., YIN, X. M. & GORES, G. J. 2004. TNF-alpha-mediated lysosomal permeabilization is FAN and caspase 8/Bid dependent. *Am J Physiol Gastrointest Liver Physiol,* 287, G436-43.

WERNEBURG, N. W., GUICCIARDI, M. E., BRONK, S. F., KAUFMANN, S. H. & GORES, G. J. 2007. Tumor necrosis factor-related apoptosis-inducing ligand activates a lysosomal pathway of apoptosis that is regulated by Bcl-2 proteins. *J Biol Chem,* 282, 28960-70.

WILSON, J., HUYNH, C., KENNEDY, K. A., WARD, D. M., KAPLAN, J., ADEREM, A. & ANDREWS, N. W. 2008. Control of parasitophorous vacuole expansion by LYST/Beige restricts the intracellular growth of Leishmania amazonensis. *PLoS Pathog,* 4, e1000179.

WOJEWODKA, G., DE SANCTIS, J. B. & RADZIOCH, D. 2011. Ceramide in cystic fibrosis: a potential new target for therapeutic intervention. *J Lipids,* 2011, 674968.

WU, B. X., RAJAGOPALAN, V., RODDY, P. L., CLARKE, C. J. & HANNUN, Y. A. 2010a. Identification and characterization of murine mitochondria-associated neutral sphingomyelinase (MA-nSMase), the mammalian sphingomyelin phosphodiesterase 5. *J Biol Chem,* 285, 17993-8002.

WU, W., LIU, P. & LI, J. 2012. Necroptosis: an emerging form of programmed cell death. *Crit Rev Oncol Hematol,* 82, 249-58.

WU, Y. T., TAN, H. L., HUANG, Q., SUN, X. J., ZHU, X. & SHEN, H. M. 2011. zVAD-induced necroptosis in L929 cells depends on autocrine production of TNFalpha mediated by the PKC-MAPKs-AP-1 pathway. *Cell Death Differ,* 18, 26-37.

WU, Y. T., TAN, H. L., SHUI, G., BAUVY, C., HUANG, Q., WENK, M. R., ONG, C. N., CODOGNO, P. & SHEN, H. M. 2010b. Dual role of 3-methyladenine in modulation of autophagy via different temporal patterns of inhibition on class I and III phosphoinositide 3-kinase. *J Biol Chem,* 285, 10850-61.

XU, X., CHUA, C. C., ZHANG, M., GENG, D., LIU, C. F., HAMDY, R. C. & CHUA, B. H. 2010. The role of PARP activation in glutamate-induced necroptosis in HT-22 cells. *Brain Res,* 1343, 206-12.

XU, Y., HUANG, S., LIU, Z. G. & HAN, J. 2006. Poly(ADP-ribose) polymerase-1 signaling to mitochondria in necrotic cell death requires RIP1/TRAF2-mediated JNK1 activation. *J Biol Chem,* 281, 8788-95.

YABU, T., SHIMUZU, A. & YAMASHITA, M. 2009. A novel mitochondrial sphingomyelinase in zebrafish cells. *J Biol Chem,* 284, 20349-63.

YAMAMOTO, A., TAGAWA, Y., YOSHIMORI, T., MORIYAMA, Y., MASAKI, R. & TASHIRO, Y. 1998. Bafilomycin A1 prevents maturation of autophagic vacuoles by inhibiting fusion between autophagosomes and lysosomes in rat hepatoma cell line, H-4-II-E cells. *Cell Struct Funct,* 23, 33-42.

YAMASHIMA, T. 2004. Ca2+-dependent proteases in ischemic neuronal death: a conserved 'calpain-cathepsin cascade' from nematodes to primates. *Cell Calcium,* 36, 285-93.

YAMASHIMA, T., KOHDA, Y., TSUCHIYA, K., UENO, T., YAMASHITA, J., YOSHIOKA, T. & KOMINAMI, E. 1998. Inhibition of ischaemic hippocampal neuronal death in primates with cathepsin B inhibitor CA-074: a novel strategy for neuroprotection based on 'calpain-cathepsin hypothesis'. *Eur J Neurosci,* 10, 1723-33.

YANG, Q. H., CHURCH-HAJDUK, R., REN, J., NEWTON, M. L. & DU, C. 2003. Omi/HtrA2 catalytic cleavage of inhibitor of apoptosis (IAP) irreversibly inactivates IAPs and facilitates caspase activity in apoptosis. *Genes Dev,* 17, 1487-96.

YEH, W. C., ITIE, A., ELIA, A. J., NG, M., SHU, H. B., WAKEHAM, A., MIRTSOS, C., SUZUKI, N., BONNARD, M., GOEDDEL, D. V. & MAK, T. W. 2000. Requirement for Casper (c-FLIP) in regulation of death receptor-induced apoptosis and embryonic development. *Immunity,* 12, 633-42.

YEH, W. C., POMPA, J. L., MCCURRACH, M. E., SHU, H. B., ELIA, A. J., SHAHINIAN, A., NG, M., WAKEHAM, A., KHOO, W., MITCHELL, K., EL-DEIRY, W. S., LOWE, S. W., GOEDDEL, D. V. & MAK, T. W. 1998. FADD: essential for embryo development and signaling from some, but not all, inducers of apoptosis. *Science,* 279, 1954-8.

YOON, Y. H., CHO, K. S., HWANG, J. J., LEE, S. J., CHOI, J. A. & KOH, J. Y. 2010. Induction of lysosomal dilatation, arrested autophagy, and cell death by chloroquine in cultured ARPE-19 cells. *Invest Ophthalmol Vis Sci,* 51, 6030-7.

YOUSEFI, S., PEROZZO, R., SCHMID, I., ZIEMIECKI, A., SCHAFFNER, T., SCAPOZZA, L., BRUNNER, T. & SIMON, H. U. 2006. Calpain-mediated cleavage of Atg5 switches autophagy to apoptosis. *Nat Cell Biol,* 8, 1124-32.

YU, H. B., KIELCZEWSKA, A., ROZEK, A., TAKENAKA, S., LI, Y., THORSON, L., HANCOCK, R. E., GUARNA, M. M., NORTH, J. R., FOSTER, L. J., DONINI, O. & FINLAY, B. B. 2009. Sequestosome-1/p62 is the key intracellular target of innate defense regulator peptide. *J Biol Chem,* 284, 36007-11.

YU, L., ALVA, A., SU, H., DUTT, P., FREUNDT, E., WELSH, S., BAEHRECKE, E. H. & LENARDO, M. J. 2004. Regulation of an ATG7-beclin 1 program of autophagic cell death by caspase-8. *Science,* 304, 1500-2.

YU, S. W., WANG, H., POITRAS, M. F., COOMBS, C., BOWERS, W. J., FEDEROFF, H. J., POIRIER, G. G., DAWSON, T. M. & DAWSON, V. L. 2002. Mediation of poly(ADP-ribose) polymerase-1-dependent cell death by apoptosis-inducing factor. *Science,* 297, 259-63.

YUAN, J. & KROEMER, G. 2010. Alternative cell death mechanisms in development and beyond. *Genes Dev,* 24, 2592-602.

ZEIDAN, Y. H. & HANNUN, Y. A. 2007. Activation of acid sphingomyelinase by protein kinase Cdelta-mediated phosphorylation. *J Biol Chem,* 282, 11549-61.

ZHA, X., PIERINI, L. M., LEOPOLD, P. L., SKIBA, P. J., TABAS, I. & MAXFIELD, F. R. 1998. Sphingomyelinase treatment induces ATP-independent endocytosis. *J Cell Biol,* 140, 39-47.

ZHANG, D. W., SHAO, J., LIN, J., ZHANG, N., LU, B. J., LIN, S. C., DONG, M. Q. & HAN, J. 2009. RIP3, an energy metabolism regulator that switches TNF-induced cell death from apoptosis to necrosis. *Science,* 325, 332-6.

ZHANG, H., ZHOU, X., MCQUADE, T., LI, J., CHAN, F. K. & ZHANG, J. 2011. Functional complementation between FADD and RIP1 in embryos and lymphocytes. *Nature,* 471, 373-6.

ZHANG, J., WANG, J. S., ZHENG, Z. K., TANG, J., FAN, K., GUO, H. & WANG, J. J. 2012. Participation of autophagy in lung ischemia-reperfusion injury in vivo. *J Surg Res*.

ZHANG, Y. & ZHANG, B. 2008. TRAIL resistance of breast cancer cells is associated with constitutive endocytosis of death receptors 4 and 5. *Mol Cancer Res,* 6, 1861-71.

ZHAO, J., JITKAEW, S., CAI, Z., CHOKSI, S., LI, Q., LUO, J. & LIU, Z. G. 2012. Mixed lineage kinase domain-like is a key receptor interacting protein 3 downstream component of TNF-induced necrosis. *Proc Natl Acad Sci U S A,* 109, 5322-7.

ZHENG, L., BIDERE, N., STAUDT, D., CUBRE, A., ORENSTEIN, J., CHAN, F. K. & LENARDO, M. 2006. Competitive control of independent programs of tumor necrosis factor receptor-induced cell death by TRADD and RIP1. *Mol Cell Biol,* 26, 3505-13.

ZHU, P., MARTINVALET, D., CHOWDHURY, D., ZHANG, D., SCHLESINGER, A. & LIEBERMAN, J. 2009. The cytotoxic T lymphocyte protease granzyme A cleaves and inactivates poly(adenosine 5'-diphosphate-ribose) polymerase-1. *Blood,* 114, 1205-16.

ZONG, W. X. & THOMPSON, C. B. 2006. Necrotic death as a cell fate. *Genes Dev,* 20, 1-15.

IX. Declaration

I hereby declare that this Ph.D. thesis entitled „Molecular and functional characterization of the signaling pathways that mediate TNF- and TRAIL-induced programmed necrosis" is a presentation of my original research work. Wherever contributions of others are involved, every effort is made to indicate this clearly, with due reference to the literature, and acknowledgement of collaborative research and discussions.

The work was done under the guidance of Prof. Dr. Dieter Adam, Institute of Immunology, The University of Kiel (German Christian-Albrechts-Universität zu Kiel, CAU) and has not been previously submitted for the award of any degree, diploma or its equivalent to any other University or Institution.

I commit myself to adhering to the standards of Good Scientific Practice of the German Research Foundation valid at the time of my research-related activities at the University.

PLACE, DATE, SIGNATURE

Parts of this thesis have been accepted for publication in:

SOSNA J., VOIGT S., MATHIEU S., LANGE A., THON L., DAVARNIA P., HERDEGEN T., LINKERMANN A., RITTGER A., CHAN F., KABELITZ D., SCHÜTZE S. & ADAM D. 2013. TNF-induced necroptosis and PARP-1-mediated necrosis represent distinct routes to programmed necrotic cell death. *Cell Mol Life Sci*, advance online publication, DOI: 10.1007/s00018-013-1381-6.

Parts of this thesis are currently submitted for publication:

GIEFING M., WINOTO-MORBACH S., SOSNA J., DÖRING C., KLAPPER W., KÜPPERS R., BÖTTCHER S., ADAM D., SIEBERT R. & SCHÜTZE S. 2013. Hodgkin-Reed-Sternberg cells in classical Hodgkin lymphoma show alterations of genes encoding the NADPH oxidase complex and impaired reactive oxygen species synthesis capacity. Submitted to *Plos One*

LUEDDE M., LUTZ M., CARTER N., VUCUR M., JACOBY C., FLÖGEL U., KLEIN T., TOLBA R., REISINGER F., SOSNA J., HIPPE H-J., LINKERMANN A., CHALARIS A., ROSE-JOHN S., ADAM D., LUEDDE T., HEIKENWAELDER M. & FREY N. 2013. RIP3 mediates inflammation and adverse remodeling after myocardial infarction. Submitted to *Circulation Research*

PLACE, DATE, SIGNATURE

X. Acknowledgements

First and foremost, I want to thank Prof. Dr. Dr. h.c. Thomas C. G. Bosch for reading, and insightful questions.

I am grateful to the headmaster of the Institute of Immunology – Prof. Dr. D. Kabelitz for giving me the opportunity to complete a Ph.D thesis in the institute.

I wish to thank Prof. Dr. D. Adam for inviting me to work in his laboratory and for the supervision as well as the help during the laboratory work. I appreciate all his contributions of time, ideas, and funding to make my Ph.D. experience productive and stimulating.

I gratefully acknowledge the funding sources that made my Ph.D. work possible. I was funded by the German Academic Exchange Service (DAAD, A/08/79433) during my thesis.

I would like to thank Prof. Dr. S. Schütze, Prof. Dr. med. R. Siebert and Dr. M. Lüdde for giving me an opportunity to take part in their investigations.

I wish to thank the whole groups of Prof. Dr. D. Adam, Prof. Dr. O. Janßen, Prof. Dr. D. Kabelitz, Prof. Dr. S. Schütze and all members of the Institute for Immunology for being very cheerful colleagues and friends which made daily life in the laboratory extremely nice and interesting, apart from being such good friends!

Thanks very much to colleague Sabine Mathieu. She always had an open ear and open mind for me, helping during practical work.

Lastly, I would like to thank my family: beloved mum and siblings – Ilona and Martin. Many great thanks to my grandfather Hubert and patient, tolerant and encouraging Stephan.

Curriculum Vitae

Justyna Maria Sosna

PERSONAL DETAILS:

Born: 23 August 1983 in Rydultowy, Silesia, Poland
Nationality: Polish
Marital status: unmarried
Gender: Female

EDUCATION and QUALIFICATION:

2002 – 2005	University of Silesia, Katowice, Poland Faculty of Biology and Environmental Protection **Bachelor's degree**: **mark 5 (very good)** **Department of Genetics** Topic: *'Evolution of human genome'.*
2005 – 2007	University of Silesia, Katowice, Poland Faculty of Biology and Environmental Protection **M. Sc. in biology: mark 5 (very good)** **Department of Genetics** Topic: *'Level of polymorphism between barley cultivars and molecular characteristic of barley mutants from Department of Genetics University of Silesia'.*
2007 – 2009	University of Silesia, Katowice, Poland Faculty of Biology and Environmental Protection **Department of Microbiology**
2009 – 2010	University of Applied Sciences in Senftenberg, Germany **M. Sc. in biotechnology mark 1.4 (very good)** Master Thesis in the Laboratory of Prof. Dr. D. Adam, Institute of Immunology, UK-SH, Kiel, Germany Topic: *'Characterization of intracellular pathways in TRAIL-induced caspase-independent programmed cell death'.*
2009 Oct. – 2013 March	**3 years scholarship by the German Academic Exchange Service (DAAD)** **Ph.D. Thesis at CAU in Kiel, Institute of Immunology**

PUBLICATIONS:

DEERBERG A., SOSNA J., THON L., BELKA C. & ADAM D. 2009. Differential protection by wildtype vs. organelle-specific Bcl-2 suggests a combined requirement of both the ER and mitochondria in ceramide-mediated caspase-independent programmed cell death. *Radiation Oncology* 4:41

SOSNA J., VOIGT S., MATHIEU S., LANGE A., THON L., DAVARNIA P., HERDEGEN T., LINKERMANN A., RITTGER A., CHAN F., KABELITZ D., SCHÜTZE S. & ADAM D. 2013. TNF-induced necroptosis and PARP-1-mediated necrosis represent distinct routes to programmed necrotic cell death. *Cell Mol Life Sci*, advance online publication, DOI: 10.1007/s00018-013-1381-6

SUBMITTED MANUSCRIPTS:

GIEFING M., WINOTO-MORBACH S., SOSNA J., DÖRING C., KLAPPER W., KÜPPERS R., BÖTTCHER S., ADAM D., SIEBERT R. & SCHÜTZE S. 2013. Hodgkin-Reed-Sternberg cells in classical Hodgkin lymphoma show alterations of genes encoding the NADPH oxidase complex and impaired reactive oxygen species synthesis capacity. Submitted to *Plos One*

LUEDDE M., LUTZ M., CARTER N., VUCUR M., JACOBY C., FLÖGEL U., KLEIN T., TOLBA R., REISINGER F., SOSNA J., HIPPE H-J., LINKERMANN A., CHALARIS A., ROSE-JOHN S., ADAM D., LUEDDE T., HEIKENWAELDER M. & FREY N. 2013. RIP3 mediates inflammation and adverse remodeling after myocardial infarction. Submitted to *Circulation Research*

XI. Appendix

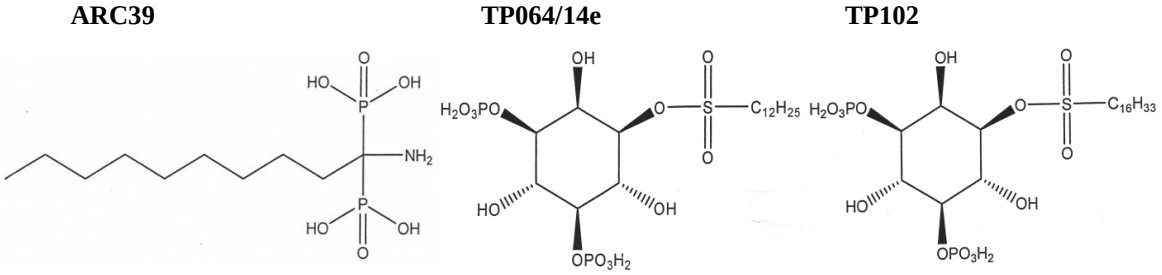

Appendix, Figure 84. Molecular structures of novel A-SMase inhibitors. ARC39 (1-aminodecan-1,1-biphospho acid) (Roth et al., 2009a, Arenz, 2010), TP064/14e (1-*O*-dodecylsulfonyl-*myo*-inositol-3,5-biphosphate) and TP102 (1-*O*-hexadecylsulfonyl-*myo*-inositol-3,5-biphosphate) (Roth et al., 2009b, Arenz, 2010).

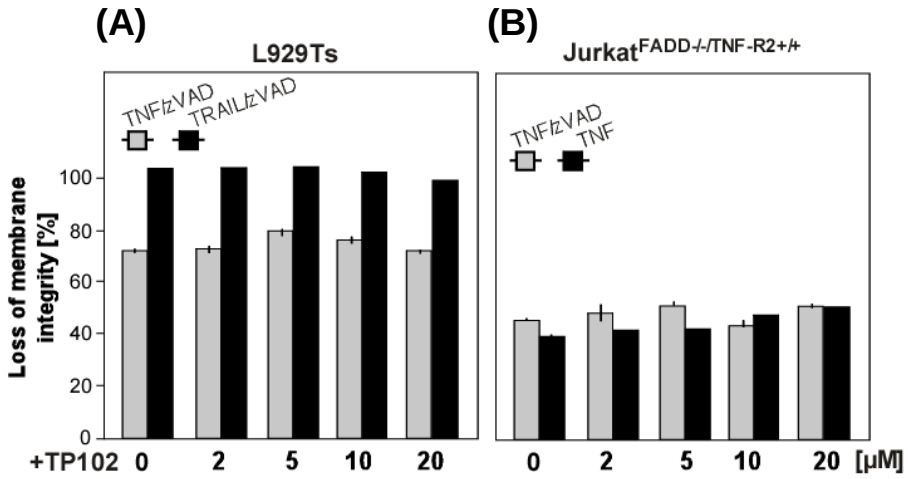

Appendix, Figure 85. The A-SMase inhibitor TP102 does not protect against TNF- or TRAIL-mediated necroptosis in murine and human cell lines. Cells were pretreated for 2 h with indicated concentrations of TP102 with subsequent addition of **(A)** 100 ng/mL hrTNF or 30 ng/mL *killer*TRAIL in combination with 20 µM zVAD-fmk for 5 h or 14 h, respectively, for murine L929Ts cells, or **(B)** 100 ng/mL hrTNF alone for 6 h or in combination with 50 µM zVAD-fmk for 6 h for human Jurkat$^{FADD-/-/TNF-R2+/+}$cells. Data were obtained by flow cytometry counting PI-fluorescence of a sample of 10,000 cells from one experiment in three replications each. Error bars indicate the respective SD.

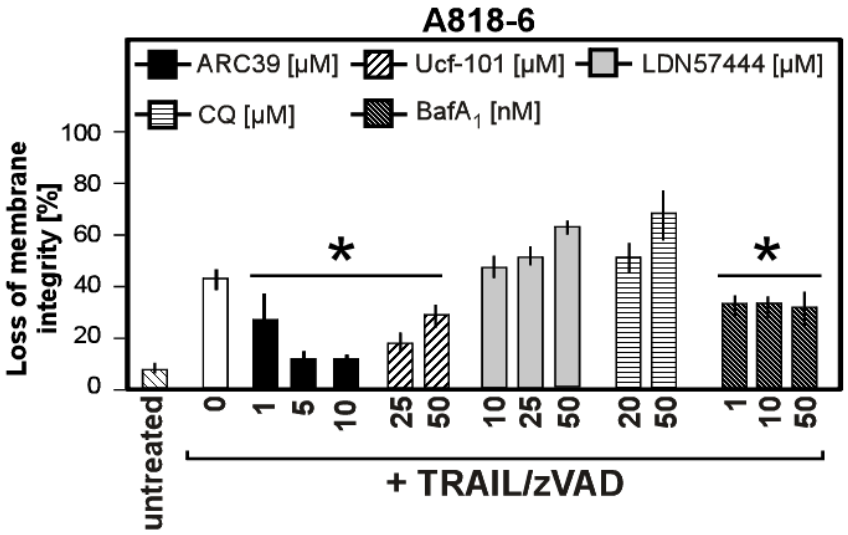

Appendix, Figure 86. Inhibitors of A-SMase, HtrA2/Omi, UCH-L1 and vacuolar-type H^+-V-ATPase protect from TRAIL-mediated necroptosis in the human pancreas adenocarcinoma cell line A818-6. Cells were pretreated for 2 h (or 3 h for LDN57444) with the indicated concentrations of the inhibitors and subsequent addition of 100 ng/mL *killer*TRAIL in combination with 50 µM zVAD-fmk for 24 h. Cell death was analyzed after PI-staining by flow cytometric determination of the fraction of PI-positive cells from 10,000 measured events. Values represent the means of at least three independent experiments, each in three repetitions. Error bars indicate the respective SD. Asterisks indicate statistical significance (t-test) $p<0.01$.

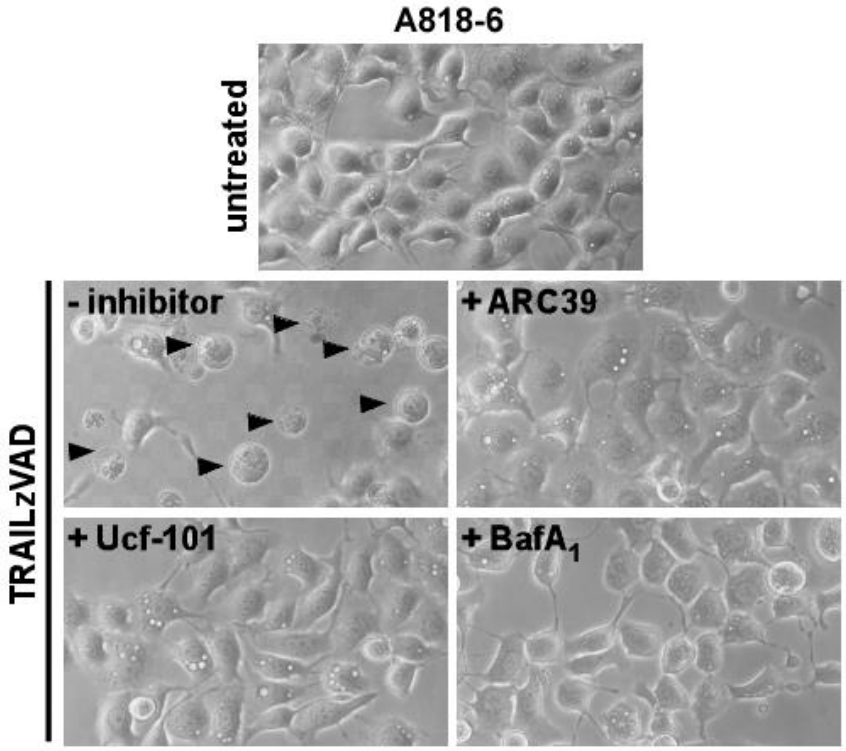

Appendix, Figure 87. Morphological changes of human A818-6 pancreas adenocarcinoma cells after induction of TRAIL-mediated necroptosis in combination with inhibitors for A-SMase, HtrA/Omi and vacuolar-type H^+-V-ATPase. Cells were pretreated for 2 h with 10 µM ARC39, 25 µM Ucf-101 or 10 µM BafA1 and subsequent addition of 100 ng/mL *killer*TRAIL in combination with 50 µM zVAD-fmk for 24 h. The images show morphological changes in A818-6 cells during TRAIL-mediated necroptosis in the absence and presence of the inhibitors. Black arrows indicate typical necroptotic morphology. Magnification 320x.

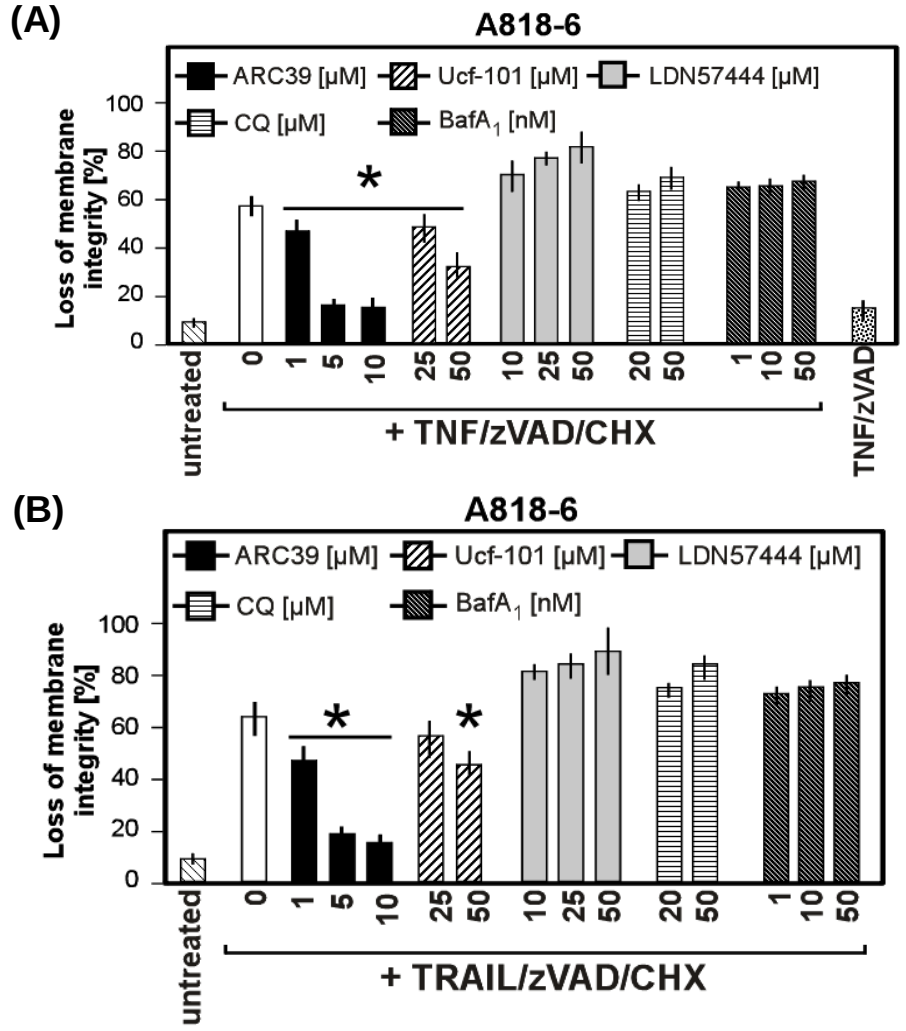

Appendix, Figure 88. Inhibitors of A-SMase, HtrA2/Omi protect from TNF- and TRAIL-mediated necroptosis in presence of CHX in human A818-6 cells. Cells were pretreated for 2 h (or for 3 h with LDN57444) with the indicated concentrations of the inhibitors with subsequent addition of **(A)** 100 ng/mL hTNF or **(B)** *killer*TRAIL in combination with 50 µM zVAD-fmk and 1 µg/mL CHX for 24 h. Cell death was analyzed after PI-staining by flow cytometric determination of the fraction of PI-positive cells from 10,000 measured events. Values represent the means of at least three independent experiments, each in three repetitions. Error bars indicate the respective SD. Asterisks indicate statistical significance (t-test) $p<0.01$.

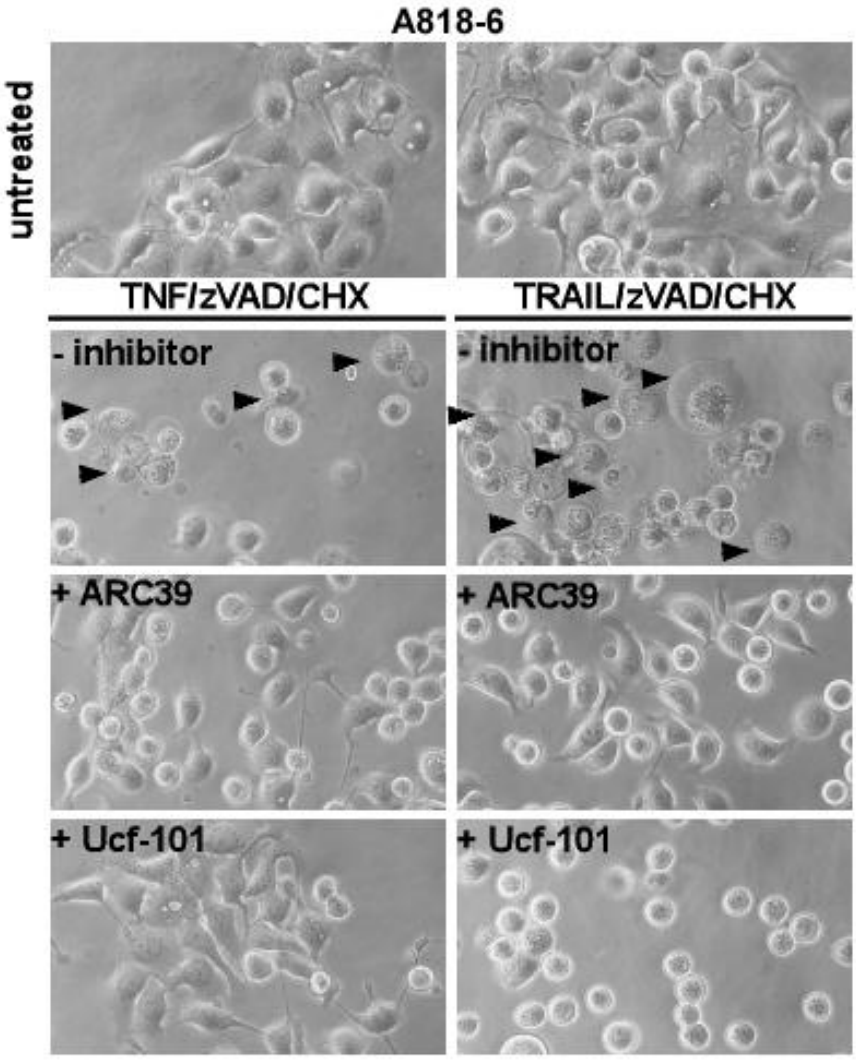

Appendix, Figure 89. Morphological changes of human A818-6 pancreas adenocarcinoma cells after induction of TNF- and TRAIL-mediated necroptosis in combination with inhibitors for A-SMase (ARC39) and HtrA/Omi (Ucf-101). Cells were pretreated for 2 h with 10 µM ARC39 or 50 µM Ucf-101 and subsequent addition of 100 ng/mL hTNF or *killer*TRAIL in combination with 50 µM zVAD-fmk and 1µg/mL CHX for 24 h. The images show morphological changes in A818-6 cells during necroptosis in the absence and presence of the inhibitors. Black arrows indicate typical necroptotic morphology. Magnification 320x.

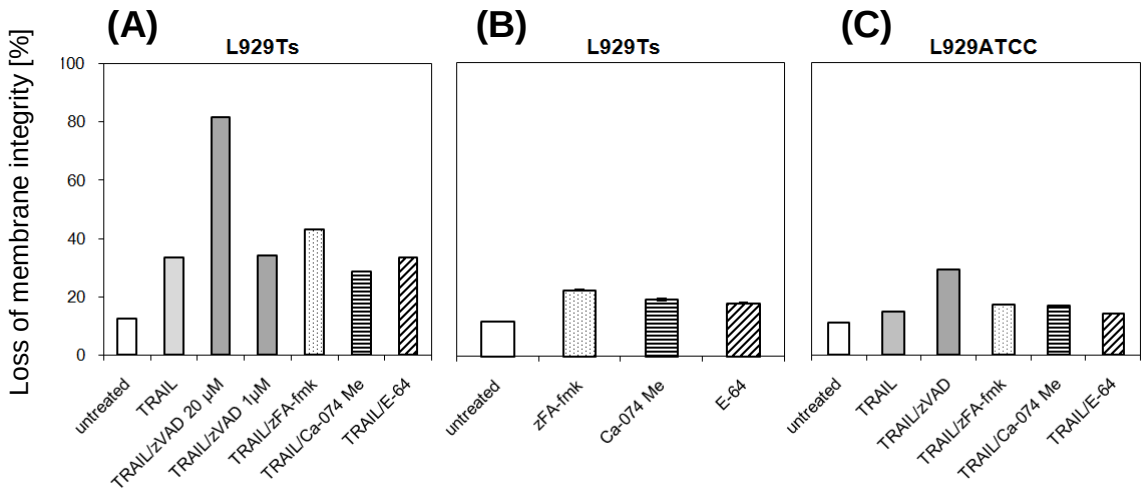

Appendix, Figure 90. TRAIL-induced necroptosis is enhanced by inhibition of caspases but not by inhibition of cathepsins. **(A)** L929Ts cells were incubated with 30 ng/mL *killer*TRAIL for 14 h in the absence or presence of 1 µM zVAD-fmk or 20 µM of zVAD-fmk, zFA-fmk, Ca-074 Me or E-64 before cell death was measured. **(B)** L929Ts cells were left untreated or treated with 20µM of each zFA-fmk, Ca-074 Me and E-64 to determine toxicity of the inhibitors themselves. **(C)** L929ATCC cells were incubated with 30 ng/mL *killer*TRAIL for 14 h in the absence or presence of 20 µM zVAD-fmk, zFA-fmk, Ca-074 Me or E-64 before cell death was determined. Data were obtained by flow cytometry counting PI-fluorescence of a sample of 10000 cells from two different experiments in three replications each. Error bars indicate the respective SD. Data taken from Sosna, 2010.

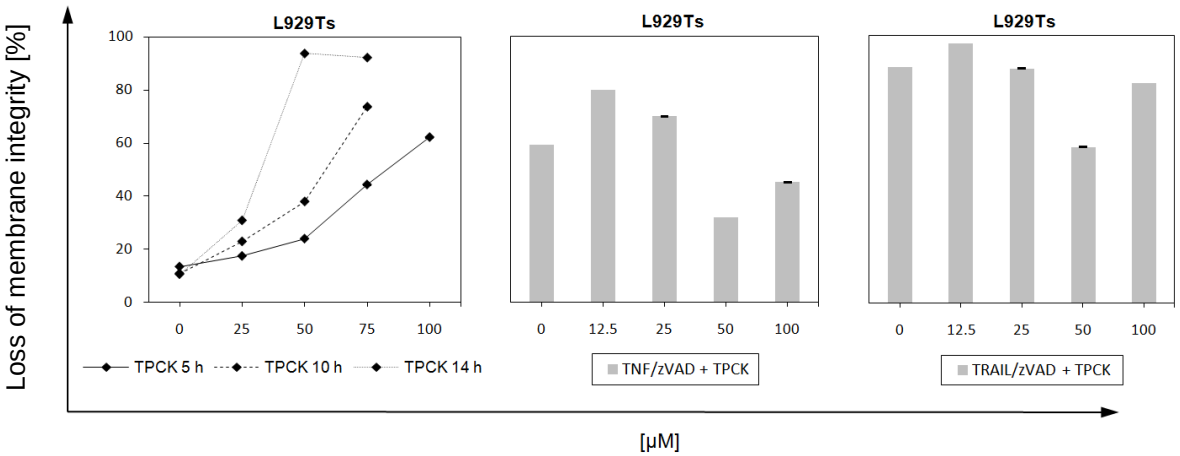

Appendix, Figure 91. TPCK protects L929Ts cells from TNF- and TRAIL-mediated necroptosis. (A) Experiment to determine the cytotoxic influence of TPCK on L929Ts cells after treatment for the indicated time points and with the indicated concentrations. Cells were stimulated **(B)** with 100 ng/mL hrTNF and 20 µM zVAD-fmk in the presence of the indicated concentrations of TPCK for 5 h or **(C)** with 30 ng/mL *killer*TRAIL and 20 µM zVAD-fmk in combination with the indicated concentrations of TPCK for 14 h. Cell death was analyzed after PI-staining by flow cytometric determination of the fraction of PI-positive cells. Values represent the means of three independent experiments, each in two repetitions. Error bars indicate the respective SD. Data taken from (Sosna, 2010).

XII. Additional results obtained in cooperation projects with other research groups

1.1. Analyses of ROS levels in Hodgkin's and non-Hodgkin's human B-cell lymphomas

Cooperation with Dr. Maciej Giefing, Prof. Dr. Reiner Siebert (Institute for Human Genetics, UK-SH) and Prof. Dr. Stefan Schütze (Institute for Immunology, UK-SH)

Genetic analyses performed in the Institute for Human Genetics (UK-SH, Kiel) had revealed functional polymorphisms of genes for NAD(P)H oxidase subunits in Hodgkin's and non-Hodgkin's B-cell lymphoma. Within the above cooperation, extensive analyses of NAD(P)H enzyme activity were performed after stimulation of the membrane-bound lymphocyte activation antigen CD30 (tumor necrosis factor receptor superfamily member 8) to establish whether the amount of ROS produced by stimulated NAD(P)H oxidase is a consequence of the observed genetic polymorphisms. In a first approach, a broad spectrum of ROS generated by NAD(P)H oxidase as well as by other mechanisms was measured simultaneously using the staining dye CM-H_2DCFDA, but a significant contribution of genetic polymorphisms between Hodgkin's and non-Hodgkin's lymphoma on NAD(P)H oxidase activity could not be detected (data not shown). Therefore, more specific measurements of the activity of NAD(P)H oxidase were performed by detecting the production of superoxide anions (O_2^-) with the staining dye DHE. In these experiments, a diminished superoxide anion production in Hodgkin's lymphoma relative to non-Hodgkin's lymphoma (which possess active NAD(P)H oxidase but bare CD30 antigen) was confirmed by comparison with the positive controls Dev1, a non-classical subtype of Hodgkin's lymphoma and Karpas299, a non-Hodgkin's lymphoma (both of them express active NAD(P)H oxidase and CD30 on the cell surface) (Appendix, Figure 92). In summary, these analyses have revealed an association between the genetic polymorphisms in NAD(P)H oxidase and the production of superoxide anions in Hodgkin's lymphomas. These results are part of a manuscript that is currently submitted for publication (Giefing M. et al., 2013). In future, it would be interesting to address the medical relevance of ROS production in Hodgkin's and non-Hodgkin's lymphomas for the application of

chemotherapeutics, as well as for the prognosis of their sensitivity towards anti-cancer drugs and for estimating the genetic instability of cancer cell lines.

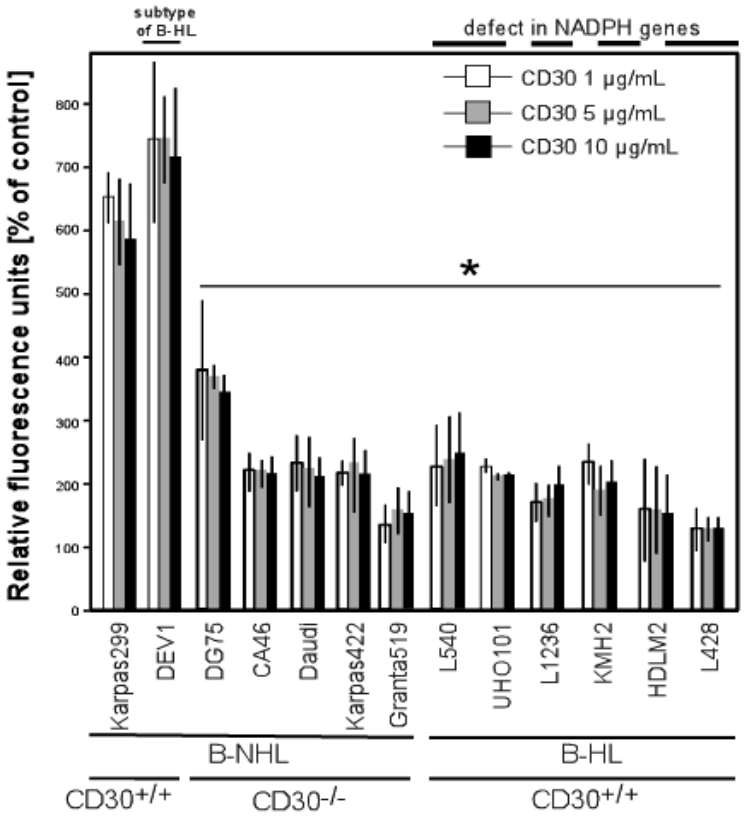

Appendix, Figure 92. Analysis of ROS in Hodgkin's and non-Hodgkin's B-cell lymphomas. Cells were treated with 1 g/mL, 5 µg/mL, or 10 µg/mL of CD30 antibody and simultaneously stained with 30 µM DHE for 30 min. Afterwards, the levels of ROS were measured by flow cytometry and calculated as relative fluorescence units in comparison to cells not stimulated with CD30 antibody. Values represent the means of three independent experiments, each in three repetitions. Error bars indicate the respective SD. Asterisks indicate statistical significance (t-test) $p<0.01$. B-NHL – B-cell non-Hodgkin's lymphoma, B-HL - B-cell non-Hodgkin's lymphoma.

1.2 Characterization of cell death, ROS levels and mitochondrial membrane potential in cardiomyocytes

Cooperation with Dr. Mark Lüdde (Institute for Molecular Cardiology, UK-SH)

Functional analyses performed in the Institute for Molecular Cardiology, UK-SH had revealed an important role of RIP3 in inflammation and adverse remodeling after myocardial infarction in cardiomyocytes from rats. As part of the above cooperation, extensive analyses of RIP3-overexpressing rat cardiomyocytes were carried out to establish which type of cell death triggers the destructive processes and to characterize the associated molecular mechanisms in more detail.

In a first set of experiments, loss of cell membrane integrity was measured (Appendix, Figure 93 A), demonstrating that overexpression of RIP3 kinase in cardiomyocytes leads to increased cell death. To more precisely define which type of cell death was triggered, additional analyses of phosphatidylserine (Ptd-L-Ser) externalization (which only occurs in apoptosis, not in programmed necrosis) were carried out. As shown in (Appendix, Figure 93 B), RIP3 overexpression elevated the amount of PI-positive cell, but not of cells which were externalizing Ptd-L-Ser, demonstrating that RIP3 kinase mediates a necrotic type of PCD in cardiomyocytes from rats. Next, the influence of RIP3 overexpression on the production of ROS as well as on changes in mitochondrial membrane potential were investigated (Appendix, Figure 94). A diminished ROS production in rat cardiomyocytes overexpressing RIP3 was revealed. By comparison, in cells overexpressing the negative control protein LacZ which is unspecific for myocardial infarction, an increase in mitochondrial membrane potential was detected. In summary, these analyses revealed an association of RIP3 kinase activity with the execution of programmed necrosis in rat cardiomyocytes. Moreover, the data suggest a participation of hypertrophic conditions associated with ischemic preconditioning and hypercontraction in cardiomyocytes affected by RIP3 kinase overexpression. These results are part of a manuscript that is currently submitted for publication (Luedde M. et al., 2013). In future, it would be interesting to address the medical relevance of these data to treat patients after myocardial infarction.

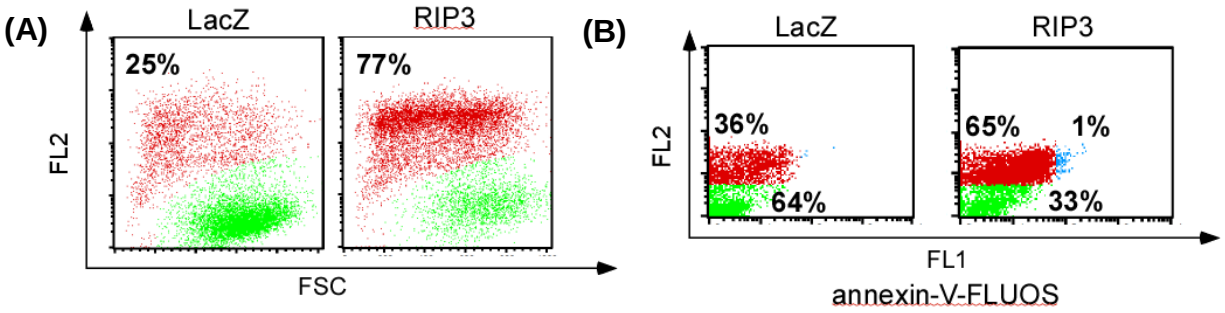

Appendix, Figure 93. Rat cardiomyocytes overexpressing RIP3 are dying through necrosis. Rat cardiomyocytes transfected with a rat RIP3 construct or LacZ vector (negative control) were provided by Dr. M. Lüdde. 3 days after transfection, FACS analysis of cell viability was performed by **(A)** measurement of PI-positive cells (FL2) (to determine loss of membrane integrity) and **(B)** by staining with annexin-V-FLUOS (FL1) (to additionally determine externalization of phosphatidylserine typical for apoptosis) and PI (FL2).

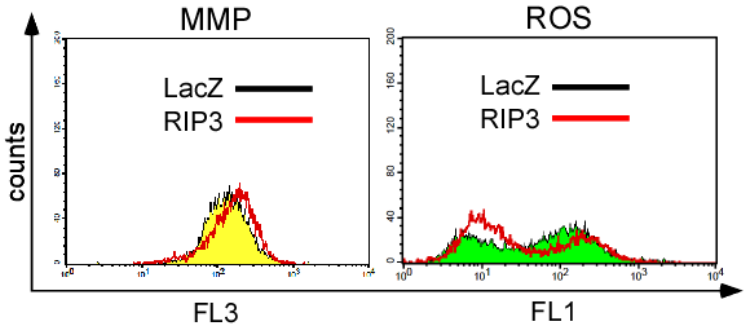

Appendix, Figure 94. Rat cardiomyocytes overexpressing RIP3 exhibit an increased mitochondrial membrane potential (MMP) and decreased levels of ROS. Rat cardiomyocytes transfected with a rat RIP3 construct or LacZ vector (negative control) were provided by Dr. M. Lüdde. 3 days after transfection, FACS analysis of MMP (FL3) was performed in parallel to detection of ROS (FL1).